AN INTRATUMORAL CONTROLLED RELEASE FORMULATION OF CLUSTERIN ANTISENSE OLIGONUCLEOTIDE AND PACLITAXEL OR DOCETAXEL FOR TREATMENT OF PROSTATE TUMORS

by

CHRISTOPHER MICHAEL KEVIN SPRINGATE

B.Sc. (Pharm), The University of British Columbia
M.Sc. (Pharm), The University of British Columbia

A THESIS SUBMITTED IN PARTIAL FULFILLMENT OF
THE REQUIREMENTS FOR THE DEGREE OF

DOCTOR OF PHILOSOPHY

in

THE FACULTY OF GRADUATE STUDIES

(Pharmaceutical Sciences)

THE UNIVERSITY OF BRITISH COLUMBIA

April 2007

ABSTRACT

The localized controlled delivery of both phosphorothioated clusterin antisense oligonucleotide (clusterin ASO) and paclitaxel or docetaxel to prostate tumors to maintain therapeutic concentrations of the agents at the target disease site was investigated in this work. The primary objectives were to develop and characterize the physicochemical properties, drug release profiles and efficacy in prostate cancer models, of intratumoral, controlled release polymeric paste formulations of clusterin ASO and paclitaxel or docetaxel.

A solvent loading process was used to complex polyanionic clusterin ASO with polycationic chitosan microparticles (microparticulate CC complexes). CC complexes were incorporated into an injectable, biodegradable paste based on a 40/60 blend of triblock copolymer poly(D,L-lactide-co-caprolactone)-block-poly(ethylene glycol)-block-(D,L-lactide-co-caprolactone) and methoxy-poly(ethylene glycol) (CC paste). CC paste formed a semi-solid implant when injected into aqueous media or tissue.

Physicochemical characterization of CC complexes showed that the amount of clusterin ASO complexed with chitosan was dependent on the ASO:chitosan ratio and the pH. *In vitro* release of ASO from CC paste in phosphate buffered saline (PBS) at 37°C was assayed by HPLC and showed that the release of ASO was influenced by ASO:chitosan ratios, pH, phosphate ion concentration and the presence or absence of polymer paste. Increasing the amount of chitosan or decreasing the pH resulted in slower ASO release rates as a result of the increased number of positively charged amine groups within the chitosan available for

complexation with ASO. *In vitro* release of clusterin ASO and its 20-, 19- and 18-mer degradation products from CC paste into human plasma at 37°C was assayed by capillary gel electrophoresis (CGE). The data showed that degradation of 21-mer clusterin ASO occurred in the plasma and suggested that the polymer paste protected ASO from nuclease degradation.

Treatment of mice bearing human prostate PC-3 or LNCaP tumors with an intratumoral injection of CC pastes loaded with clusterin ASO plus paclitaxel or docetaxel reduced mean tumor volumes and serum PSA levels by more than 50% and 70%, respectively.

Complexation of clusterin ASO with chitosan and incorporation into polymeric paste with paclitaxel or docetaxel produced *in vitro* controlled release of the agents and *in vivo* efficacy over four weeks following a single intratumoral injection in solid human prostate tumors in mice.

TABLE OF CONTENTS

LIST OF TABLES

LIST OF FIGURES

Page

LIST OF ABBREVIATIONS

ANOVA	analysis of variance
ASO	antisense oligonucleotide
b	intercept
C	concentration
CC complexes	clusterin ASO:chitosan microparticulate complexes
CC paste:	polymeric paste loaded with microparticulate CC complexes
CE	capillary electrophoresis
CGE	capillary gel electrophoresis
clusterin ASO	21-mer antisense oligonucleotide, fully pohophorothioated, sequence 5'-CAG CAG CAG AGT CTT CAT CAT-3', targeted against clusterin protein
cm	centimeter
conc	concentration
CpG	cytosine-phosphate-guanine (5'-3')
CV	coefficient of variation
D	diffusion coefficient
dC/dx	concentration gradient
DMEM	Dulbecco's Modified Eagle Medium culture media
DNA	deoxyribonucleic acid
DOPE	dioleoylphosphatidylethanolamine
DRE	digital rectal examination
DSC	differential scanning calorimetry
EDTA	ethylenediaminetetraacetic acid
EVA	poly(ethylene-co-vinyl acetate)
FBS	fetal bovine serum
g	gram
g	equivalent gravity force
GPC	gel permeation chromatography
h	hour
HCl	hydrochloric acid
HPLC	high pressure liquid chromatography

J	flux
KCl	potassium chloride
kPa	kilopascals
kV	kilovolts
k_1	a constant
k_2	a constant
L	liter
LHRH	luteinizing hormone-releasing hormone
m	meter
m	slope
M	amount of material
MePEG	methoxy-poly(ethylene glycol)
MePEG 350	MePEG with molecular weight of 350 $g \cdot mol^{-1}$
mer	nucleotide
mg	milligram
M_{GPC}	peak molecular weight
min	minute
mL	milliliter
mm	millimeter
MMO	mismatch oligonucleotide phosphorothioate
M_i	molecular weight of polymer chains with degree of polymerization i
M_n	number average molecular weight
mRNA	messenger ribonucleic acid
M_w	weight average molecular weight
NaBr	sodium bromide
NaCl	sodium chloride
$NaClO_4$	sodium perchlorate
$NaClO_4 \cdot H_2O$	sodium perchlorate monohydrate
NaOH	sodium hydroxide
n_i	is the number of molecules with the number of repeat units i
N, N oligonucleotide	full-length 21-mer clusterin ASO, sequence 5'-CAG CAG CAG AGT CTT CAT CAT-3'

N-1, N-1 oligonucleotide	20-mer clusterin ASO degradation product or standard, sequence 5'-CAG CAG CAG AGT CTT CAT CA-3'
N-2, N-2 oligonucleotide	19-mer clusterin ASO degradation product or standard, sequence 5'-CAG CAG CAG AGT CTT CAT C-3'
N-3, N-3 oligonucleotide	18-mer clusterin ASO degradation product or standard, sequence 5'-CAG CAG CAG AGT CTT CAT-3'
OD	optical density
OD_{260}	optical density at a wavelength of 260 nm
oligo	oligonucleotide
PBS	phosphate buffered saline
PCL	poly(ε-caprolactone)
PDi	polydispersity index
PEG	poly(ethylene glycol)
PEI	polyethylenimine
PEO	poly(ethylene oxide)
PDLLA	poly(D,L-lactide)
PGA	poly(glycolide)
pH	negative logarithmic value of the hydrogen ion concentration
pKa	pH at which 50% of an acid is ionized
pK_0	pKa or theoretical pKa of an acid in a zero ionic strength solution
PLA	poly(lactide)
PLGA	poly(lactide-co-glycolide)
PLLA	poly(D-lactide)
PLC	poly(D,L-lactide-random-caprolactone) copolymer
PLC-PEG-PLC	triblock copolymer of PLC and PEG in the form of PLC-block-PEG-block-PLC
Poloxomer 407	triblock copolymer of PEO and PPO in the form of PEO-block-PPO-block-PEO
PPO	poly(propylene oxide)
PS	phosphorothioate
PSA	prostate specific antigen
RNA	ribonucleic acid
RPMI 1640	Roswell Park Memorial Institute 1640 culture media
R^2	coefficient of determination

s	second
S	cross-section of area
SEM	scanning electron microscopy
siRNA	small interfering ribonucleic acid
'Stains-all'	4,5,4',5'-dibenzo-3,3'-diethyl-9-methyl-thiacarbocyanine bromide
T	unit of time
TBE	Trizma® base, boric acid and EDTA buffer
t_c	time for a polymer solution at concentration c to flow through a viscometer
TEMED	N,N,N',N'-tetramethylethylenediamine
TNM	tumor, nodes and metastasis classification system for prostate cancer (further abbreviations within the TNM system are given in Table 1)
Tr	retention time
Trizma® base	Tris base, tris[hydroxyl-methyl]aminomethane
Trizma® HCl	Tris HCl, tris[hydroxymethyl] aminomethane hydrochloride
T_{25}, T_{25} oligonucleotide	25-mer thymidine oligonucleotide internal standard, sequence 5'-TTT TTT TTT TTT TTT TTT TTT TTT T-3' (T_{25})
UV-Vis	ultraviolet-visible light; ultraviolet-visible light spectroscopy
w_i	the weight fraction of the molecules with the number of repeat units i
X	distance of a diffusant's movement perpendicular to the surface of a barrier
2'-MOE	2'-O-(2-methoxyethyl)
η	viscosity
η_{sp}	specific viscosity
η_{rel}	relative viscosity
$[\eta]$	intrinsic viscosity
$[\eta]_H$	Huggins intrinsic viscosity
$[\eta]_K$	Kraemer intrinsic viscosity
$[\eta]_{SC}$	Solomon-Ciuta intrinsic viscosity
µg	microgram
µL	microliter

ACKNOWLEDGEMENTS

This dissertation is the result of seeds planted in my brain after reading several articles on ASOs, ribozymes and other therapeutic oligonucleotides. As a pharmacist I was fascinated that these mRNA targeted oligonucleotides may one day be used to treat patients with fewer resulting side effects than observed from the use of traditional non-specific cytotoxic agents. Although the clinical development of therapeutic oligonucleotides had been hobbled by drug delivery issues I felt that some of these issues may be overcome through the research and development of an appropriate polymeric delivery system. I proposed these ideas to Dr. Helen Burt and - to my surprise and delight – she took me on as a PhD student. Thank you, Dr. Burt, for your guidance, patience and providing an intellectually stimulating laboratory environment during this work. Your leadership, mentorship and commitment to your students have served as an inspiration to me throughout this project. I particularly appreciate your helping to develop my critical thinking processes, writing skills and high academic standards.

I owe a special thanks to the other members of my research committee, Drs. Marcel Bally, Martin Gleave, Ron Reid and Peter Soja, for your helpful questions and discussion. Dr. Bally, thank you for your suggestions regarding the *in vitro* complexation and drug release studies. Dr. Gleave, thank you for sharing your thoughts regarding the *in vitro* Western blot and *in vivo* efficacy studies. Dr. Reid, thank you for your helpful general suggestions regarding the oral comprehensive exam and the research program. Dr. Soja, thank you for doing such a great job chairing the committee.

I had the pleasure of working with numerous creative and intelligent people on a day to day basis in Dr. Burt's laboratory. John Jackson, the laboratory manager and a research scientist, was particularly helpful with technical trouble shooting and providing feedback on experimental design. Thank you to the other lab members and former members, Kevin Letchford, Chiming Yang, Clement Mugabe, Jinfang Wang, Tobi Higo, Karen Long, Wes Wong, Melanie ter Borg, Mandip Bajwa and Drs Ruiwen Shi, Christine Allen, Jason Zastre, Sanching Linda Liang, Jianjun John Lu, Katherine Haxton and Chris Tudan, for your intellectual challenges and valuable suggestions. I give special thanks to Kelly-Ann Babiuk, Jennifer Tam, Mary Hoang, Jessica Chong and Karen Chu for helping me with the drug release studies and to Drs. Xichen Zhang and Richard Liggins for synthesizing the triblock copolymer.

I was fortunate to receive encouragement from several faculty members and former members during this project including Drs. John McNeil, Frank Abbot, James Orr, Jack Diamond, David Fielding, Kathleen MacLeod, Wayne Riggs, Brian Rodrigues, Arun Verma, Judith Soon, Brian Cairns and Adam Frankel. Thank you, Dr. Keith McKerlane, for lending me your capillary electorphoresis instrumentation and materials during the initiation of this project. Thank you, Dr. Kishor Wasan, for our discussions on the design of animal studies. Thank you, Dr. Marc Levine, for your feedback on my presentations to the faculty.

Thank you, Dr. Gleave, for providing your animal and wet bench facilities at the Prostate Centre / Jack Bell Research Centre for the *in vivo* efficacy studies and Western blots, respectively. I am grateful, Virginia Yago, for your patience in teaching me animal handling, surgical techniques and helping with the animal studies. I am thankful, Shannon Sinneman, for your assistance with the Western blots.

Thank you, ARC Pharmaceuticals Inc., for financial support of these studies. Drs. Charles Winternitz and Johanne Cashman, your discussions on method development and animal studies, respectively, were very helpful.

Thank you, Mom and Dad, sister and brothers, for your encouragement throughout this project. Thank you, my two daughters, Robyn who was with me when I started and Georgia who joined us along the way.

DEDICATION

I dedicate this thesis to my wife Cynthia.

1. PROJECT OVERVIEW AND BACKGROUND

1.1 PROJECT OVERVIEW

Prostate cancer is the second most common cause of cancer-related deaths in men, with over 30,000 estimated deaths from prostate cancer in North America annually (Carson, III, 2006). Despite androgen ablation treatment initially resulting in high response rates, remissions are temporary because surviving tumor cells usually progress from an androgen dependent to an androgen independent phenotype (Gleave et al., 2005). That the agents used to kill neoplastic cells may also be mediating the chemoresistant phenotype, is one of the main obstacles to curing advanced prostate cancer. New therapeutic strategies designed to inhibit the emergence of this phenotype need to be developed to have a significant impact on survival of patients.

Clusterin protein inhibits apoptosis and as a result, its overexpression assists in the formation of a prostate cancer phenotype that is resistant to chemotherapy, radiation and androgen ablation (Miyake et al., 2000d; Miyake et al., 2003; Zellweger et al., 2003) and is associated with poor clinical outcomes (Chi et al., 2005). However, pro-apoptotic stimulation results in an increase in clusterin protein expression in the clinical setting (July et al., 2002). Antisense oligonucleotides (ASOs) are single strands of deoxyribonucleic acid (DNA) between approximately 15 to 25 nucleotides long (Stahel and Zangemeister-Wittke, 2003) that prevent the expression of specific genes by hybridizing to messenger ribonucleic acid (mRNA) in a sequence-specific manner via Watson-Crick base pairing. Paclitaxel (Kuruma et al., 2003) and

docetaxel (Sinibaldi et al., 2002) are cytotoxic agents that have shown modest responses against prostate cancer when administered intravenously. The combination of clusterin ASO with paclitaxel enhanced apoptosis and reduced human prostate PC-3 (Miyake et al., 2000a) and LNCaP (Miyake et al., 2000b) cancer cell growth and tumor volume in mice xenograft models, following systemic administration.

The clinical application of ASOs has been hampered by a number of drug delivery issues including poor targeting of ASOs to the site of action, rapid elimination from the body, degradation by nucleases and inefficient cellular uptake (Brignole et al., 2003; Vinogradov et al., 2004; Wang et al., 2003b). A limited number of studies have demonstrated *in vitro* that oligonucleotides incorporated into poly(lactide-co-glycolide) (PLGA) microspheres were released in a sustained manner (De Rosa et al., 2002; Hussain et al., 2002) and that the degradation of the oligonucleotides was inhibited (Lewis et al., 1998). However, there have been few investigations of delivery methods that might more effectively locate and maintain therapeutic concentrations of ASOs at the target disease site.

Effective combination therapy using clusterin ASO and paclitaxel or docetaxel depends on the design of an effective drug delivery system. Intratumoral injection of therapeutic agents directly into the prostate gland to localize the agents at the site of tumors is a practical and clinically feasible approach, given the success of brachytherapy in prostate cancer, where radioactive seeds are implanted directly into prostate tissue. Therefore, a delivery system that localizes clusterin ASO and paclitaxel or docetaxel at the site of action, protects clusterin ASO

from degradation and provides controlled release of clusterin ASO and paclitaxel or docetaxel, would represent a significant advance in prostate cancer chemotherapy.

The goal of this research project was to develop a clusterin ASO and paclitaxel or docetaxel loaded polymer-based formulation suitable for intratumoral delivery in prostate cancer. Our research group has developed an intratumoral biodegradable polymeric "paste" for the delivery of paclitaxel (Jackson et al., 2000). The paste is based on a 40/60 w/w blend of a triblock copolymer of poly(D,L-lactide-co-caprolactone)-block-poly(ethylene glycol)-block-poly(D,L-lactide-co-caprolactone) (PLC-block-PEG-block-PLC) and methoxy-poly(ethylene glycol) (MePEG) and can be injected through a 22 gauge needle. Following injection into water, phosphate buffered saline (PBS) or tissue at 37°C, the MePEG dissolved out of the formulation and the remaining formulation set to a semi-solid depot or implant. The polymeric paste released paclitaxel *in vitro* in PBS at 37°C in a controlled manner over several weeks (Jackson et al., 2004). Following intratumoral administration of paclitaxel loaded paste into xenograft LNCaP murine models, decreased tumor volumes and serum prostate specific antigen (PSA) levels were observed (Jackson et al., 2000).

Complexing polyanionic ASO with a polycationic polymer microparticle and incorporating this into the polymeric paste may help to control the release of the ASO from the paste. Polycationic chitosan has been dissolved in weak acids to form polyelectrolyte complexes or coacervated complexes with polyanionic genes and ASOs to increase *in vitro* transfection efficiency and *in vivo* efficacy (Erbacher et al., 1998). In this work, polyanionic clusterin ASO

was loaded into polycationic chitosan microparticles by a solvent loading process to form clusterin ASO:chitosan microparticulate complexes (CC complexes) which may provide a sustained release of clusterin ASO. To our knowledge, ASOs have not previously been complexed with microparticulate chitosan and incorporated into polymeric paste for intra-tumoral injection; and clusterin ASO and paclitaxel or docetaxel combination therapy has not previously been administered intra-tumorally.

The thesis is divided into three main sections. The first part of the thesis addresses the development and qualification of analytical methods, including the analysis of clusterin ASO and its oligonucleotide degradation products in human plasma. CGE methods were developed for separation and quantitation of oligonucleotides differing in length by only one base. The second part of the thesis describes the characterization of clusterin ASO:chitosan microparticulate complexes and the formulation development work in which the clusterin ASO:chitosan microparticulate complexes and paclitaxel or docetaxel were loaded into the triblock copolymer/MePEG paste. Release profiles of paclitaxel, docetaxel and clusterin ASO from the polymeric pastes were evaluated. Degradation of clusterin ASO in the presence of chitosan or paste was determined. The third section of the thesis evaluates the effect of intratumoral administration of clusterin ASO:chitosan microparticulate complexes and paclitaxel or docetaxel loaded into the triblock copolymer/MePEG paste in human prostate cancer xenograft models. Mice bearing PC-3 tumors were treated and tumor volume evaluated. Mice

bearing LNCaP tumors were treated and both tumor volume and serum PSA level were determined.

1.2 PROSTATE CANCER

1.2.1 Epidemiology

With greater than 30,000 estimated deaths yearly from prostate cancer in North America, this disease is the second most common cause of cancer-related deaths in men (Carson, III, 2006). Prostate cancer is an age-related disease, with the majority of all diagnosed cases occurring in patients aged 65 years and older (Levy et al., 1998; Konstantinos, 2005). Race, family history (genetics), diet and environmental (or geographical) factors have all been associated with prostate cancer, although their roles in prostate tumor etiology are uncertain and a singular, definitive cause of the disease has not been clearly identified (Gronberg, 2003; Konstantinos, 2005). African-American men have the highest risk of developing prostate cancer, while Asian populations have the lowest risk (Quinn and Babb, 2002; Bono, 2004). Racial and heredity differences in the occurrence of prostate cancer may be related to genetics, including gene mutations, chromosome abnormalities, decreased gene expression and loss of genes (Gronberg, 2003; Konstantinos, 2005). Low fat / high fiber diets and high lycopene intake are associated with a lower risk of prostate cancer (Bono, 2004; Carson, III, 2006; Konstantinos, 2005).

1.2.2 Screening

Prostate cancer (shown in Figure 1.1) is screened by digital rectal examination (DRE) (Routh and Leibovich, 2005), determining PSA levels (So et al., 2003) and by transrectal ultrasound of the prostate (Carson, III, 2006). Levels and rates of increase of serum PSA are higher in patients with prostate tumors than those without (So et al., 2003). Approximately 40 to 50% of prostate tumors detected by DRE have spread beyond the prostate, while approximately 70 to 90% of prostate cancers detected from abnormal PSA serum levels are localized to the prostate (Routh and Leibovich, 2005). Combining DRE and serum PSA level testing appears to be more accurate than using only one of the screening tests (Konstantinos, 2005). Patients with PSA serum levels equal to or greater than 4 $ng \cdot mL^{-1}$ are generally recommended to have a prostatic biopsy (So et al., 2003), although there is a suggestion that this threshold level should be lowered to 2.6 $ng \cdot mL^{-1}$, depending on the age of the patient (Routh and Leibovich, 2005). Prostatic biopsy may be performed using a transrectal ultrasonography to assist in guiding a needle for the removal of tissue specimens or cores. Tumor histology may be analyzed using the Gleason grading system (Carson, III, 2006).

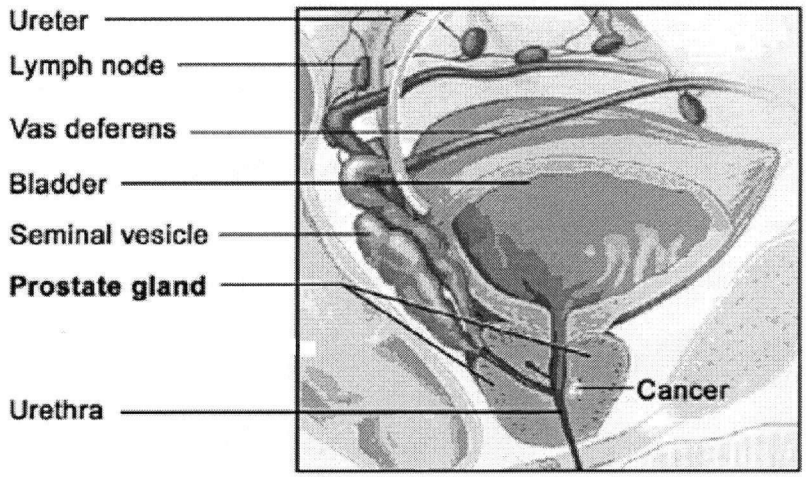

Figure 1.1 Schematic of the prostate, prostate cancer and surrounding tissues. Adapted from the U.S. National Institute's of Health, National Cancer Institute's web site: http://www.cancer.gov.

1.2.3 Staging

Prostate cancers are classified by the Gleason score and/or the tumor, nodes and metastasis (TNM) system and these systems have been reviewed in several publications (Konstantinos, 2005; Carson, III, 2006; Routh and Leibovich, 2005). The Gleason score denotes the dominant and non-dominant histological patterns and thus is an index for prognosis. The TNM system (summarized in Table 1.1) is more widely used than the Gleason score and is based on the clinical progression of the cancer. T1a-T1c designates a clinically undetectable tumor through to a cancer found incidentally or identified by needle biopsy because of increased serum PSA. T2a-T2c designates a tumor confined to one or both lobes of the prostate. T3a-T3c designates an extracapsular extension or invasion of the seminal vesicles by the cancer. T4-T4b designates a tumor that has invaded areas near the prostate (except seminal vesicles). Hence,

stages T3a – T4b represent a tumor localized to the prostate and surrounding tissues and that has not spread to the lymph nodes or otherwise metastasized. N1-N3 designates cancer that has spread to one or more lymph nodes. M1 represents distant metastasis. TNM, Gleason score and PSA level have been used in combination to predict the pathological stage of prostate cancers (Konstantinos, 2005; Carson, III, 2006; Routh and Leibovich, 2005).

1.2.4 Genetics

Men with one primary relative with prostate cancer have a two- to three-fold greater risk of developing prostate cancer than those without. Those with several first-degree or second-degree relatives with a prostate tumor are at even greater risk (Gronberg, 2003). A number of gene polymorphisms are thought to be associated with an increased risk of prostate cancer, including those in the following genes: hormone-regulating genes androgen receptor, cytochrome P450 (CYP17), steroid-5-alpha-reductase type 2 (Lindstrom et al., 2006), 3-β-hydroxysteroid dehydrogenases (Chang et al., 2002), 17-β-hydroxysteroid dehydrogenases (Kraft et al., 2005), insulin growth factor I (Gronberg, 2003), PSA (So et al., 2003), vitamin D receptor (Schwartz, 2005), glutathione S-transferase (Agalliu et al., 2006) and HPC2/ELAC2 (Yokomizo et al., 2004).

Table 1.1 Summary of the tumor, nodes and metastasis (TNM) staging system for prostate cancer. Adapted from Konstantinos (2005), Routh and Leibovich (2005) and Carson, III (2006).

Tumor stage	Definition
Primary tumor	
TX	Primary tumor cannot be assessed
T0	No evidence of primary tumor
T1	Clinically inapparent tumor, not palpable or visible by imaging
T1a	Tumor found incidentally by histology in ≤ 5% of resected tissue
T1b	Tumor found incidentally by histology in > 5% of resected tissue
T1c	Tumor identified by needle biopsy (biopsy taken, for example, because of elevated serum prostate specific antigen level)
T2	Tumor confined within prostate, palpable or visible
T2a	Tumor involves ≤ 50% of 1 prostate lobe
T2b	Tumor involves > 50% of 1 prostate lobe but not both lobes
T2c	Tumor involves both prostate lobes
T3	Tumor extends through the prostate capsule
T3a	Extracapsular extension of tumor (unilateral or bilateral)
T3b	Tumor invades seminal vesicle(s)
T4	Tumor is fixed or invades adjacent structures other than seminal vesicles
T4a	Tumor invades bladder neck, external sphincter and/or rectum
T4b	Tumor invades other areas near prostate (to the floor and/or wall of pelvis)
(Lymph) Node	
NX	Regional lymph nodes cannot be assessed
N0	No regional lymph node metastasis
N1	Metastasis in 1 lymph node < 2 cm
N2	Metastasis(es) in 1+ lymph nodes 2 - 5 cm
N3	Metastasis(es) in 1+ lymph nodes ≥ 5 cm
Metastasis	
MX	Presence of metastasis cannot be assessed
M0	No distant metastasis
M1	Distant metastasis
M1a	Nonregional lymph node(s)
M1b	Metastasis in bone(s)
M1c	Other site(s) with or without bone disease

1.2.5 Initiation, promotion and progression

Gene mutations which result from damage to the genome may result in normal cells becoming cancerous (Chung et al., 2005). Mechanisms within cells, such as incorrect replication of DNA, attack of DNA by free radicals, or the instability of particular nucleotide bases may all cause damage resulting in mutations. In addition, external influences such as radiation (for example, ultra-violet or ionizing) or chemical carcinogens can also cause damage resulting in mutations (McKenzie and Kyprianou, 2006). The transformation of normal cells to cancerous cells, also includes mechanisms by which the genes that normally control cell proliferation and death, undergo mutational damage, resulting in the inactivation of tumor suppressor genes (genes that normally inhibit the proliferation of cells) and the expression of oncogenes (genes that stimulate the proliferation of cells and/or protect cells from apoptosis) (Sherbet, 2005). The transformation of normal cells to cancerous cells, also includes the requirement that these cells avoid replicative senescence (to become immortal) and garner appropriate amounts of oxygen and nutrients to sustain a high rate of proliferation (McKenzie and Kyprianou, 2006). The environment of the cancer cells or tumor also appears to play a role in the development of primary tumors and metastases (Chung et al., 2005).

Carcinogenesis has three-stages: initiation, promotion and progression. Initiation involves changes to DNA by carcinogens. Although most DNA lesions are either repaired or eliminated by cell death (Sherbet, 2005), promotion involves persistent DNA lesions that become

permanent mutations in the cell line following cellular proliferation. These cells may have selective growth advantages. Promotion begins when these cells multiply into focal aggregates and involves the process of the expansion of clonal selection into tumors. Progression may take place over a period of years or be accelerated by endogenous or exogenous factors (Sherbet, 2005). With progression comes a change in the physiological properties of the cancerous cells. These changes include the emergence of new growth regulatory mechanisms and the ability to mobilize, invade and escape recognition by the immune system (McKenzie and Kyprianou, 2006).

1.2.6 Androgen dependence and progression to androgen independence

Initially, the survival and proliferation of prostate cancer cells is dependent on androgen (Gleave et al., 2005). Androgen ablation causes prostate cancer cell death through apoptosis, but despite high initial response rates, remissions are temporary because surviving tumor cells usually proliferate eventually (Gleave et al., 2005). Thus, one of the main obstacles to curing advanced prostate cancer by androgen ablation is androgen independent progression. Progression to androgen independence is a complex process involving variable combinations of clonal selection, adaptive up-regulation of anti-apoptotic survival genes androgen receptor transactivation in the absence of androgen from mutations, or increased levels of co-activators and alternative growth factor pathways (McKenzie and Kyprianou, 2006). That is, the agents used to kill neoplastic cells may also be mediating the chemoresistant phenotype (Gleave et al.,

2005). As a result, in order to have a significant impact on survival, new therapeutic strategies designed to inhibit the emergence of this phenotype may have to be developed.

1.2.7 Inhibitors of apoptosis in hormone- and chemo-resistance

Development of resistance to hormonal or chemotherapy is a common feature of numerous type of solid tumors (McKenzie and Kyprianou, 2006). Many studies on mechanisms of chemo-resistance have focused on regulation of drug transport and metabolism. For example, up-regulation of drug efflux proteins that pump the drug out of cells, such as the multiple drug resistance protein P-glycoprotein expressed by the MDR1 gene, may be one mechanism of drug resistance (Stuart et al., 2000). Chemoresistance may also result from alterations in the apoptotic machinery, due to increased activity of anti-apoptotic pathways or expression of anti-apoptotic genes (Gleave et al., 2005). Identification of such aberrant signaling pathways and gene expression may help not only to elucidate the mechanisms by which androgen independence and chemoresistance arise, but may also aid in identifying therapeutic targets for chemosensitization (McKenzie and Kyprianou, 2006). Of particular relevance to the development of androgen independent progression and hormone resistant prostate cancer are those survival proteins up-regulated after apoptotic triggers such as androgen ablation, that function to inhibit cell death (Gleave et al., 2005). Proteins known to fulfill these criteria include anti-apoptotic members of the B cell lymphomas protein family including Bcl-2 (Miyake et al., 2000f) and Bcl-xL (Miyake et al., 2000c), HER-2 (neu or c-erbb-2) (Craft et al., 1999), c-myc (Napoli et al., 2006), heat

shock proteins 72 and 27 (Gibbons et al., 2000) , survivin (Pennati et al., 2004) and clusterin (Miyake et al., 2000f).

1.2.8 Tissue environment and growth

The physiological environment of tumors is hypoxic, contains greater levels of lactate (Bhujwalla et al., 2001), has lower extracellular pH and similar or slightly higher intracellular pH (Evelhoch, 2001; Raghunand and Gillies, 2001) than healthy tissue. There are differences in the vasculature, metabolism and physiological properties of prostate cancer compared to other cancers (Bhujwalla et al., 2001).

Tumors stimulate the formation of blood vessels to provide the nutrients necessary for growth (Brannon-Peppas and Blanchette, 2004). If a tumor is successful in stimulating the formation of new blood vessels and accessing existing blood vessels, then the outside of the tumor will continue to replicate and grow. Tumor vasculature is generally defective ("leaky") and chaotically organized, resulting in an enhanced permeation and retention of drugs administered intravenously (Brannon-Peppas and Blanchette, 2004). The inside of the tumor remains poorly vascularized with little supply of nutrients and becomes necrotic. Transport of intravenously administered drugs into these interior regions of a tumor is poor or non-existent (Jain, 1999) and remains a challenge for treatment of solid tumors.

1.2.9 Animal models of prostate cancer

Prostate cancer is heterogeneous, varying widely in its biologic aggressiveness, androgen sensitivity and histologic appearance (Gleave et al., 2005). Thus, it is unrealistic to expect that a single animal model will fully describe the clinical condition (Chung et al., 2005). However, insights and understanding into the nature of human prostate cancer have come from the development and use of different types of tumor models including Shionogi (Miyake et al., 1999), PC (for example, PC-82) (Kyprianou et al., 1990), LAPC (for example, LAPC-4) (Craft et al., 1999), PAC120 (Legrier et al., 2003), DU-145 (Wang et al., 2003a), CRW22 (Bubendorf et al., 1999), PC-3 (Stephenson et al., 1992; Pettaway et al., 1996) and LNCaP (Thalmann et al., 1994; Thalmann et al., 2000). The molecular mechanisms of prostate cancer, including processes leading to progression to androgen independence, cannot be reproduced in monolayer tissue cultures and must be studied in a limited number of available tumor model systems (Chung et al., 2005). The PC-3 (Stephenson et al., 1992; Pettaway et al., 1996) and LNCaP (Thalmann et al., 1994; Thalmann et al., 2000) human prostate tumor systems are well-established models for lethal, androgen independent prostate tumors with metastatic potential that use changes in gene expression and tumor volume as endpoints for androgen independent progression (Miyake et al., 2000a). Furthermore, the LNCaP model expresses PSA and so uses PSA as an endpoint for androgen independence progression (Stephenson et al., 1992; Miyake et al., 2000b).

1.2.10 Treatments for prostate cancer

Radical prostatectomy or external beam radiation are generally considered the best treatments for localized prostate cancer (Carson, III, 2006), while external beam radiation and androgen ablation are commonly used for advanced prostate cancer (Konstantinos, 2005; Routh and Leibovich, 2005). Additional treatment options for prostate tumors include cryotherapy, high intensity focused ultrasound, brachytherapy, chemotherapy and watchful waiting (Konstantinos, 2005; Carson, III, 2006; Routh and Leibovich, 2005). There is presently no effective chemotherapeutic treatment for prostate cancer that might complement these methods or be used to treat non-responding patients or patients receiving no treatment (Miyake et al., 2000a). In particular, there is an urgent need for novel therapeutic strategies that could prevent prostate cancer cells from becoming resistant to hormone ablation or chemotherapeutic agents.

1.2.10.1 Watchful waiting

Watchful waiting is a treatment option for older men with early stage, slow-growing prostate cancer in which patients are monitored by DRE and measuring serum PSA levels. Watchful waiting is sometimes used in place of prostatectomy, radiation or other treatments to avoid or delay the side effects of those treatments. Watchful waiting is often used for patients with a life expectancy of greater than 10 years with stage T1a prostate cancer or for patients with a life expectancy of less than 10 years with a stage T1b – T2b prostate tumor (Konstantinos, 2005; Routh and Leibovich, 2005).

1.2.10.2 Prostatectomy

Radical prostatectomy involves the removal of the complete prostate gland and the seminal vesicles (Routh and Leibovich, 2005). Surgery is usually used for patients with a life expectancy of greater than 10 to 15 years and stage T1a to T2c prostate cancer (Goldenberg et al., 1998). Radical prostatectomy remains the only theoretical cure for prostate tumors and greater than 70% of patients undergoing surgery remain tumor-free for over 7 to 10 years (Routh and Leibovich, 2005). Radical prostatectomy results in a decrease in the likelihood of local tumor progression and metastases. Although the ten-year survival rates of surgical patients range from 44 to 88%, there is only a small absolute reduction in the chance of death 10 years post surgery. Complications from surgery include death and depending on patient age and surgical technique, erectile dysfunction (Goldenberg et al., 1998). However, erectile function often improves over time following surgery (Routh and Leibovich, 2005).

1.2.10.3 External beam radiation

Older patients with stage T1b - T2c prostate cancer and all patients with stage T3 or T4 prostate cancer are usually treated with external beam radiation therapy (Konstantinos, 2005). Recently developed techniques, including three-dimensional conformal radiotherapy and intensity modulated radiation therapy, deliver radiation directly to the tumor while sparing most of the surrounding tissue. External beam radiotherapy has similar efficacy to prostatectomy. Side effects of external beam radiation include chronic bowel complications, erectile dysfunction

and incontinence. An estimated 80,000 prostate cancer patients in North America undergo external beam radiation therapy yearly and greater than 50% of these patients experience post-radiation recurrences of the disease. Thus it is estimated that approximately 40,000 patients in North America experience post-radiation failure per year, yet there is no effective treatment for these patients (Konstantinos, 2005).

1.2.10.4 Brachytherapy

Brachytherapy involves treating prostate tumors with implants of radioactive seeds (Konstantinos, 2005; Carson, III, 2006). Brachytherapy may be used for patients with a life expectancy of greater than 10 years who are not candidates for prostatectomy. Advantages of brachytherapy over external beam radiation include the requirement for only one session and the delivery of higher radiation doses over a shorter period of time (Crook et al., 2001). Side effects of brachytherapy include rectal discomfort, urinary voiding symptoms and erectile dysfunction (Konstantinos, 2005; Carson, III, 2006).

1.2.10.5 Androgen ablation

Hormonal therapy involves bilateral orchiectomy (surgical castration) or medical castration with luteinizing hormone-releasing hormone (LHRH) analogs or LHRH antagonists (Gleave et al., 1999). Orchiectomy, LHRH analogs and LHRH antagonists interfere with normal endocrine flow. Hormonal therapy is the most effective, albeit usually palliative, treatment for patients with advanced, stage T4 - M1 prostate cancer (Konstantinos, 2005). Hormonal therapy

is also being investigated as a potential supplementary treatment alongside radical prostatectomy (Carson, III, 2006) or radiation therapy for localized prostate cancer. As an inexpensive therapy with low morbidity, surgical castration is the gold standard of hormonal therapy for patients with metastatic prostate cancer (Gleave et al., 1999). However, for psychological reasons, many patients may not accept surgical castration, resulting in an increased use of LHRH analogs and LHRH antogonists. LHRH analogs include buserelin, goserelin, leuprolide and triptorelin as 1, 3, 4 or 12 month controlled release implants. Side effects of LHRH analogs include hot flashes, erectile dysfunction, osteoporosis and lethargy (Carson, III, 2006). LHRH antagonists include flutamide, bicalutamide and nilutamide and may be used in combination with surgical castration or LHRH agonists to assist in completing the androgen blockade. Side effects of LHRH antagonists include gynecomastia, decreased night vision, nausea and alcohol intolerance (Gleave et al., 1999). Approximately 40,000 patients in North America undergo androgen ablation therapy each year. Approximately 80% of patients treated with androgen ablation have objective responses (Gleave et al., 1999). Unfortunately, nearly all of these cases progress to androgen independence over approximately two years (Konstantinos, 2005). Progression to androgen independence remains the principle obstacle to improving the morbidity and mortality in such patients (Gleave et al., 1999).

1.2.10.6 Chemotherapy

Patients with androgen independent prostate cancer and rising PSA serum levels may be treated with chemotherapy. Although the cancer response rate is poor and long-term survival rates are minimally affected by current chemotherapy regimens, there may be some palliative benefits (Gleave et al., 1999). Bone pain is usually treated with palliative therapy including radioisotope treatment and the administration of bisphosphonates. In addition, bisphosphonates inhibit osteoporosis and fractures following castration (Konstantinos, 2005). Earlier clinical trials with cyclophosphamide, estramustine, vincristine, mitoxantrone, paclitaxel and/or docetaxel administered immediately after (adjuvant therapy) or administered before (neoadjuvant therapy) radical prostatectomy or radiation therapy had feasibility and safety as their primary endpoints (Kelly et al., 2003; Kuruma et al., 2003; Behrens et al., 2003). The addition of chemotherapy resulted in an increase in side effects ranging from anemia, neutropenia, deep vein thrombosis, to fatigue and nausea and vomiting (Sinibaldi et al., 2002; Smith et al., 2003). Although some of the studies showed a small objective response rate, most of the studies used small numbers of patients and it is unclear whether the overall survival of patients was increased with adjuvant or neoadjuvant therapy (Gleave and Kelly, 2005). However, the results of these studies suggested that chemotherapy is reasonably safe and does not significantly complicate radiotherapy or surgery (Sinibaldi et al., 2002). Docetaxel has recently been shown to increase survival in patients with androgen independent prostate cancer (Logothetis, 2002; Gleave and Kelly, 2005). As a result, there are currently several Phase III studies underway that are

investigating the use of various agents including docetaxel as neoadjuvant or adjuvant therapy and are using overall survival or progression-free survival as the primary endpoint (Gleave and Kelly, 2005).

1.3 CLUSTERIN

1.3.1 Clusterin gene, messenger ribonucleic acid and protein

Clusterin protein is also called testosterone-repressed prostate message-2, sulphated glycoprotein-2 and apolipoprotein J (Miyake et al., 2000d; Frasoldati et al., 1995; Hardardottir et al., 1994). Clusterin protein is found in most mammalian physiological fluids, including plasma, cerebrospinal fluid, urine and semen (Jones, 2002). Clusterin protein may play a role in several different normal physiological processes including development, sperm maturation, complement regulation, lipid transport, protection of cells at tissue-fluid boundaries, phagocyte recruitment, clearance of debris, control of cell matrix and cell-cell interactions, and cell cycle regulation (Jones, 2002; Trougakos, 2006). Clusterin protein is associated with various pathological processes in the initiation and growth of cancers, including the inhibition of apoptotic cell death. Clusterin protein inhibits stress-induced protein precipitation and the transcription of clusterin protein is regulated by heat shock factor-1 (Caccamo et al., 2006). Thus it appears that clusterin protein may work like a small heat shock protein during cell stress to stabilize protein conformations and inhibit protein precipitation, that is, clusterin acts as a chaperone protein (Gleave and Chi, 2005). Clusterin is a cytoprotective protein whose expression is enhanced by

pro-apoptotic stimuli and provides resistance to prostatic cancers that are being treated with chemotherapy, radical prostatectomy or radiotherapy (Miyake et al., 2000d; Miyake et al., 2000b).

1.3.2 Rationale of clusterin protein as an anti-prostate cancer target

The overexpression of clusterin protein in clinical prostate cancer specimens is associated with poor clinical outcomes (July et al., 2002). Biopsy specimens taken before radical prostatectomy from patients who had received neoadjuvant hormonal therapy, had greater clusterin protein levels than specimens taken from patients who had not received neoadjuvant hormonal therapy (Chi et al., 2005). These data suggest that pro-apoptotic stimulation resulted in an increase in clusterin protein expression in a cell survival manner in human tumors (July et al., 2002; Miyake et al., 2005). Increases in clusterin protein expression have also been observed in the rat prostate and various human prostate cancer xenograft models following pro-apoptotic stimulation (Sensibar et al., 1991; Miyake et al., 2000b; Miyake et al., 2000a). Clusterin protein inhibits apoptosis and as a result, its overexpression assists in the formation of a prostate cancer phenotype that is resistant to chemotherapy, radiation and androgen ablation (Miyake et al., 2000d; July et al., 2002, Miyake et al., 2003; Zellweger et al., 2003). As discussed later in this thesis in sections 1.5.2 and 1.5.3, inhibiting the expression of clusterin protein increased the sensitivity of a number of different cancer models to chemotherapy, radiotherapy and hormonal therapy. Together, these studies suggest that clusterin protein is an important anti-cancer target.

1.4 ANTISENSE OLIGONUCLEOTIDES (ASOs)

ASOs are single strands of DNA or ribonucleic acid (RNA), between approximately 15 to 25 nucleotides long (Stahel and Zangemeister-Wittke, 2003). ASOs and other therapeutic oligonucleotides, including small interfering ribonucleic acids (siRNAs) and ribozymes, are expected to provide treatments against a number of different diseases (Tomari and Zamore, 2005; Yu et al., 2005; So et al., 2005).

1.4.1 Mechanism of action and pharmacology

ASOs prevent the expression of specific genes by hybridizing to mRNA in a sequence-specific manner via Watson-Crick base pairing. ASOs are complementary to the mRNA, that is, the "sense" strand of a specifically targeted gene. The ASO hybridizes with mRNA forming a mRNA/DNA or mRNA/RNA duplex, eventually resulting in the inhibition of the expression of the target gene (Gibson, 1996). Several mechanisms have been proposed to explain the decreased protein expression following hybridization and are given in Figure 1.2. The most commonly accepted mechanism involves the oligonucleotide/mRNA hybrid serving as a substrate for RNase H or other RNases which cleave mRNA (Walder and Walder, 1988). Other putative mechanisms include the inhibition of transcription by the formation of a triple helix with the ASO binding to the double-stranded DNA, prevention of splicing, inhibition of ribosomal read-through, prevention of ASO transport and alternative splicing or translational arrest (Crooke, 1997; Crooke, 1999). By inhibiting the production of specific proteins involved

in the progression of a disease, it is possible to use ASOs for therapeutic purposes. In addition, some ASOs with cytosine-phosphate-guanine (CpG) sequences also have immunostimulatory effects (Rothenfusser et al., 2004).

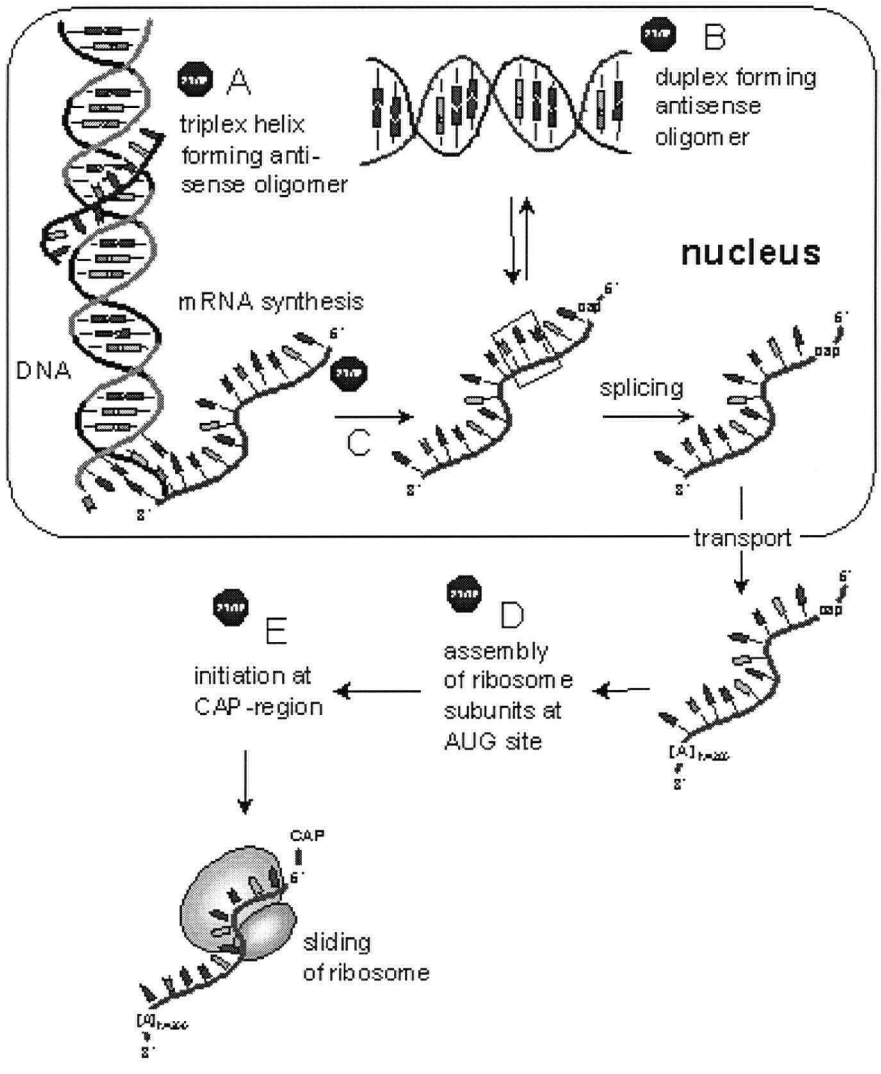

Figure 1.2 Putative mechanisms of action for antisense oligonucleotides include **A)** the inhibition of transcription by the formation of a triple helix with the ASO binding to the double-stranded DNA or **B)** inhibition of translation by the most commonly accepted mechanism, which involves the ASO/mRNA hybrid serving as a substrate for RNase H or other RNases which cleave mRNA. Other putative mechanisms include **C) to E)** prevention of splicing, prevention of ASO transport, inhibition of ribosomal read-through and alternative splicing or translational arrest. Adapted from Noe and Kaufhold (2000).

1.4.2 Chemistry

Phosphodiester ASOs are susceptible to cleavage by both plasma and cellular nucleases and have been shown *in vivo* to have half-lives ranging from a few to thirty minutes following intravenous administration, or *in vitro* to have half-lives ranging from a few minutes to three hours. Examples of chemical modifications made to ASOs to improve their physical, biochemical and pharmacokinetic properties are given in Figure 1.3. Phosphorothioated ASOs, termed "first generation" ASOs, have a non-bridging phosphate oxygen substituted with sulphur (Stahel and Zangemeister-Wittke, 2003). Phosphorothioated ASOs are resistant to nuclease degradation compared to phosphodiester ASOs and have increased *in vivo* serum half-lives of several hours (Agrawal et al., 1991; Gilar et al., 1997). A number of clinical trials have been completed using phosphorothioated ASOs with administration via either frequent or continuous intravenous infusions. "Second generation" ASOs possess a phosphorothioated backbone and also include an additional modification to the backbone, sugar or the heterocycle (Henry et al., 2001). Modifications to the 2' position of the ribose appear to be the most successful in improving the pharmacokinetic properties of second generation ASOs, such as 2'-O-(2-methoxyethyl) (2'-MOE) (Tereshko et al., 1998; Geary et al., 2001). In addition to having greater resistance to degradation and significantly longer half-lives than the first generation ASOs, some second generation ASOs also have improved affinity for mRNA and thus increased potency (Tereshko et al., 1998). Further improvements may be made with "third generation"

ASOs, including for example, peptide nucleic acids, in which the negatively charged backbone is replaced with a neutral amide linkage (Gait, 2003).

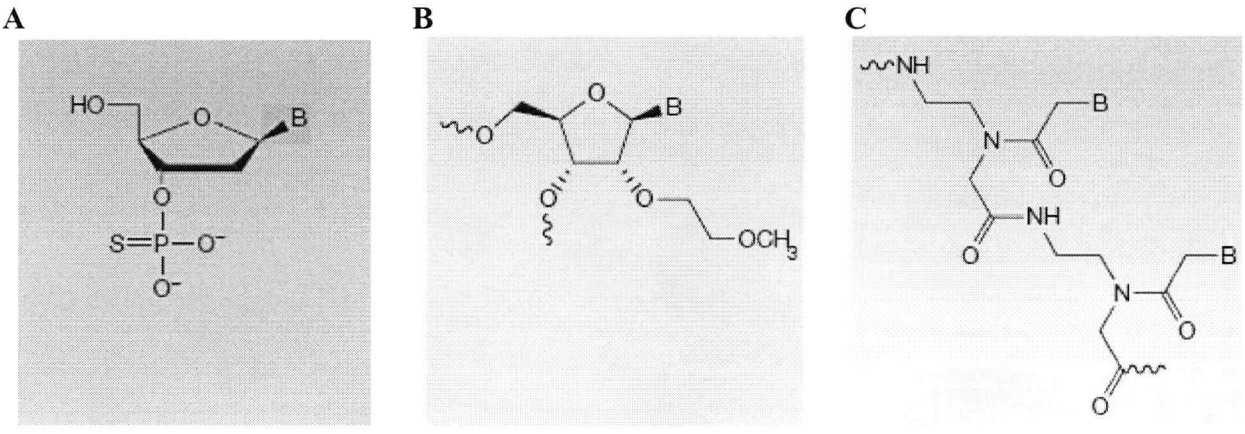

Figure 1.3 Chemical modifications made to ASOs to improve their physical, biochemical and pharmacokinetic properties. The structural group "B" represents the base. **A)** "First generation" ASOs have a non-bridging phosphate oxygen substituted with sulphur. **B)** "Second generation" ASOs include an additional modification to the backbone, sugar or the heterocycle. The example shown is a 2'-O-(2-methoxyethyl) (2'-MOE) substitution on the ribose. **C)** "Third generation" ASOs include neutral backbones including peptide nucleic acids as given in the example. Adapted from Gleave and Monia (2005).

1.4.3 Use in prostate cancer

ASOs have been targeted against a number of different genes known to be implicated in various cancers. ASOs have been evaluated as therapeutic agents either alone, or as sensitizers in combination with chemotherapy, radiotherapy or hormonal therapy against several prostate cancer gene targets, including X-linked inhibitor of apoptosis protein (Amantana et al.,

2004), survivin (Fornaro et al., 2003), 2-5A-telomerase (Kondo et al., 2000), mouse double minute 2 (MDM2) (Wang et al., 2003a), RAF-1 (Tolcher et al., 2002), protein kinase C alpha (Tolcher et al., 2002), androgen receptor (AR) (Eder et al., 2002), insulin-like growth factor binding proteins 2 (IGFBP-2) (Kiyama et al., 2003) and 5 (IGFBP-5) (Miyake et al., 2000e), Bcl-2 (Miyake et al., 1999), Bcl-xL (Miyake et al., 2000c) and clusterin (Miyake et al., 2000b).

1.4.4 Issues associated with ASOs as therapeutic agents

One of the attractions of ASOs as therapeutic agents is that in theory, they should be less toxic than traditional non-specific chemotherapeutic agents that inhibit the proliferation of all rapidly dividing cells. The toxicity of phosphorothioated ASOs usually results from the compounds being polyanionic and also from the phosphorothioate backbone (Gleave and Monia, 2005). Only infrequently have toxicities been due to the sequence of a specific ASO. The more common toxicities associated with phosphorothioated ASOs include thrombocytopenia, leukopenia, anemia, elevation in hepatic transaminases, decreased serum complement activity and increased clotting times, fever, hypotension, asthenia and rigors (Shaw et al., 1997; Nemunaitis et al., 1999; Waters et al., 2000; O'Brien et al., 2005).

The clinical application of therapeutic oligonucleotides such as ASOs (Veeramachaneni et al., 2004), ribozymes (Pennati et al., 2004), siRNAs (Caplen and Mousses, 2003), CpG immune modulators (Rothenfusser et al., 2004), aptamers (Grate and Wilson, 2001) and other oligonucleotides (Cho-Chung et al., 2003) has been hampered by a number of drug

delivery issues. These include poor targeting of oligonucleotides to the site of action, rapid elimination from the body, degradation by nucleases and inefficient cellular uptake (Brignole et al., 2003; Vinogradov et al., 2004; Wang et al., 2003b).

Increasing the length of an oligonucleotide increases its number of internal sequences and thus increases the potential number of different RNA targets for the oligonucleotide. That is, increasing the length of an oligonucleotide may result in a decrease in specificity. Thus, an oligonucleotide that acts through an antisense mechanism may potentially cause the cleavage of a number of different mRNA species (Shuttleworth et al., 1988).

The CpG motif (5'-3') has been demonstrated to stimulate the immune system, (Klinman et al., 2003; Yamamoto et al., 1992). Certain CpG motif-containing sequences stimulated the production of interferon in murine spleen cells, which in turn resulted in the stimulation of natural killer cell activity. The length of the oligonucleotide played a role in this process, as shown by a reduction in stimulatory activity caused by reducing the length of the oligonucleotides from 45- to 15-mers. Unmethylated CpG motifs (both 6-mers and longer) have been shown to activate B-cells independent of T-cell activation (Krieg et al., 1995).

Sequence specific protein binding has been demonstrated for some phosphorothioated oligonucleotides. For example, phosphorothioated oligonucleotides have been shown to bind to and inhibit the function of tyrosine kinase $p210^{bcr\text{-}abl}$, or thrombin in clotting (Bergan et al., 1994). Secondary oligonucleotide structure was shown, in addition to the sequence, to have an effect on the ability of the oligonucleotides to bind to the proteins involved.

1.4.5 Pharmacokinetics

Due to the relatively rapid elimination of first generation ASOs, these drugs have generally been given by continuous subcutaneous or intravenous infusion over several weeks, or administered daily. Continuous subcutaneous infusion of ASO at 3 mg/kg/d resulted in a plasma steady-state concentration of approximately 1 $\mu g \cdot mL^{-1}$ and mean plasma elimination half-life of 7 hours. Continuous intravenous infusion of ASO at 7 mg/kg/d resulted in steady state plasma concentrations of approximately 4 to 6 $\mu g \cdot mL^{-1}$ (Raynaud et al., 1997; Tolcher et al., 2005). Oblimersen, a phosphorothioate ASO, showed variable plasma concentrations and a mean plasma half life of 7.5 h following continuous infusion in patients. The uptake of ASOs in tumors is dependent on the ASO chemistry. Nakajima et al. (2000) showed that following arterial infusion, first and second generation phosphorothioated ASOs were accumulated in tumors to a greater extent than phosphodiester ASO.

1.4.6 Experimental controls

ASOs target mRNA and inhibit the production of protein, rather than targeting the protein directly. Since proteins may be produced continuously and may degrade at different rates, reduction of the protein levels by ASOs and the resulting biological effects are dependent upon the half-life of the protein. Most proteins have a half-life ranging from a few minutes to a day and thus, their mRNAs are appropriate targets for ASOs. However, proteins with half-lives on the order of days would require an extended period before the results of treatment with an

ASO could be observed (Stein and Krieg, 1994). ASOs are potentially unable to inhibit the function of proteins that are regulated post-translationally. In addition, if a cell adjusts the half-life of a protein relative to mRNA production, then the inhibition or degradation of mRNA may not significantly decrease the levels of protein within the cell (Stein, 1999b). ASOs have been shown to also have nonspecific effects on proteins (not based on an antisense mechanism). Therefore, in studies involving the down-regulation of proteins by ASOs, appropriate controls should be used to determine whether the biochemical or biological effects are due to an antisense mechanism or to non-specific effects (Bock et al., 1992; Stein, 1998; Stein, 2000; Crooke, 2000). In this thesis, the control oligonucleotide was the same length and had the same sequence of bases as the ASO of interest, except that 2 nucleotide bases were replaced with incorrect nucleotides, creating a 2-base "mismatch" control oligonucleotide.

1.4.7 Assays

ASOs are commonly assayed *in vitro* by ultraviolet-visible light spectroscopy (UV-Vis), HPLC or CGE. HPLC and CGE methods often use UV-Vis or laser-induced fluorescence detectors, or are used in conjunction with mass spectrometry. When mass spectorometry is employed it is generally performed using electrospray ionization or matrix-assisted laser desorption ionization, which in turn is often used in combination with time of flight mass analysis (von Brocke et al., 2003; Williams et al., 2003; Hail et al., 2004; Willems et al., 2005).

Analysis has also been completed on ASOs using an enzyme-linked immunosorbent assay (Chi et al., 2005).

1.4.8.1 Ultraviolet-visible light spectroscopy

UV-Vis is a relatively easy and sensitive technique for the analysis of oligonucleotides and provides quantitative data, providing the samples are purified (Schweitzer and Engels, 1997). UV-Vis does not differentiate between a parent oligonucleotide and differing chain lengths. However, the shape of the absorbance curve does give some qualitative information about the purity of the sample (Schweitzer and Engels, 1997). Since UV-Vis is relatively sensitive, it is frequently used as the method of detection for chromatographic procedures.

1.4.8.2 High pressure liquid chromatography (HPLC)

Either reverse phase or anion exchange HPLC of oligonucleotides can provide reasonably good separation for strands of 15-20 bases or shorter and when the backbone is unmodified (Zhang et al., 2005). However, HPLC methods often fail to separate oligonucleotides that differ by only a single nucleotide when phosphodiester oligonucleotides are longer than 15-20 bases and/or have modified backbones, including second generation ASOs (Horvath and Aradi, 2005). The separation of oligonucleotides longer than approximately 20 bases and differing in length by two or more nucleotides has been performed using HPLC (Zhang et al., 2005).

Reverse phase HPLC is used for the analysis or purification of crude oligonucleotide synthesis mixtures because the separation is based on the hydrophobic interactions between the stationary phase of the column and terminal synthesis protection groups such as dimethoxytrityl (Zhang et al., 2005). The dimethoxytrityl group is separated from the oligonucleotide following HPLC purification. Reverse phase HPLC is also often used for the analysis of oligonucleotides with modified backbones resulting in hydrophobic/neutral molecules that do not separate well in anion exchange columns or by electrophoresis. Typical reverse phase HPLC columns are of the C_{18} type (Zhang et al., 2005).

In general, anion exchange HPLC columns contain silica particles or organic polymers with attached cationic groups (Horvath and Aradi, 2005). The separation of different length oligonucleotides is due to the ionic interactions of the anionic molecules with the cationic stationary phase. Shorter oligonucleotides elute more quickly than longer oligonucleotides and the retention times are not greatly influenced by nucleotide composition. Mobile phases typically consist of two salt phases in phosphate buffer run on a gradient of increasing salt concentration to elute the oligonucleotides (Horvath and Aradi, 2005). Organic solvents such as acetonitrile are often included in concentrations of approximately 5-20% v/v in the mobile phase to reduce hydrophobic interactions between the oligonucleotides and the column, resulting in better separation between oligonucleotides of different lengths (Horvath and Aradi, 2005; Metelev and Agrawal, 1992).

1.4.8.3 Slab polyacrylamide gel electrophoresis

The influence of an electric field causes charged oligonucleotides to migrate based on their mass to charge ratio (Aynie et al., 1996). Because the mass to charge ratio of oligonucleotides is approximately the same for oligonucleotides of different lengths, a gel is used in combination with an electric field. This results in the separation of the oligonucleotides based on their molecular weight due to the interaction of the oligonucleotides with the gel (de Semir et al., 2002). Oligonucleotides are generally separated with a polyacrylamide gel that has entanglements and/or is cross-linked. Oligonucleotides with modified neutral backbones will not migrate under electrophoresis. Polyacrylamide gel electrophoresis (PAGE) with radiolabeling gives good separation of oligonucleotides differing by only a single nucleotide (Aynie et al., 1996). However, this technique is, at best, semi-quantitative. In addition, although the instrumentation is relatively simple and inexpensive, slab gel electrophoresis is laborious, not particularly sensitive and does not provide complete structural information about the metabolites. For example, if two oligonucleotides differ by only one oligonucleotide, PAGE will not easily determine if the shorter oligonucleotide is missing a nucleotide from the 3' or the 5' end. Radiolabeling is used to increase the sensitivity of slab gel electrophoresis (Aynie et al., 1996). The polyacrylamide gel can be obtained by cross-linking acrylamide monomers with a cross-linking agent such as *N,N'*-methylene bisacrylamide (in a w/w ratio of 1:20 cross-linking agent:acrylamide). The pore size of the resulting gel is controlled by the concentration of the cross-linking agent. The gel is usually formed between two glass plates, resulting in a gel which

has the shape of a slab. A denaturing agent, usually urea at 6 to 7 $mol \cdot L^{-1}$, is used to minimize sequence dependent effects to assist in separating oligonucleotides based on their length. Buffers generally consist of tris[hydroxyl-methyl]aminomethane (Trizma® base), boric acid and ethylenediaminetetraacetic acid (EDTA) at approximately pH 8.3. Visualization of the oligonucleotides in slab gels may be performed by fluorescence, UV-Vis shadowing, silver staining or autoradiography (Aynie et al., 1996; DeDionisio and Lloyd, 1996; de Semir et al., 2002).

1.4.8.4 Capillary gel electrophoresis

CGE has been used with good results for quantitation and separation of oligonucleotides differing by only one nucleotide (Williams et al., 2003). The oligonucleotide samples are injected into the capillary by immersing the capillary into the sample and applying an electric field (termed electrokinetic injection). Both capillary ends are then immersed in a buffer and as voltage is applied, oligonucleotides migrate through the gel in the capillary based on the same principles as for slab gel electrophoresis. The drawback to the use of cross-linked polyacrylamide gels is that they have a relatively short lifetime, resulting in the capillary requiring a new gel approximately every two hours (Williams et al., 2003). The gels are also sensitive to handling and thus need to be prepared on a regular basis. UV-Vis detection provides direct determination of oligonucleotides (Froim et al., 1997). Laser-induced fluorescence detection of fluorescent indicators can provide greater selectivity and sensitivity than UV

detectors, however, the signal from fluorescent indicators is quenched by the denaturants that separate oligonucleotides of different lengths, thus allowing the fluorescent indicators to provide either selectivity or sensitivity at one time (Belenky et al., 1995). Peak broadening results from CGE analysis of phosphorothioates and has been overcome by increasing the theoretical plates of the capillary. Non-linear correlations between sample concentration and peak area due to electrokinetic injections being affected by the buffer composition have been overcome by the use of an internal standard (an oligonucleotide of similar length with appropriate separation from the parent oligonucleotide) (von Brocke et al., 2003; Williams et al., 2003; Benesova-Minarikova et al., 2005).

Analysis of biological samples by CGE is dependent on extraction methods that purify the oligonucleotide and metabolites from biological impurities, including residual salts or buffer ions that interfere with the electrokinetic injection, migration and UV-Vis detection of the oligonucleotide (Chen et al., 1997). Extraction of oligonucleotides from biological matrices in preparation for CGE analysis has been accomplished by the use of two separate steps (Leeds et al., 1996). The first step involves an anion-exchange (solid-phase) cartridge and high salt concentrations to remove the oligonucleotide and metabolites from proteins and lipids. The second step thus involves a reverse-phase (solid-phase) cartridge to desalt the oligonucleotide and metabolites. Some methods have included an additional membrane desalting step to increase the UV signal (Leeds et al., 1996). The drawback of the solid-phase extractions is that they are time consuming and laborious (Leeds et al., 1996; Yu et al., 2001).

1.4.8.5 Western blots for proteins

As ASOs are used to decrease the expression of a specific protein, assaying for the target protein following treatment with an ASO, provides information on the ASO's effectiveness. The length of time between treatment and measurement of target protein expression levels is important for two reasons. First, there is a lag between the incubation of cultured cells *in vitro* with ASOs or their administration *in vivo* and the cellular uptake of the ASOs, resulting in a delay of their inhibition of the translation of the protein of interest from the targeted mRNA. Second, ASOs inhibit the production of new protein and unless they have non-antisense effects, they do not affect the amount of previously expressed protein. Accordingly, in order to detect a decrease in the levels of the protein of interest, the required period of administration of ASOs *in vivo* or their incubation with cultured cells *in vitro* will be dependent on the protein's half-life. Generally, an incubation or administration period equal to approximately one to two half-lives is used to observe changes in expression of the target protein.

To determine the expression of a specific protein by Western blot, the cells are lysed and centrifuged, leaving the protein in solution in the supernatant. The total amount of protein is determined and equal amounts of protein are then subjected to gel electrophoresis to separate the individual proteins by molecular weight. The proteins are transferred onto a nitrocellulose membrane, where they bind to the nitrocellulose. The nitrocellulose membrane is incubated with a primary monoclonal antibody against the specific protein of interest. The nitrocellulose

membrane is incubated with a probe- (e.g. horseradish peroxidase-) conjugated secondary antibody against the primary monoclonal antibody. The specific protein is subsequently detected by determining the amount of probe (for example, using chemiluminescence to determine the amount of horseradish peroxidase) (Leung et al., 2000; Miyake et al., 2000b). The advantages of Western blots include the determination of the approximate molecular weight of the detected protein, specificity for the protein of interest and the semi-quantitative nature of the method. Immunoprecipitation or an enzyme-linked immunosorbent assay is sometimes used to verify Western blot analysis. The disadvantages of Western blotting include the requirement of an appropriate antibody directed against the protein of interest, the need for a relatively large number of cells and the time consuming nature of the method.

1.5 COMBINATION OF CLUSTERIN ASO AND TAXANES IN PROSTATE CANCER

1.5.1 Paclitaxel and docetaxel

Paclitaxel and docetaxel (shown in Figure 1.4) are both members of the class of compounds called taxanes. Paclitaxel was originally extracted from the bark of *Taxus brevifolia* (Western yew or Pacific yew) while docetaxel is a semi-synthetic derivative of 10-deacetyl baccatin III, which is extracted from *Taxus baccata* (European yew) (Wani et al., 1971; Baloglu et al., 2004). Taxanes have a characteristic 20 carbon tricyclic taxane ring skeleton, but have different substituents at the C-10 and on the C-13 side chain. The structure of the C-13 side

chain is important for anti-cancer activity. Paclitaxel and docetaxel are hydrophobic molecules with low aqueous solubilities. The solubility of paclitaxel is approximately 1 $\mu g \cdot mL^{-1}$ (Liggins et al., 1997). The commercial formulation of paclitaxel for intravenous injection (Taxol®) is formulated in polyoxyethylated castor oil (Cremophor EL®) and ethanol, while the commercial formulation of docetaxel for intravenous injection (Taxotere®) is formulated in polysorbate 80 (ten Tije et al., 2003).

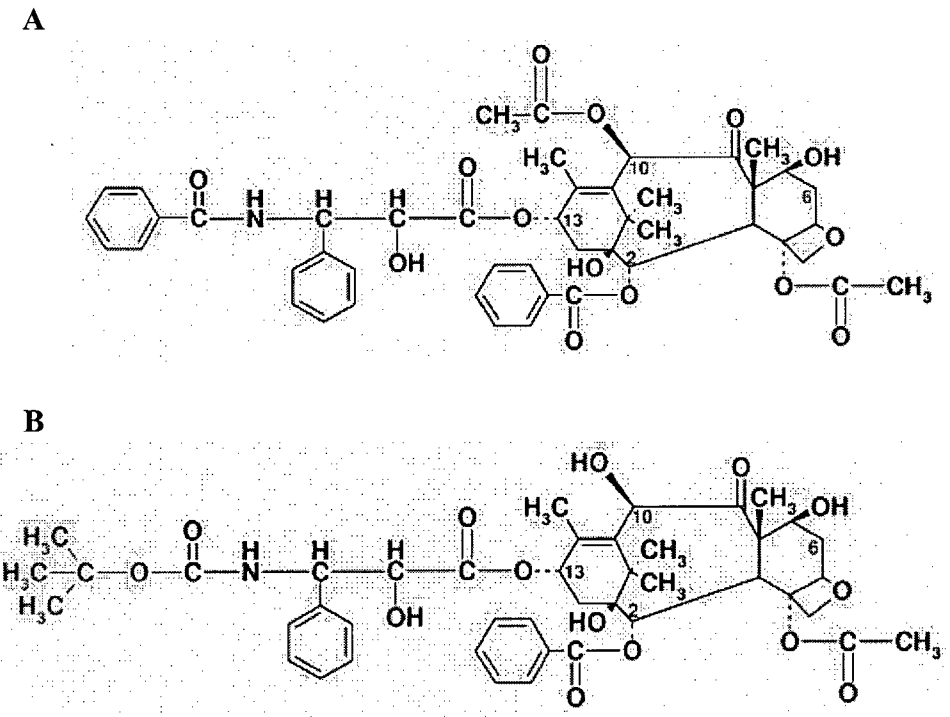

Figure 1.4 The chemical structure of **A)** paclitaxel and **B)** docetaxel. The numbers 2, 6, 10 and 13 are the numbers assigned to carbons in the structure by the International Union of Pure and Applied Chemistry. Adapted from BioMed Central website at www.biomedcentral.com.

1.5.1.1 Pharmacology and toxicity

Paclitaxel and docetaxel bind to β-tubulin, promoting the polymerization of tubulin dimers into microtubules, while inhibiting the disassembly of the microtubules (Berchem et al., 1999). Docetaxel has approximately twice the affinity of paclitaxel for β-tubulin (Pienta, 2001). Microtubules are components of the mitotic spindle, which is involved in a number of cellular functions including cell motility and cell division. The result of paclitaxel and docetaxel inhibiting the depolymerization of microtubules is to arrest the cell cycle at the late G2/M phase (Berchem et al., 1999). Paclitaxel and docetaxel also induce the phosphorylation of the anti-apoptotic proteins Bcl-2 and Bcl-xL, resulting in their inactivation, apoptosis and cell death (Leung et al., 2000). Docetaxel is a more potent inducer of Bcl-2 phosphorylation (Stein, 1999a).

Several phase II trials showed that paclitaxel administered in combination with epirubicin or estramustine phosphate and/or etoposide plus carboplatin against androgen independent prostate cancer in men was tolerated, with primarily hematologic toxicity being observed (Meluch et al., 2003; Smith et al., 2003; Vaughn et al., 2004; Neri et al., 2005). Toxicities increased with dose and included neutropenia, thrombocytopenia, thromboembolism, anemia, myelosuppression, peripheral neuropathy, fatigue and reversible alopecia. Treatment-related deaths were observed in a small number of patients (generally due to sepsis) and one patient had deep vein thrombosis (Meluch et al., 2003; Smith et al., 2003; Vaughn et al., 2004; Neri et al., 2005). Treatment of hormone refractory prostate cancer patients with docetaxel plus

estramustine or prednisone and compared to mitoxantrone plus prednisone in phase III studies, showed that most toxicities associated with docetaxel were of low grade (for example, loss of sensation in the fingers and toes) rather than life-threatening (Petrylak, 2005). Toxicities that were observed in some patients included febrile neutropenia, cardiovascular events (for example, cardiac ischemia or deep vein thrombosis), neurosensory changes, nausea, vomiting and lacrimation (Petrylak et al., 2004; Tannock et al., 2004).

1.5.1.2 Activity in prostate cancer

Paclitaxel and docetaxel have been shown to be clinically effective against numerous cancer types and are approved as chemotherapy agents against breast and ovarian cancers (Vasey et al., 2004). Leung et al. (2000) showed that micellar paclitaxel inhibited LNCaP cell growth (IC_{50} = 6 nmol·L^{-1}). The LNCaP human prostate cancer cell line is androgen dependent but it regresses after castration and then later recurs as an androgen-independent cell line (Thalmann et al., 1994). DNA laddering confirmed that paclitaxel induced apoptosis at concentrations of ≥ 1 nmol·L^{-1} in these cells (Leung et al., 2000). *In vivo*, intravenous administration of micellar paclitaxel in castrated athymic male mice bearing LNCaP tumors, resulted in regression of the tumors. After three cycles of treatment with paclitaxel, the serum PSA level had decreased 96% and the tumor volume had decreased 91% (Leung et al., 2000). Gleave and coworkers have shown that paclitaxel decreased the tumor volume *in vivo* in both PC-3 (Miyake et al., 2000a) and Shionogi tumor models (Miyake et al., 2000f). These reports confirmed the activity of

paclitaxel against prostate cancer cell lines commonly used as models for both androgen dependent and independent human prostate cancer.

Several phase II trials showed that paclitaxel administered in combination with epirubicin or estramustine phosphate and/or etoposide plus carboplatin against androgen independent prostate cancer in men resulted in median survival of 10 to 16 months, median time to disease progression of 6 to 8 months, partial objective responses in 15 to 58% of patients and a greater than 50% reduction in serum PSA levels in 35 to 58% of patients (Vaughn et al., 2004; Neri et al., 2005; Smith et al., 2003; Meluch et al., 2003). Treatment of hormone refractory prostate cancer patients with docetaxel plus estramustine or prednisone and compared to mitoxantrone plus prednisone in phase III studies, showed that patients treated with the docetaxel regimens had a two month longer median survival period, delayed time to progression, greater decreases in serum PSA levels and improved pain responses (Petrylak et al., 2004; Tannock et al., 2004). Based on these data, it has been suggested that docetaxel or paclitaxel may be useful as neoadjuvant or adjuvant therapies in patients with tumors that are locally advanced with poor prognoses. Although encouraging, these clinical results with paclitaxel or docetaxel against androgen independent prostate cancer were modest and highlight the requirement for therapeutics that target the molecular basis of chemoresistance and androgen independence (Gleave and Chi, 2005).

1.5.1.3 Pharmacokinetics and absorption, distribution, metabolism and excretion

Several phase II trials treating androgen independent prostate cancer patients with paclitaxel plus epirubicin or estramustine phosphate and/or etoposide plus carboplatin used regimens including paclitaxel administered by infusion over 1 hour and repeated weekly (Meluch et al., 2003; Vaughn et al., 2004; Neri et al., 2005; Smith et al., 2003). Premedications included dexamethasone, diphenhydramine and an H_2 receptor antagonist (Vaughn et al., 2004; Neri et al., 2005; Smith et al., 2003; Meluch et al., 2003). Some protocols also administered ondansetron (Neri et al., 2005) or granisetron (Smith et al., 2003) for nausea and vomiting. Some protocols administered warfarin to prevent thromboembolism (Vaughn et al., 2004). Two phase III studies treating hormone refractory prostate cancer patients with docetaxel plus estramustine or prednisone, used regimens including docetaxel administered by 1 hour infusion dosed every 3 to 6 weeks (Petrylak et al., 2004; Tannock et al., 2004).

Following intravenous administration of paclitaxel or docetaxel, these agents are extensively and rapidly bound to plasma proteins with both agents primarily bound to albumin and docetaxel also bound to α_1-acid glycoprotein (Rowinsky and Donehower, 1995; Urien et al., 1996). The pharmacokinetics of paclitaxel and docetaxel are very complex. Maximum plasma concentration and area under the plasma concentration versus time curve of these agents vary markedly between patients, doses and length of infusion periods (Wiernik et al., 1987a; Wiernik et al., 1987b; Huizing et al., 1993; Huizing et al., 1995; Bruno et al., 2001; Baker et al., 2006). Paclitaxel has a mean distribution-phase half-life of 20 minutes and a mean terminal elimination

half-life of 4.9 hours (Kuhn, 1994; Straubinger, 1996). Hence, despite extensive plasma protein binding, initial plasma clearance is rapid. Paclitaxel has a mean steady state volume of distribution of 110 $L \cdot m^{-2}$ (Kuhn, 1994). Paclitaxel and docetaxel distribute into most tissues, including tumors. However, paclitaxel and docetaxel do not readily cross the blood brain barrier and are not found in the central nervous system or the testes (Spencer and Faulds, 1994). Mean clearance of paclitaxel from plasma is approximately 20 $L \cdot h^{-1} \cdot m^{-2}$ (Kuhn, 1994; Rowinsky and Donehower, 1995). Paclitaxel and docetaxel are primarily eliminated by hepatic metabolism and biliary clearance (Seidman et al., 1996; Shou et al., 1998), with excretion in the feces (Marchettini et al., 2002) and little excretion in the urine (Wiernik et al., 1987a; Clarke and Rivory, 1999). Paclitaxel and docetaxel are primarily metabolized by cytochrome P450 isoform CYP3A and paclitaxel is also metabolized by CYP2C (Cresteil et al., 1994; Shou et al., 1998).

Paclitaxel or docetaxel have been administered intraperitoneally in order to expose intraperitoneal tumors (for example, ovarian carcinoma) to greater concentrations of the agents and for longer periods of time than could be provided by intravenous infusion (Baker et al., 2006).

1.5.2 Clusterin ASO

A clusterin ASO 21-mer sequence of 5'-CAG-CAG-GAG-AGT-CTT-CAT-CAT-3', corresponding to the human clusterin translation initiation site, was identified as the most potent of 10 different potential ASO sequences targeting different regions of the clusterin gene (Miyake

et al., 2000a). Clusterin ASO has been shown to down-regulate the expression of clusterin protein and increase the sensitivity of a tumor to radiotherapy, chemotherapy and hormonal therapy in a number of cancer models, including prostate, bladder, kidney, lung and breast cancer models (Miyake et al., 2000a; Miyake et al., 2002b; Miyake et al., 2002a; Cao et al., 2005; Biroccio et al., 2005; Gleave and Miyake, 2005; Duggan et al., 2002; Miyake et al., 2002a). Clusterin ASO inhibited the expression of clusterin protein in human prostate tumor cells *in vitro* and in xenograft models in a sequence-specific and dose-dependent manner (Miyake et al., 2000b; Miyake et al., 2000a; Miyake et al., 2000d; Sensibar et al., 1995).

A phase I study showed that the use of clusterin ASO as neoadjuvant therapy to radical prostatectomy resulted in a dose-dependent decrease in clusterin mRNA and protein expression and an increase in cell apoptosis (Chi et al., 2005). Patients received 40 to 640 mg administered via two hour intravenous infusions on days 1, 3, 5, 8, 15, 22 and 29, followed by radical prostatectomy within 7 days of the last dose. Additional neoadjuvant therapy included buserelin acetate and flutamide. Administration of clusterin ASO at the highest dose resulted in a significant reduction in clusterin mRNA and protein levels and an increase in cell apoptosis (Chi et al., 2005). There was no dose-limiting toxicity observed in these patients. Hematologic side effects were thrombocytopenia, leukopenia and anemia. Non-hematologic side effects included fever, fatigue and rigors. Transient increases in hepatic alanine transaminase and aspartate transaminase were observed in some patients (Chi et al., 2005).

Pharmacokinetics were investigated during the same Phase I study described above (Chi et al., 2005). As the dose was increased between 40 and 640 mg, mean peak plasma levels increased between 4 and 75 $\mu g \cdot mL^{-1}$, respectively, and the mean area under the curve increased between 8 and 347 $\mu g \cdot h \cdot mL^{-1}$. The mean half-life also increased with increase in dose between 0.5 and 3.3 hours, respectively, and mean volume of distribution ranged between 3 and 12 L. Prostate tissue levels of clusterin ASO increased in a dose-dependent manner and were in the range of 0.7 and 4.8 μg clusterin ASO / g prostate tissue (Chi et al., 2005).

1.5.3 Clusterin ASO and taxanes as combination therapy

Although numerous specific molecular targets for cancer, including oncogenes and tumor suppressor genes, have been identified recently, non-specific cytotoxic drugs are still used in many anti-cancer regimens (Miyake et al., 2000a). The use and dose of cytotoxic agents is limited by toxicity and the development of drug resistance. A treatment strategy of using ASOs that inhibit the expression of oncogenes, in combination with cytotoxic agents, may be a means to achieve efficacy with reduced doses of the cytotoxic agent. This strategy may result in a decrease in side effects and potentially avoid early development of drug resistance. At the molecular level, a common therapeutic approach for treating tumors is to induce apoptosis in cancer cells (Narayanan, 1997). Gleave and coworkers (Gleave and Miyake, 2005; Gleave and Chi, 2005) have proposed that treatments causing apoptosis may be improved and the emergence or progression of the androgen independent phenotype delayed, by including agents that target

increases in gene expression stimulated by chemotherapy, androgen withdrawal or radiotherapy. The use of ASOs that block the expression of anti-apoptotic genes, in combination with cytotoxic agents that promote apoptosis, has been shown to accelerate the process of apoptosis (Narayanan, 1997).

siRNA targeted to inhibit the expression of clusterin has been shown to increase the chemosensitivity of PC-3 cells *in vitro* (Trougakos et al., 2004), while clusterin ASO has been demonstrated to increase the sensitivity of PC-3, LNCaP and Shionogi prostate tumors in mice to paclitaxel (Miyake et al., 2003) *in vitro* and *in vivo* (Miyake et al., 2000b; Miyake et al., 2000a; Miyake et al., 2000d). Since prostate cancer has modestly responded to treatment with the taxanes, paclitaxel (Kuruma et al., 2003) and docetaxel (Sinibaldi et al., 2002) in the clinic, a suitable therapeutic strategy might be to combine clusterin ASO treatment with paclitaxel or docetaxel. Clusterin ASO is currently being investigated in combination with chemotherapy, via systemic administration in prostate, breast and lung cancers in separate Phase II studies (Gleave and Monia, 2005).

As reviewed by Gleave and Miyake (2005), following treatment with radiation, clusterin protein expression increased *in vitro* and *in vivo* in a dose-dependent manner in PC-3 cells. Inhibiting the expression of clusterin protein in PC-3 cells with clusterin ASO *in vitro* and *in vivo* resulted in increased apoptotic cell death and a greater reduction in tumor volume, respectively, following treatment with radiation (Gleave and Miyake, 2005). In addition, studies with different LNCaP cell lines showed that LNCaP cells that over-expressed clusterin protein

were less sensitive to radiation than other LNCaP cells (Gleave and Miyake, 2005). The local intratumoral administration, using brachytherapy injection templates, of the combination therapy approach consisting of the chemosensitization effects of clusterin ASO with the cytotoxic effects of paclitaxel or docetaxel, may hopefully prove to be effective in the treatment of patients with post-radiation recurrences of local prostate cancer. As discussed earlier in this thesis in section 1.2.10.3, there is no additional effective treatment for these patients.

Efficacy has been achieved using systemically administered paclitaxel and clusterin ASO combination therapy in human prostate cancer xenograft models. However, the dose of paclitaxel was close to the maximum tolerated dose (Miyake et al., 2000a). No apparent toxicity following the systemic administration of clusterin ASO in the mice was observed. Although improved chemical modifications of the phosphorothioated ASO backbone has resulted in increased resistance to nuclease degradation with a resulting increase in tissue half-lives and time between intravenous administrations (Henry et al., 2001), the efficacy of both clusterin ASO and paclitaxel or docetaxel combination therapy is dependent on both drug concentration and drug exposure time to the diseased tissue. However, clusterin ASO, paclitaxel and docetaxel are poorly targeted to the diseased tissue when administered intravenously.

1.6 CELLULAR UPTAKE AND DELIVERY ISSUES OF ASOs

1.6.1 Challenges of ASO delivery and cellular uptake

The development of ASOs and other therapeutic oligonucleotides in the clinic has been slowed due to a number of drug delivery issues. These include poor targeting of oligonucleotides to the site of action, rapid elimination from the body, degradation by nucleases and inefficient cellular uptake (Brignole et al., 2003; Vinogradov et al., 2004; Wang et al., 2003b). Systemically administered ASOs are rapidly cleared from the bloodstream due to uptake by the liver, which in turn inhibits the delivery of ASOs to other organs or tissues. ASOs (naked or alone) injected directly into tissue are rapidly taken up by the lymphatic system (Waters et al., 2000). Barriers to cellular uptake and nuclear localization of ASOs include the lipophilic cell membrane, endosomal release and nuclear transport (Lysik and Wu-Pong, 2003). Although ASOs (naked or alone) are generally poorly taken up by cells *in vitro*, when large enough doses are administered systemically or the ASOs are localized at the site of action, they may be satisfactorily taken up by targeted cells *in vivo* (Akhtar et al., 2000).

1.6.2 Cellular uptake of ASOs

Several methods have been used to investigate the cellular uptake and distribution of oligonucleotides within cells. Autoradiography, using either ^{3}H-, ^{14}C-, ^{35}S-, or ^{125}I-radiolabeled oligonucleotide has been used in combination with light or electron microscopy autoradiography. Radio-labeling of oligonucleotides followed by measurement of radioactivity associated with the

cells or analysis of radioactivity following extraction and gel electrophoresis have also been used to quantitate cellular uptake of oligonucleotides (Schweitzer and Engels, 1997). Flow cytometry using fluorescent-labeled oligonucleotides has been used for the quantification of oligonucleotide uptake in cells (Tonkinson and Stein, 1994; Krieg et al., 1993). Methods such as immunohistochemistry and fluorescently tagging ASOs have been used to determine the location of oligonucleotides within cells, following uptake (Leonetti et al., 1991).

As reviewed by Lysik and Wu-Pong (2003), the mechanism of cellular uptake of ASOs is poorly understood (Krieg, 2001) and may be dependent on ASO chemistry, cell type and cell cycle. A number of mechanisms for the cellular uptake of ASOs have been proposed with adsorptive endocytosis (shown in Figure 1.5), including pinocytosis (Stein et al., 1993) and potocytosis (Zamecnik et al., 1994), being the most widely accepted cell uptake mechanism (Yakubov et al., 1989; Krieg, 2001). Pinocytosis is endocytotic cellular uptake via local infoldings of the cell membrane (Mellman, 1996) and potocytosis is endocytotic cellular uptake via caveolar pits (Mellman, 1996). Adsorptive endocytosis involves a two step process (Lysik and Wu-Pong, 2003). In the first step, the ASO binds to the cellular membrane in apparently a non-sequence specific manner (Krieg, 2001). In the second step, the ASO is endocytosed and transported into the cytoplasm inside the endosome. It appears that the rate limiting step in ASO hybridizing with its target is the release of ASO from the endosome (Krieg, 2001). Following endocytosis, the ASO may be unable to escape from the endosome and eventually becomes degraded by lysozymes (Loke et al., 1989) or alternatively escapes from the endosome. If the

ASO escapes from the endosome, it is generally accepted that the ASO accumulates in the perinuclear organelles or is transported into the nucleus (Zamecnik et al., 1994). However, the mechanisms of endosomal escape and nuclear transport are not understood (Lysik and Wu-Pong, 2003).

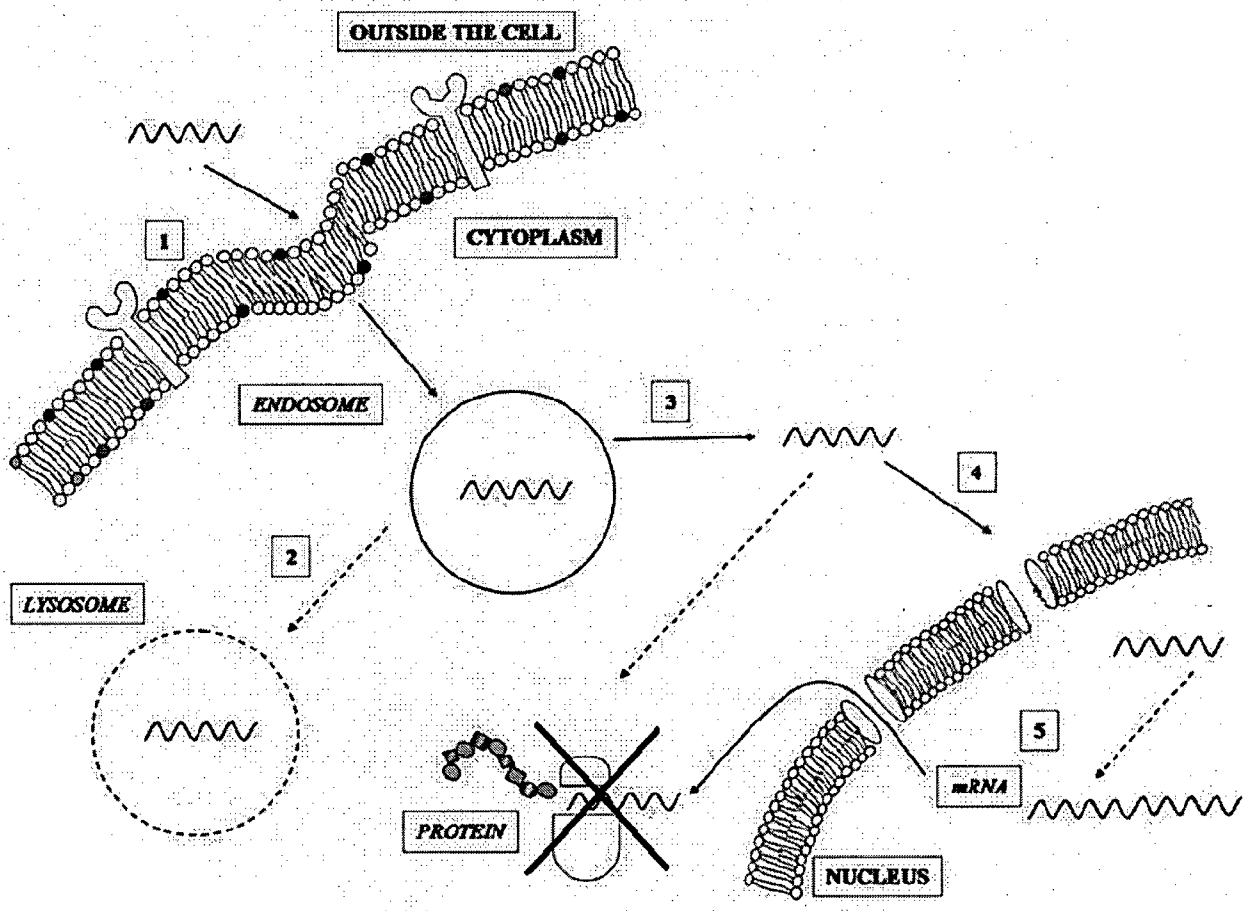

Figure 1.5 Schematic representation of postulated adsorptive endocytosis mechanism of cellular uptake of ASOs. **1)** Adsorption to the cell membrane and endosomal uptake into the cytoplasm. **2)** Potential lysosomal degradation of ASO. **3)** Release from the endosome. **4)** Entry into nucleus. **5)** Inhibition of protein expression (detailed in Figure 1.2). Adapted from Roth and Sundaram (2004).

Cellular uptake of ASOs is dependent on the chemical structure of the ASO (Lysik and Wu-Pong, 2003). Although ASOs with phosphodiester or phosphorothioate backbones (shown in Figure 1.3) are polyanionic and this may inhibit their uptake through the lipophilic cell membrane, polyanionic ASOs are thought to bind to cell surface proteins, which aids in adsorptive endocytosis. Neutral ASOs, such as peptide nucleic acids (shown in Figure 1.3), are poorly bound to cell surface proteins and show little endocytosis or cellular uptake (Lysik and Wu-Pong, 2003).

1.6.3 Strategies to deliver and enhance cell uptake of ASOs

Various methods are used to improve the cellular uptake of oligonucleotides, decrease their rate of degradation by nucleases, extend systemic circulation time and/or provide a controlled release of oligonucleotides. These methods include modifying the chemical backbone and side groups of oligonucleotides (Nakajima et al., 2000; Zellweger et al., 2001), preparing oligonucleotide conjugates (Juliano, 2005), complexing oligonucleotides with cationic or polycationic moieties including lipids (Oupický et al., 2000), amino acids (Ferreiro et al., 2001) and polymers (Robaczewska et al., 2001), and incorporating oligonucleotides into polymeric matrices (De Rosa et al., 2002; Zellweger et al., 2001; Allerson et al., 2005; Juliano, 2005; Oupický et al., 2000; Ferreiro et al., 2001; Robaczewska et al., 2001).

1.6.3.1 Lipoplexes

Cationic liposomes are comprised of cationic lipids such as N-[1-(2,3-dioleoyloxy) propyl]-N,N,N-trimethylammonium methyl sulfate (shown in Figure 1.6) (Capaccioli et al., 1993; Jaaskelainen et al., 1994) mixed with, for example, dioleoylphosphatidylethanolamine (DOPE) in a 1:1 ratio (Maurer et al., 1999). Lipoplexes (shown in Figure 1.6) are cationic liposomes complexed with polyanionic DNA, including ASOs. These complexes form spontaneously with polyanionic DNA through an electrostatic interaction with the cationic head groups, thus neutralizing the charge on the ASOs (Meidan et al., 2000). The physicochemical properties of lipoplexes are influenced by their components including lipids and ASO sequence, and by the lipoplex environment such as pH and ionic strength (Meidan et al., 2001).

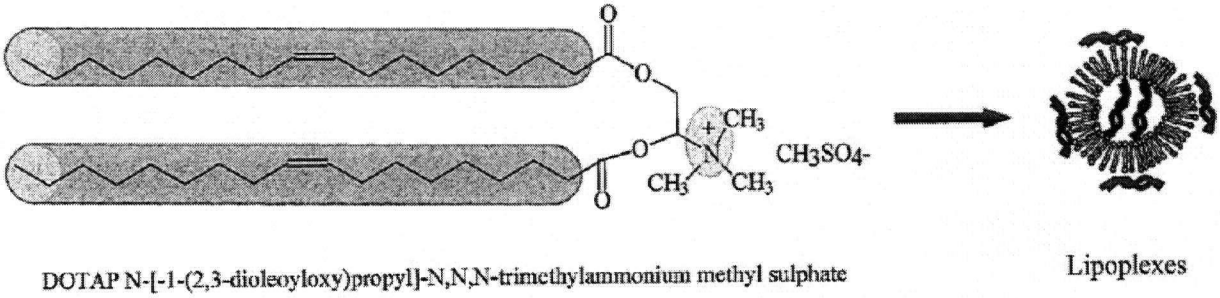

Figure 1.6 Structure of N-[1-(2,3-dioleoyloxy) propyl]-N,N,N-trimethylammonium methyl sulfate, a cationic lipid commonly used in the formation of lipoplexes. Adapated from Brown et al. (2001).

Incorporating oligonucleotides into cationic liposomes to form lipoplexes (Islam et al., 2000) has been the most widely used strategy to improve the *in vitro* and *in vivo* cellular uptake of ASOs (Semple et al., 2001), provide ASOs with protection from degradation by nucleases (Capaccioli et al., 1993) and increase their systemic circulation following intravenous administration. Unfortunately, cationic liposomes show dose dependent toxicity (Capaccioli et al., 1993). Less toxic lipoplexes have been formulated by using novel lipids or other materials, such as the pyridinium-based amphiphile 1-methyl-4(dioleoyl)methyl-pyrimidinium chloride, mixed with DOPE. (Shi et al., 2001). There are a number of commercially supplied examples of cationic lipids commonly used to prepare lipoplexes for *in vitro* transfection of ASOs, including Lipofectin®, Lipofectamine® and Oligofectamine® (Miyake et al., 2000a; Albrecht et al., 1996; Cui et al., 2004).

The primary mechanism of cellular uptake of lipoplexes is generally accepted to be via endocytosis (Zelphati and Szoka, 1996) (shown in Figure 1.5). Lipoplexes are usually prepared with cationic lipid and polyanionic oligonucleotide ratios that provide a slight positive charge, in order to provide increased cellular uptake through interaction with the negatively charged cell membranes (Maurer et al., 1999). DOPE is incorporated into lipoplexes to aid in the destabilization of endosomes and enhancement of ASO release from endosomes (Jaaskelainen et al., 1994). Cholesterol or a cholesterol derivative is often added to the lipids to increase the stability of the liposomes (Maurer et al., 1999). Cellular uptake of lipoplexes has

been enhanced through the use of targeting ligands. For example, galactosylated lipids have been used to target asialoglycoprotein receptors (Managit et al., 2005).

ASO was incorporated into liposomes before incorporation into 20 or 27% w/v poloxamer 407 gel in order to provide a controlled release and improved cellular uptake of ASO for an ocular formulation (Bochot et al., 1998). Little or no difference in ASO release was observed between poloxamer 407 gels with or without liposomes and 100% of the loaded ASO was released in approximately 6 to 24 hours. Approximately 15 to 25% of the ASO was released from the poloxamer 407 gels while still encapsulated in the liposomes; the remaining ASO was released as free ASO (Bochot et al., 1998).

1.6.3.2 Polyplexes

Polyplexes (shown in Figure 1.7) are cationic polymers complexed with polyanionic DNA (Felgner et al., 1997). Linear polycationic polymers employed in polyplexes include diethylaminoethyl-modified dextran, poly(L-lysine), poly(N-ethyl-4-vinylpyridinium bromide), linear polyethylenimine (PEI), chitosan and poly(dimethylaminoethyl methylacrylate) (De Smedt et al., 2000; Brown et al., 2001; Yoo et al., 1999; Ferreiro et al., 2001; Robaczewska et al., 2001; Gao et al., 2005). Chitosan is described in more detail in section 1.9.3 of this thesis. Branched polycationic polymers used to prepare polyplexes include polyamidoamine dendrimers, fractured dendrimers (partially degraded polyamidoamine dendrimers) and branched PEI (De Smedt et al.,

2000). A number of polycationic polymers, including poly(L-lysine), polyamidoamine dendrimers and PEI have been associated with toxicities (Shoji and Nakashima, 2004).

Complexing oligonucleotides with cationic polymers to form polyplexes has been used to inhibit degradation of oligonucleotides by nucleases and enhance their *in vitro* and *in vivo* cellular uptake (Wagner, 2004). Similar to lipoplexes, the most accepted mechanism for cellular uptake of unmodified polyplexes is by endocytosis (Godbey et al., 1999) (shown in Figure 1.5) including potocytosis and phagocytosis (Lungwitz et al., 2005). The mechanism of cellular uptake of lipoplexes may be dependent on cell type. Cellular internalization of lipoplexes is influenced by the net positive charge of the complexes, length of incubation and concentration (Lungwitz et al., 2005). Following endocytosis, ASO:PEI complexes may be too stable for the ASO to be released from endosomes into the cytoplasm (Shoji and Nakashima, 2004). Similar to lipoplexes, targeting ligands such as PEG or galactose have been covalently bonded to cationic polymers in an effort to improve the delivery and biocompatibility characteristics of polyplexes (Hu et al., 2001; Murthy et al., 2003; Gao et al., 2005).

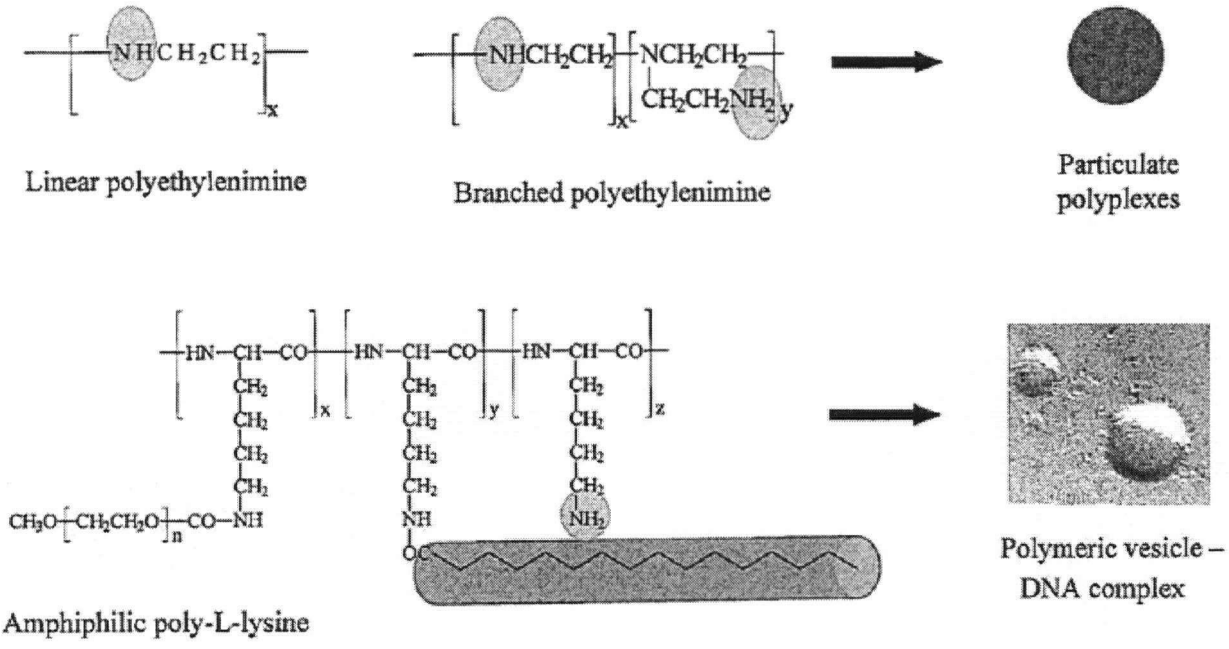

Figure 1.7 Structure of selected cationic polymers complexed with polyanionic DNA to form polyplexes. Adapted from Brown et al. (2001).

1.6.3.3 Nanoparticulates and microparticulates

Nanoparticulates and microparticulates are particles, matrices or shells usually comprised of biodegradable polymers and have diameters in the nanometer and micrometer ranges, respectively. ASOs have been incorporated into nanoparticles of cyanoacrylates such as polyisohexylcyanoacrylate or polyisobutylcyanoacrylate, to increase their cellular uptake and protect the ASOs from nuclease degradation (Chavany et al., 1992). Due to the polyanionic charge of ASOs, loading levels of ASOs in cyanoacrylates are low. ASO loading levels in cyanoacrylates have been increased to loading efficiencies of approximately 50% by complexing the ASO with hydrophobic cations such as cetyltrimethylammonium bromide to neutralize the

ASOs prior to loading into nanoparticles (Berton et al., 1999). However, cetyltrimethylammmonium bromide is cytotoxic and less than 10% of the ASO was released from ASO:cetyltrimethylammonium complex loaded cyanoacrylate microspheres over 60 days (Berton et al., 1999).

Several groups have incorporated ASOs into PLGA microspheres and reported sustained release of the ASOs *in vitro* over approximately 4 to 8 weeks; however, maximum ASO loading of these formulations was only 0.003% w/v (Hussain et al., 2002), 0.03% w/w (Lewis et al., 1998) and 0.3% w/w (De Rosa et al., 2003). Scaled to 100 mg of microspheres these formulations would have contained a total of only approximately 3 to 300 μg of ASO. Hydrophilic ASOs are poorly incorporated into hydrophobic PLGA during the preparation of microspheres, even when using multi-step water-in-oil-in-water emulsion methods (Hussain et al, 2002; Lewis et al., 1998; De Rosa et al., 2003). Lewis et al. (1998) showed that loading ASO into PLGA microspheres inhibited the degradation of the ASO when incubated in 10% serum *in vitro* (degradation data were not provided by Hussain et al. (2002) or De Rosa et al. (2003)). The loading efficiency of ASOs in PLGA microspheres was increased by complexing the ASOs with PEI at N/P ratios of 13/1 and 35/1 before preparing the microspheres (De Rosa et al., 2003). No free oligonucleotide was released from the ASO/PEI complex loaded PLGA microspheres for up to 60 days. Only 4 to 10% of the loaded ASO was released as ASO/PEI complexes over 45 days from PLGA microspheres loaded with ASO/PEI complexes with a N/P ratio of 13/1 and for PLGA microspheres loaded with ASO/PEI complexes "...with a N/P ratio of 35, the percentage

of released complex even decreased with time." (De Rosa, 2003). The authors suggested that the carboxylic end-groups of PLGA may interact with the ASO/PEI complexes, providing for the absorption [sic] of the ASO/PEI complexes onto the surface of the microspheres and a corresponding slow and incomplete release of the ASO (De Rosa, 2003).

1.6.3.4 Other strategies

A number of other strategies have been employed to improve the delivery of ASOs. Carrier molecules, such as poly(L-lysine), have been conjugated to ASOs to enhance binding to cell membranes (Lysik and Wu-Pong, 2003), fusogenic peptides to promote binding to cell receptors (Soukchareun et al., 1998) and cholesterol to enhance the release of ASOs from endosomes (Krieg, 2001). Cyclodextrins, which are amphiphilic cyclic oligosaccharides, have been used to deliver ASOs (Epa et al., 2000).

1.7 BIODEGRADABLE POLYMERIC DRUG DELIVERY SYSTEMS

1.7.1 General applications

Polymeric drug delivery systems are being developed in an effort to meet the requirements of prolonged and better controlled drug delivery (Grassi and Grassi, 2005) of a broad range of drug types and classes, including small molecules, vaccines, peptides, proteins and oligonucleotides. As discussed in several excellent reviews, including (Langer, 1990; Robinson, 1997; Siepmann and Gopferich, 2001; Kanjickal and Lopina, 2004), the field of polymeric drug delivery research is large and growing.

1.7.2 Polymer structure and nomenclature

A polymer may be defined as a large molecule composed of many smaller repeating units called monomers, which are covalently bonded together (Cowie, 1973). The physical properties of a polymer are related to its chemical structure and its environment. The morphology of a polymer may be defined by its constitution, configuration and conformation. Constitution depicts the atoms, sequence of the monomers, functional groups (including backbone groups, end groups and pendant groups), branch chains and molecular weight distribution of the polymer. Configuration describes the orientation of atoms and groups around atoms within the polymer backbone (Hall, 1988). Configuration thus includes a description of chirality, isomerism and rigidity. Conformation depicts the three dimensional arrangement of a polymer, which is dependent on its constitution, configuration and environment (Billmeyer, 1984). Polymer chains are likely to form a random coil when there are no external ordering forces acting on the chains. Polymer chains may also become folded or form helices (Billmeyer, 1984).

Polymers are named on the basis of their structure and/or on the basis of the monomers from which they are formed (Wilks, 2000). Polymers in this work are named using the name of the monomers from which they are formed and parentheses are used when the name of the monomers has more than one word (Wilks, 2000). Polymers that have only one type of repeating unit are called homopolymers, while polymers that have two or more different monomers are referred to as copolymers (Grulke, 1994). Figure 1.8 shows the structure of random, diblock and triblock copolymers. A random copolymer, also called a statistical

copolymer, has randomly organized different repeating units. A block copolymer has two or more long blocks of monomers, with at least one block containing one or more kinds of monomers that are different from at least one other block of repeating units (Grulke, 1994).

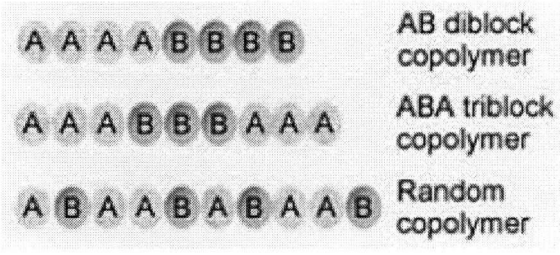

Figure 1.8 Schematic of diblock, triblock and random copolymers. Adapted from the Materials Science and Engineering Laboratory NIST Center for Neutron Research website: http://www.ncnr.nist.gov.

1.7.3 Biodegradable polyesters

Numerous different classes of biodegradable polymers have been used for drug delivery including polyesters, polyanhydrides, poly(ortho esters), phosphorus containing polymers, polysaccharides, peptides and proteins (Al Malyan et al., 2006). The most important class of biodegradable polymers is the polyesters (Fung and Saltzman, 1997; Sinha and Trehan, 2003). Within the class of polyesters the following polymers (shown in Figure 1.9) are the most significant in terms of drug delivery applications: poly(ε-caprolactone) (PCL), poly(lactide) (PLA), poly(glycolide) (PGA), PLGA, poly(β-hydroxybutyrate) and poly(β-hydroxybutyrate-co-hydroxyvalerate) (Hasirci et al., 2001; Sinha and Trehan, 2003; Freiberg and Zhu, 2004).

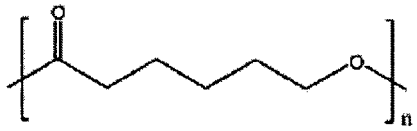

poly(ε-caprolactone) (PCL)

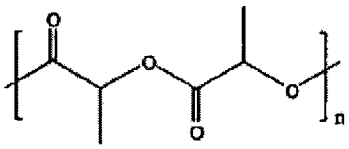

poly(lactide) (PLA)

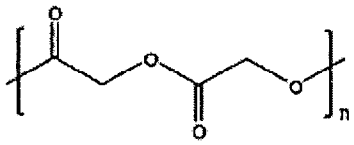

poly(glycolide) (PGA)

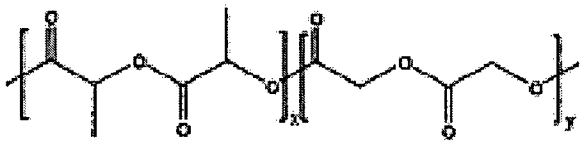

poly(lactide-co-glycolide) (PLGA)

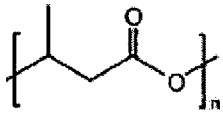

poly(β-hydroxybutyrate)

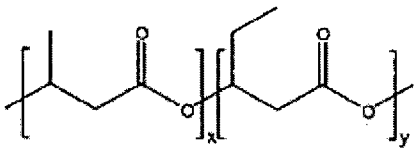

poly(β-hydroxybutyrate-co-hydroxyvalerate)

Figure 1.9 The chemical structures of polyesters commonly used in biodegradable drug delivery systems. Adapted from Shi (2003).

1.7.4 Mechanisms of drug release from polyesters

Controlled release polymeric drug delivery systems consist primarily of two types of systems: matrix and reservoir. Reservoir drug delivery systems utilize a polymeric membrane which surrounds a core of drug. This thesis is focused on a matrix type of drug delivery system, with drug distributed throughout a polymeric matrix (Sinha and Trehan, 2003). The potential mechanisms of drug release from matrix systems include initial release from the matrix surface, polymer swelling and drug diffusion through the swollen polymer, drug diffusion through intact

polymer or pores and channels within the matrix, and polymer biodegradation and erosion (Sinha and Trehan, 2003; Kanjickal and Lopina, 2004; Grassi and Grassi, 2005). Drug release from biodegradable polymeric matrices is usually complex, involving several drug release mechanisms (Grassi and Grassi, 2005; Freiberg and Zhu, 2004).

1.7.6.1 Swelling

Swelling controlled release drug delivery systems involve a drug incorporated into a hydrophilic polymeric matrix, termed a hydrogel (Grassi and Grassi, 2005). Penetration of water into the matrix from the system's environment alters the size and physical properties of the matrix, which in turn alter the release of drug from the matrix. The rate of drug release from an unswollen, dehydrated gel, is dependent on the rate of water uptake into the matrix and the rate of drug diffusion (Grassi and Grassi, 2005).

1.7.6.2 Biodegradation and erosion

Biodegradation is the chemical or enzymatic degradation of polymer chain backbones and is termed "scission" (Sinha and Trehan, 2003). Biodegradation of polyesters used in drug delivery occurs primarily by hydrolysis. Following biodegradation, material is physically lost from the bulk matrix and this is termed erosion (Sinha and Trehan, 2003). Bulk and/or surface degradation and erosion may occur, depending on the rate of diffusion of water into the matrix and the rate of degradation (Grassi and Grassi, 2005). Bulk degradation and erosion takes place when water rapidly penetrates the matrix and degradation and erosion occur throughout the

matrix. Surface degradation and erosion occur when degradation and erosion of the polymer chains is more rapid than the penetration of water into the matrix (Sinha and Trehan, 2003; Grassi and Grassi, 2005).

The release of drugs from biodegradable matrices is influenced not only by the rate of degradation and erosion of the matrix, but also by the diffusion of drug from the matrix (Sinha and Trehan, 2003). The primary mechanism of release from these types of systems may vary during the release period and the mechanisms and kinetics of drug release from these types of matrices are usually complex (Grassi and Grassi, 2005).

1.7.6.2 Diffusion

Matrix diffusion controlled release drug delivery systems involve either a drug dissolved in a matrix (termed a monolithic solution) or partially dissolved in a matrix with the rest of the drug distributed throughout the matrix as particles (termed a monolithic dispersion) (Baker, 1987; Park et al., 1993). The release of drugs from diffusion controlled matrix systems may be described by Fick's laws of diffusion (Grassi and Grassi, 2005). Fick's first law shows that flux (J) is proportional to the drug diffusion coefficient (D) and the concentration gradient of the drug (dC/dx) and is given by the equation (Kanjickal and Lopina, 2004)

$$J = -D(dC/dx) \qquad \textbf{Equation 8}$$

C is the concentration of the drug and x is distance of drug movement perpendicular to the surface of the barrier. At steady state flow, the amount of material (M) that is transported

through a cross-section of area (S) per unit of time (t), that is, diffusion through a unit area, is described by the following equation (Kanjickal and Lopina, 2004)

$$J = dM/S \cdot dt \qquad \textbf{Equation 9}$$

No concentration gradient is present in monolithic solutions prior to the start of drug release. However, as drug is released from the surface of the matrix into the media, a concentration gradient is established with a greater drug concentration in the center of the matrix, resulting in drug diffusing down the concentration gradient to the surface of the matrix to be released. The rate of drug release is dependent on the diffusivity of the drug in the matrix (Grassi and Grassi, 2005). The rate of drug release from monolithic dispersions is influenced by the amount of drug loaded in the matrix. At drug loading levels of approximately 5% or less, the drug in the dispersed particles dissolves into the matrix and diffuses to the surface of the matrix, in a similar manner to that of monolithic solutions (Higuchi, 1961). At higher loading levels, released drug leaves behind pores in the matrix which become filled with fluid from the environment. The pores in turn assist in the release of drug remaining in the matrix (Baker, 1987). At drug loading levels of greater than approximately 20 to 30%, there are enough pores created by the release of drug to form continuous channels throughout the matrix to its surface. At these higher loadings, the majority of drug is released by diffusion through these channels and the rate of drug release is dependent on drug solubility and diffusivity in the fluid in the channels (Baker, 1987).

1.7.5 Factors influencing drug release from polyesters

Drug release from biodegradable polymer matrices is influenced by a number of factors, including properties related to the drug (such as solubility, pKa, molecular weight and loading), properties of the polymer (including hydrophilicity, molecular weight, crystallinity and glass transition temperature) and the size and geometry of the delivery system (Freiberg and Zhu, 2004; Grassi and Grassi, 2005). The drug partition coefficient between the matrix and its environment, diffusivity of the drug in the matrix and drug release rate are influenced by the solubility of the drug in the polymer and the release media (Grassi and Grassi, 2005). The molecular weight of the polymer and the drug both influence the diffusivity and drug release rate from diffusion controlled release systems. Drugs with lower molecular weights have greater diffusion coefficients and faster release rates than those with higher molecular weights (Pitt and Schindler, 1980; Chien, 1991). Crystalline regions of semicrystalline polymers have lower free volume and therefore lower rates of diffusion of drug and water molecules, compared to amorphous regions (Chien, 1991). Hence, the degree of crystallinity and glass transition temperature of a polymer matrix influence drug release rate (Sinha and Trehan, 2003; Freiberg and Zhu, 2004).

Increasing drug loading in monolithic solutions and monolithic dispersions results in an increase in concentration gradient and an increase in drug release rate (Chien, 1991). Furthermore, increasing drug loading in monolithic dispersions results in the formation, or formation of greater numbers of, pores and channels for diffusion (Baker, 1987). Decreasing the

size of a delivery system results in an increase in surface area per amount of material and an increase in drug release rate (Freiberg and Zhu, 2004). The geometry of a delivery system may affect its length of diffusion path and surface area, which influence the drug release rate (Grassi and Grassi, 2005).

1.7.6 Polymeric drug delivery systems in prostate cancer

LHRH analogs have been formulated in a number of polymeric controlled release systems and approved for use in men by the Therapeutic Products Directorate in Canada and by similar regulatory agencies in other territories. Examples of the formulations include PLGA implants, PLGA microspheres (Moul and Civitelli, 2001) and PLGA dissolved in N-methyl pyrrolidone injectable liquid (Perez-Marrero and Tyler, 2004). Following subcutaneous or intramuscular injection, these formulations form a depot for controlled drug release between 1 to 12 months (Fung and Saltzman, 1997; Cox et al., 2005; Moul and Civitelli, 2001).

As reviewed by Liggins and Burt (Liggins and Burt, 2002), a series of diblock copolymers of MePEG and poly(D,L-lactide) (MePEG-block-PDLLA) have been investigated for preparing micellar paclitaxel for intravenous or intraperitoneal administration. Paclitaxel has been solubilized in aqueous micellar solutions of diblock copolymers above the critical micelle concentration. The diblock copolymers were amphiphilic polyether-polyester copolymers or amphiphilic triblock polyether copolymers. Micellar paclitaxel administered systemically in murine xenograft models of human leukaemia, lung and prostate tumors was shown to be as, or

more, efficacious than the commercial Taxol® formulation. The micellar paclitaxel formulations had lower toxicity than the commercial Taxol® formulation, resulting in a higher maximum tolerated dose of paclitaxel in the micellar formulations (Zhang et al., 1997b; Zhang et al., 1997a; Leung et al., 2000).

Paclitaxel has been incorporated into a number of different microsphere formulations for direct injection into tumors in prostate cancer animal models. Injection of paclitaxel loaded PLGA microspheres directly into PC-3 tumors in mice resulted in a decrease in tumor volume or complete tumor regression (Sahoo et al., 2004). Injection of paclitaxel loaded polilactofate (a biodegradable polyphosphoester) microspheres into LNCaP tumors grown in mice, resulted in a decrease in tumor volume and serum PSA level (Lapidus et al., 2004). Docetaxel incorporated into PDLLA-block-PEG microspheres was recently shown to be efficacious against human LNCaP prostate tumors in a mice xenograft model (Farokhzad et al., 2006).

1.8 INTRATUMORAL POLYMERIC DRUG DELIVERY SYSTEMS

Polymeric drug delivery systems are being developed for intratumoral or tumor resection site delivery, in an attempt to provide localized, high drug concentrations over a sustained period of time (Luo and Prestwich, 2002). Examples of the polymeric delivery systems for resection site or intratumoral administration include solid implants (Brem and Gabikian, 2001), microparticulates (Liggins et al., 2000) and pastes (Jackson et al., 2000).

1.8.1 Solid implants

Implantable polymeric wafers of poly(bis-p-[carboxyphenoxy]propane-co-sebacic acid) (termed polifeprosan 20) loaded with carmustine are approved for interstitial chemotherapy of brain tumors (Guerin et al., 2004). The polymer wafers have been loaded with other chemotherapy agents such as paclitaxel and further investigated for interstitial chemotherapy of brain tumors (Walter et al., 1994). Implantable rods of PLGA have been proposed for the intratumoral delivery of beta-lapachone (Wang et al., 2006) or 5-fluorouracil (Qian et al., 2002).

1.8.2 Microparticulates

Rather than inserting a solid implant into a tumor or resection site, delivery systems are being developed that allow for intratumoral injection of microparticulates which provide a localized depot and controlled drug release. Fung and Saltzman (1997) provide a review of studies using polymeric microspheres loaded with chemotherapy agents and injected intratumorally in various animal tumor models and applications in prostate cancer are described in the previous section 1.7.8.

1.8.3 Liquid and semi-solid formulations

Several strategies have been developed to provide an injectable polymeric drug delivery system for intratumoral administration, which is liquid at room temperature and forms a gel, semi-solid or solid at body temperature (Zentner et al., 2001; Chenite et al., 2000). The drug is encapsulated within the polymer matrix as it gels or solidifies. Following solidification, the

drug is released by mechanisms similar to those of pre-formed matrices (Eliaz and Szoka, Jr., 2002).

A number of biodegradable, thermoreversible polymer hydrogels have been developed for the intratumoral delivery and controlled release of chemotherapy agents (Jackson et al., 2004). The polymers used in these gels form a free-flowing sol when in aqueous solution at room temperature. When the temperature is increased to 37°C, these systems undergo a reversible sol-gel transition to become a transparent gel (Jackson et al., 2004). Following the incorporation of paclitaxel into a thermoreversible gel and injection directly into human breast tumors in a mouse xenograft model, paclitaxel was slowly cleared from the injection site over approximately 6 weeks with minimal distribution into any organs outside of the tumor (Zentner et al., 2001).

Injectable liquid implant systems have also been developed from water insoluble polymers, such as PLGA, dissolved in a water soluble solvent such as glycofurol (Eliaz and Szoka, Jr., 2002) or benzyl benzoate (Wang et al., 2004). Following injection of the polymer/solvent system into an aqueous environment, the water miscible solvent diffuses out from the polymer solution, leaving the polymer to coagulate or precipitate to form a solid polymeric matrix. Using a different injectable implant system approach, it was shown that chitosan in polyol salts is a liquid at room temperature and forms a gel at body pH and temperature (Chenite et al., 2000)

Our research group has developed injectable polymeric "paste" systems that set to implants without the need for organic solvents, for the controlled release of paclitaxel following local application at tumor resection sites (Winternitz et al., 1996). PCL was blended with low molecular weight MePEG (PCL/MePEG 80/20 w/w) to reduce the viscosity and lower the melting point of PCL to about 40 to 45°C. The melted paste could be injected and then solidified at 37°C (Winternitz et al., 1996).

1.9 INTRATUMORAL DELIVERY OF CLUSTERIN ASO AND TAXANES

1.9.1 Ideal features

Effective combination therapy for treatment of prostate cancer using clusterin ASO and paclitaxel or docetaxel depends on the design of an effective drug delivery system. An intratumoral drug delivery system for clusterin ASO and paclitaxel or docetaxel should provide controlled release and high localized concentrations of ASO and taxane within the tumor tissue. Ideal features of a formulation for intratumoral delivery are suggested to include the following characteristics:

- biocompatible and biodegradable,
- provide a homogeneous dispersion of drug(s) within the biomaterial matrix,
- sterilizable,
- easily injected into tissue,
- formation of a depot following injection,

- chemical stability of drugs within the matrix is maintained and
- controlled release of the drugs for one month or greater at the tumor site.

1.9.2 Triblock/MePEG polymeric paste

Our research group has developed an intratumoral, injectable, biodegradable polymeric "paste" for the delivery of paclitaxel (Jackson et al., 2000; Jackson et al., 2004). The paste was based on a triblock copolymer (shown in Figure 1.10A) of random poly(lactide-co-caprolactone) (PLC) with PEG in the form of PLC-block-PEG-block-PLC, blended with MePEG (shown in Figure 1.10B) in a 40/60 w/w ratio. The triblock copolymer is a hydrophobic, waxy, semi-solid (Jackson et al., 2004). The MePEG used in this work had a molecular weight of 350 $g \cdot mol^{-1}$., is an injectable liquid and soluble in water at ambient and body temperatures. MePEG 350 has a well established biocompatibility and is used extensively in pharmaceutical preparations. Characterization of this paste by Jackson et al. (2000; 2004) showed that the hydrophobic, waxy, semi-solid triblock copolymer was miscible with the liquid MePEG and that paclitaxel dissolved in a series of these blends up to 15% w/w drug loading. Formulations of triblock copolymer blended with MePEG in a 40/60 w/w ratio with 10% w/w paclitaxel could be injected through a 22 gauge needle without heating. Following injection into water, PBS or tissue at 37°C, the MePEG diffused out of the formulation and the remaining formulation, consisting primarily of the triblock copolymer, set to a semi-solid depot or implant. As shown in Figure 1.10C, during the first two weeks of incubation the triblock copolymer degraded from a

measured molecular weight of 16,700 $g \cdot mol^{-1}$ (calculated molecular weight was 15,333 $g \cdot mol^{-1}$) to approximately 13,000 to 14,000 $g \cdot mol^{-1}$. Little change in molecular weight was determined during weeks 3 and 4, after which rapid and extensive weight loss was measured during weeks 5 and 6. It was shown that the polymeric paste released paclitaxel and a number of other drugs *in vitro* in PBS at 37°C in a controlled manner over several weeks (Jackson et al., 2000; Jackson et al., 2004). Following intratumoral administration of paclitaxel-loaded paste into xenograft LNCaP murine models, decreased tumor volume and serum PSA levels were observed (Jackson et al., 2000).

1.9.3 Chitosan

Chitosan is an injectable, biocompatible (Lee et al., 1995; Richardson et al., 1999) and biodegradable (Mi et al., 2002) polycationic polysaccharide that has been used in a number of pharmaceutical and biomedical applications (Di Martino et al., 2005).

1.9.3.1 Structure and physicochemical properties

Chitosan (shown in Figure 1.11) is composed of N-acetylglucosamine and N-D-glucosamine monomers joined by β(1,4) glycosidic bonds. Chitosan is a deacetylation product of chitin, which is found in the exoskeleton of crustaceans. A general deacetylation process involves hydrolyzing the N-aetyl linkages of chitin by incubation in 40 to 50% w/v sodium hydroxide solution at 110 to 120°C for several hours, followed by rinsing and drying (Hon, 1996). Chitosan

A

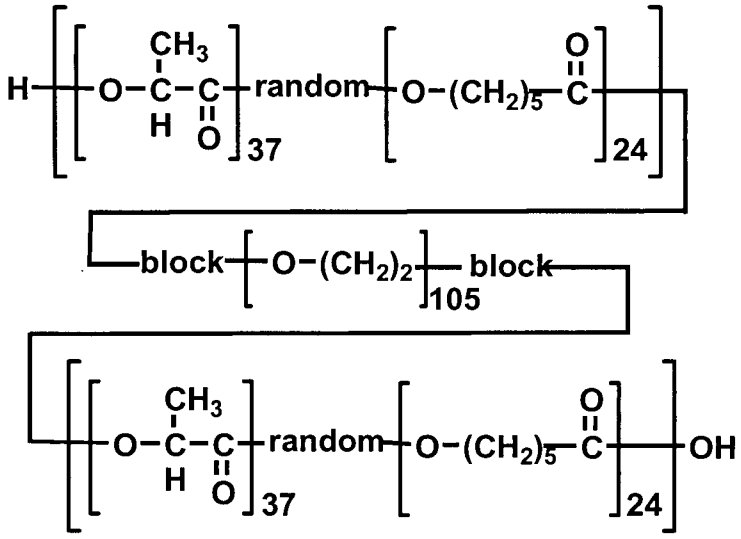

B

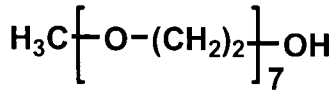

C

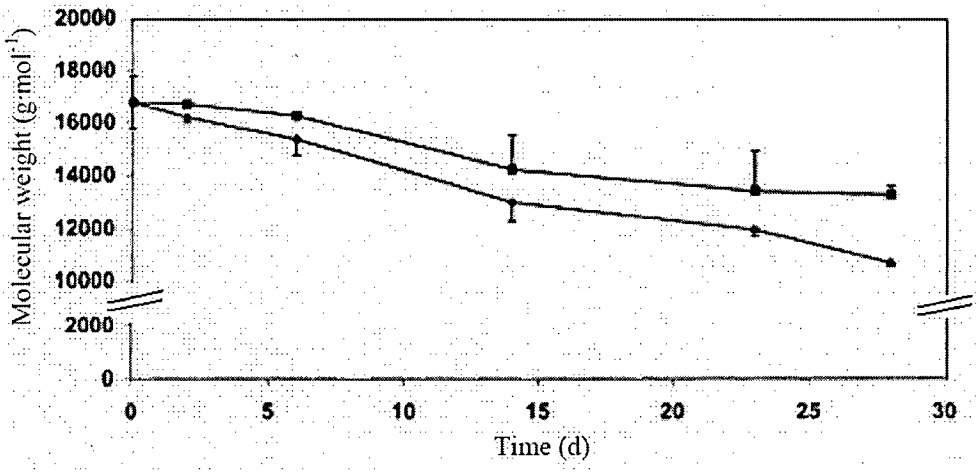

Figure 1.10 **A)** The chemical structure of triblock copolymer poly(D,L-lactide-random-caprolactone)-block-poly(ethylene glycol)-block-poly(D,L-lactide-random-caprolactone) (PCL-block-PEG-block-PCL) where 37 and 24 are the average number of lactide and caprolactone repeat units, respectively, within each poly(D,L-lactide-random-caprolactone) block and 105 is the average number of ethylene glycol repeat units. **B)** The chemical structure of methoxy-poly(ethylene glycol) (MePEG) where 7 is the average number of ethylene glycol repeat units. **C)** The degradation profile of triblock copolymer. Adapted from Jackson et al. (2000; 2004).

is available commercially with different degrees of deacetylation and even from the same supplier the degree of deacetylation may vary from lot to lot (Henriksen et al., 1997).

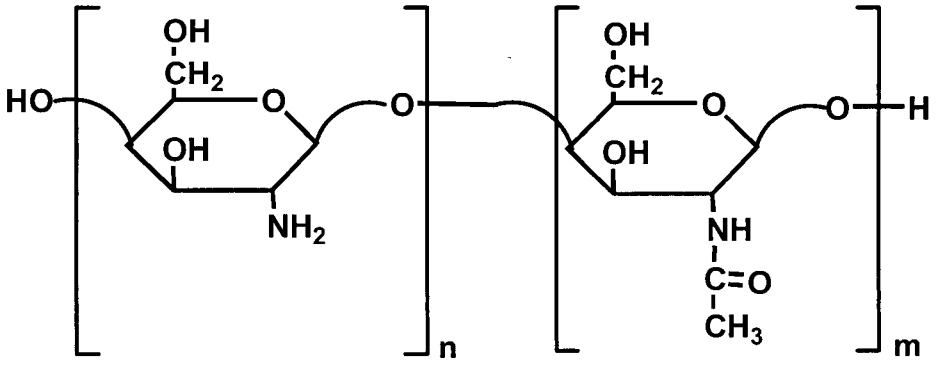

Figure 1.11 The chemical structure of chitosan where **n** and **m** are the average number of deacetylated monomers and monomers retaining the acetyl group, respectively. The amine groups of the deacetylated monomers may be protonated.

The charge density of chitosan is influenced by its degree of deacetylation (and thus the degree of amine groups that may be protonated) and the pH of the media. As the degree of deacetylation was decreased from 95 to 78% and the ionic strength of the media was increased from 0.01 to 0.1, the pKa of high molecular weight chitosan was shown to range from 5.5 to 7.1 (Romoren et al., 2003; Peng et al., 2005). Thus chitosan is a polycation at weakly acidic pH (Henriksen et al., 1997) and soluble at low pH. A 1 to 2% acetic acid solution or a 0.1 $mol \cdot L^{-1}$ hydrochloric acid solution is frequently used to dissolve chitosan. Chitosan behaves as a linear polyelectrolyte in solution (Richardson et al., 1999).

1.9.3.2 Biocompatibility and biodegradation

Chitosan incorporated into films, microparticles and fibers, has been shown to be biocompatible with various tissues both *in vivo* and *in vitro* (Jameela and Jayakrishnan, 1995; Rao and Sharma, 1997; Richardson et al., 1999; Illum et al., 2001; Mi et al., 2002). Chitosan has shown molecular weight and concentration dependent *in vitro* cytotoxicity towards the murine melanoma cell line B16F10. The cytotoxicity was also salt dependent with the order in decreasing toxicity of chitosan hydrochloride, chitosan hydroglutamate, glycol chitosan and chitosan hydrolactate. However, when compared to poly(L-lysine) which had an IC_{50} of 0.05 ± 0.01 mg·mL^{-1}, the chitosan hydrochloride which had an IC_{50} of 0.21 ± 0.04 mg·mL^{-1}, was found to be less toxic (Carreño-Gómez and Duncan, 1997). Other groups have shown that the toxicity of chitosan was decreased with lower molecular weight chitosan and that purified lower molecular weight chitosan showed no cytotoxicity or hemolysis (Richardson et al., 1999).

Chitosan has been shown to be hemostatic and this activity appears to be independent of the normal/classical clotting cascade (Rao and Sharma, 1997). It causes hemagglutination of erythrocytes in human and a number of animal species (Rao and Sharma, 1997). It has been suggested that the agglutination effect of chitosan on cells is influenced by its molecular weight and is due to its polycationic chains interfering with anionic residues of molecules on cell surfaces (Evans and Kent, 1962; Rao and Sharma, 1997).

Evidence suggests that chitosan breaks down *in vivo* by enzymatic degradation (Lee et al., 1995) via lysozyme hydrolysis of glycosidic bonds in chitosan (Freier et al., 2005). The

biodegradation of chitosan is influenced by its degree of deacetylation (Nordtveit et al., 1996). It may take several weeks to months for chitosan to degrade (Rao and Sharma, 1997; Mi et al., 2002; Freier et al., 2005). Following intramuscular injection in rats, glutaraldehyde cross-linked chitosan microspheres degraded into a loose and porous structure over 12 weeks (Mi et al., 2002). Microspheres prepared from genipin cross-linked chitosan and injected intramuscularly in rats showed no significant degradation after 20 weeks (Mi et al., 2002). The degradation of chitosan incubated *in vitro* in buffer with lysozyme was found to be dependent on the degree of deacetylation, with those samples with a very high or low degree of deacetylation having the slowest degradation rates (Freier et al., 2005).

1.9.3.3 Sterilization

Chitosan has been sterilized by dry heat, saturated steam autoclaving, γ-irradiation, microwave irradiation, glutaraldehyde and ethylene oxide (Rao and Sharma, 1997; Lim et al., 1998; Lim et al., 1999; Wong et al., 2002). Sterilizing chitosan fibers and films by gamma irradiation resulted in chain scission. The viscosity average molecular weight and the glass transition temperature of the chitosan both decreased with increasing irradiation doses (Lim et al., 1998).

1.9.4 Use of chitosan to enhance cellular delivery of ASOs and plasmids

The amine groups on the N-D-glucosamine residues of chitosan and its derivatives are protonated at neutral or lower pH, producing a polycationic polymer that has been shown to

effectively condense and deliver plasmids/genes (high molecular weight DNA) and ASOs *in vitro* and *in vivo* (Renbutsu et al., 2005; Gao et al., 2005; Freier et al., 2005; Mi et al., 2002; Ishii et al., 2001; Ramos et al., 2005). There are numerous examples of chitosan being used to enhance the delivery and cellular uptake of plasmid (high molecular weight DNA) *in vitro* and *in vivo* by condensing the plasmid DNA (MacLaughlin et al., 1998; Ishii et al., 2001; Chen et al., 2003; Park et al., 2003) and protecting it from degradation by nucleases (Erbacher et al., 1998; Sato et al., 2001; Mao et al., 2001).

Similar to other lipoplexes and polyplexes discussed previously in sections 1.6.3.1 and 1.6.3.2, it has been demonstrated that plasmid DNA/chitosan complexes are internalized by endocytosis following adsorbtion to the cell surface (Venkatesh and Smith, 1998). Chitosan undergoes enzymatic degradation in the endosome and the degradation of the polysaccharide increases the number of degraded chitosan molecules which increases the osmolarity of the endosomes (Köping-Höggård et al., 2001). As a result, the endosomes take in water, swell and burst, releasing their contents into the cytoplasm (Ishii et al., 2001).

The strength of the binding between the polyanionic DNA and polycationic chitosan depends on the degree of protonation (positive charge) of the amine groups on the polysaccharide chains (Romoren et al., 2003), which is dependent on the degree of deacetylation of the chitosan and the pH of the environment. The effect of various physicochemical properties of chitosan on plasmid transfection efficiency has been investigated (Köping-Höggård, 2003). Chitosan molecular weight, plasmid concentration and charge ratio affected the stability of

plasmid DNA/chitosan complexes. It has been demonstrated that strong complex stability results in low *in vivo* expression levels and that decomplexation and/or uptake may be the rate-limiting steps in cell uptake of plasmid DNA (not endosomal release) (MacLaughlin et al., 1998). Chitosan complexed with calf thymus plasmid DNA has been shown to protect the DNA from degradation *in vitro* by the nuclease DNAase II (Richardson et al., 1999) and serum nucleases (Erbacher et al., 1998). However, the ability of chitosan to protect genes from degradation and to increase their transfection *in vitro*, was found to be dependent on the type of cell line used (Erbacher et al., 1998). Other groups have shown that plasmid DNA/chitosan complexes protected the DNA following intramuscular injection *in vivo* (Leong et al., 1998).

Genes or oligonucleotides have typically been complexed with chitosan by first dissolving the chitosan in weak acid and mixing with genes or oligonucleotides to form polyelectrolyte complexes or coacervated complexes with mean diameters generally between 100 to 1500 nm (Erbacher et al., 1998; MacLaughlin et al., 1998; Mao et al., 2001; Gao et al., 2005; Ramos et al., 2005). As described in more detail in Chapter 3 in this thesis, we used microparticulate chitosan that swelled as a clusterin ASO solution was absorbed into the microparticles by a solvent loading process.

1.10 THESIS GOAL, HYPOTHESES AND OBJECTIVES

The goal of this research project was to develop a clusterin ASO and paclitaxel or docetaxel loaded polymeric paste formulation suitable for the intra-tumoral treatment of prostate cancer.

Our working hypotheses were as follows.

1. The incorporation of clusterin ASO:chitosan complexes and paclitaxel or docetaxel into a biodegradable polymeric paste will control the release of both clusterin ASO and paclitaxel or docetaxel.
2. A clusterin ASO:chitosan complex and paclitaxel or docetaxel loaded biodegradable polymeric paste formulation injected intra-tumorally into a localized human prostate tumor grown in a mouse model will inhibit tumor growth.

The research objectives were as follows.

1. To develop an extraction and desalting method and a CGE assay that provides single base separation and quantitation of clusterin ASO and its 20-, 19- and 18-mer oligonucleotide degradation products from human plasma.
2. To complex clusterin ASO with chitosan microparticles and characterize the influence of clusterin ASO:chitosan ratio and pH on the physicochemical properties.

3. To characterize the influence of clusterin ASO:chitosan ratio, pH and the loading of complexes into polymeric paste on clusterin ASO *in vitro* release profiles in PBS and human plasma.

4. To determine the efficacy of intratumoral administration of clusterin ASO:chitosan complexes and paclitaxel or docetaxel loaded biodegradable polymeric paste in PC-3 and LNCaP human prostate xenograft tumor models in mice.

2. DEVELOPMENT AND QUALIFICATION OF ANALYTICAL METHODS[1]

2.1 INTRODUCTION

The development of precise, accurate and reproducible analytical methods for the drugs and ASO components of the intratumoral drug and ASO loaded polymeric paste was an important aspect of this research project. The intratumoral paste was based on a blend of microparticulate complexes of chitosan and clusterin ASO together with either paclitaxel or docetaxel in a polymer matrix. The polymer matrix was a blend of triblock copolymer PLC-block-PEG-block-PLC with low molecular weight MePEG (shown in Figure 1.10).

A method of determining the molecular weight of chitosan was required as this parameter varies depending on the selection of a particular commercial source. Viscometry or GPC are commonly used to obtain information regarding the molecular weight of polymers (Strlic and Kolar, 2003). Viscometry only provides the viscometric average of molecular weight (Cowman and Matsuoka, 2005). GPC provides detailed data on the molecular weight averages and distribution (Winzor, 2003). GPC separates polymer chains based on their effective thermodynamic radius in solvent, which is indiscernible from their hydrodynamic volume (Shearwin and Winzor, 1990). Chitosan exhibits complex hydrodynamic behaviour, which is influenced by its degree of deacetylation and the solvent (Knaul et al., 1998). A GPC universal

---

[1] A version of this Chapter is in preparation for submission.

calibration curve may be constructed from information on the molecular weight, [η] and GPC retention time of a set of standards (Winzor, 2003). Although polymer molecular weight standards are often comprised of a different polymer than the polymer of interest, the standards and polymer of interest are generally of the same broad class of polymers in order to decrease hydrodynamic volume differences (Winzor, 2003). The polysaccharide pullulan is commonly used as a molecular weight standard for other polysaccharides in aqueous or organic solvents (Eremeeva, 2003).

Paclitaxel and docetaxel have been quantitatively analyzed by HPLC (Monsarrat et al., 1990; Marchettini et al., 2002). Our research group has previously developed and qualified an extraction method and HPLC assay for paclitaxel (Burt et al., 1995; Liggins et al., 2000). The HPLC method for paclitaxel was modified and adapted for docetaxel analysis and is described in this chapter.

As reviewed by Schweitzer and Engels (1997) and Leeds and Cummins (2001), analysis of ASOs has been performed using a number of methods, including UV-Vis spectrometry, reverse phase HPLC, anion exchange HPLC, PAGE, CGE, cloning and sequencing, hybridization, mass spectrometry and nuclear magnetic resonance. A simple method of quantitation was desired in order to determine the quantity of received oligonucleotides from suppliers and to determine the concentration of oligonucleotide standards prepared for other analysis methods. Small numbers of samples of relatively pure ASO solutions are commonly quantitated by UV-Vis spectroscopy as this is a simple and accurate method for determining total

ASO content (Schweitzer and Engels, 1997). However, UV-Vis spectroscopy does not differentiate between oligonucleotides which differ in length by several nucleotide bases (Leeds and Cummins, 2001).

A method of quantitation with short analysis times that could be automated was desired for clusterin ASO for analysis of numerous drug release study samples in phosphate buffered saline (PBS). Reverse phase HPLC is reserved for hydrophobic, backbone-modified ASOs (Zhang et al., 2005) and more typically, anion exchange HPLC is used for ASOs with charged backbones (Horvath and Aradi, 2005). With short preparation and analysis times, HPLC systems allow for relatively rapid through-put of larger numbers of samples. It is noted that most HPLC methods fail to separate oligonucleotides that differ in length by only a single nucleotide (Leeds and Cummins, 2001).

Exonucleases in plasma metabolize phosphorothioated ASOs by cleaving a nucleoside from either the 5' or the 3' end of the oligonucleotide (shown in Figure 2.1). A method of separation and quantitation of clusterin ASO and its degradation products was required for the analysis of these oligonucleotides in human plasma. Of the various methods used to analyze ASOs, CGE and perhaps mass spectrometry are the only methods that can be used to separate and quantify phosphorothioated oligonucleotides differing in length by only 1 nucleotide (Leeds and Cummins, 2001). The disadvantages of using CGE for ASO analysis is that preparation is more laborious and analysis times are longer than those required for HPLC, an internal oligonucleotide standard is required and salt or buffer in the sample interferes with the

method (von Brocke et al., 2003; Benesova-Minarikova et al., 2005). The long run-times required by CGE may be overcome in part, by sequentially injecting a number of different

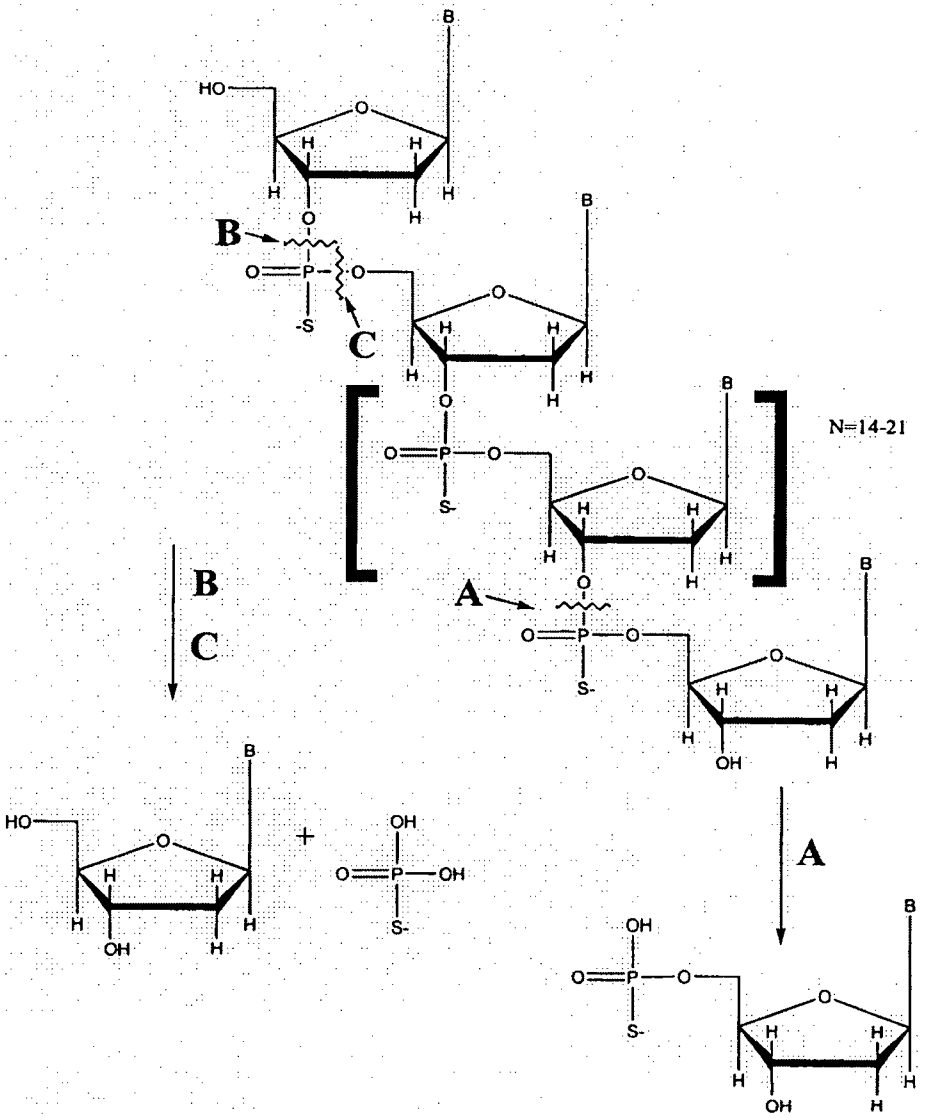

Figure 2.1 Exonucleolytic cleavage of phosphorothioate ASOs. **A)** Exonucleolytic cleavage from the 3' end of the oligonucleotide liberates a 5'-nucleoside monothiophosphate. **B)** Exonucleotide cleavage from the 5' end of the oligonucleotide liberates a nucleoside and leaves a 5'-phophorothioate attached to the oligonucleotide. **C)** 5' phosphatases rapidly cleave the 5' thiophosphate from the oligonucleotide. Adapted from Leeds and Cummins (2001).

samples onto the capillary without waiting for the first samples to elute (Williams et al., 2003). Analysis of biological or buffered oligonucleotide samples by CGE is dependent on lengthy extraction methods that purify the oligonucleotide from biological impurities including salts (Leeds et al., 1996; Yu et al., 2001).

The qualification or validation of analytical methods has been reviewed by a number of journal and industry publications (Shah et al., 1992; ICH, 1996; Shah, 1998; USFDA, 2000). To qualify a method means to show that it is suitable for its intended use and that there is an assurance that the method will perform consistently to predefined criteria on a routine basis (Shah et al., 1992). Qualification requirements may vary with the type of test or assay (ICH, 1996). Information required for qualification include specificity, linearity, range, accuracy, precision, detection limit and quantitation limit (USFDA, 2000).

In this chapter, we report the results of the development and qualification of analytical methods for chitosan, paclitaxel, docetaxel and clusterin ASO. The objectives of this study were to:

1. Develop a GPC method to determine the molecular weight of chitosan.
2. Develop an HPLC method to quantify docetaxel.
3. Develop and qualify extraction procedures for ASO from plasma samples and HPLC and CGE methods for 21-mer clusterin ASO and its 20-, 19- and 18-mer degradation products.

2.2 MATERIALS, EQUIPMENT AND STOCK SOLUTIONS

2.2.1 Drugs, standards and polymers

Paclitaxel was obtained from Sigma Chemical Co. (USA). Docetaxel was obtained from Aventis Pharmaceuticals Inc. (Canada). Clusterin ASO, 21-mer (N oligonucleotide), sequence 5'-CAG CAG CAG AGT CTT CAT CAT-3', fully phosphorothioated, was obtained from La Jolla (USA), TriLink BioTechnologies (USA) and the Nucleic Acid – Protein Service at The University of British Columbia (Canada) (NAPS). Clusterin ASO degradation standards, 20-mer (N-1 oligonucleotide) sequence 5'-CAG CAG CAG AGT CTT CAT CA-3', 19-mer (N-2 oligonucleotide) sequence 5'-CAG CAG CAG AGT CTT CAT C-3' and 18-mer (N-3 oligonucleotide) sequence 5'-CAG CAG CAG AGT CTT CAT-3'; and thymidine internal standard, 25-mer, sequence 5'-TTT TTT TTT TTT TTT TTT TTT TTT T-3' (T_{25}), were all fully phosphorothioated and were obtained from NAPS. Chitosan, biomedical grade, lot 30310A, was obtained from Carbomer, Inc. (USA).

2.2.2 General laboratory materials

N,N,N',N'-tetramethylethylenediamine (TEMED) was obtained from Bio-Rad (USA). Plastic vials with attached caps, 0.5 mL, 1.5 mL and 2 mL, were obtained from Eppendorf (USA) and Sarstedt (USA). HPLC grade acetonitrile, ACS grade EDTA, ACS reagent grade hydrochloric acid (HCl) and 15 mL glass culture tubes with polytetrafluoroethylene lined plastic caps were all obtained from Fisher Scientific Company (USA). N.F. grade boric acid was

obtained from Sel-Win Chemicals Ltd. (Canada). Acrylamide, ammonium persulphate, sodium salt of bromophenol blue (3',3",5',5"-tetrabromophenolsulfonephthalein) and N,N'-methylene bisacrylamide were all electrophoresis reagent grade and obtained from Sigma (USA). ACS reagent grade potassium chloride (KCl), 99% purity iodoacetic acid, sodium bicarbonate, ACS reagent grade sodium bromide (NaBr), sodium hydroxide (NaOH), sodium perchlorate monohydrate ($NaClO_4 \cdot H_2O$), 4,5,4',5'-dibenzo-3,3'-diethyl-9-methyl-thiacarbocyanine bromide ('Stains-all'), 1-ethyl-2-[3-(3-thylnaphthol[1,2-d]thiazolin-2-ylidene)-2-methyl-propenyl] naphthol[1,2-d]thiazolium bromide), reagent grade Trizma® base and reagent grade (tris[hydroxymethyl] aminomethane hydrochloride) (Trizma® hydrochloride) were all obtained from Sigma (USA). All water was distilled and deionized via a Milli-RO Water System obtained from Millipore (USA). Filters with 0.45 μm pore size (types HA and HV) were obtained from Millipore (USA). Filters with a 0.45 μm pore size and Luer lock were obtained from Mandel (USA).

2.2.3 General preparation of stock solutions, buffers and gels

Unless otherwise indicated, all HPLC and CGE stock solutions, buffers and gels were stirred or shaken until clear, filtered through a 0.45 μm filter, placed in glass bottles, capped and stored at 4°C until used.

2.2.4 HPLC

All HPLC methods used HPLC instrumentation consisting of 1 mL sample vials with lids, 600S controller, 600S, 717plus autosampler, 515 HPLC pump and Millenium[32] Version 3.20 software and were obtained from Waters (USA).

2.2.4.1 HPLC of paclitaxel and docetaxel

A Nova-Pak® C_{18} column with 3.9 mm internal diameter x 15 cm length and UV-Vis 486 Tunable Absorbance detector were obtained from Waters (USA). Paclitaxel mobile phase was prepared by mixing 580 mL of acetonitrile, 37 mL of water and 5 mL of methanol. Docetaxel mobile phase was prepared by mixing 500 mL of acetonitrile with 500 mL of water.

2.2.4.2 HPLC of clusterin ASO

A DNAPac™ PA-100 anion exchange column with 4 mm internal diameter x 25 cm length was obtained from Dionex (USA). UV-Vis 486 Tunable Absorbance detector was obtained from Waters (USA). A 1 $mol \cdot L^{-1}$ $NaClO_4$ stock solution was prepared by making 140.5 g $NaClO_4 \cdot H_2O$ up to 1 L. A 1 $mol \cdot L^{-1}$ Tris base stock solution was prepared by making 60.55 g Trizma® base up to 500 mL. A 1 $mol \cdot L^{-1}$ Tris HCl stock solution was prepared by making 78.8 g Trizma® HCl up to 500 mL. A 1 $mol \cdot L^{-1}$ Tris buffer (pH 8) was prepared by adding approximately 300 mL of 1 $mol \cdot L^{-1}$ Tris HCl to a 500 mL flask and making up to pH 8 with 1 $mol \cdot L^{-1}$ Tris base (approximately 50 mL). Mobile phase A and mobile phase B were prepared using modifications to the methods of Agrawal et al. (1990), Metelev and Agrawal (1992) and

Chen et al. (1997) . Mobile phase A was prepared by mixing 10 mL of 1 M Tris buffer (pH 8), 5 mL of 1 M $NaClO_4$, 585 mL filtered water and 400 mL acetonitrile. Mobile phase B was prepared by mixing 10 mL of 1 M Tris buffer (pH 8), 300 mL of 1 M $NaClO_4$, 290 mL filtered water and 400 mL acetonitrile.

2.2.5 Ultraviolet-visible light spectroscopy

Diode array 8452A UV-Vis spectrophotometer was obtained from Hewlett-Packard (USA). UV-Visible ChemStation Rev. A.09.01 software was obtained from Agilent Technologies (USA).

2.2.6 Slab gel electrophoresis

Polyacrylamide slab gel electrophoresis cell, spacers of 0.5, 1 and 1.5 mm thickness and 10-well combs of 0.5, 1 and 1.5 mm thickness were Mini-Protean® II models and were obtained from Bio-Rad (USA). PowerPac 300 powersource was obtained from Biorad (USA). A 10 x TBE stock solution was prepared by weighing out 109 g of Trizma® base, 55 g of boric acid and 7.5 g of EDTA and making up to 1 L with water. A 1 x TBE solution was prepared by making 100 mL of 10 x TBE stock solution up to 1 L with water. Immediately before use, a 19% w/v acrylamide stock solution was prepared by mixing 21 g of urea, 5 mL of 10 x TBE buffer and 23.75 mL 40% w/v acrylamide stock solution and making up to 50 mL with water. A 10% w/v ammonium persulphate stock solution was prepared by adding 1 g of ammonium persulphate and 10 mL of water to a 20 mL glass scintillation vial. A 0.05% w/v bromophenol

blue tracking dye solution was prepared by adding 5 mg of bromophenol blue and 10 mL of formamide to a 20 mL glass scintillation and vial. A 0.01 % w/v 'stains-all' solution was prepared by mixing 0.1 g of 'Stains-all', 300 mL of formamide and 700 mL of 1 x TBE stock solution.

2.2.7 Capillary gel electrophoresis

Plastic 0.5 mL sample vials with blue rubber caps, plastic 0.5 gel vials with metal springs, inserts and grey caps, glass 2.0 mL inlet/outlet buffer/water/waste vials with orange rubber caps, P/ACE MDQ CE with autosampler and P/ACE MDQ UV detector module were obtained from Beckman Coulter, Inc. (USA). DNA capillaries with 100 μm internal diameter, 7 M urea buffer kit, Tris-borate buffer kit and ssDNA 100-R lyophilized polyacrylamide gel were all designated by the supplier as "eCAP™" and were obtained from Beckman Coulter, Inc. (USA). Tris-borate/urea buffer was prepared according to the manufacturer's instructions by adding 135 mL of water and the dry urea from the 7 M urea buffer kit to the Tris-borate buffer kit with stirring. The ssDNA 100-R gel was received as a 1 g lyophilized product and rehydrated by pipetting the appropriate volume of Tris-borate/urea buffer into the gel vial. This was followed by stirring with a magnetic stirrer for approximately five hours (without vacuum) until the gel was completely dissolved in the buffer.

2.2.8 Extraction and desalting of oligonucleotides

AccuBond^{II} ODS-C18 cartridges ("500 mg, 3 mL") and AccuBond^{II} SPE SAX Cartridges ("500 mg, 3 mL") (termed "AccuBond^{II} SAX cartridges") were obtained from Agilent Technologies, Inc. (USA). PD-10 Sephadex™ G-25 M columns were obtained from Amersham Biosciences AB (Sweden). Sep-Pak® Vac Accell™ Plus QMA cartridges ("100 mg, 1 cc"), Sep-Pak® Classic C18 cartridges ("~ 100 mg, ~ 1 mL") and Sep-Pak® Cartridges Vac C_{18} ("500 mg, 3 cc") (termed "Sep-Pack® C_{18} cartridges") were obtained from Waters Corp. (USA). Aqueous nitrocellulose type VS filters with a 27 or 45 mm diameter and 0.025 μm pore size and aqueous type GV filters with a 0.22 μm pore size were obtained from Millipore (USA). Disposable 16 mL lime glass culture tubes were obtained from VWR (USA). Sodium heparin human plasma was obtained from Bioreclamation, Inc. (USA). Nitrogen gas was obtained from Praxair Canada Inc. (Canada). Reacti-Therm III drying/heating block apparatus was obtained from Pierce (USA).

Strong anion exchange load/run buffer (10 mmol·L^{-1} Tris-HCl, 0.5 mol·L^{-1} KCl, 20% v/v acetonitrile, pH 11.0) was prepared by mixing 1.58 g of Tris-HCl, 37.3 g of KCl and 200 mL of acetonitrile and making up to 1 L with water. Strong anion exchange elution buffer (10 mmol·L^{-1} Tris-HCl, 0.5 mol·L^{-1} KCl, 1.0 mol·L^{-1} NaBr, 30% v/v acetonitrile, pH 9.0) was prepared by mixing 1.58 g of Tris-HCl, 37.3 g of KCl, 102.9 g NaBr and 300 mL of acetonitrile and making up to 1 L with water. Dilution buffer (10 mmol·L^{-1} Tris-HCl, 0.5 mol·L^{-1} KCl, 1.0

mol·L^{-1} NaBr, pH 9.0) was prepared by mixing 1.58 g of Tris-HCl, 37.3 g of KCl and 102.9 g NaBr and making up to 1 L with water. The three buffers' pHs were adjusted by dropwise addition of 10 mol·L^{-1} NaOH and/or 10 mol·L^{-1} HCl solutions.

2.3 METHODS

2.3.1 Paclitaxel and docetaxel HPLC assays

Paclitaxel was quantitated by HPLC based on a modification of the procedure previously developed and qualified by our research group (Burt et al., 1995; Liggins et al., 2000). Paclitaxel was extracted by adding 1 mL of dichloromethane to each aqueous sample and shaking for 5 s to allow the paclitaxel to partition into the organic phase. The aqueous phase was discarded and the organic phase dried at 60° under a gentle stream of nitrogen gas. The residue was dissolved in 1 mL of acetonitrile:water v/v 60:40 by vortexing for 10 s. The solution was then transferred into HPLC sample vials and capped. Paclitaxel was assayed at ambient temperature with an injection volume of 20 µL and the paclitaxel mobile phase (acetonitrile:water:methanol 58:37:5 v/v) flowing at a rate of 1 mL·min^{-1}. Detection was via UV-Vis at a wavelength of 232 nm. The modification of the published procedure concerned the partial conversion of paclitaxel in aqueous media to 7-epitaxol (Ringel and Horwitz, 1987; Chmurny et al., 1992). Paclitaxel and 7-epitaxol have similar extinction coefficients, so the areas under both the paclitaxel and 7-epitaxol peaks were combined to determine the total quantity of paclitaxel being assayed. The paclitaxel HPLC assay was further modified and adapted for

docetaxel analysis by changing the mobile phase from acetonitrile:water:methanol 58:37:5 v/v to acetonitrile:water 50:50 v/v. Calibration curves were constructed for the paclitaxel and docetaxel HPLC assays using a minimum of five standards and a blank. The HPLC system was calibrated each day of use by preparing calibration curves similar to those used during qualification of the assays. Linearity of the calibration curves was measured and expressed as R^2.

2.3.2 Oligonucleotide ultraviolet-visible light spectroscopy assay

UV-Vis is commonly used to quantitate oligonucleotide stock solutions due to the accuracy of direct weighing of solid samples being hampered by hydration of samples in the solid state (due to the ionic nature of the molecules) and due to the potential of salt contamination. The optical density (OD) is the determination of absorbance and is used to quantify oligonucleotides in solution as reviewed by Schweitzer and Engels (Schweitzer and Engels, 1997). According to Beer's Law (Heirwegh, 1987)

$$OD = \varepsilon \cdot c \cdot l \qquad \textbf{Equation 10}$$

where ε is the extinction coefficient, c is the concentration and l is the path length of the cuvette. The calculation of the extinction coefficient for single strand oligonucleotides can be made (Gray et al., 1995) by estimating the stacking interaction between bases and taking this estimation into account by multiplying the sum of the individual extinction coefficients by 0.9 (Schweitzer and

Engels, 1997). Using one centimeter cuvettes and a volume of one milliliter, the extinction coefficient is thus calculated according to the following equation (Schweitzer and Engels, 1997)

$$\varepsilon = ((A \cdot 15.34)\,(G \cdot 12.16)\,(T \cdot 8.70)\,(C \cdot 7.60)) \cdot 0.9 \cdot 1000 \qquad \textbf{Equation 11}$$

where A, G, T and C correspond to the numbers of each of the specific bases, respectively, in the oligonucleotide and the units are $mol \cdot L^{-1} \cdot cm^{-1}$. The concentration of an oligonucleotide in solution is thus obtained by rearranging the above equation to (Schweitzer and Engels, 1997)

$$c = (OD_{260}/\varepsilon) \cdot l \qquad \textbf{Equation 12}$$

The absorbance maximum of oligonucleotides is generally found at a wavelength of 260 nm (the minimum at approximately 230 nm) and thus the OD at this wavelength is referred to as the OD_{260} (Schweitzer and Engels, 1997). Calibration curves were constructed from OD_{260} values plotted against serial dilutions of clusterin ASO stock solutions to ensure that the OD_{260} values correlated with concentration. Linearity of the calibration curves was measured and expressed as R^2.

2.3.3 Clusterin ASO HPLC assay

The clusterin ASO anion exchange HPLC methods were adapted from Agrawal et al. (1990), Metelev and Agrawal (1992) and Chen et al. (1997) . The initial clusterin ASO anion exchange HPLC assay was performed in the following manner. Clusterin ASO was assayed at ambient temperature using an injection volume of 20 μL. The mobile phase was started with a flow rate of 1 $mL \cdot min^{-1}$ and 100% mobile phase A. Over 10 min using linear gradients, the

mobile phase was changed to a flow rate of 2 $mL \cdot min^{-1}$ and 100% mobile phase B. Between 11 to 12 min using linear gradients, the flow rate was increased to 2.5 $mL \cdot min^{-1}$ and the mobile phase changed to 100% mobile phase A. These conditions were used for the remainder of each run. The detection wavelength was 260 nm and the total run time was 15 min per sample.

The sample run time of the clusterin ASO HPLC assay was decreased to 8.5 min by increasing the mobile phase flow rate to 2 $mL \cdot min^{-1}$ during the first 10 min, maintaining a flow rate of 2 $mL \cdot min^{-1}$ during the remainder of the run and using a non-linear, "accelerated" gradient as the initial mobile phase (100% mobile phase A) was changed to 100% mobile phase B. The final clusterin ASO HPLC assay was performed as follows. The mobile phase started with a 100% mobile phase A and over 5.5 min using a non-linear "accelerated" gradient the mobile phase was changed to 100% mobile phase B and this was maintained until 7.0 min. Between 7.0 and 7.1 min the mobile phase was rapidly changed to 100% mobile phase A and this was maintained for the remainder of each run. The total run time was 8.5 min per sample.

2.3.4 Slab gel electrophoresis of clusterin ASO and degradation products

Slab gel electrophoresis was used as a method to check the purity of received oligonucleotides and to verify samples analyzed using capillary gel electrophoresis. Polyacrylamide gel electrophoresis (PAGE) slabs were prepared by transferring 50 mL of 19% w/v acrylamide stock solution and pipetting 300 µL of 10% w/v ammonium persulphate stock solution and 30 µL of N,N,N',N'-tetramethylethylenediamine (TEMED) into a 100 mL beaker

while stirring. The gel was immediately pipetted between two sets of glass plates with 1.5 mm spacers. The sample well former (comb) was inserted and the gel allowed to polymerize for approximately 45 min. The apparatus was placed in an ice bath and the gels were equilibrated in TBE buffer at constant voltage of 250 V for 30 min. Each well was loaded with 10 μL of 0.016 $\mu g \cdot \mu L^{-1}$ of appropriate oligonucleotide (0.16 μg of each appropriate oligonucleotide per well). The gels were run at a constant voltage of 250 V until the bromophenol blue tracking dye reached the bottom of the gels and then for a further 30 min (approximately 2.5 h in total). The gels were stained by incubating them in approximately 200 mL of the 0.01% w/v 'stains-all' stock solution for 1 h. The gels were de-stained by rinsing approximately every 10 min for 2 hours with water.

2.3.5 Clusterin ASO capillary gel electrophoresis assay

The procedures for CGE analysis were adapted and modified from DeDioniso et al. (1993), Leeds et al. (1996) and Chen et al. (1997) . A series of experiments were performed to develop and optimize the capillary length, gel concentration, capillary temperature, voltage and equilibration period for quantitation of 21-mer clusterin ASO (N oligonucleotide) and its 20-, 19- and 18-mer degradation products (N-1, N-2 and N-3 oligonucleotides, respectively). The CGE assay conditions are summarized in Table 2.1.

Table 2.1 Summary of parameter settings used to achieve optimal resolution of 21-mer clusterin ASO (N oligonucleotide) and its 20-, 19- and 18-mer (N-1, N-2 and N-3 oligonucleotides, respectively) degradation product standards.

Parameter	Optimal setting for resolution	Setting used for analysis
Capillary length to detector (cm)	50	50
Electrokinetic injection	30 s at 10 kV	30 s at 10 kV
Gel concentration (% w/v)	15 to 17	16.7
Capillary temperature (°C)	60[b]	30
Voltage ($V \cdot cm^{-1}$)	300	350
Equilibration time (min)	0 to 90	0

[a] Capillary length to detector of 50 cm provides a total capillary length 60.2 cm.
[b] A temperature of 60 °C gave baseline resolution and a run time of ≤ 35 min. However, this temperature stressed various components of the instrumentation.
[c] Optimal voltage for a running temperature of 30 °C was 350 $V \cdot cm^{-1}$.

Before use, the ssDNA 100-R gel was stirred with a polytetrafluoroethylene coated magnetic stir bar for 5 min. A 200 µL aliquot of the gel was then transferred to a 0.5 mL plastic vial (with plastic inserts, metal spring and grey cap) and centrifuged for 3 min at 2,000 rpm in GS-6 centrifuge (Beckman Coulter, Inc., USA). Standards of 75 µL volume were usually diluted with 75 µL of T_{25} internal standard at a concentration of 2 $\mu g \cdot mL^{-1}$ in 0.5 mL plastic vials (with blue rubber caps) and capped. This provided a final volume of 150 µL, a twice-fold dilution of the standards and a final T_{25} internal standard concentration of 1 $\mu g \cdot mL^{-1}$. The relative retention time was taken as the quotient of the retention time of the analyte divided by the retention time of T_{25}. The relative peak area was taken as the quotient of the peak area of the analyte divided by the peak area of T_{25}, adjusted for the concentrations of the analyte and the T_{25}.

The capillary was packed with fresh gel after approximately 2 to 4 hours of assaying, by rinsing the capillary for 15 min with water at approximately 600 kPa and filling with gel for 20 min at approximately 400 kPa. After packing the capillary with fresh gel and between sample injections, the capillary ends were rinsed by dipping them in water for 30 seconds. Samples were stored at 4°C until electrokinetic injection onto the capillary. Samples were separated over 80 to 110 min and detected at a wavelength of 254 nm.

The following procedure for CGE analysis were adapted and modified from Williams et al. (2003). After replacing the gel in the capillary with fresh gel, the effective time to run each sample was decreased by injecting samples every 12 min rather than waiting 80 to 110 min for the first sample to elute. Following the sixth injection, the samples were separated for 80 to 110 min. We termed this method of piggy-backing samples on effectively the same run, as the "train method". The peaks for the oligonucleotides were detected on the resulting chromatogram of the sixth injection before packing the capillary with fresh gel again.

2.3.6 Oligonucleotide extraction and desalting method

Although a CGE method was developed and qualified for 21-mer clusterin ASO and its 20-, 19- and 18-mer degradation products differing in length by only nucleotide base, even low concentrations of salt inhibited effective electrokinetic injection of the samples onto the capillary and interfered with UV-Vis detection of the samples (Leeds and Cummins, 2001). Method development studies for the extraction and desalting of 21-mer clusterin ASO and its 20-

, 19- and 18-mer degradation product standards from plasma and serum were carried out using three basic steps: 1) extraction from the biological matrix sample using a strong anion exchange cartridge, 2) desalting of the sample using a reverse phase cartridge and 3) a final desalt step using a filter or membrane. The strong anion exchange load/run buffer, strong anion exchange elution buffer and the dilution buffer were adapted from Leeds et al. (1996). A number of different strong anion exchange cartridges, reverse phase cartridges and filters or membranes were tested in various combinations using T_{25} as a model oligonucleotide spiked into water until a method was found that extracted the oligonucleotide and removed enough of the salt so that the sample could be electrokinetically injected onto a capillary and detected by UV-Vis for CGE analysis. After a preliminary method was developed, the volumes and concentrations of the various buffers, acetonitrile solution and water were varied to increase the amount of oligonucleotide extracted and decrease the salt content in the final sample. Samples were analyzed by HPLC at each step of the extraction to determine if low or zero absorbance readings observed via CGE were due to a lack of oligonucleotide being extracted, or due to salt in the samples. Following optimization of the extraction and desalting of T_{25} spiked into water at different concentrations, the oligonucleotide was spiked into both rabbit and human plasma and extracted and desalted. The method for extracting and desalting oligonucleotides from plasma is detailed below.

AccuBond II SPE SAX cartridges were equilibrated with 1 mL acetonitrile, followed by 1 mL water and finally 3 mL strong anion exchange load/run buffer. Plasma samples

(volume range of 0.1 to 1 mL) were spiked with 0.5 mL of T_{25} internal standard at a concentration of 2 $\mu g \cdot mL^{-1}$ (1 μg of T_{25}) and vortexed for 10 seconds. Samples were diluted with 5 mL of strong anion exchange loading/running buffer and loaded onto separate AccuBond II SPE SAX cartridges. The AccuBond II SPE SAX cartridges were rinsed with 3 mL strong anion exchange load/run buffer. The eluent was collected from the AccuBond II SPE SAX cartridges with 3 mL of strong anion exchange elution buffer.

Sep-Pak® Vac C18 cartridges were equilibrated with 1 mL acetonitrile, followed by 1 mL water and finally 3 mL of dilution buffer. The eluent from the AccuBond II SPE SAX cartridges was diluted with 6 mL of dilution buffer to lower the acetonitrile concentration in the mixture to 10% and loaded onto Sep-Pak® Vac C18 cartridges. Sep-Pak® Vac C18 cartridges were rinsed with 5 mL water and the eluent collected with 4 mL of 20% acetonitrile solution.

The eluent from the Sep-Pak® Vac C18 cartridges was dried under nitrogen gas at 60°C and the samples reconstituted with 100 µL water and vortexing. Samples were transferred onto separate Type VS filters floating on 2 L water in a 2 L beaker. After 30 min, 75 µL of each sample was transferred into a 0.5 mL CGE sample vial (blue rubber caps), diluted two-fold with 75 µL water, capped and assayed by CGE.

2.3.7 Qualification of clusterin ASO HPLC and capillary gel electrophoresis assays

The retention time, specificity, linearity, range, accuracy, precision (injection repeatability, intra-day precision, inter-day precision), detection limit and quantitation limit were

determined for clusterin ASO using the HPLC assay and for 21-mer clusterin ASO and its 20-, 19- and 18-mer degradation products using the CGE assay.

2.3.8.1 Specificity

Specificity of the HPLC and CGE assays was determined by first determining the oligonucleotide retention time and relative retention time compared to internal standard, respectively. Representative chromatograms of blank replicates (HPCL) and internal standard spiked replicates (CGE) were then observed for a lack of peaks at the retention time and relative retention time, respectively. Specificity of the CGE assay was further investigated with available impurities by spiking samples with various combinations of T_{25} internal standard, 21-mer clusterin ASO standard and clusterin ASO 20-, 19- and 18-mer degradation product standards and demonstrating that the assay result was unaffected by the presence of oligonucleotides differing in length by only 1 mer. In addition, specificity of the CGE assay was demonstrated by incubating clusterin ASO in 50% fetal bovine serum to produce degradation products (impurities) and demonstrating that the assay separated the anticipated degradation products.

2.3.8.2 Linearity

Linearity was evaluated over a range of a minimum of 5 concentrations by preparing and assaying serial dilutions of sets of standards. The instrumentation signals were plotted against the standards' concentrations and linearity was expressed as the coefficient of determination (R^2) of a least squares linear regression line. For the HPLC assay, clusterin ASO

was dissolved in water over a concentration of approximately 0.5 to 50 $\mu g \cdot mL^{-1}$. Four sets of calibration curves were prepared on each of four days, to produce sixteen calibration curves and a single standard curve consisting of each of the sixteen standards data points for each concentration. For the CGE assay, separate calibration curves were prepared for each of N-3, N-2, N-1 and N oligonucleotides standards dissolved in water over a concentration of approximately 0.07 to 6 $\mu g \cdot mL^{-1}$ and spiked with T_{25}. For each oligonucleotide standard, four sets of calibration curves were prepared on each of two days to produce eight calibration curves and a single standard curve consisting of each of the eight standards data points for each concentration.

2.3.8.3 Range

The range was determined from the linearity studies and established by confirming that the assay provided an acceptable degree of linearity, accuracy and precision within the specified range.

2.3.8.4 Accuracy

Accuracy of the HPLC and CGE assays was determined by assembling a calibration curve and comparing three different standards at each concentration against the calibration curve for four days and two days, respectively. Accuracy was expressed in terms of the deviation (bias) of each of the three standards and their mean bias compared to the daily calibration curve.

2.3.8.5 Precision

Injection repeatability precision was expressed in terms of the coefficient of variation (CV) of the mean of four repeat injections of the same standard on one day. Intra-day precision was expressed in terms of the CV of the mean of the four standards data points for each concentration, on each of four days for the HPLC assay and on each of two days for the CGE assay. Inter-day precision was expressed in terms of the mean of all standards data points collected for each concentration. For the HPLC assay, sixteen standards data points were collected for each clusterin ASO concentration over four days. For the CGE assay, nine standards' data points were collected for each concentration over three days for 21-mer clusterin ASO and its 20-, 19- and 18-mer degradation product standards.

2.3.8.6 Detection limit

The detection limit was calculated from the equation (ICH, 1996)

$$\text{detection limit} = 3.3\sigma / s \qquad \textbf{Equation 13}$$

where σ is the standard deviation of the y-intercepts of the sixteen and nine calibration curves for the HPLC and CGE assays, respectively, and s is the mean slope of the sixteen and nine calibration curves, respectively.

2.3.8.7 Quantitation limit

The quantitation limit was calculated from the equation (ICH, 1996)

$$\text{quantitation limit} = 10\sigma / s \qquad \textbf{Equation 14}$$

and subsequently qualified by the analysis of a number of samples prepared at a concentration near the quantitation limit.

2.4 RESULTS

2.4.1 Paclitaxel and docetaxel HPLC assays

A representative HPLC calibration curve for paclitaxel is given in Figure 2.2. The paclitaxel calibration curves, constructed during the initial qualification of the assay and on each day of sample analysis, all had R^2 values of greater than 0.99 based on standards ranging from approximately 0.8 to 50 $\mu g \cdot mL^{-1}$.

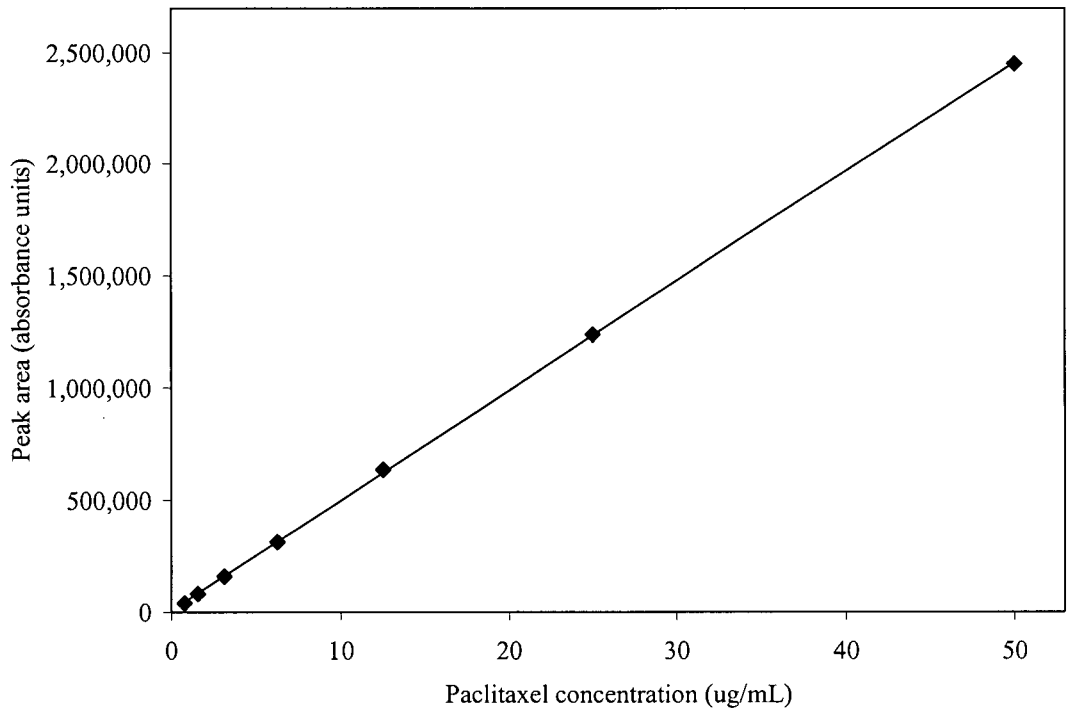

Figure 2.2 Representative paclitaxel HPLC calibration curve.

Regression analysis parameters ($y = mx + b$, R^2):
$m = 48{,}970$, $b = 7{,}596$, $R^2 = 1.000$

A representative HPLC calibration curve for docetaxel is given in Figure 2.3. The docetaxel calibration curves, constructed during the initial qualification of the assay and on each day of sample analysis, all had R^2 values of greater than 0.98 based on standards ranging from approximately 1 to 100 $\mu g \cdot mL^{-1}$.

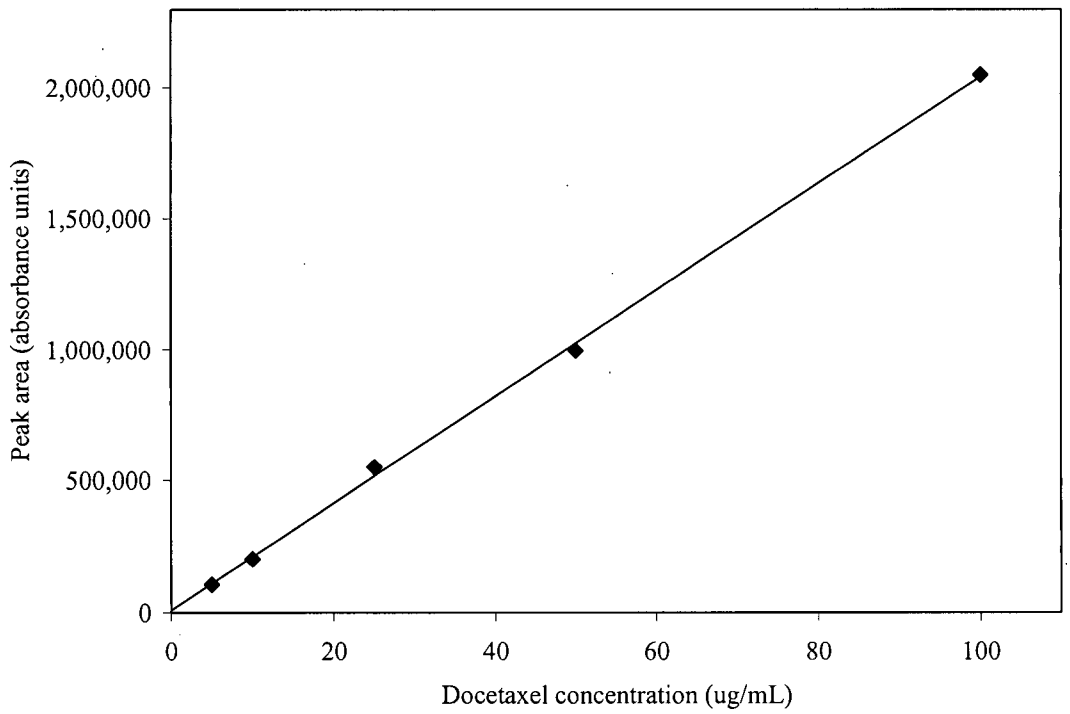

Figure 2.3 Representative docetaxel HPLC calibration curve.

Regression analysis parameters ($y = mx + b$, R^2):
$m = 20{,}340$, $b = 6{,}874$, $R^2 = 0.999$

2.4.2 Oligonucleotide ultraviolet-visible light spectroscopy assay

Curves were constructed from OD_{260} values plotted against clusterin ASO concentrations to ensure that the OD_{260} values correlated with a decrease in concentration as the ASO stock solutions were diluted. A representative OD_{260} curve for clusterin ASO is given in Figure 2.4. The curves constructed from the OD_{260} correlated with clusterin ASO concentrations and had R^2 values greater than 0.99 based on an absorbance range of approximately 0.01 to 1.

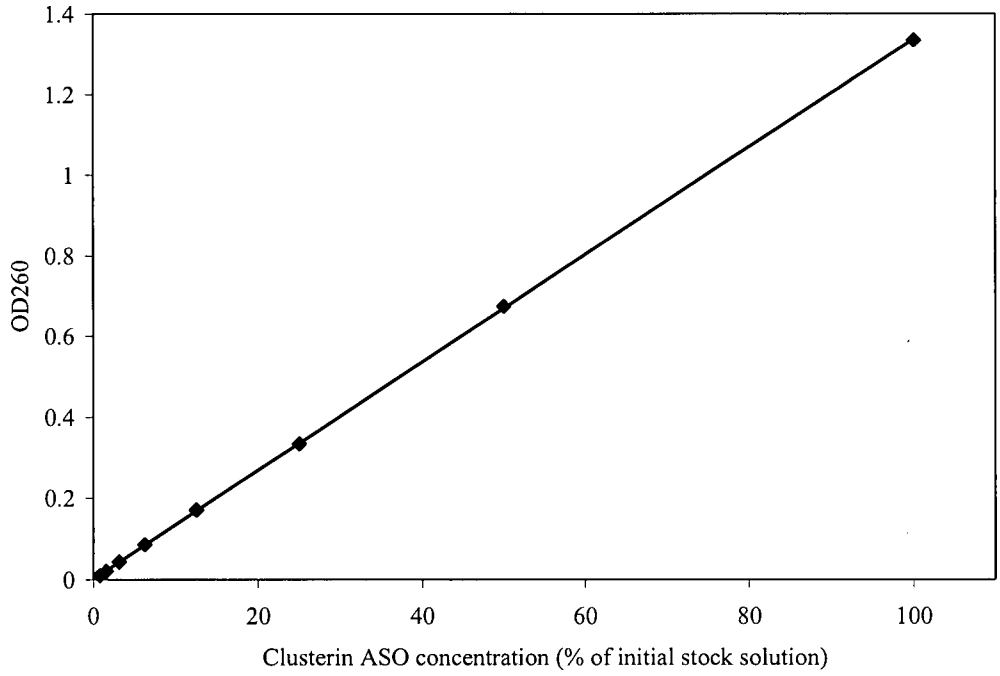

Figure 2.4 Representative curve correlating optical density at a wavelength of 260 nm (OD_{260}) to serial dilutions of clusterin ASO stock solution. From Equations 11 and 12, it was calculated that the initial stock solution (OD_{260} = 1.342) had a clusterin ASO concentration of 39.3 $\mu g \cdot mL^{-1}$.

Regression analysis parameters ($y = mx + b$, R^2):
$m = 0.0134$, $b = 0.00152$, $R^2 = 1.000$

2.4.3 Clusterin ASO HPLC assay

The specificity, linearity, accuracy and precision were determined for the clusterin ASO HPLC assay within the range of 1 to 50 $\mu g \cdot mL^{-1}$ and are summarized in Table 2.2. Appendix 1 provides the detailed tables and figures from which Table 2.2 was prepared. Representative blank and clusterin ASO spiked chromatograms are shown in Figures A1.1 and A1.2, respectively. Sixteen calibration curves (four a day for four days) were combined and plotted as a standard curve. A representative calibration curve and the standard curve are given in Figures A1.3 and A1.4, respectively. The accuracy of three sets of standards was determined against a daily calibration curve on each day for four days and is summarized in Tables A1.1 through A1.4. Summaries of intra-day and inter-day precision for the calibration curves are shown in Tables A1.5 and A1.6, respectively.

Table 2.2 Summary of values of qualification parameters for clusterin ASO HPLC assay.

Qualification parameter	Result
Specificity – retention time (min)	6.3 ± 0.1[a]
Specificity – interfering peaks	None observed
Linearity – 16 calibration curves (R^2)	All ≥ 0.999
Linearity – combined standard curve (R^2)	1.000
Range	1 to 50 $\mu g \cdot mL^{-1}$
Accuracy – bias (%)	All < 15, except 1 $\mu g \cdot mL^{-1}$ was ≤ 25
Accuracy – mean bias (%)	All < 15, except 1 $\mu g \cdot mL^{-1}$ was ≤ 20
Precision - injection repeatability (% CV)	12.6
Precision - intra-day (% CV)	All < 15, except 1 $\mu g \cdot mL^{-1}$ was ≤ 16
Precision - inter-day (% CV)	All < 15, except 1 $\mu g \cdot mL^{-1}$ was = 15
Detection limit ($\mu g \cdot mL^{-1}$)	0.316
Quantitation limit ($\mu g \cdot mL^{-1}$)	0.958

[a] The initial clusterin ASO HPLC assay had a run time of 15 min with a retention time of 11.6 ± 0.1 min. During the project the run time and retention times were shortened to 8.5 and 6.3 ± 0.1 min, respectively, by increasing the mobile phase flow rate and using an "accelerated" gradient to change from mobile phase A to mobile phase B.

2.4.4 Clusterin ASO slab gel electrophoresis assay

Slab gel electrophoresis (shown in Figure 2.5) provided separation between full-length 21-mer clusterin ASO and its 20-, 19- and 18-mer degradation product standards.

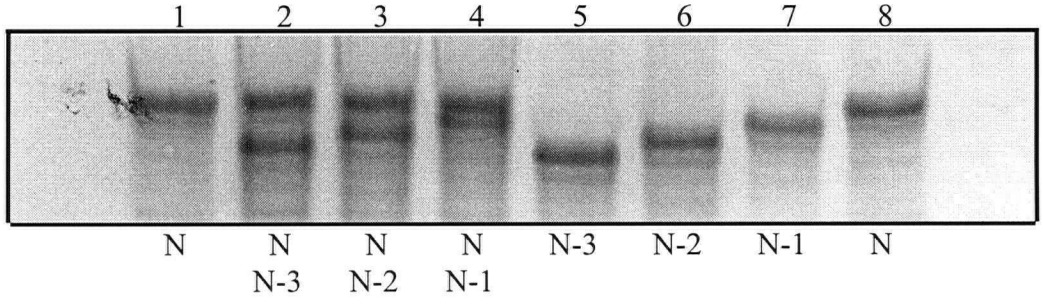

Figure 2.5 'Stains-all' stained denaturing 19% w/v polyacrylamide gel. Lanes 1 and 8: 21-mer clusterin ASO (N oligonucleotide). Lanes 5, 6 and 7: 18-mer (N-3 oligonucleotide), 19-mer (N-2 oligonucleotide) and 20-mer degradation standards (N-1 oligonucleotide), respectively. Lane 2: N and N-3. Lane 3: N and N-2. Lane 4: N and N-1. All oligonucleotides were loaded at 0.16 µg per appropriate lane.

2.4.5 Clusterin ASO capillary gel electrophoresis assay

The specificity, linearity, accuracy and precision were determined for the CGE assay for 21-mer clusterin ASO and its 20-, 19- and 18-mer degradation product standards within the range of 0.13 to 6.3 $\mu g \cdot mL^{-1}$ and are summarized in Table 2.3. Appendix 2 provides the detailed tables and figures from which Table 2.3 was prepared. Summaries of the characteristics of the relative retention times of N-3, N-2, N-1 and N oligonucleotides to the T_{25} internal standard retention time are shown in Table A2.1. Representative CGE chromatograms of blanks and N-3, N-2, N-1 and N oligonucleotide standards are shown in Figures A2.1 through A2.4. Representative chromatograms of N-1 spiked with potentially peak-interfering N-2 and N oligonucleotides, are shown in Figures A2.5 and A2.6. Eight calibration curves (four a day for two days) were combined and plotted as a standard curve for each N-3, N-2, N-1 and N oligonucleotide. Representative calibration curves of N-3, N-2, N-1 and N oligonucleotides are shown in Figures A2.7 through A2.10, respectively, and their standard curves are shown in Figures A2.11 through A2.14, respectively. A representative calibration curve prepared from N-1 oligonucleotide standard spiked with potentially peak-interfering N-2 and N oligonucleotides is given in Figure A2.15. The accuracy of three sets of standards for each N-3, N-2, N-1 and N oligonucleotide was determined against a daily calibration curve on each day for two days and is summarized in Tables A2.2 through A2.5, respectively. Summaries of intra-day and inter-day precision for the calibration curves are shown in Tables A2.6 and A2.7, respectively. The

detection limits and quantitation limits for the N-3, N-2, N-1 and N oligonucleotides are summarized in Table A2.8.

Table 2.3 Summary of values of qualification parameters for clusterin ASO CGE assay. The results are the range of values for 21-mer clusterin ASO (N oligonucleotide) and its 20-, 19- and 18-mer (N-1, N-2 and N-3 oligonucleotides) degradation product standards. Eight calibration curves were determined for each oligonucleotide (four a day on each of two days). T_{25} oligonucleotide was used as an internal standard.

Qualification parameter	Result
Specificity –relative retention time (min)	0.879 (N-3); 0.890 (N-2); 0.908 (N-1); 0.925 (N)[a]
Specificity – interfering peaks	None observed[b]
Linearity – 8 calibration curves (R^2)	All $\geq$ 0.958
Linearity – combined standard curve (R^2)	0.993
Range	0.13 to 6.3 $\mu g \cdot mL^{-1}$
Accuracy – bias (%)	All $\leq$ 25, except as noted[c]
Accuracy – mean bias (%)	All $\leq$ 21
Precision - intra-day (% CV)	All $\leq$ 20, except 0.2 $\mu g \cdot mL^{-1}$ was $\leq$ 24
Precision - inter-day (% CV)	All $\leq$ 20
Detection limit ($\mu g \cdot mL^{-1}$)	0.035 to 0.044
Quantitation limit ($\mu g \cdot mL^{-1}$)	0.107 to 0.133

[a] The coefficient of variation (CV) was $\leq$ 1% for all concentrations and oligonucleotides, except for N-2 at 1.8 $\mu g \cdot mL^{-1}$, which had a CV of 2.1%.

[b] Approximately $\geq$ 75% baseline separation was observed between oligonucleotides differing in length by 1 mer.

[c] N-3, first standard at 0.6 $\mu g \cdot mL^{-1}$ and second standard at 1.8 $\mu g \cdot mL^{-1}$ had CVs of 38% and 27%, respectively. N-2, first standard at 0.2 $\mu g \cdot mL^{-1}$ had a CV of 34%. N, second standard at 0.6 $\mu g \cdot mL^{-1}$ and third standard at 0.2 $\mu g \cdot mL^{-1}$ had CVs of 29 and 41%, respectively.

2.4.6 Extraction and desalting of clusterin ASO

The extraction and desalting of 1.5 $\mu g \cdot mL^{-1}$ T_{25} oligonucleotide spiked in rabbit and human plasma samples and assayed by CGE, resulted in sharp peaks as shown in Figure 2.6. To illustrate the utility of the extraction and desalting method combined with the CGE assay, 21-mer clusterin ASO was spiked in 50% fetal bovine serum and incubated at 37 °C for 24 hours. The CGE chromatograms for samples taken at 1 min, 2 hours and 24 hours, are given in Figure 2.7. The full-length 21-mer clusterin ASO and its 20-, 19- and 18-mer degradation products can be clearly observed in Figure 2.7C.

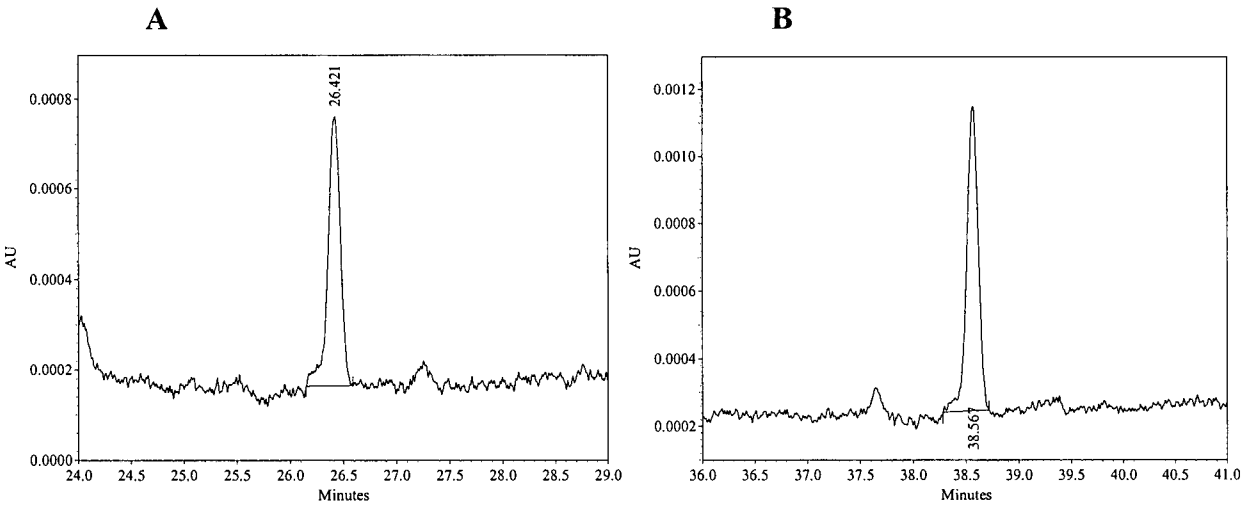

Figure 2.6 Capillary gel electrophoresis chromatogram following the extraction and desalting of T_{25} spiked at a final concentration of 1.5 $\mu g \cdot mL^{-1}$. into **A)** rabbit plasma and **B)** human plasma.

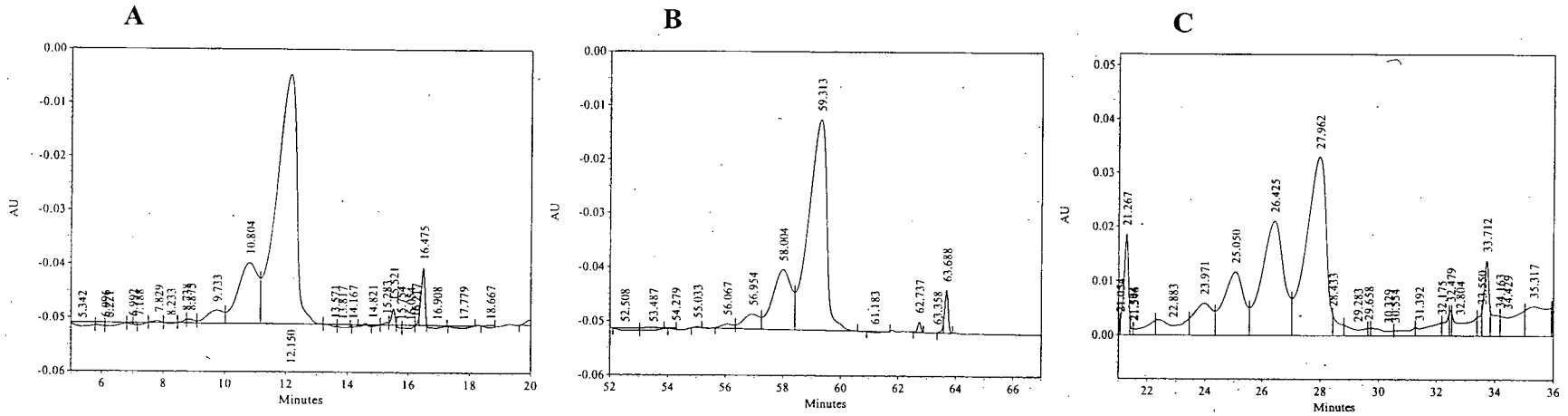

Figure 2.7 CGE chromatograms following the incubation of 21-mer clusterin ASO in 50% fetal bovine serum at 37 °C. Samples were spiked with T_{25} internal standard immediately before extraction and analysis. **A)** Incubation for 1 min. Peak retention times of 9.7, 10.8, 12.1 and 16.5 min represent 19-mer degradation product (N-2 oligonucleotide), 20-mer degradation product (N-1 oligonucleotide), 21-mer clusterin ASO (N oligonucleotide) and T_{25} internal standard, respectively. **B)** Incubation for 2 h. Peak retention times of 57.0, 58.0, 59.3 and 63.5 min represent N-2, N-1, N and T_{25}, respectively. **C)** Incubation for 24 h. Peak retention times of 24.0, 25.0, 26.4, 28.0 and 33.7 min represent 18-mer degradation product (N-3 oligonucleotide), N-2, N-1, N and T_{25}, respectively.

2.5 DISCUSSION

Paclitaxel and docetaxel HPLC calibration curves (Figures 2.2 and 2.3) indicated linearity over paclitaxel and docetaxel concentration ranges of 1 to 50 $\mu g \cdot mL^{-1}$ and 1 to 100 $\mu g \cdot mL^{-1}$, respectively.

The clusterin ASO UV-Vis OD_{260} method demonstrated linearity (Figure 2.4) over the absorbance range of 0.01 to 1 (equivalent to 0.293 to 29.3 $\mu g \cdot mL^{-1}$ clusterin ASO). The specificity, linearity, accuracy and precision data for the clusterin ASO HPLC assay over the concentration range of 1 to 50 $\mu g \cdot mL^{-1}$ are summarized in Table 2.2. Except where noted, CVs were less than 15% and were taken to be acceptable (Shah, 1992). The quantitation limit was determined from Equation 14 to be 0.958 $\mu g \cdot mL^{-1}$ and this has the same order of magnitude as the lowest concentration of standards, 1 $\mu g \cdot mL^{-1}$, whose inter-day precision, bias and mean bias were acceptable. The quantitation limit from this study was thus taken to be 1 $\mu g \cdot mL^{-1}$.

The slab gel electrophoresis method developed in this work separated 21-mer clusterin ASO and its 20-, 19- and 18-mer degradation product standards (Figure 2.5), differing in length by only one nucleotide base. This method was useful qualitatively to support the results obtained while developing the CGE method for separation and quantitation of these oligonucleotides differing in length by only one nucleotide base.

Using the method of 12 min separation for the first five electrokinetic injections after replacing the gel in the capillary with fresh gel and a separation time of greater than 80 min for

the sixth electrokinetic injection before repacking the capillary with fresh gel, the mean time per sample was less than 40 min. Williams et al. (2003) obtained a run time of approximately 20 min per sample, however, our method provided for greater resolution between oligonucleotides differing in length by only 1 mer.

The specificity, linearity, accuracy and precision data determined for the CGE assay for 21-mer clusterin ASO and its 20-, 19- and 18-mer degradation product standards over the concentration range of 0.13 to 6.3 $\mu g \cdot mL^{-1}$ are summarized in Table 2.3. We achieved approximately 75% baseline separation when oligonucleotides differing in length by 1 mer were co-injected. This allowed for individual oligonucleotides to be readily quantitated (Figures A2.5 and A2.6). The CVs for the accuracy data, with a very few exceptions, were equal to or less than 25% (Tables A2.2 through A2.5), which was a little higher than the preferred 15 to 20% suggested by Shah et al. (1992). Hence, a calibration curve was obtained each day that samples were run. Intra-day and inter-day precisions generally showed CVs less than 20% (Tables A2.6 and A2.7, respectively). The quantitation limits were determined from Equation 14 to be less than or equal to 133 $ng \cdot mL^{-1}$. The quantitation limit for this method was thus taken to be 0.13 $\mu g \cdot mL^{-1}$. von Brock et al. (2003) coupled CGE to an electrospray ionization-mass spectrometer and obtained a lower limit of detection, but did not show the separation of oligonucleotides differing in length by only 1 mer.

By using strong anion exchange extraction, reverse-phase desalting and filter/osmosis desalting steps in sequence to prepare samples, oligonucleotides could be extracted from plasma.

Analyzing these preparations via CGE provided single-base separation (Figure 2.7) and quantitation of the full-length 21-mer clusterin ASO and its 20-, 19- and 18-mer degradation products. This method provided for the extraction of larger volumes of plasma than other reported methods (Leeds et al., 1996). The extraction and CGE assay of 21-mer clusterin ASO and its 20-, 19- and 18-mer degradation products were determined to be acceptable for future studies over the range of 0.13 to 6.3 $\mu g \cdot mL^{-1}$.

2.6 CONCLUSIONS

1. The paclitaxel and docetaxel HPLC methods were acceptable with linear ranges of 1 to 50 and 1 to 100 $\mu g \cdot mL^{-1}$, respectively.
2. An anion exchange HPLC method was developed and qualified for the analysis of clusterin ASO in the range of 1 to 50 $\mu g \cdot mL^{-1}$. A CGE method was developed and qualified for the analysis of 21-mer clusterin ASO and its 20-, 19- and 18-mer oligonucleotide degradation products in plasma in the range of 0.13 to 6.3 $\mu g \cdot mL^{-1}$.

3. PHYSICOCHEMICAL CHARACTERIZATION AND DRUG RELEASE[2]

3.1 INTRODUCTION

In Chapter 1 of this thesis, we have discussed the selection of clusterin ASO and paclitaxel or docetaxel as suitable combination therapies for the intratumoral treatment of localized prostate tumors. Prostate cancer patients have demonstrated modest responses following intravenous administration of paclitaxel (Kuruma et al., 2003) or docetaxel (Sinibaldi et al., 2002). Furthermore, the use of clusterin ASO resulted in increased sensitivity of PC-3, LNCaP and Shionogi prostate tumors in mice to paclitaxel (Miyake et al., 2000b).

There are very few studies of delivery methods that might more effectively locate and maintain therapeutic concentrations of oligonucleotides, including ASOs, at the target disease site. ASOs targeted against c-myc and incorporated into triblock copolymer poly(ethylene oxide-block- propylene oxide-block- ethylene oxide) (poloxamer 407) gel were released *in vitro* over several days, whereas the same ASOs incorporated into poly(ethylene-co-vinyl acetate) (EVA) matrices were released *in vitro* over several weeks (Edelman et al., 1995). When these formulations were implanted perivascularly in a rat carotid artery model of restenosis, only the EVA formulation demonstrated efficacy after two weeks, indicating that the efficacy of ASOs

---

[2] A version of Figure 3.9 of this Chapter has been published (Springate, CMK, JK Jackson, ME Gleave and HM Burt. Efficacy of an intratumoral controlled release formulation of clusterin antisense oligonucleotide complexed with chitosan containing paclitaxel or docetaxel in prostate cancer xenograft models. *Cancer Chemother Pharmacol* (2005) 56:239-247). A version of the remainder of this Chapter is in preparation for submission.

may be influenced by their duration of release from a polymeric implant (Edelman et al., 1995). The most commonly used polymer for preparing controlled release delivery systems for ASOs has been PLGA. De Rosa et al. (2002) incorporated oligonucleotides into PLGA microspheres in the absence or presence of polyethylenimine and demonstrated controlled release of the oligonucleotides *in vitro* over 30 days (De Rosa et al., 2002). Other groups showed that oligonucleotides incorporated into PLGA microspheres were released *in vitro* in a sustained manner for 20 to 56 days (Cleek et al., 1997; Lewis et al., 1998; Hussain et al., 2002). The release rate of the ASO from the microspheres was influenced by ASO loading, ASO length, PLGA molecular weight, microsphere size and the pH of the release medium used. Incorporation of the ASO in the microspheres improved their stability in serum but did not impair their hybridization capability with specific mRNA (Lewis et al., 1998).

Ribozymes are catalytic RNA oligomers approximately 30 to 36 mers in length that bind to and cleave specific mRNA sequences. Due to their similar size, physicochemical properties and molecular targets, ribozymes are somewhat analogous to ASOs for controlled release purposes. Our research group incorporated ribozymes into microspheres of poly(L-lactide) (PLLA) or PLGA and into paste comprised of PCL blended with MePEG. The PLLA microspheres released the ribozymes *in vitro* in a controlled manner for 11 days before disintegrating, while the PLGA microspheres and the PCL/MePEG paste provided sustained release of the ribozymes for over 50 days (Jackson et al., 2002).

Chitosan is a biocompatible, biodegradable polysaccharide composed of N-acetylglucosamine and N-D-glucosamine monomers (Figure 1.11). The amine on the N-D-glucosamine residues is protonated at a lower pH, producing a polycationic polymer that has been shown to effectively condense and deliver plasmids/genes (high molecular weight DNA) *in vitro* and *in vivo* (Renbutsu et al., 2005; Freier et al., 2005; Mi et al., 2002; Ishii et al., 2001; Ramos et al., 2005). Chitosan and its derivatives have been complexed with polyanionic genes and ASOs to increase *in vitro* transfection efficiency and *in vivo* efficacy (Gao et al., 2005). Genes or oligonucleotides have typically been complexed with chitosan by first mixing the chitosan with a dilute acid or buffer at low pH, thereby increasing the number of cationic amine sites on the chitosan to dissolve the polysaccharide (Ramos et al., 2005; MacLaughlin et al., 1998). The chitosan solution is then mixed with genes or oligonucleotides to form complexes. Due to cooperative electrostatic interactions between the polycationic chitosan and the polyanionic DNA, these mixtures resulted in polyelectrolyte complexes or coacervated complexes with mean diameters generally between 100 to 1500 nm (Erbacher et al., 1998; Mao et al., 2001; Gao et al., 2005).

Our research group is studying the intratumoral, controlled delivery of drugs, in solid prostate tumors (Jackson et al., 2000; Jackson et al., 2004). An injectable and biodegradable polymeric paste consisting of a triblock copolymer composed of PLC-block-PEG-block-PLC (Figure 1.10A) blended with MePEG (Figure 1.10B) at a w/w ratio of 40/60, was developed for intratumoral administration and controlled release of paclitaxel (Jackson et al., 2000). The

addition of low molecular weight MePEG to the triblock copolymer resulted in a blended polymeric "paste" that could be injected by syringe through a 22 gauge needle. In aqueous media or a tissue environment, the paste set to a semisolid implant at 37°C (Jackson et al., 2004). This intratumoral formulation was effective at inhibiting the growth of human prostate tumors grown in mice when loaded with 10 mg of paclitaxel (Jackson et al., 2000).

To our knowledge, chitosan has not been used to control the release of oligonucleotides from polymer-based implants or depot formulations. One of the goals of this thesis was to prepare a delivery system that localizes clusterin ASO at the site of action, protects the ASO from degradation and provides controlled release of the ASO. Polyanionic clusterin ASO was loaded into polycationic chitosan microparticles by a solvent loading process to form clusterin ASO:chitosan microparticulate complexes (CC complexes). Unlike the colloidal or coacervate complexes formed from chitosan and oligonucleotide solutions, CC complexes were formed using microparticulate chitosan that swelled as the clusterin ASO solution was sorbed into the microparticles. CC complexes were dried and incorporated into the triblock copolymer/MePEG polymeric paste by blending.

In this chapter, we report the results of the development and physicochemical characterization of clusterin ASO complexed with chitosan and incorporated into injectable, biodegradable polymeric paste with paclitaxel or docetaxel. The objectives of these studies were to:

1. Determine the influence of clusterin ASO to chitosan ratio and pH on the physicochemical properties of CC complexes.
2. Determine the release characteristics of clusterin ASO from CC complexes and paste formulations, and the influence of clusterin ASO:chitosan ratio, pH and phosphate concentration on release rates.
3. Characterize the release profiles of paclitaxel, docetaxel and clusterin ASO from taxane and clusterin ASO loaded CC paste formulations selected for *in vivo* evaluation.

3.2 MATERIALS

3.2.1 General lab materials and equipment

HPLC grade acetonitrile, ACS reagent grade hydrochloric acid (HCl), 70% isopropyl alcohol and 15 mL glass culture tubes with polytetrafluoroethylene lined plastic caps were obtained from Fisher Scientific (USA). KCl, NaBr, NaOH, $NaClO_4 \cdot H_2O$, sodium chloride, sodium phosphate monobasic, sodium phosphate dibasic, Trizma® base and Trizma® HCl were obtained from Sigma Chemical Co. (USA). Sodium heparin human plasma and EDTA rabbit

plasma (NZW) were obtained from Bioreclamation Inc. (USA). F-12 nutrient mixture, fetal bovine serum (FBS), penicillin/streptomycin (10 000 units/10 000 μg per mL), Oligofectamine™ and Opti-Mem I were obtained from Invitrogen Incorporation (USA). N,N,N',N'-tetramethylethylenediamine (TEMED), Kaleidoscope protein molecular weight marker and blotter paper were obtained from Bio-Rad (USA).

3.2.2 Drugs, polymers and standards

Paclitaxel was obtained from Sigma Chemical Co. (USA). Docetaxel was obtained from Aventis Pharmaceuticals Inc. (Canada). Clusterin ASO, 21-mer (N oligonucleotide), sequence 5'-CAG CAG CAG AGT CTT CAT CAT-3', fully phosphorothioated, was obtained from La Jolla (USA), TriLink BioTechnologies (USA) and the Nucleic Acid – Protein Service at The University of British Columbia (Canada) (NAPS). Clusterin ASO degradation standards, 20-mer (N-1 oligonucleotide) sequence 5'-CAG CAG CAG AGT CTT CAT CA-3', 19-mer (N-2 oligonucleotide) sequence 5'-CAG CAG CAG AGT CTT CAT C-3' and 18-mer (N-3 oligonucleotide) sequence 5'-CAG CAG CAG AGT CTT CAT-3', and thymidine oligonucleotide internal standard, 25-mer, sequence 5'-TTT TTT TTT TTT TTT TTT TTT TTT T-3' (T_{25}) were all fully phosphorothioated and were obtained from NAPS.

Chitosan (shown in Figure 1.11), biomedical grade, lot 30310A, was obtained from Carbomer, Inc. (USA) and had a manufacturer reported degree of deacetylation of 82 to 87%. MePEG (shown in Figure 1.10B) with MW 350 $g \cdot mol^{-1}$ was obtained from Union Carbide

(USA). Triblock copolymer (shown in Figure 1.10A) of PLC-block-PEG-block-PLC is described in in Chapter 1.

3.3 METHODS

3.3.1 Preparation of formulations

Complexation data have been reported using a chitosan amine/DNA phosphate ratio (termed N/P ratio) (Ishii et al., 2001) or DNA phosphate/chitosan amine ratio (termed P/N ratio), which based on the maximum theoretical charge of the chitosan amine groups are sometimes referred to as a "charge ratio" (Köping-Höggård et al., 2001). However, few chitosan amines are protonated at physiological pH. Using a format similar to that employed by Lee et al. (2000), we report clusterin ASO:chitosan ratios on a w/w basis. The formulations used in this work were prepared with the final compositions as summarized in Table 3.1. Formulations for physicochemical characterization studies were prepared as follows: clusterin ASO solutions were prepared at a concentration of 1 $mg \cdot mL^{-1}$ in 10 $mmol \cdot L^{-1}$ phosphate buffered saline (PBS) at pH 6.6, 7.0 and 7.4. Suspensions of chitosan microparticles were also prepared in PBS at pH 6.6, 7.0 and 7.4, by vortexing chitosan in 1 mL PBS for 10 s in a 2 mL Eppendorf tube. Clusterin ASO:chitosan microparticulate complexes, termed "CC complexes", were prepared using a solvent loading method, by adding 1 mL of 1 $mg \cdot mL^{-1}$ clusterin ASO solution to 1 mL of the appropriate concentration of chitosan suspension and vortexing for 10 s. The chitosan

swelled in the aqueous clusterin ASO solution and the CC complexes were allowed to equilibrate for approximately 12 hours at room temperature before analysis.

Formulations for clusterin ASO release and bioactivity studies were prepared as follows: clusterin ASO solutions were prepared at a concentration of 2 $mg \cdot mL^{-1}$ in PBS at pH 7.4. CC complexes with clusterin ASO:chitosan w/w ratios between 1:0.5 and 1:16 were prepared using a solvent loading method, by carefully pipetting the 2 $mg \cdot mL^{-1}$ clusterin ASO solution onto the appropriate amount of chitosan powder in the corner of a 20 mL glass scintillation vial. The chitosan swelled in the aqueous clusterin ASO solution and the CC complexes were dried overnight. Clusterin ASO alone (no chitosan) was dried by pipetting the 2 $mg \cdot mL^{-1}$ clusterin ASO solution into the corner of an empty glass scintillation vial and drying overnight. Polymeric paste was prepared in 1 g batches by blending 400 mg triblock copolymer and 600 mg MePEG in a 20 mL glass scintillation vial at 40°C in a water bath. An appropriate amount of polymeric paste was added to dried CC complexes or clusterin ASO alone and blended with a spatula at 40°C for 10 min to achieve homogeneous formulations. The paste containing the CC complexes was termed "CC paste". These formulations were stored at 4°C until further use.

Table 3.1. Summary of the composition of clusterin ASO:chitosan microparticle complexes (CC complexes) and CC complexes in triblock/MePEG 40/60 polymeric paste (CC paste) formulations for *in vitro* physicochemical characterization and drug release studies. The CC paste 1:2 + paclitaxel and CC paste + docetaxel formulations were also used for *in vivo* evaluation in Chapter 4.

Formulation name	Composition (mg)				
	Clusterin ASO	Chitosan	Paclitaxel	Docetaxel	Polymeric paste
Phys/chem studies					
CC complex 1:0.5	1	0.5	—	—	—
CC complex 1:1	1	1	—	—	—
CC complex 1:2	1	2	—	—	—
CC complex 1:3	1	3	—	—	—
CC complex 1:4	1	4	—	—	—
CC complex 1:5	1	5	—	—	—
CC complex 1:6	1	6	—	—	—
CC complex 1:7	1	7	—	—	—
CC complex 1:8	1	8	—	—	—
CC complex 1:12	1	12	—	—	—
CC complex 1:16	1	16	—	—	—
Release studies					
ASO alone	1	-	—	—	—
ASO in paste	1	-	—	—	49
CC complex 1:2	1	2	—	—	—
CC complex 1:6	1	6	—	—	—
CC paste 1:0.5	1	0.5	—	—	48.5
CC paste 1:1	1	1	—	—	48
CC paste 1:2	1	2	—	—	47
CC paste 1:3	1	3	—	—	46
CC paste 1:4	1	4	—	—	45
CC paste 1:6	1	6	—	—	43
CC paste 1:2 + paclitaxel	2	4	1	—	93
CC paste 1:2 + docetaxel	2	4	—	1	93

3.3.2 Physicochemical characterization

3.3.2.1 Determination of chitosan molecular weight

The [η] of chitosan and a GPC universal calibration curve based on pullulan standards is reported in Appendix 4. The GPC conditions for chitosan analysis were the same as for the pullulan standards. Briefly, chitosan replicates were prepared as a 0.1% w/v solution in 0.25 $mol \cdot L^{-1}$ acetic acid and 0.25 $mol \cdot L^{-1}$ sodium acetate and assayed by GPC at ambient temperature with an injection volume of 20 μL and a mobile phase of 0.25 $mol \cdot L^{-1}$ acetic acid and 0.25 $mol \cdot L^{-1}$ sodium acetate. The replicates were eluted through Ultrahydrogel 2000 and Unltrahydrogel 1000 columns (Waters, USA) joined in series. The M_{GPC} of chitosan was calculated from the GPC universal calibration curve (Figure A3.2).

3.3.2.2 Scanning electron microscopy

Scanning electron micrographs (SEMs) were taken of dried chitosan alone and dried CC complexes. Samples were mounted on graphite studs with DAG 154 colloidal graphite in alcohol from Acheson Colloids Ltd. (Canada) using double sided tape. Mounted samples were coated with a 100 Å gold/palladium 60/40 film using a Hummer Sputter Coater. Images were taken using a Hitachi SEM (Japan) with 20 kV beam at various magnifications.

3.3.2.3 Swelling and particle size analysis

The swelling of chitosan microparticles in PBS at different pH values was determined after incubation for 12 and 24 hours. Each sample consisted of approximately 10 mg chitosan

powder accurately weighed into a 2 mL Eppendorf tube. Samples were suspended in 1 mL of PBS at pH 6.6, 7.0 or 7.4 and vortexed for 10 s. After 12 or 24 hours the samples were centrifuged at 18,000 g for 5 min and the supernatant carefully withdrawn. The swollen chitosan microparticles were weighed and swelling reported as a percentage of dry weight. Three replicates were used per group. The particle size distributions of CC complexes were determined in PBS at different pH values. Chitosan alone and CC complexes containing 1 mg clusterin ASO and between 0.5 and 16 mg chitosan were suspended in a total of 10 mL of PBS at pH 6.6, 7.0 or 7.4. Samples were vortexed for 10 s immediately before analysis. Particle size distributions were determined using a Mastersizer 2000 laser diffraction particle size analyzer (Malvern Instruments, USA). Three replicates were used per group.

3.3.2.4 Intrinsic pKa of chitosan

Chitosan suspensions were prepared by adding 10 mL of dilute solutions of $NaClO_4$ with ionic strength of 0, 0.01, 0.05, 0.075 or 0.1, to 10 mg of chitosan powder. To protonate the amine groups on chitosan microparticles, 20 μL of 10 $mol \cdot L^{-1}$ HCl was added to each suspension as this was approximately the amount of HCl required to achieve stoichiometric protonation of the chitosan amine groups. Potentiometric titration was performed by adding NaOH solution dropwise at a concentration of 0.1, 1 and/or 10 $mol \cdot L^{-1}$ and converting to an equivalent amount of 0.1 $mol \cdot L^{-1}$ NaOH solution. The pKa was determined for chitosan at the various ionic strengths and then plotted against ionic strength. The intrinsic pKa (pK_0) of chitosan was

determined using a second degree polynomial best fit line of the pKa versus ionic strength plot and taking pK_0 to be the pKa at an ionic strength of zero.

3.3.2.5 Zeta potential

The zeta potential of CC complexes was determined at different pH values. Chitosan alone and CC complexes containing 1 mg clusterin ASO and between 0.5 and 16 mg chitosan were suspended in a total of 10 mL of PBS at pH 6.6, 7.0 or 7.4. Samples were vortexed for 10 s immediately before analysis. Zeta potential measurements were taken using a Zetasizer 3000 HS zeta potentiometer from Malvern Instruments (USA). Three replicates were used per group.

3.3.2.6 Complexation studies

The amount of clusterin ASO complexed within the chitosan microparticles was determined at different pH values. Samples consisted of clusterin ASO alone and CC complexes containing 1 mg clusterin ASO and between 0.5 and 16 mg chitosan suspended for approximately 12 hours in 2 mL of PBS at pH 6.6, 7.0 or 7.4. To ensure that samples were at equilibrium within 12 hours, CC complexes with a clusterin ASO:chitosan ratio of 1:2 were analyzed for differences in clusterin ASO loadings between 12 and 24 hours. Samples were vortexed for 10 s and then centrifuged at 18,000 g for 5 min. Clusterin ASO concentrations in the supernatant were determined spectrophotometrically at a wavelength of 260 nm using a diode array 8452A spectrophotometer from Hewlett Packard (USA). The amount of clusterin ASO complexed with the chitosan pellet was taken to be the difference between the total amount of

clusterin ASO added and the clusterin ASO measured in the supernatant. Three replicates were used per group.

3.3.3 *In vitro* drug release studies

3.3.3.1 Clusterin ASO release into PBS or human plasma

The appropriate amount of each CC complex or CC paste formulation, containing 1 mg clusterin ASO, was placed in the bottom of 1.5 mL Eppendorf tubes. One milliliter of PBS at 37°C was added to the tubes and the tubes were incubated without shaking or agitation at 37°C. At various time points, all the supernatant was removed for clusterin ASO analysis by HPLC and replaced with fresh buffer at 37°C. Five replicates were used per group. Following HPLC analysis, the remaining volumes of PBS release media containing the clusterin ASO, corresponding to each different formulation, were pooled and diluted to a concentration of 5 $\mu mol \cdot L^{-1}$ clusterin ASO for treatment of PC-3 cells.

Studies were completed in the same manner using human plasma in place of PBS. The full-length 21-mer clusterin ASO and three of its catabolites differing in length by the loss of one, two and three bases, 20-mer, 19-mer and 18-mer, respectively, were extracted and desalted from the withdrawn supernatant and analyzed by CGE. Five replicates were used per group.

3.3.3.2 Influence of ASO to chitosan ratio and pH on clusterin ASO release

The influence of clusterin ASO to chitosan ratio and pH on the *in vitro* release profiles of clusterin ASO released from CC pastes was investigated in PBS. The appropriate amount of each formulation, containing 1 mg clusterin ASO, was placed in the bottom of 1.5 mL

Eppendorf tubes. One milliliter of PBS at pH 6.6, 7.0 or 7.4 at 37°C was added to the tubes and the tubes were incubated without shaking or agitation at 37°C. At various time points, all the supernatant was removed for clusterin ASO analysis by HPLC and replaced with fresh buffer at 37°C. Four replicates were used per group.

3.3.3.3 Influence of phosphate concentration on clusterin ASO release

The influence of sodium phosphate concentration on the *in vitro* release profiles of clusterin ASO released from CC pastes was investigated in PBS. CC pastes containing 1 mg clusterin ASO with clusterin ASO:chitosan ratio of 1:2 were prepared and placed in the bottom of 1.5 mL Eppendorf tubes. PBS was prepared at pH 7.4 at a sodium phosphate concentration of 0.5, 1, 8 or 50 $mmol \cdot L^{-1}$ and made isotonic with differing concentrations of sodium chloride. One milliliter of PBS at 37°C at the appropriate sodium phosphate concentration was added to the tubes and the tubes were incubated without shaking or agitation at 37°C. At various time points, all the supernatant was removed for clusterin ASO analysis by HPLC and replaced with fresh buffer at 37°C. Four replicates were used per group.

3.3.3.4 Paclitaxel, docetaxel and clusterin ASO release from CC pastes

The release of clusterin ASO and paclitaxel or docetaxel from CC pastes containing clusterin ASO and paclitaxel/docetaxel, was determined. The formulations used for these release studies are described in Table 3.1 as CC paste 1:2 + paclitaxel and CC paste 1:2 + docetaxel. Approximately 100 mg of clusterin ASO and paclitaxel or docetaxel loaded CC paste was placed in the bottom of 15 mL culture tubes and cooled to 4 °C to form solid pellets. Fifteen milliliters

of PBS at 37 °C was added to the tubes. The tubes were incubated at 37 °C and at various time points the supernatant was removed and replaced with fresh PBS at 37 °C to maintain sink conditions. Clusterin ASO and paclitaxel or docetaxel concentrations were determined by HPLC analysis of the withdrawn supernatant. After 35 d, the residual clusterin ASO remaining in the carrier paste was released by adding 3 mL of 50 $mmol \cdot L^{-1}$ phosphate buffer at pH 10 to each replicate, followed by vortexing and sonicating. Four replicates were used per group.

3.3.4 *In vitro* bioactivity of released clusterin ASO

3.3.4.1 Tumor cell line and treatment of cells

A study was carried out to determine whether the clusterin ASO released into the PBS release media was bioactive *in vitro*. Human prostate cancer PC-3 cells were from the American Type Culture Collection (USA). Cells were maintained in PC-3 media consisting of F-12 nutrient mixture, 1.176 g sodium bicarbonate, 111 mL FBS (equivalent to 10% FBS) and 11 mL penicillin/streptomycin mixture made up to 1 L with distilled water. Approximately $1x10^6$ PC-3 cells were plated into 10 cm diameter plates with 10 mL of PC-3 media per plate. One day after plating the cells, release media containing clusterin ASO from the various formulations was incubated with 4 $\mu g \cdot mL^{-1}$ Oligofectamine™ for 20 minutes in serum-reduced Opti-Mem I before treating PC-3 cells in 10 cm plates. The *in vitro* concentration responses of clusterin ASO on clusterin mRNA and protein levels in human prostate cancer PC-3 (Miyake et al., 2000a), LNCaP (Miyake et al., 2000b) and Shionogi (Miyake et al., 2000d) cells have been well

characterized. Evidence from these studies demonstrated that treatment of these cell lines with 500 nmol·L^{-1} of clusterin ASO resulted in a reduction of approximately 40 to 80% of clusterin mRNA and corresponding reductions in clusterin protein expression. A final clusterin ASO concentration of 500 nmol·L^{-1} was thus chosen for treatment of PC-3 cells in this work. After 4 hours of clusterin ASO treatment, serum-containing media was added to the plates to increase the serum concentration to 10%. The cells were treated again 24 hours later. Two days after the second treatment the cells were harvested for clusterin protein analysis by Western blot. Three replicates were used per group.

3.3.4.2 Western blots and densitometry

Samples containing 30 μg of protein from lysates of *in vitro* PC-3 cells were electrophoresed on a 1.5 mm SDS – 10% polyacrylamide gel and transferred to a BioTrace NT nitrocellulose membrane (Pall-Gelman Labs, USA) using a Mini-Protean III System with Mini Trans-blot module and a Power-Pac 300 power supply, all from Bio-Rad (USA). The filters were blocked overnight at 4°C in TBST (2.42 g Tris base, 8 g sodium chloride, 3.8 mL of 1 mol·L^{-1} hydrochloric acid, 1 g Tween®, made up to 1 L with distilled water) containing 5% nonfat milk powder, washed three times and then incubated for 1 hour with a 1:500 diluted clusterin goat polyclonal antibody from Santa Cruz Biotechnology, Inc. (USA) or 1:2000 diluted vinculin mouse monoclonal antibody from Sigma (USA). The membranes were then washed five times and incubated for 1 hour with 1:5000 diluted horseradish peroxidase conjugated rabbit

antigoat or goat antimouse antibody. Specific proteins were detected using an enhanced chemiluminescence ECL™ Kit from GE Healthcare (USA). Protein expression was quantitated by densitometry using Fluor Chem™ version 2.01 software (Alpha Innotech Corp., USA).

3.3.5 *In vitro* degradation of clusterin ASO

One mg of clusterin ASO either alone or complexed with chitosan in a w/w ratio of clusterin ASO:chitosan of 1:6 was incubated in 1 mL of 50% plasma at 37 °C for four days. At various time points each sample was vortexed and 100 μL withdrawn for oligonucleotide extraction, desalting and analysis by CGE.

3.3.6 Analytical methods

Unless otherwise indicated, all HPLC and CGE stock solutions, buffers and gels were stirred or shaken until clear, filtered through a 0.45 μm filter, placed in glass bottles, capped and stored at 4°C until used. All HPLC methods used HPLC instrumentation consisting of 1 mL sample vials with lids, 600S controller, 600S, 717plus autosampler, 515 HPLC pump and Millenium[32] Version 3.20 software and were all obtained from Waters (USA).

3.3.6.1 Paclitaxel and docetaxel analysis by HPLC

A Nova-Pak® C_{18} column with 3.9 mm internal diameter x 15 cm length and UV-Vis 486 Tunable Absorbance detector were obtained from Waters (USA). Paclitaxel mobile phase was prepared by mixing 580 mL of acetonitrile, 37 mL of water and 5 mL of methanol. Docetaxel mobile phase was prepared by mixing 500 mL of acetonitrile with 500 mL of water.

3.3.6.2 Clusterin ASO analysis by anion exchange HPLC

The anion exchange HPLC analysis of clusterin ASO is described in detail in Chapter 2. Briefly, the injection volume was 20 μL, the column was a DNAPac™ PA-100 anion exchange column with 4 mm internal diameter x 25 cm length (obtained from Dionex, USA), the detection wavelength was 260 nm and the mobile phase was run at a constant 2 $mL \cdot min^{-1}$. Mobile phase A (0.01 $mol \cdot L^{-1}$ Tris buffer pH 8, 0.005 $mol \cdot L^{-1}$ $NaClO_4$ and 40% v/v acetonitrile) was run for 2 minutes, followed by a linear gradient to mobile phase B (0.01 $mol \cdot L^{-1}$ Tris buffer pH 8, 0.3 $mol \cdot L^{-1}$ sodium perchlorate and 40% v/v acetonitrile) over 5 minutes, followed by 2 minutes of 100% mobile phase A.

3.3.6.3 Clusterin ASO extraction and analysis by capillary gel electrophoresis

The extraction, desalting and CGE assay for 21-mer clusterin ASO and its 20-, 19- and 18- mer degradation products is described in detail in Chapter 2. Briefly, to prepare plasma samples for CGE analysis, AccuBond^{II} SAX cartridges, 500 mg, 3 mL (Agilent Technologies, USA), were equilibrated with 1 mL acetonitrile, followed by 1 mL water and finally 3 mL strong anion exchange load/run buffer (10 $mmol \cdot L^{-1}$ Trizma® HCl, 0.5 $mol \cdot L^{-1}$ KCl, 20% v/v acetonitrile, pH 11.0). Plasma samples were diluted with at least 5 mL strong anion exchange load/run buffer and spiked with 0.5 mL of 2 $\mu g \cdot mL^{-1}$ T_{25} internal standard before vortexing for 10 s and loading onto an AccuBond^{II} SAX cartridge. AccuBond^{II} SAX cartridges were washed with 3 mL strong anion exchange load/run buffer and the oligonucleotides eluted with 3 mL

strong anion exchange elution buffer (10 mmol·L^{-1} Trizma® HCl, 0.5 mol·L^{-1} KCl, 1.0 mol·L^{-1} NaBr, 30% v/v acetonitrile, pH 9.0). The eluent from each cartridge was diluted with 6 mL dilution buffer (10 mmol·L^{-1} Trizma® HCl, 0.5 mol·L^{-1} KCl, 1.0 mol·L^{-1} NaBr, pH 9.0) to lower the acetonitrile concentration in the mixture to 10%. In preparation for the first desalting step, Sep-Pak® Vac C_{18} cartridges, 500 mg, 3 mL (Waters Division of Millipore, USA), were equilibrated with 1 mL acetonitrile, followed by 1 mL water and finally 3 mL dilution buffer. The diluted eluent from each AccuBond^{II} SAX cartridge was loaded onto a separate Sep-Pak® Vac C_{18} cartridge. Sep-Pak® Vac C_{18} cartridges were washed with 5 mL water and the oligonucleotides eluted with 3 mL of 20% v/v acetonitrile solution. The Sep-Pak® Vac C_{18} eluent then underwent a second desalting step by drying down under nitrogen gas at 40°C and reconstituting with 100 µL water and vortexing for 10 s. Each sample was pipetted onto a nitrocellulose VS type, aqueous, 0.025 µm, 45 mm filter (Millipore, USA) floating on 1 L of water in a 1 L beaker. After 30 min, 75 µL of each sample was pipetted into a 0.5 mL CGE vial (Beckman Coulter, USA), diluted to 150 µL with distilled water and assayed by CGE.

Briefly, 21-mer clusterin ASO and its 20-, 19- and 18- mer degradation products extracted and desalted from plasma were assayed by CGE using a P/ACE MDQ capillary electrophoresis system with a P/ACE MDQ UV-Vis detector module and 32 Karat Version 5.0 software. An eCAP™ DNA capillary with 100 µm internal diameter, length to detector of 50 cm and total length of 60.2 cm was used. An eCAP™ Tris-borate/urea buffer and eCAP™ ssDNA

100-R polyacrylamide gel were prepared according to the manufacturer's instructions. All instrumentation and materials were from Beckman Coulter, Inc. (USA). The capillary was packed with fresh gel after every fourth sample run by rinsing the capillary for 10 min with distilled water and filling with gel for 20 min under high pressure. Clusterin ASO and catabolites were assayed at 30°C with a 30 s electrokinetic injection at 10 kV followed by a separation voltage of 21.1 kV for approximately 80 min and a detection wavelength of 254 nm.

3.3.7 Statistical analysis

Statistical analysis was completed using Microsoft Office Excel 2003 software. Differences in the *in vitro* release and bioactivity of clusterin ASO were analyzed using the Tukey test or analysis of variance (ANOVA), respectively.

3.4 RESULTS

3.4.1 Physicochemical characterization

3.4.1.1 Chitosan molecular weight, swelling and particle size

The medical grade chitosan used in these studies showed a broad molecular weight distribution and an M_{GPC} of 360,000 $g \cdot mol^{-1}$. Swelling of chitosan microparticles was determined after incubation in PBS at different pHs for 12 or 24 hours. Chitosan incubated for 12 hours in PBS at pH 6.6, 7.0 and 7.4 swelled to 630 ± 70, 660 ± 40 and 600 ± 40 percent of the dry chitosan weight, respectively. There was no difference in swelling between samples

incubated at different pHs and no change in swelling was determined between 12 and 24 hours incubation. Particle size distributions were determined via laser diffraction after incubation for approximately 12 hours in PBS at pHs 6.6, 7.0 and 7.4 for chitosan alone and CC complexes with clusterin ASO:chitosan ratios ranging from 1:0.5 to 1:16. Chitosan alone and CC complexes at the different pHs and different ASO:chitosan ratios all had broad particle size distributions with particles ranging in diameter from approximately 10 to 850 μm with a mean diameter of approximately 200 μm. Particle morphology was further investigated by SEM after drying. A representative SEM of CC complexes prepared at a clusterin ASO:chitosan ratio of 1:4 is provided in Figure 3.1 and shows the irregular morphology and broad size range of the particles.

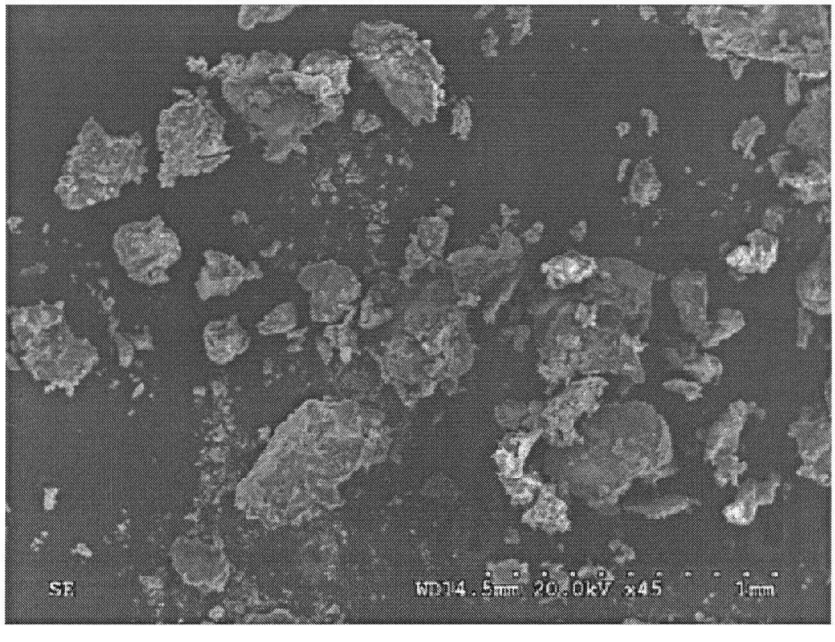

Figure 3.1 Representative scanning electron micrograph of clusterin ASO:chitosan microparticle complexes (CC complexes) at a ratio of 1:4. The complexes were prepared in PBS at pH 7.4 and dried.

3.4.1.3 Intrinsic pKa of chitosan

Chitosan suspensions were stirred in $NaClO_4$ at ionic strengths between 0 and 0.1 to which HCl was added to achieve stoichiometric protonation of the chitosan amine groups. Potentiometric titration curves were prepared by adding NaOH solution to the suspension while recording the pH of the mixture. A representative titration curve for chitosan in $NaClO_4$ with an ionic strength of 0.01 is given in Figure 3.2A. As shown in Figure 3.2B, the pKa of chitosan ranged from 6.2 to 6.7 over ionic strengths ranging from 0 to 0.1 ($NaClO_4$ concentrations of 0 to 0.1 $mol \cdot L^{-1}$). A best fit line for this plot was determined using a second order polynomial equation of $y = 39.9x^2 - 8.92x + 6.21$. The pK_0 of chitosan was taken as the pKa on this curve at an ionic strength of zero and was determined to be 6.2.

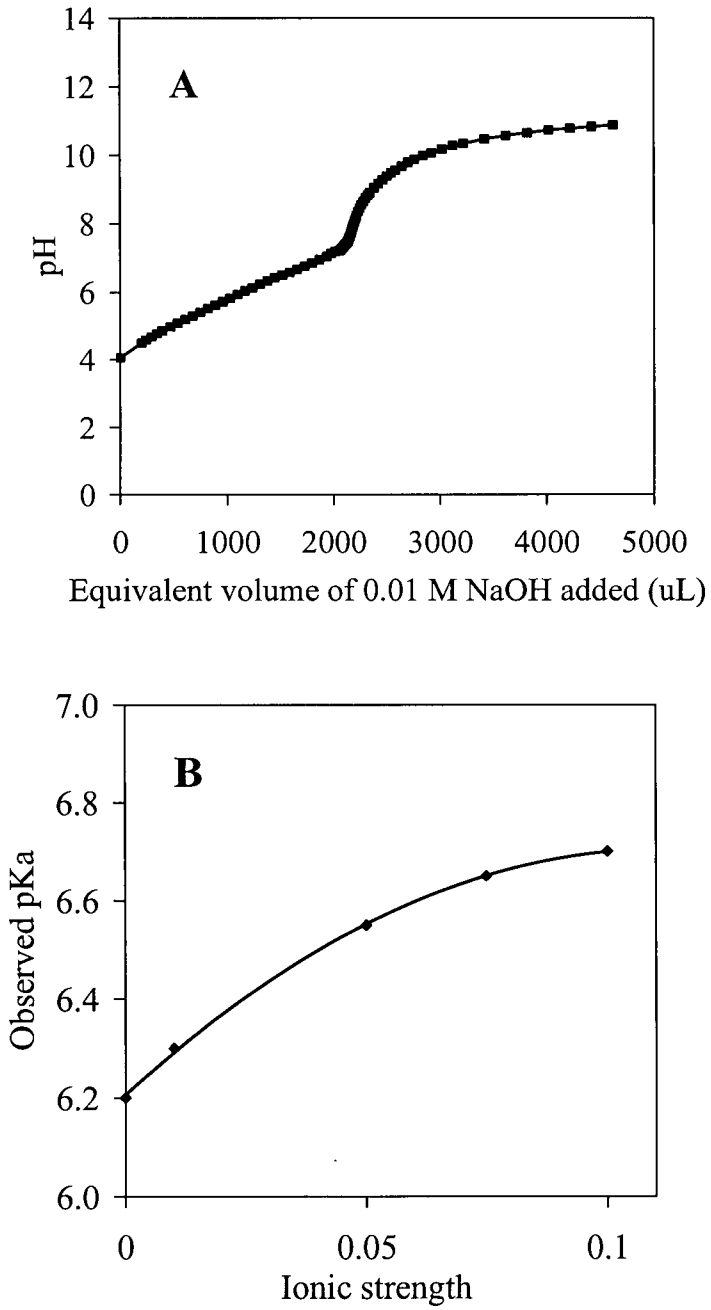

Figure 3.2 **A)** Representative potentiometric titration plot: effect of addition of sodium hydroxide solution to a 10 mL suspension of chitosan (0.1% w/v in 0.01 mol·L^{-1} sodium perchlorate - ionic strength of 0.01) on the pH of the system. Prior to adding the sodium hydroxide, 20 µL of 1 mol·L^{-1} hydrochloric acid were first added to achieve stoichiometric protonation of the chitosan amine groups. **B)** Plot of observed pKa of 0.1% w/v chitosan in sodium perchlorate solutions varying in ionic strength between 0 and 0.1. A best fit line for this plot was determined using a second order polynomial equation of $y = 39.9x^2 - 8.92x + 6.21$. The pK_0 of chitosan was taken as the pKa on this curve at an ionic strength of zero and was determined to be 6.2.

3.4.1.4 Zeta potential

The zeta potentials of CC complexes with clusterin ASO:chitosan ratios between 1:0.5 and 1:16 were measured at pHs 6.6, 7.0 and 7.4. As shown in Figure 3.3 the zeta potentials became increasingly less negatively charged as the amount of chitosan was increased in the CC complexes. At pHs 6.6 and 7.0, ASO:chitosan ratios of 1:4 or those containing greater amounts of chitosan had positive zeta potentials. At pH 7.4, only ASO:chitosan ratios of 1:7 or those containing greater amounts of chitosan had neutral or small positive zeta potentials.

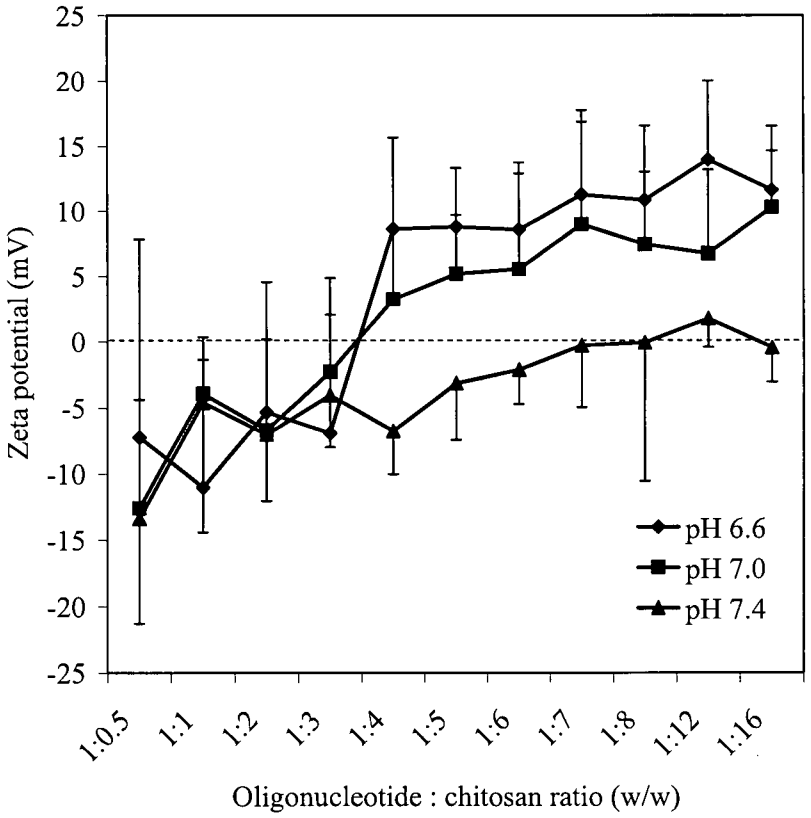

Figure 3.3 Effect of clusterin ASO:chitosan ratio on the zeta potential values for clusterin ASO:chitosan microparticle complexes buffered at different pHs. CC complexes containing 1 mg clusterin ASO and between 0.5 to 16 mg chitosan were suspended in 10 mL of PBS at pH 6.6, 7.0 or 7.4. Data points and error bars represent means ± standard deviation ($n = 3$).

3.4.1.5 Complexation studies

The uptake of clusterin ASO into chitosan microparticles incubated for approximately 12 hours at different pHs was determined by centrifuging the CC complexes and analyzing clusterin ASO in the supernatant. The amount of clusterin ASO complexed into the chitosan pellet was calculated as the difference between the total amount of clusterin ASO added and the amount of clusterin ASO determined to be in the supernatant. The samples were shown to be at equilibrium within 12 hours incubation, since the difference in clusterin ASO uptake into chitosan microparticles between 12 and 24 hours was equal to or less than 1.2%. As observed in Figure 3.4 the amount of clusterin ASO in the pellet increased as the amount of chitosan was increased in the CC complexes. CC complexes at pHs 6.6, 7.0 and 7.4, with clusterin ASO:chitosan ratios of 1:4 to 1:6 or higher amounts of chitosan, were determined to have $\geq 95 \pm 2\%$ of the clusterin ASO in the chitosan pellet.

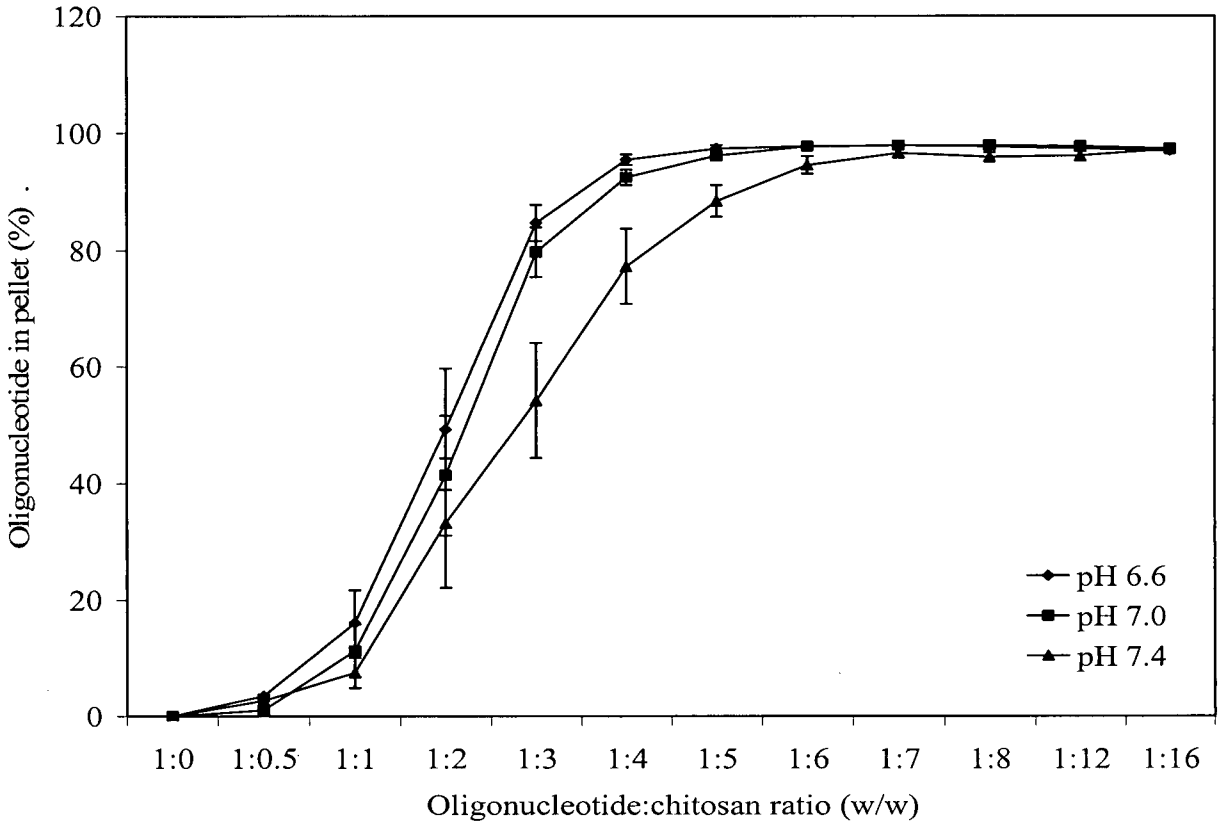

Figure 3.4 Effect of clusterin ASO:chitosan ratio on the loading of clusterin ASO into chitosan microparticles buffered at different pHs. CC complexes containing 1 mg clusterin ASO and between 0.5 to 16 mg chitosan were suspended in 2 mL of PBS at pH 6.6, 7.0 or 7.4, incubated overnight and centrifuged at 18,000 g for 5 min to pellet the chitosan and associated clusterin ASO. The amount of clusterin ASO in the pellet was calculated by subtracting the amount of clusterin ASO in the supernatant from the total amount of clusterin ASO added. Data points and error bars represent means ± standard deviation (n = 3).

3.4.2 *In vitro* drug release studies

3.4.2.1 Clusterin ASO release into PBS or human plasma

In vitro release profiles are given in Figure 3.5 for clusterin ASO released from polymeric paste, CC complexes and CC pastes into PBS at 37°C. All release profiles showed biphasic release of clusterin ASO. Clusterin ASO was released more rapidly for the first 2 to 7 days, followed by a slower release or no release for the remainder of the study. Statistical differences between total cumulative release at 28 days for the different formulations are illustrated by a schematic diagram showing results of Tukey tests (Figure 3.5). The cumulative release and residual amounts of clusterin ASO for the various formulations are summarized in Table 3.2. The total amounts of clusterin ASO that could be accounted for (or recovered) on completion of the released studies ranged from 79 to 101% for the various formulations. Figure 3.5A shows the clusterin ASO release profile from polymeric paste compared to clusterin ASO alone (no formulation). When clusterin ASO was incubated alone in PBS a total of 91 ± 1% of the clusterin ASO was recovered on day 1. Clusterin ASO released from polymeric paste in a controlled manner over the first 7 days, followed by a slower release averaging 1 μg/day from day 7 to day 18, after which no clusterin ASO was detected in the release media for the remainder of the study. Figure 3.5B gives the clusterin ASO release profiles from CC complexes compared to clusterin ASO alone. Clusterin ASO released from CC complexes in a rapid manner for the first 1 to 2 days, followed by a slower release averaging 1 to 4 μg/day for the next

several days until days 5 to 6. No clusterin ASO was detected from days 6 through 12, followed by clusterin ASO being released from days 12 to 28 at an average rate of 5 and 0.5 μg/day for clusterin ASO:chitosan ratios of 1:2 and 1:6, respectively. The extent of clusterin ASO release at 28 days was significantly higher for 1:2 complexes compared to 1:6 complexes ($p < 0.05$). Figure 3.5C demonstrates the clusterin ASO release profiles from CC pastes compared to clusterin ASO in paste (no chitosan). Clusterin ASO released from CC pastes in a controlled manner over the first 4 to 5 days, followed by a slower release for the remainder of the 28 day study, averaging 0.1 to 0.3 μg/day. As shown in Table 3.2, the total clusterin ASO accounted for (or recovered) at the end of the study from CC paste with a clusterin ASO:chitosan ratio of 1:6 was 79 ± 11%, which was lower than the recovery for the other formulations. The cumulative amounts released at 28 days were significantly different for all paste and CC paste formulations ($p < 0.05$).

Table 3.2 Cumulative *in vitro* release and residual analysis of clusterin ASO from various formulations incubated in phosphate buffered saline with sodium phosphate concentration of 10 mmol·L^{-1} (pH 7.4) at 37°C and analyzed by anion exchange HPLC. The composition of each formulation is given in Table 3.1.

Formulation (ratios are w/w ASO:chitosan)	**Cumulative ASO released by 28 days (% of ASO loaded)**	**Residual ASO in each pellet at 28 days[a] (% of ASO loaded)**	**Total ASO released + in each pellet at 28 days[b] (% of ASO loaded)**
ASO alone[c]	91 ± 1	n/a	91 ± 1
ASO in paste	86 ± 6	0	86 ± 6
CC complex 1:2	69 ± 3	30 ± 5	99 ± 2
CC complex 1:6	38 ± 8	56 ± 5	94 ± 6
CC paste 1:2	44 ± 4	57 ± 7	101 ± 7
CC paste 1:6	20 ± 7	59 ± 8	79 ± 11

[a] Amount of clusterin ASO remaining in the semi-solid pellet at the end of the release study.
[b] Sum of the cumulative release and the amount of clusterin ASO remaining in the semi-solid pellet at the end of the release study.
[c] Clusterin ASO alone (no formulation) incubated under the same conditions as the various formulations.

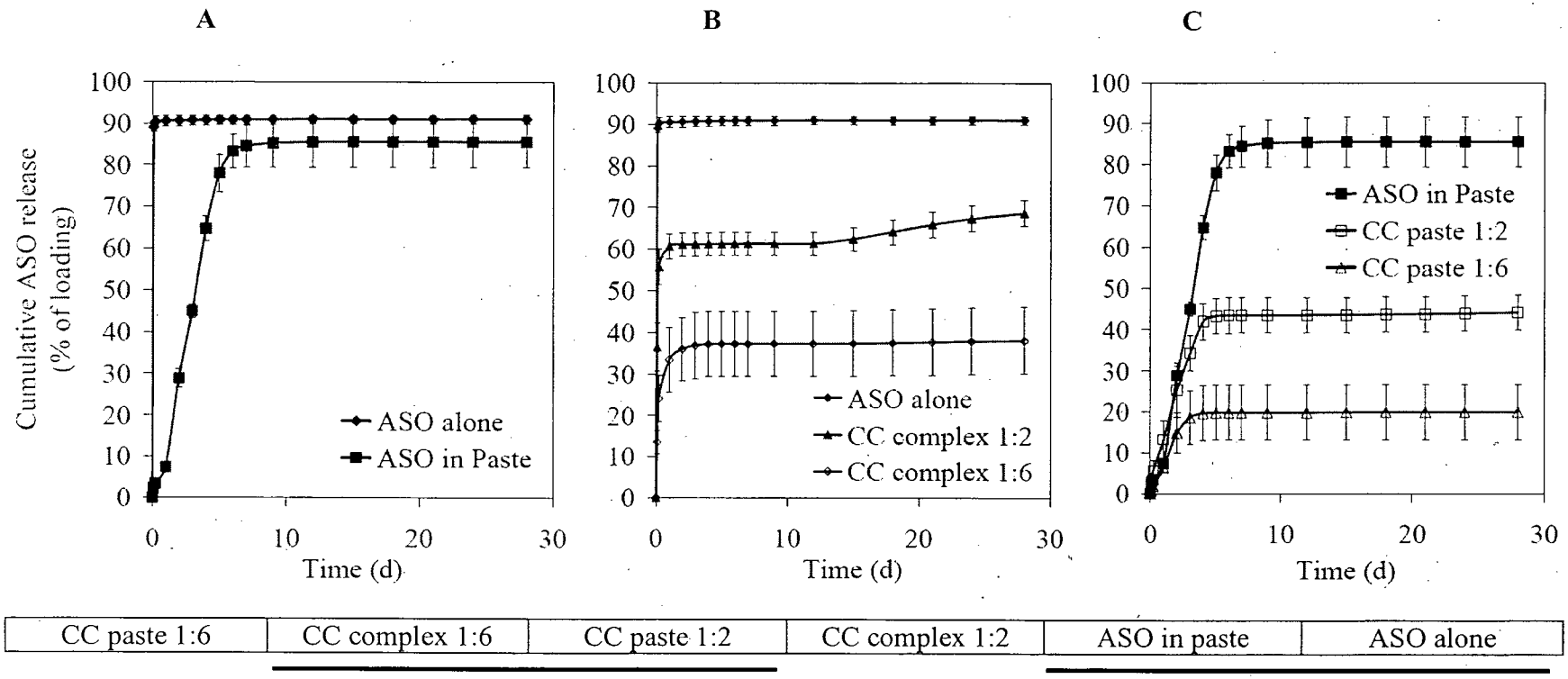

Figure 3.5 Effect of clusterin ASO:chitosan ratio on the *in vitro* release profiles of clusterin ASO from various formulations incubated in phosphate buffered saline with sodium phosphate concentration of 10 mmol·L^{-1} (pH 7.4) at 37°C and analyzed by anion exchange HPLC. Each formulation was loaded with 1 mg clusterin ASO and the composition of each formulation is given in Table 3.1. **A)** triblock/MePEG 40/60 w/w polymeric paste. **B)** clusterin ASO:chitosan microparticle complexes (CC complexes). **C)** CC complexes loaded into polymeric paste (CC paste). Data points and error bars represent the mean ± standard deviation (n = 5). Below the figures is a schematic representation of the results of Tukey tests of significant differences in total extent of clusterin ASO release at 28 days. Dark lines identify formulations between which no significant difference ($p > 0.05$) was observed. .

In vitro release profiles are given in Figure 3.6 for full-length 21-mer clusterin ASO released from polymeric paste, CC complexes and CC pastes into human plasma at 37°C. Similar to release in PBS (Figure 3.5), the feature that was common to all of the release profiles in plasma from CC complexes, polymeric paste and CC paste, was biphasic release of clusterin ASO. Clusterin ASO was released more rapidly for approximately the first week, followed by a slower release or no release for the remainder of the study. The cumulative release and residual amounts of the 21-mer clusterin ASO and the 20-, 19- and 18-mer degradation products for the various formulations are summarized in Table 3.3. Figure 3.6A shows the 21-mer clusterin ASO release profile from polymeric paste compared to clusterin ASO alone (no formulation). After incubation alone in plasma for 1 day, 88 ± 12% of the clusterin ASO was recovered as the sum of amounts of the 21-mer clusterin ASO and the 20-, 19- and 18-mer catabolites. The 21-mer clusterin ASO released from polymeric paste in a controlled manner over the first 7 days, followed by a slower release averaging 0.3 μg/day from day 7 to day 10, after which no oligonucleotides were detected in the plasma for the remaining 21 days. Figure 3.6B gives the 21-mer clusterin ASO release profiles in plasma from CC complexes compared to clusterin ASO alone. The 21-mer clusterin ASO released from CC complexes in a controlled manner for the first 3 to 4 days, followed by a slower release averaging 3 to 4 μg/day for the next several days until day 7. No oligonucleotides were detected in the plasma from days 7 through 28. For the CC complexes at the end of the study, 62 to 64% of the clusterin ASO was accounted for as the sum of amounts of the 21-mer clusterin ASO and 20-, 19- and 18-mer catabolites, which was lower than the recovery from polymeric paste and CC paste formulations, which had a total recovery of 91 to approximately 100% (Table 3.3). Figure 3.6C demonstrates the 21-mer clusterin ASO release profiles in plasma from CC pastes compared to clusterin ASO in paste (no

chitosan). The 21-mer clusterin ASO released from CC pastes in a controlled manner over the first 7 days, after which no oligonucleotides were detected in the plasma for the remainder of the study. The overall amounts released at 28 days were significantly different for all paste and CC paste formulations ($p < 0.05$). As summarized in Table 3.3, at the end of 28 days, CC pastes had residual 21-mer clusterin ASO amounts of 20 and 44% for clusterin ASO:chitosan ratios of 1:2 and 1:6, respectively, while polymeric paste (no chitosan) and CC complexes had residual amounts of zero and 1 to 2%, respectively.

Table 3.3 Cumulative *in vitro* release and residual analysis of full-length 21-mer clusterin ASO and its 20-, 19- and 18-mer degradation products from various formulations incubated in human plasma at 37°C and analyzed by capillary gel electrophoresis.

Formulation name	Cumulative 21-mer ASO released by 28 days (% of ASO loaded)	Residual 21-mer ASO in each pellet[a] at 28 days (% of ASO loaded)	Total 21-mer ASO released + in each pellet at 28 days[b] (% of ASO loaded)	Cumulative release of 20-, 19- and 18-mer oligos (% of ASO loaded)	Residual 20-, 19- and 18-mer oligos at 28 days[c] (% of ASO loaded)	Total 21-mer ASO and 20-, 19- & 18-mer oligos released + in each pellet at 28 days[d] (% of ASO loaded)
ASO alone[e]	79	n/a	79 ± 6	9	n/a	88 ± 12
ASO in paste	80	0	80 ± 5	14	0	93 ± 9
CC complex 1:2	55	1	57 ± 7	6	1	64 ± 8
CC complex 1:6	52	2	55 ± 10	6	1	62 ± 12
CC paste 1:2	55	20	75 ± 9	8	3	86 ± 19
CC paste 1:6	33	44	76 ± 8	10	5	91 ± 13

[a] Amount of full-length 21-mer clusterin ASO remaining in the semi-solid pellet at the end of the release study.
[b] Sum of the cumulative release and the amount of full-length 21-mer clusterin ASO remaining in the semi-solid pellet at the end of the release study.
[c] Sum of the amounts of 20-, 19- and 18-mer degradation products remaining in the semi-solid pellet at the end of the release study.
[d] Sum of the cumulative release and the amounts of 21-mer full-length clusterin ASO plus 20-, 19- and 18-mer degradation products in the semi-solid pellet at the end of the release study.
[e] Clusterin ASO alone (no formulation) was incubated under the same conditions as the various formulations.

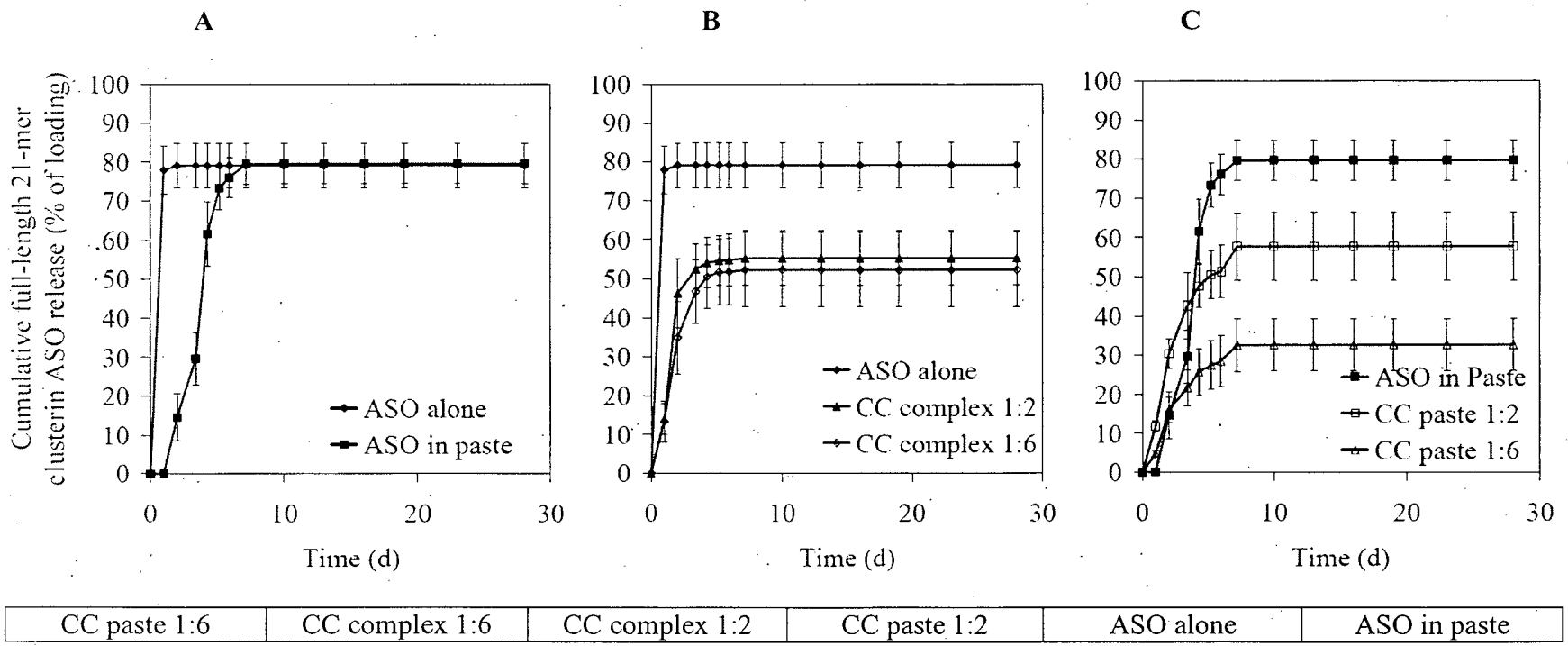

Figure 3.6 Effect of clusterin ASO:chitosan ratio on the *in vitro* release profiles of full-length 21-mer clusterin ASO from various formulations incubated in human plasma at 37°C and analyzed by capillary gel electrophoresis. Each formulation was loaded with 1 mg clusterin ASO and the composition of each formulation is given in Table 3.1. **A)** triblock/MePEG 40/60 w/w polymeric paste. **B)** clusterin ASO:chitosan microparticle complexes (CC complexes). **C)** CC complexes loaded into polymeric paste (CC paste). Data points and error bars represent the mean ± standard deviation (n = 5). Below the figures is a schematic representation of the results of Tukey tests of significant differences in total extent of clusterin ASO release at 28 days. Dark lines identify formulations between which no significant difference ($p > 0.05$) was observed.

3.4.2.2 Influence of ASO to chitosan ratio and pH on clusterin ASO release from CC paste into PBS

In vitro release profiles are giving in Figure 3.7 for clusterin ASO released from CC pastes containing clusterin ASO:chitosan ratios ranging from 1:0.5 to 1:4, into PBS at 37°C at pH 6.6, 7.0 or 7.4. Similar to release in other PBS and plasma studies (Figures 3.5C and 3.6C), the feature that was common to all of the release profiles in PBS from CC paste, was roughly biphasic release of clusterin ASO. Clusterin ASO was released more rapidly for approximately the first week, followed by a slower release for the remainder of the study. Statistical differences between total cumulative release at 28 days for the different formulations are illustrated by a schematic diagram showing results of Tukey tests (Figure 3.7). The rate and extent of clusterin ASO released from the CC pastes was reduced with a decrease in pH and was reduced with an increase in chitosan content. Figure 3.7C demonstrates that at pH 7.4 approximately 85 to 100% of clusterin ASO was released by 28 days from CC pastes with clusterin ASO:chitosan ratios of 1:0.5 to 1:1 whereas 30 to 40% of clusterin ASO was released at 28 days for ASO:chitosan ratios of 1:2 to 1:4. Figures 3.7A and 3.7B show that with a reduction in pH to 7.0 or 6.6, approximately 30 to 55% of clusterin ASO was released by 28 days from CC pastes with clusterin ASO ratios of 1:0.5 to 1:1.

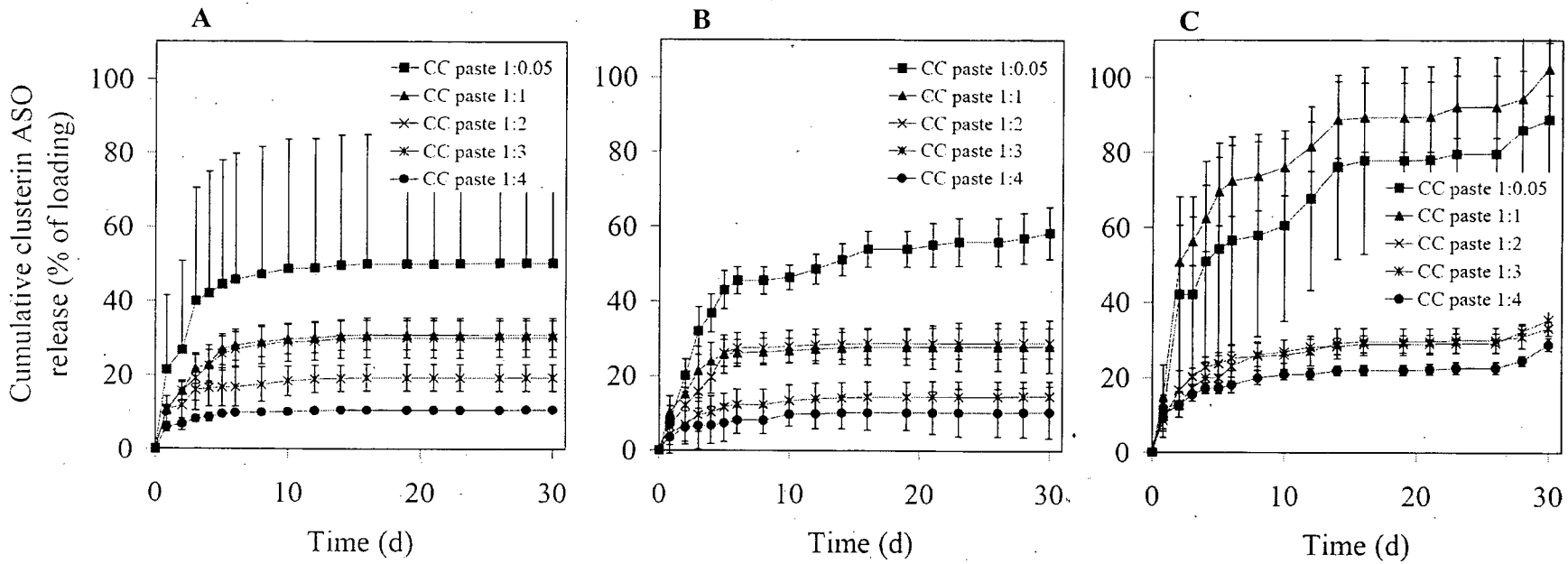

pH	6.6	7.0	7.0	6.6	7.0	7.0	7.4	6.6	6.6	7.4	7.4	6.6	7.0	7.4	7.4
ASO:chitosan	1:4	1:4	1:3	1:3	1:2	1:1	1:4	1:2	1:1	1:3	1:2	1:0.5	1:0.5	1:0.5	1:1

Figure 3.7 Effect of clusterin ASO:chitosan ratio and environmental pH on the *in vitro* release profiles of clusterin ASO. Clusterin ASO was complexed with chitosan microparticles (CC complexes) at various ratios and incorporated into polymeric paste (CC pastes) before being released into phosphate buffered saline at 37°C at various pHs and analyzed by HPLC. Each formulation was loaded with 1 mg clusterin ASO and the ratio of clusterin ASO:chitosan is given in each figure. **A)** pH 6.6, **B)** pH 7.0 and **C)** pH 7.4. Data points and error bars represent the mean ± standard deviation ($n = 3$). Below the figures is a schematic representation of the results of Tukey tests of significant differences in total extent of clusterin ASO release at 30 days. Dark lines identify pH and clusterin ASO:chitosan ratios between which no significant difference ($p > 0.05$) was observed.

3.4.2.3 Influence of sodium phosphate concentration on clusterin ASO release from CC paste into PBS

In vitro release profiles are given in Figure 3.8 for clusterin ASO released from CC pastes with a clusterin ASO:chitosan ratio of 1:2, into isotonic PBS at sodium phosphate concentrations ranging from 0.5 to 50 mmol·L^{-1}. Clusterin ASO was released from the CC paste in a biphasic manner. An initial rapid release for the first 1 to 2 days was followed by a gradual slowing of the release rate for the remainder of the 28 day study. The rate and extent of clusterin ASO release increased as the sodium phosphate concentration was increased in the release media. The total amount of clusterin ASO released at 28 days increased from approximately 40 to 100% as the sodium phosphate concentration was increased from 0.5 to 50 mmol·L^{-1}.

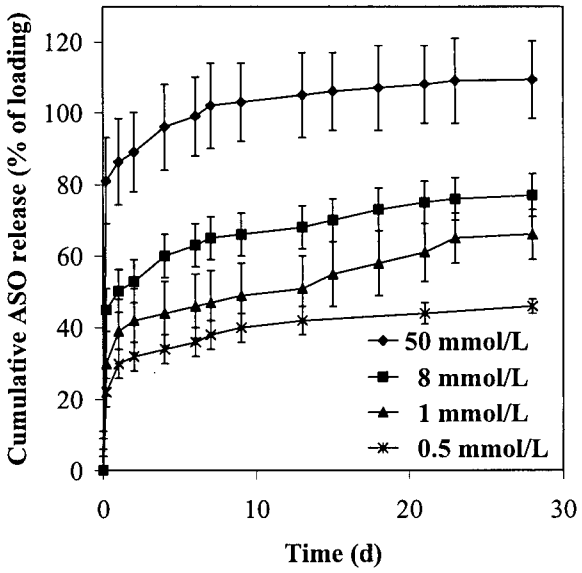

Figure 3.8 Effect of sodium phosphate concentration on the *in vitro* release profiles of clusterin ASO. Clusterin ASO was complexed with chitosan microparticles at a ratio of 1:2 and incorporated into polymeric paste (CC pastes) before being released into phosphate buffered saline at 37°C and analyzed by HPLC. The concentration of sodium phosphate is given for each release profile in the legend. Data points and error bars represent the mean ± standard deviation (n = 4).

3.4.2.4 Characterization of paclitaxel, docetaxel and clusterin ASO release from CC paste formulations used in *in vivo* efficacy studies

In vitro release studies were carried out for paclitaxel, docetaxel and clusterin ASO in PBS (pH 7.4) at 37°C from CC paste formulations used for *in vivo* evaluation in Chapter 4. The release profiles of paclitaxel and clusterin ASO from CC paste 1:2 + paclitaxel and the release profile of docetaxel from CC paste 1:2 + docetaxel are given in Figure 3.9. The components of the formulations are given in Table 3.1. Paclitaxel released in a controlled, almost linear manner from the paste. After five weeks, a total of six percent of the loaded paclitaxel had been released. Docetaxel rapidly released in a short burst phase during the first day followed by a slower release phase over the following 22 days. After 23 days, a total of 40% of the loaded docetaxel had been released. Clusterin ASO was complexed with chitosan as a ratio of 1:2 and was released in roughly a biphasic manner. Over the first 11 days there was a faster release of ASO, followed by a slower phase of release over the following 23 days. Analysis of residual clusterin ASO at 34 days and mass balance determinations, when the amount of clusterin ASO released by 34 days was added to the amount of residual clusterin ASO, accounted for a total amount of approximately 100% of the loaded clusterin ASO.

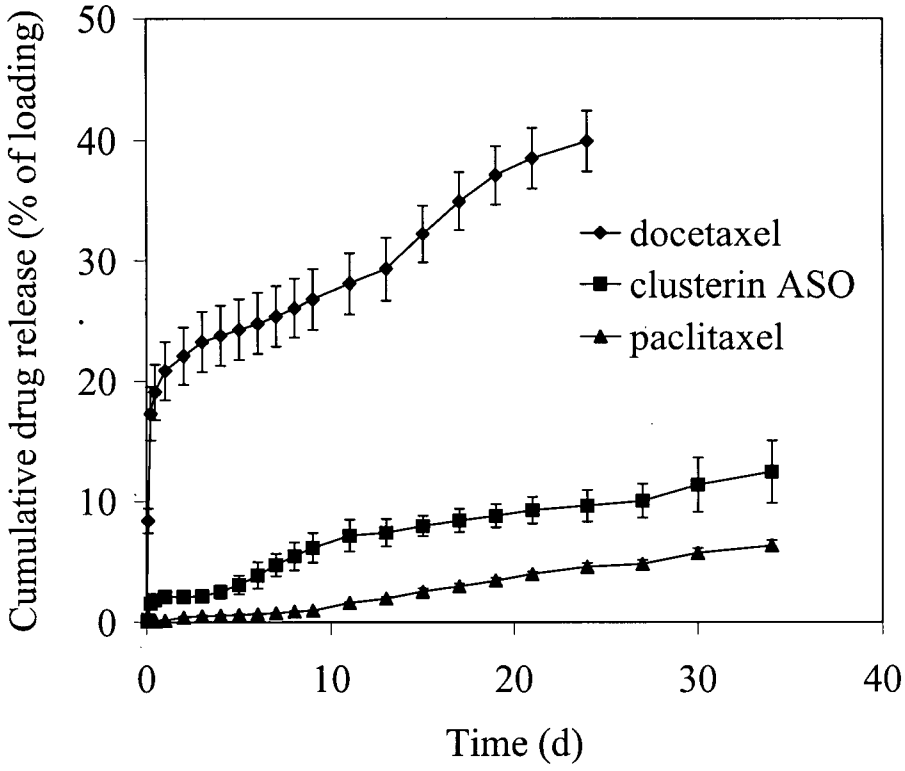

Figure 3.9 *In vitro* release profiles of paclitaxel, docetaxel and clusterin ASO from formulations used for *in vivo* evaluation in Chapter 4. Formulation constituents are summarized in Table 3.1. Each formulation consisted of 2 mg of clusterin ASO complexed with chitosan (CC complexes) at a w/w ratio of 1:2 and 1 mg of either paclitaxel (CC paste plus paclitaxel) or docetaxel (CC paste plus docetaxel) incorporated into polymeric paste (CC pastes). The clusterin ASO release profile shown is from the CC paste plus paclitaxel formulation. Data points and error bars represent means ± standard deviation ($n = 4$).

3.4.2.3 Bioactivity of released clusterin ASO

The *in vitro* bioactivity of clusterin ASO released into PBS from polymeric paste, CC complexes and CC pastes was investigated by treating PC-3 cells with the released clusterin ASO and analyzing changes in clusterin protein levels. A representative set of Western blots for clusterin protein and vinculin protein (housekeeping protein) is provided in Figure 3.10A and demonstrates the inhibition of the expression of the unprocessed 60 kDa form of clusterin protein following treatment with clusterin ASO alone or clusterin ASO released from the various formulations. Figure 3.10B shows the relative clusterin protein expression following densitometry and standardization of the clusterin protein expression of the no treatment group to 100%. Treatment with clusterin ASO alone (no formulation) and clusterin ASO released from the various formulations resulted in 52 to 62% inhibition of the expression of clusterin protein, which was significantly greater than the 22% inhibition of expression which resulted from treatment with mismatch control oligonucleotide ($p < 0.05$, ANOVA). There was no difference in clusterin protein expression between treatments with clusterin ASO alone and clusterin ASO released from the various formulations.

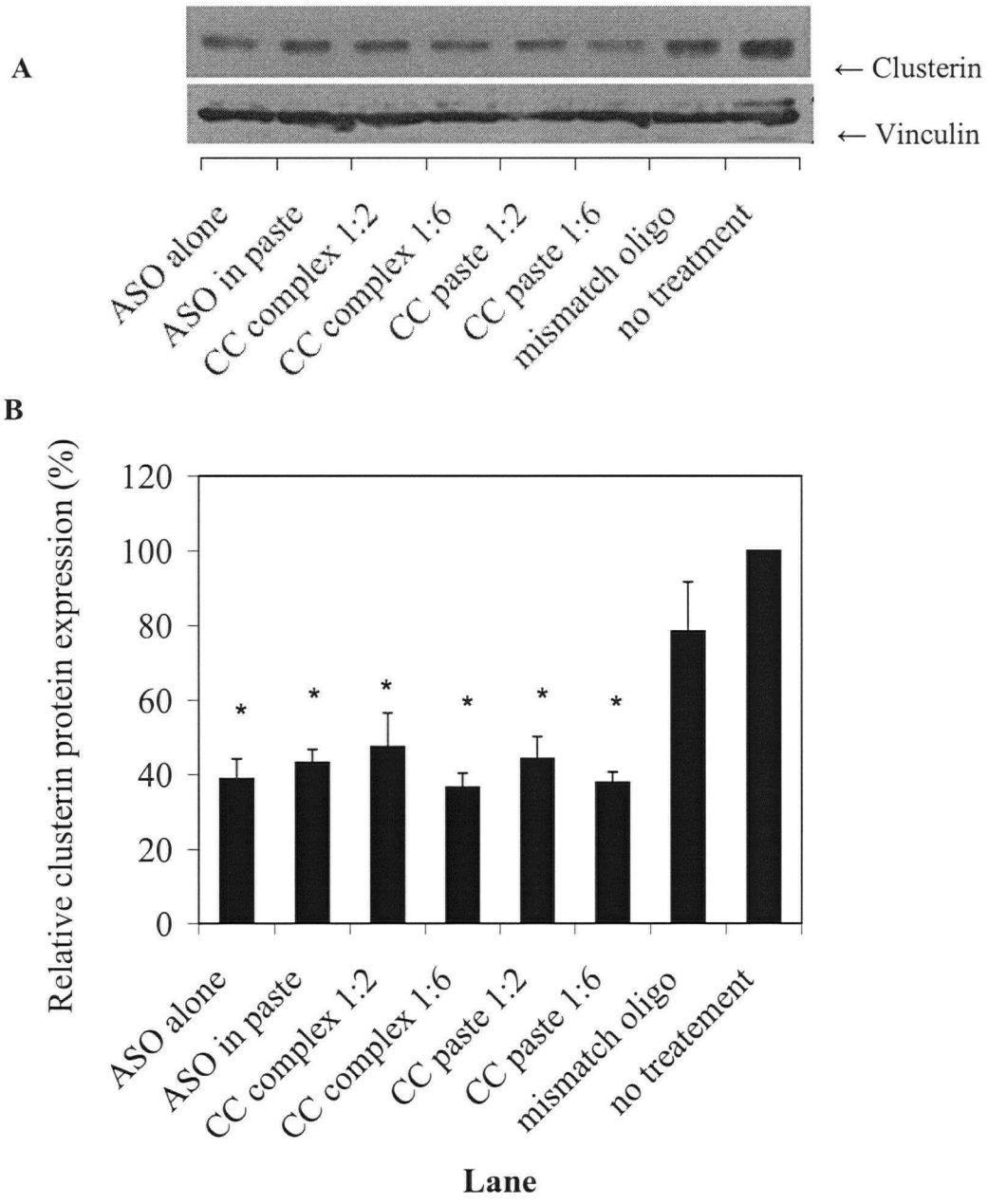

Figure 3.10 Effect of clusterin ASO formulations (given in Table 3.1) on the *in vitro* bioactivity of clusterin ASO. Clusterin ASO released from the formulations into PBS was analyzed by HPLC and the ASO concentration standardized to 500 nmol·L^{-1} before treating PC-3 cells. **A)** Representative Western blots of clusterin protein and vinculin (housekeeping) protein in PC-3 cells. **B)** Densitometry of Western blots' bands. Clusterin expression was divided by vinculin expression and reported as a percent of clusterin expression following standardizing the no treatment control group to 100%. Data bars and error bars represent the mean ± standard deviation (n = 4). (*) denotes significant difference in clusterin expression from mismatch oligonucleotide control treatment (ANOVA, $p < 0.05$).

3.4.3 *In vitro* degradation of clusterin ASO

The stability of full length 21-mer clusterin ASO either alone or complexed with chitosan at a w/w ratio of 1:6 was determined in 50% human plasma incubated at 37°C for 4 days. In addition, the amounts of the 20-, 19- and 18-mer degradation products were determined. As shown in Figure 3.11A, at the end of 4 days approximately 40% of the full-length clusterin ASO remained from both the clusterin ASO (no chitosan) and the CC complex 1:6 samples. At the end of 4 days an amount of 20-mer degradation oligonucleotide equivalent to approximately 20% of the initial 21-mer clusterin ASO was determined to be present in both the clusterin ASO (no chitosan) and the CC complex 1:6 samples (Figure 3.11B).

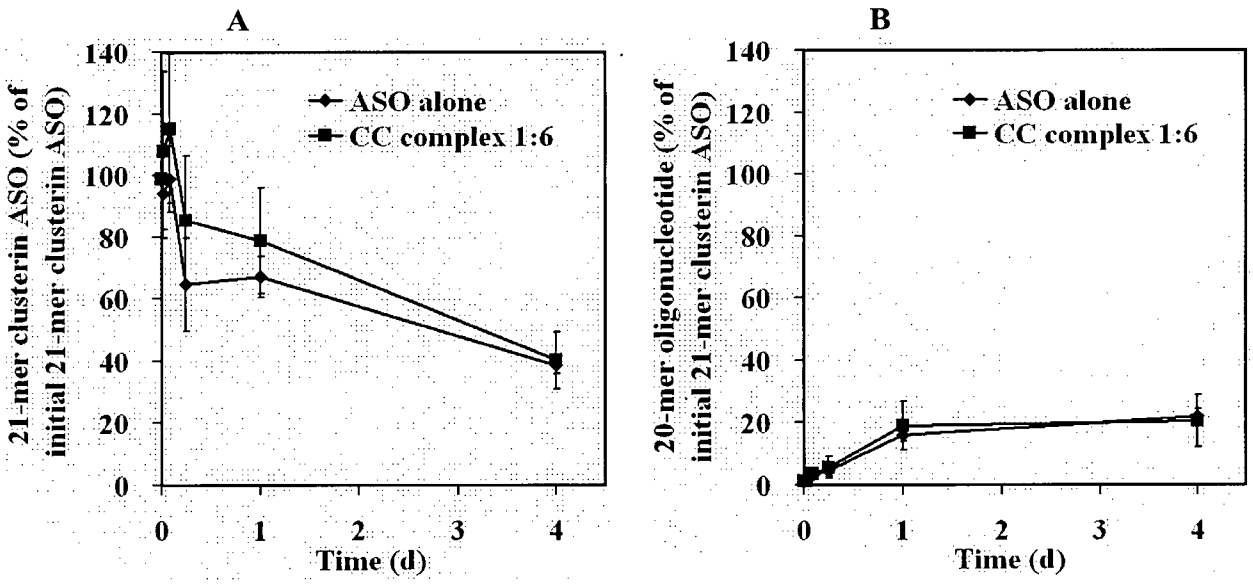

Figure 3.11 Effect of chitosan on the *in vitro* stability of full-length 21-mer clusterin ASO either alone or in a clusterin ASO:chitosan complex at a w/w ratio of 1:6 (CC complex 1:6) incubated in 50% human plasma at 37 °C for 4 days. Each replicate was loaded with 1 mg clusterin ASO. At various time points the oligonucleotides were extracted and analyzed by capillary gel electrophoresis. **A)** The amount of full-length 21-mer clusterin ASO. **B)** The amount of 20-mer clusterin ASO degradation product. Each formulation was incubated in 50% plasma from three different lots and data points and error bars represent the mean ± standard deviation.

3.5 DISCUSSION

The clinical application of ASOs has been hampered by a number of drug delivery issues including poor targeting of ASOs to the site of action, rapid elimination from the body, degradation by nucleases and inefficient cellular uptake (Brignole et al., 2003; Vinogradov et al., 2004; Wang et al., 2003b). A limited number of studies have demonstrated *in vitro* that oligonucleotides incorporated into PLGA microspheres could be released in a sustained manner (De Rosa et al., 2002; Hussain et al., 2002) and that the degradation of the oligonucleotides could be inhibited (Lewis et al., 1998). There have been few investigations of methods that might more effectively locate and maintain therapeutic concentrations of oligonucleotides including ASOs at the target disease site. We proposed that complexing polyanionic clusterin ASO with polycationic chitosan microparticles using a solvent loading process and incorporating these microparticulate complexes into a polymeric paste may help to control the release of the ASO from the paste.

Chitosan is a biocompatible material with an established history of use as a plasmid and antisense oligonucleotide complexation and cell transfection agent (Renbutsu et al., 2005; Gao et al., 2005). The amine group on the N-D-glucosamine residue is capable of accepting a proton in acidic solutions and the potential maximum number of positive charges on chitosan is limited by the number of N-D-glucosamine monomers. For plasmid transfection either water soluble chitosan derivatives or particulate chitosan dissolved in solutions at pH less than 4 were used to condense DNA into nanoparticulate suspensions. The condensation resulted from the

ionic interaction between the protonated amine groups on chitosan in solution and the negative charge on the backbone of DNA chains (Ramos et al., 2005). In this study, insoluble microparticulate chitosan was found to swell by approximately 600% in aqueous media at approximately neutral pH so that amine groups within the chitosan hydrogel matrix might be exposed to water without dissolution. By soaking these microparticles in aqueous solutions containing clusterin ASO, followed by drying, it was possible to load the microparticulate chitosan with clusterin ASO to provide a complex that might be used for controlled release purposes. The strength of the binding between the polyanionic clusterin ASO and the polycationic chitosan depends on the degree of protonation (positive charge) of the amine groups on the polysaccharide chains (Romoren et al., 2003). The charge density of chitosan is influenced by the degree of deacetylation of the chitosan and the pH of the media. The effect of pH on the charge on the chitosan chains may best be described by the pKa which reports the pH at which 50% of the amine groups are protonated. Using chitosan with a degree of deacetylation of approximately 85%, the pKa value of the polysaccharide was found to lie between 6.2 and 6.7 at ionic strengths of 0 and 0.1, respectively (Figure 3.2B). Similarly, others showed that the pKa of high MW chitosan ranged from 5.5 to 7.1 as the degree of deacetylation was decreased from 95 to 78% while the ionic strength of the media was increased from 0.01 to 0.1 (Romoren et al., 2003; Peng et al., 2005). The chitosan microparticles swelled in PBS and CC complexes had mean diameters of approximately 200 μm which is larger than coacervate complexes made by Ishii (Ishii et al., 2001) or the condensation plasmid:chitosan complexes used for plasmid

transfection (Erbacher et al., 1998; Mao et al., 2001; Gao et al., 2005). The larger diameter of these microparticulate CC complexes may assist in providing a depot or implant type of formulation following intratumoral injection, compared to the colloidal or coacervate nanoparticulate complexes.

Clusterin ASO was found to bind to microparticulate chitosan so that all of the clusterin ASO in solution could be fully bound and removed from solution by increasing the chitosan content of CC complexes to a clusterin ASO:chitosan ratio of 1:4 or higher (Figure 3.4). This binding was pH dependent so that as the pH dropped from 7.4 to 7.0 and 6.6, the number of positive charges in the chitosan microparticles increased and more clusterin ASO could be bound for a given amount of chitosan. Previous work by others using plasmid:chitosan condensation complexes showed similar patterns, with plasmid association with chitosan increasing at plasmid:chitosan ratios containing higher amounts of chitosan and a similar pH dependence to those observed in this study (Lee et al., 2001; Köping-Höggård et al., 2001; Romoren et al., 2003). These effects of weight ratios and pH on the net charge of the microparticles was further supported by zeta potential determinations. The microparticulate charge (as measured by electrophoresis in a zeta potential instrument) increased from approximately –10 mV to positive values as chitosan content of CC complexes increased with greater rates of change occurring as the pH dropped from 7.4 to 7.0 and 6.6 (Figure 3.3). As the amount of chitosan was increased relative to clusterin ASO or as the pH was decreased, the number of protonated chitosan amines increased, resulting in less negatively charged or more positively charged CC complexes and a corresponding change in zeta potential values for the microparticles. The zeta potential values of polyelectrolyte complexes or coacervated complexes formed from ASO or plasmids and chitosan have also been shown by others to become less negatively charged or more positively charged as

the chitosan content was increased or the pH decreased (Erbacher et al., 1998; Mao et al., 2001; Gao et al., 2005). The polyanionic clusterin ASO formed electrostatic complexes (Papisov and Litmanovich, 1988) with the polycationic chitosan, somewhat similar to precipitation complexes formed between chitosan and plasmid DNA (Erbacher et al., 1998; MacLaughlin et al., 1998; Ishii et al., 2001) and the same as complexes reported by others between chitosan and oligonucleotides (Hayatsu et al., 1997). It generally requires only a minimum of six to ten salt bonds to form a cooperative system (Papisov and Litmanovich, 1988), so it is likely that the chitosan amine groups formed a coordinated system of salt bonds with the clusterin ASO thiophosphate groups (Vinogradov et al., 1998) resulting in strong complexes (Ho et al., 2002).

The microparticulate CC complexes are difficult to suspend in aqueous media or to inject through syringe/needle assemblies due to sedimentation or aggregation during injection. However, when CC complexes were incorporated homogenously into a polymeric paste (CC pastes) consisting of a 40/60 blend of triblock copolymer (Figure 1.10A) and MePEG (Figure 1.10B), sedimentation and aggregation issues were overcome and the formulation was easily injected through a 22 gauge needle at room temperature. It has been shown that following injection of the polymeric paste into aqueous media or into a tumor, the hydrophilic MePEG rapidly partitioned and diffused out from the paste into the surrounding aqueous compartment or tissue fluids (Jackson et al., 2000). The remaining hydrophobic triblock copolymer then solidified (Jackson et al., 2000) due to both an increased melting temperature and precipitation of hydrophobic drug in the polymer matrix as water entered the matrix (Jackson et al., 2004).

Clusterin ASO released from polymeric paste, CC complexes and CC pastes *in vitro* in PBS in a bioactive form (Figure 3.10), suggesting that the clusterin ASO was released from the various formulations as "free" ASO, that is, the ASO was not complexed with chitosan when it was released from the various formulations. When suspended in polymeric paste in the uncomplexed form, all the clusterin ASO released into either PBS or plasma in approximately one week (Figures 3.5A and 3.6A). In this case the controlled release over a short time period may have resulted from the uniform, hemispherical geometry of the paste pellets which may have determined the rate of entry of water into the core of the pellet and, therefore, subsequent release of the ASO. The uncomplexed ASO-in-paste system would have little practical application *in vivo* where the geometry of the paste would be highly variable following intratumoral injection. Clusterin ASO released from CC pastes *in vitro* in both PBS and plasma (Figures 3.5C and 3.6C) in a sustained manner over the first 4 to 7 days, followed by no or very little release for the remainder of the study. Modeling the cumulative release of ASO in both PBS and human plasma against the square root of time for the first several days resulted in a linear relationship for ASO in paste and CC paste (data not shown), suggesting that ASO was released from polymeric paste formulations in the presence or absence of chitosan, at least in part, via diffusion controlled release. However, clusterin ASO released from CC complexes *in vitro* in both PBS and plasma in a rapid manner over the first 1 to 4 days, followed by a slower release phase for the next several days (Figures 3.5B and 3.6B). Modeling plots of these non-paste release profiles showed no linear relationship (data not shown), suggesting that ASO was released from chitosan complexes by a different mechanism than simply diffusion alone.

Increasing the chitosan content of CC complexes or lowering the pH, released clusterin ASO from CC pastes in a slower manner and to a lesser extent (Figure 3.7). As the

chitosan content is increased or the pH is decreased the number of positively charged amine sites available to form electrostatic bonds and coordinated complexes with negatively charged clusterin ASO thiophosphate groups would be increased and provide for a slower release of clusterin ASO. Indeed, we observed that as the clusterin ASO to chitosan ratio was changed from 1:0.5 to 1:4 that the amount of ASO released during both the rapid initial phase over the first week and the remainder of the study was decreased. It is likely that the ASO dissociated from the chitosan microparticles mainly in the free form and that these species would be in equilibrium. Some of the free ASO would be released from the paste via diffusion and re-equilibration would lead to the formation of additional free ASO, resulting in the controlled release of ASO that we observed from several of our formulations over four weeks.

The rate and extent of clusterin ASO release from CC pastes in PBS increased as the sodium phosphate concentration was increased in the release media (Figure 3.8). Phosphate ions may compete with or shield the polyanionic clusterin ASO chains from positively charged binding sites on the chitosan. A similar scenario is encountered in the HPLC analysis of ASO concentration described in this study whereby following binding of the clusterin ASO to the cationic solid phase of the HPLC column, the clusterin ASO may be eluted using a gradient of increasing perchlorate ions as these ions (like phosphate ions) compete with the clusterin ASO for sites on the column, thereby displacing (or "releasing") the ASO. This competitive ion effect supports the zeta potential, complexation and release data which point towards clusterin ASO interacting with chitosan microparticles through electrostatic bonds to form microparticulate CC complexes (Mao et al., 2001; Peng et al., 2005).

CC paste formulations used in the *in vivo* evaluation in Chapter 4 contained paclitaxel or docetaxel and CC complexes (compositions described in Table 3.1). Paclitaxel and docetaxel were released *in vitro* into PBS (pH 7.4) at 37°C in a controlled manner with approximately 6 and 40%, respectively, of the loaded drug released by 28 days (Figure 3.9). Previous studies using a similar paste formulation loaded with 10% w/w paclitaxel but without chitosan produced a slow release of paclitaxel over 35 days, such that approximately 40% of the loaded dose was released (Jackson et al., 2000). Another study in which 1 to 30% w/w paclitaxel was loaded in a paste based on PCL or a PCL/MePEG blend, showed very slow release of paclitaxel over 20 days, such that approximately 5 to 20% of the loaded dose was released (Winternitz et al., 1996; Jackson et al., 2004). It is anticipated that the remaining clusterin ASO and paclitaxel or docetaxel would be released as the biodegradable chitosan and triblock copolymer undergo degradation.

Natural phosphodiester backbone oligonucleotides are rapidly degraded *in vivo*, primarily by 3'-exonucleases in plasma. Modifying oligonucleotides by replacing one of the non-bridging oxygen atoms on each of the internucleoside phosphate groups with a sulphur atom (termed fully phosphorothioated oligonucleotide) provides some resistance to nuclease degradation (Gilar et al., 1997). At the termination of the CC paste release studies after four weeks, totals of cumulative release plus residual clusterin ASO in PBS for all the formulations evaluated, accounted for approximately 80 to 100% of the loaded clusterin ASO (Table 3.2). However, similar determinations in human plasma accounted for approximately 75% of the full-

length 21-mer clusterin ASO as a percent of the loaded clusterin ASO in CC pastes and only approximately 55% of the full-length 21-mer clusterin ASO in CC complexes without polymeric paste (Table 3.3). We suggest from these data that while some degradation of clusterin ASO occurred in plasma due to nucleases, CC paste formulations may have protected the clusterin ASO from nuclease degradation. We also suggest that in the case of CC complexes without paste, nucleases present in plasma (but not present in PBS) penetrated the swollen chitosan hydrogel matrix and degraded the clusterin ASO, leaving only 1 to 2% of the full-length 21-mer clusterin ASO in the CC complexes at the end of the study (Table 3.3). The degradation study showed no difference in the degradation profiles of full-length 21-mer clusterin ASO when incubated in 50% human plasma alone or complexed with chitosan at a ratio of 1:6 (Figure 3.11). These data provide additional evidence that the ASO complexed to chitosan was not protected from degradation by nucleases in plasma. However, in the case of CC pastes, nucleases were blocked from penetrating the CC complexes by the semi-solid/waxy triblock copolymer, leaving 25 to 44% of the full-length 21-mer clusterin ASO in the CC pastes at the end of the release study in plasma (Table 3.3).

3.6 CONCLUSIONS

1. Clusterin ASO:chitosan ratio and pH both influenced the electrostatic interaction and binding of clusterin ASO with chitosan in CC complexes.

2. The rate and extent of clusterin ASO release was influenced by clusterin ASO:chitosan ratio, pH and phosphate concentration. The release profiles were also affected by the incorporation of the clusterin ASO into polymeric paste.

3. Our data suggest that CC paste may have protected clusterin ASO from nuclease degradation *in vivo* in human plasma.

4. Clusterin ASO released from the various formulations suppressed the expression of clusterin protein in PC-3 cells *in vitro*.

5. Paclitaxel, docetaxel and clusterin ASO were released *in vitro* in a controlled manner from CC paste formulations used for *in vivo* evaluation.

4. *IN VIVO* EFFICACY IN PROSTATE CANCER XENOGRAFT MODELS[3]

4.1 INTRODUCTION

The clinical application of therapeutic oligonucleotides such as antisense oligonucleotides (Veeramachaneni et al., 2004), ribozymes (Pennati et al., 2004), siRNA (Caplen and Mousses, 2003), CpG immune modulators (Rothenfusser et al., 2004), aptamers (Grate and Wilson, 2001) and other oligonucleotides (Cho-Chung et al., 2003) has been hampered by a number of drug delivery issues. In particular, lack of delivery of oligonucleotides to the target site, poor cellular uptake, and short tissue half-lives with rapid elimination and degradation of oligonucleotides by nucleases, has limited the efficacy of oligonucleotides *in vivo* (Wang et al., 2003b). However, there have been few investigations of methods that might more effectively locate and maintain therapeutic concentrations of oligonucleotides at the target disease site.

Clusterin protein has been shown to inhibit apoptosis (Miyake et al., 2000d) and as a result, its overexpression assists in the formation of a prostate cancer phenotype that is resistant to chemotherapy (Miyake et al., 2003), radiation (Zellweger et al., 2003) and androgen ablation (July et al., 2002). *si*RNA targeted to inhibit the expression of clusterin has been shown to increase the chemosensitivity of PC-3 cells *in vitro* (Trougakos et al., 2004), while antisense

---

[3] A version of this Chapter has been published (Springate, CMK, JK Jackson, ME Gleave and HM Burt. Efficacy of an intratumoral controlled release formulation of clusterin antisense oligonucleotide complexed with chitosan containing paclitaxel or docetaxel in prostate cancer xenograft models. *Cancer Chemother Pharmacol* (2005) 56:239-247).

oligonucleotide targeted at clusterin has been demonstrated to increase the sensitivity of PC-3 (Miyake et al., 2000a) and LNCaP (Miyake et al., 2000b) tumors in mice to paclitaxel (Miyake et al., 2003). ASOs inhibit gene expression by hybridizing with complementary messenger ribonucleic acid (mRNA) regions of a target gene and forming RNA/DNA duplexes (Crooke, 2000). The PC-3 cell line is an androgen independent human prostate cancer cell line that does not secrete PSA, while the LNCaP cell line is the only androgen dependent human prostate cancer cell line that is immortalized *in vitro* and secretes PSA (Miyake et al., 2000b). Since prostate cancer has responded to treatment with the taxanes paclitaxel (Kuruma et al., 2003) and docetaxel (Sinibaldi et al., 2002) in the clinic, we have suggested that a suitable therapeutic strategy might be to combine clusterin antisense oligonucleotide treatment with paclitaxel or docetaxel.

There is interest in the local delivery of paclitaxel to tumors in order to reduce the systemic side effects of this cytotoxic agent. Paclitaxel has been incorporated into microspheres for intratumoral delivery in prostate cancer (Lapidus et al., 2004). Our group has developed intratumoral biodegradable polymeric pastes for the delivery of paclitaxel and other anticancer agents (Jackson et al., 2000; Jackson et al., 2004). Decreased tumor volume and serum PSA levels were observed following intratumoral administration of paclitaxel loaded paste (10 mg paclitaxel in 100 mg paste) into xenograft LNCaP murine models (Jackson et al., 2000). The paste was based on a biodegradable triblock copolymer of PLC-block-PEG-block-PLC blended with MePEG in a 40/60 w/w ratio and 100 mg paste was injected intratumorally into each mouse. For these studies, we chose a dose of 1 mg of paclitaxel or docetaxel per 100 mg of paste

in order to decrease the local inflammation and inhibition of wound healing toxicity observed in the previous study (Jackson et al., 2000). Previous studies have shown that treatment of PC-3 and LNCaP cells *in vitro* with 500 $nmol \cdot L^{-1}$ of clusterin ASO or doses of 0.25 mg and above of clusterin ASO administered daily to mice has resulted in a significant reduction of clusterin mRNA and protein expression (Miyake et al., 2000a; Miyake et al., 2000b; Miyake et al., 2000d). We selected a dose of 2 mg clusterin ASO per 100 mg of paste.

The intratumoral polymeric paste delivery systems for controlled delivery of both clusterin ASO and paclitaxel or docetaxel to the tumor site were developed and characterized as described in the previous chapter of this thesis. It was shown that clusterin ASO complexed with chitosan microparticles (microparticulate CC complexes) and incorporated into an injectable biodegradable polymeric paste comprised of a 40/60 w/w blend of a waxy triblock copolymer and low molecular weight MePEG (CC paste), along with paclitaxel or docetaxel, provided controlled release of "free" clusterin ASO, paclitaxel and docetaxel *in vitro*. When incubated in human plasma, there was some evidence that the CC paste protected the clusterin ASO from degradation by nucleases.

In this chapter, we report the results from intratumoral injection of the CC paste + paclitaxel and CC paste + docetaxel formulations into human PC-3 and LNCaP tumors in mice. The objectives of this study were to:

1. Evaluate the effect on tumor volume of intratumoral delivery of CC paste with paclitaxel or docetaxel in a human PC-3 prostate tumor xenograft model.
2. Evaluate the effect on tumor volume and serum PSA level of intratumoral delivery of CC paste with paclitaxel in a human LNCaP prostate tumor xenograft model.

4.2 MATERIALS, STOCK SOLUTIONS AND EQUIPMENT

Clusterin ASO and mismatch oligonucleotide phosphorothioate (MMO) (used as a control oligonucleotide) were obtained from the Nucleic Acid Protein Service Unit at The University of British Columbia (Canada). The sequence of the clusterin ASO was 5'-CAG CAG CAG AGT CTT CAT CAT-3'. Paclitaxel, sodium perchlorate monohydrate, Trizma® base and Trizma® hydrochloride were obtained from Sigma-Aldrich Co. (USA). Docetaxel was obtained from Aventis Pharmaceuticals Inc (Canada). Medical grade chitosan was obtained from Carbomer, Inc. (USA). MePEG MW 350 $g \cdot mol^{-1}$ was obtained from Union Carbide (USA). Biodegradable triblock copolymer with a structure of PLC-block-PEG-block-PLC is described in detail in Chapter 1. Sodium chloride and HPLC grade acetonitrile were obtained from Fisher Scientific (USA). Water was distilled and deionized using a Milli-RO Water System obtained

from Millipore (USA). Matrigel was obtained from Becton Dickinson Labware (USA). Roswell Park Memorial Institute 1640 (RPMI 1640) culture media was obtained from Terry Fox Laboratory (Canada). FBS and Dulbecco's Modified Eagle Medium culture media (DMEM) were obtained from Life Technologies, Inc. (USA).

4.3 METHODS

4.3.1 Preparation of formulations

Formulations of an injectable polymeric paste loaded with clusterin ASO or MMO and chitosan complexes (CCs), referred to as CC paste, were prepared with or without paclitaxel/docetaxel loading. The polymer paste was prepared in 1 g batches by blending 600 mg of MePEG and 400 mg of PLC-block-PEG-block-PLC triblock copolymer in a 20 mL glass scintillation vial at 40 °C in a water bath. The clusterin CCs or MMO CCs were prepared by dissolving the appropriate amount of oligonucleotide in 500 μL of water and adding the solution to 40 mg of chitosan in a 20 mL glass scintillation vial. The chitosan swelled and the complexes were dried overnight at 37 °C. The clusterin CCs or MMO CCs and paclitaxel or docetaxel were added in differing amounts to the polymer paste by blending with a spatula for 10 min at 40 °C to achieve homogeneous formulations as summarized in Table 4.1. The preparations were drawn up into 1 mL plastic syringes, capped and stored at 4 °C until use.

Table 4.1 Summary of the constituents in the formulations prepared for *in vivo* efficacy studies. Formulations I through V and I through III were used in the *in vivo* PC-3 and LNCaP tumor efficacy studies, respectively.

Treatment number	Constituent (% w/w)					
	Clusterin ASO	Mismatch oligonu-cleotide	Chitosan	Paclitaxel	Docetaxel	Carrier paste
I	2		4	1		93
II		2	4	1		93
III	2		4			94
IV		2	4		1	93
V	2		4		1	93

4.3.2 Mice and tumor cell lines

"Principles of laboratory animal care" (NIH publication No. 85-23, revised 1985) were followed or standards equivalent to the UKCCCR guidelines for the welfare of animals in experimental neoplasia (Br J Cancer 58:109-113, 1998) were complied with at all times. The health of the animals was observed by monitoring body weight and general appearance (shiny coat, clear nose, gait, etc.). BALB/c strain mice 6 to 8 weeks old and weighing approximately 25 g were obtained from Charles River Laboratory (Canada). PC-3 cells were obtained from the American Type Culture Collection (USA). PC-3 cells were grown in DMEM supplemented with 5% heat-inactivated FBS. LNCaP cells were grown in RPMI 1640 supplemented with 5% FBS.

4.3.3 PC-3 treatment protocols

Mice were anesthetized with methoxyflurane and injected into the subcutaneous space of the flank region with 1 x 10^6 PC-3 cells in 100 μL Matrigel (Matrigel was used to assist with the growth of the cells *in vivo*). Mice were randomly assigned into the following treatment

groups: I) clusterin ASO CC paste with paclitaxel, II) MMO CC paste with paclitaxel, III) clusterin ASO CC paste, IV) MMO CC paste with docetaxel and V) clusterin ASO CC paste with docetaxel. Tumors were injected with 100 μL of the appropriate paste after the tumor reached 1 cm in diameter.

4.3.4 LNCaP treatment protocols

Mice were anesthetized with methoxyflurane and injected into the subcutaneous space of the flank region with 2 x 10^6 LNCaP cells in 75 μL Matrigel and 75 μL RPMI 1640 and 5% RBS. In LNCaP tumors, serum PSA levels correlate with tumor progression (Miyake et al., 2000b). When the serum PSA levels increased above 10 $ng \cdot mL^{-1}$ and the tumor volume reached 200 to 300 mm^3, the mice were anesthetized with methoxyflurane and castrated. Mice were randomly assigned into treatment groups I to III as per the PC-3 treatment protocols. After the serum PSA levels decreased, tumors were injected with 100 μL of the appropriate paste after the serum PSA levels had increased above 60 $ng \cdot mL^{-1}$ and tumor volumes had reached 150 to 650 mm^3. Mean tumor volumes and serum PSA levels were similar at the beginning of treatment in each group.

4.3.5 Determination of tumor volume and serum prostate specific antigen levels

Tumor volumes were measured and calculated weekly using the formula length x width x depth x 0.5236. Blood samples were taken weekly from mice with LNCaP tumors via tail vein incision. A kit obtained from Abbott IMX (Canada) was used according to the

manufacturer's protocol to determine the serum PSA levels. Data were graphed showing the mean and standard deviation for each group.

4.3.6 Statistical analysis

Statistical analysis was completed using Microsoft Excel software. The *in vivo* effects of clusterin ASO and paclitaxel or docetaxel were analyzed using an ANOVA method.

4.4 RESULTS

4.4.1 Effect of intratumoral formulations on PC-3 tumor growth

The pastes were injected through a 22-gauge needle into PC-3 and LNCaP tumors. The pastes set to a waxy solid implant in approximately 1 h at the injection site following injection of the pastes into a tumor and left a palpable semi-solid implant in the tumor for approximately three to four weeks. As shown in Figures 4.1 and 4.2, groups treated with clusterin ASO alone (treatment group #III) had a rapid growth of tumors such that by four weeks the mean tumor volume was approximately 3000 mm^3. Groups treated with MMO / paclitaxel and MMO / docetaxel (treatment groups #II and #IV, respectively) at four weeks had a mean tumor volume of approximately 1500 and 500 mm^2, respectively. Intra-tumoral formulations containing clusterin ASO with paclitaxel and clusterin ASO with docetaxel (treatment groups #I and V, respectively) significantly reduced mean tumor volume by more than 50% four weeks after treatment, compared to MMO with paclitaxel and MMO with docetaxel, respectively ($P = 0.06$ for both comparisons).

4.4.2 Effect of intratumoral formulations on LNCaP tumor growth and PSA levels

As shown in Figures 4.3 and 4.4, the group treated with clusterin ASO alone (treatment group #III) had a rapid growth in tumors such that by four weeks the mean tumor volume and serum PSA level were approximately 1370 mm^3 and 500 $ng \cdot mL^{-1}$, respectively. The group treated with MMO with paclitaxel (treatment group #II) at four weeks had a mean tumor volume and serum PSA level of approximately 1370 mm^3 and 400 $ng \cdot mL^{-1}$, respectively. Intra-tumoral formulations containing both clusterin ASO with paclitaxel (treatment group #I) significantly reduced mean tumor volume ($P < 0.001$) and serum PSA level ($P = 0.08$) by more than 50 and 70%, respectively, four weeks after treatment compared to MMO with paclitaxel.

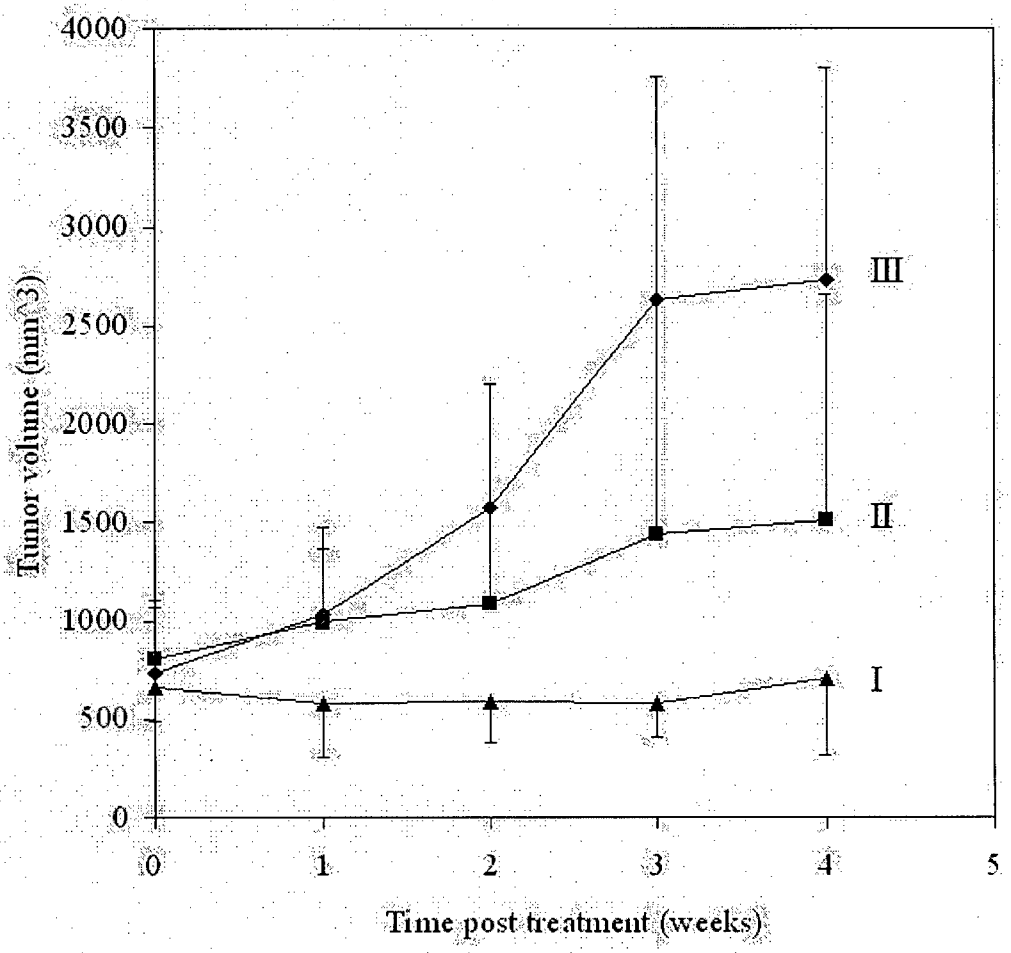

Figure 4.1 Effect of CC-paste loaded with clusterin ASO and paclitaxel on tumor volume in mice with PC-3 tumors following intra-tumoral administration. Treatment protocols are summarized in Table 4.1. (◆) 2% w/w clusterin ASO CC-paste alone (no paclitaxel) (treatment #III); (■) 2% w/w MMO CC-paste with 1% w/w paclitaxel (treatment #II); (▲) 2% w/w clusterin ASO CC-paste with 1% w/w paclitaxel (treatment #I). Data points and error bars represent the mean ± standard deviation. Results are shown for a minimum of four mice (if less than four mice remained in any group, then the data are not shown).

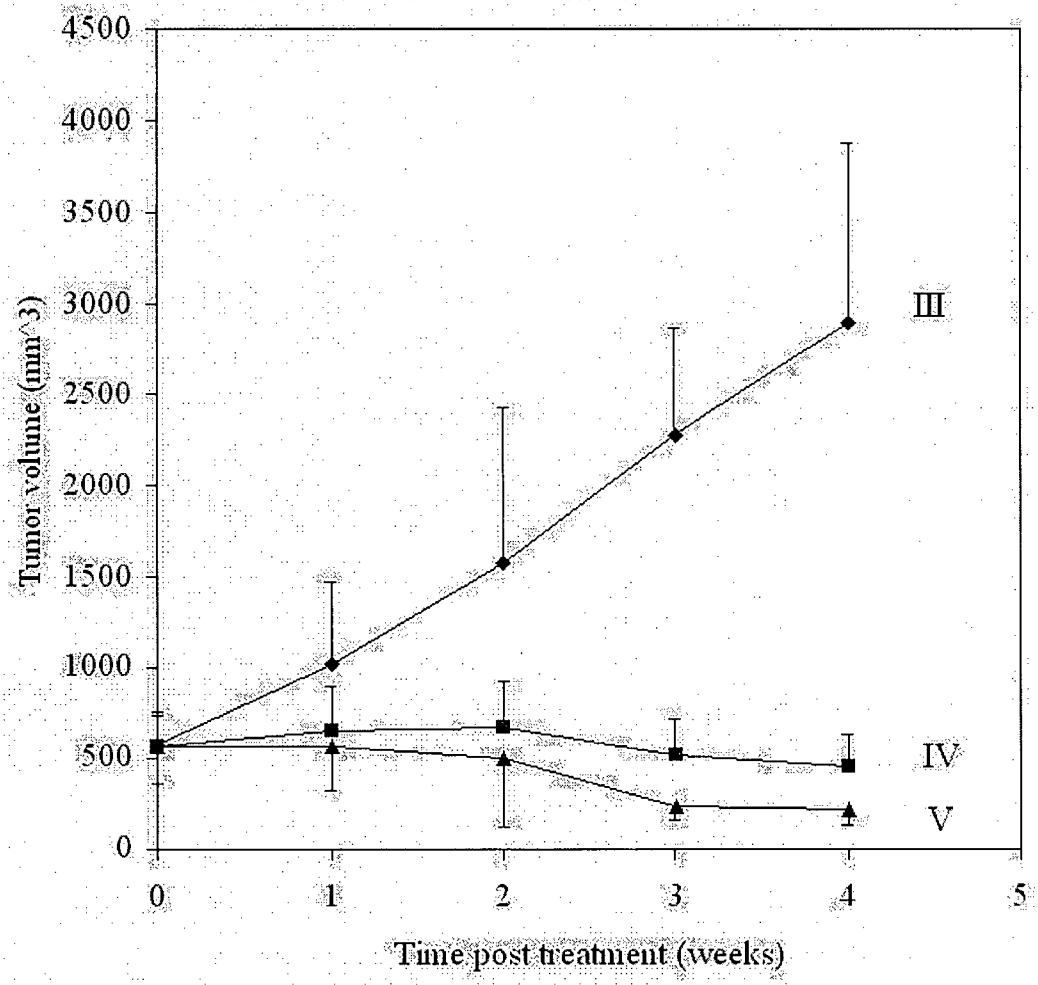

Figure 4.2 Effect of CC-paste loaded with clusterin ASO and docetaxel on tumor volume in mice with PC-3 tumors following intra-tumoral administration. Treatment protocols are summarized in Table 4.1. (◆) 2% w/w clusterin ASO CC-paste alone (no docetaxel) (treatment #III); (■) 2% w/w MMO CC-paste with 1% w/w docetaxel (treatment #IV); (▲) 2% w/w clusterin ASO CC-paste with 1% w/w docetaxel (treatment #V). Data points and error bars represent the mean ± standard deviation. Results are shown for a minimum of four mice (if less than four mice remained in any group, then the data are not shown).

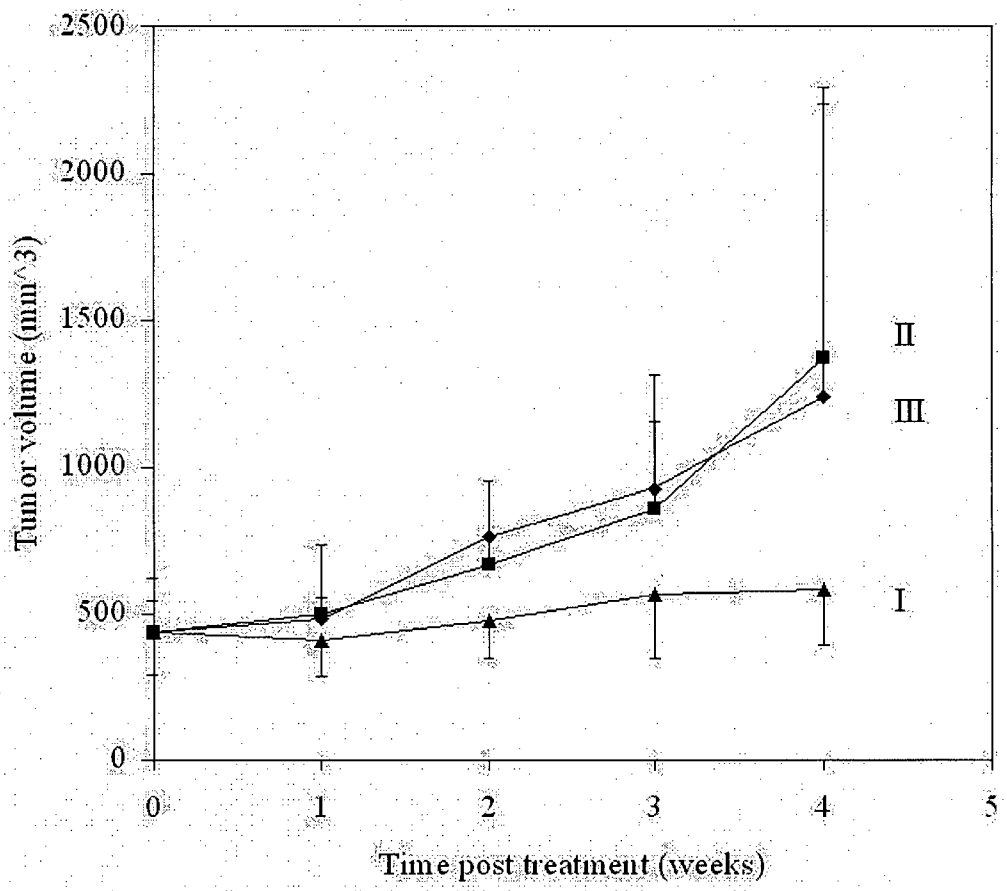

Figure 4.3 Effect of CC-paste loaded with clusterin ASO and paclitaxel on tumor volume in mice with LNCaP tumors following intra-tumoral administration. Treatment protocols are summarized in Table 4.1. (◆) 2% w/w clusterin ASO CC-paste alone (no paclitaxel) (treatment #III); (■) 2% w/w MMO CC-paste with 1% w/w paclitaxel (treatment #II); (▲) 2% w/w clusterin ASO CC-paste with 1% w/w paclitaxel (treatment #I). Data points and error bars represent the mean ± standard deviation. Results are shown for a minimum of four mice (if less than four mice remained in any group, then the data are not shown).

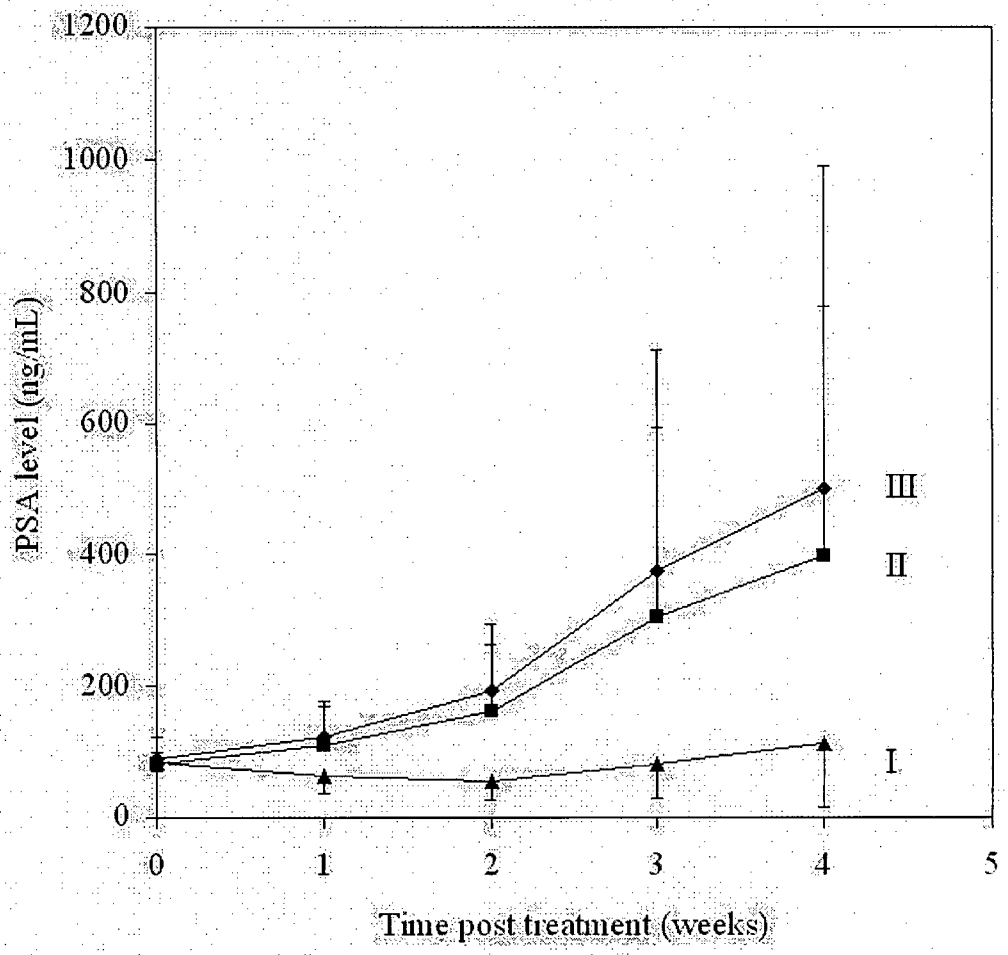

Figure 4.4 Effect of CC-paste loaded with clusterin ASO and paclitaxel on serum PSA level in mice with LNCaP tumors following intra-tumoral administration. Treatment protocols are summarized in Table 4.1. (◆) 2% w/w clusterin ASO CC-paste alone (no paclitaxel) (treatment #III); (■) 2% w/w MMO CC-paste with 1% w/w paclitaxel (treatment #II); (▲) 2% w/w clusterin ASO CC-paste with 1% w/w paclitaxel (treatment #I). Data points and error bars represent the mean ± standard deviation. Results are shown for a minimum of four mice (if less than four mice remained in any group, then the data are not shown).

4.5 DISCUSSION

The polymer formulations used in this work were pastes at room temperature that could be injected through a 22-gauge needle into tumors. Targeting the clusterin ASO:chitosan complexes into the tumor via direct injection is an advantage compared to other routes of administration, since this route bypasses the healthy tissue where the basic extracellular environment may otherwise provide for the release of the oligonucleotide from the complex before reaching the tumor site. Indeed, the uptake and expression of plasmid DNA *in vitro* has been shown to be dependent on the pH of the cell media, with the greatest uptake and expression resulting from media at pH 7.0 (Ishii et al., 2001).

In an effort to decrease systemic drug levels and corresponding systemic side effects, paclitaxel was incorporated into injectable sustained release formulations consisting of biodegradable polymeric microspheres (Lapidus et al., 2004) or paste (Jackson et al., 2000) for local delivery. Clusterin has been shown to be an anti-apoptotic gene that conferred resistance to androgen ablation, increased the rate of progression to androgen independence (Miyake et al., 2000d) and provided resistance to cytotoxic agents in PC-3 (Miyake et al., 2000a) and LNCaP (Miyake et al., 2000b) prostate cancer cells. Miyake et al. (2000a) used cultured PC-3 cells and a PC-3 tumor model in mice to show that clusterin ASO reduced the expression of clusterin mRNA and clusterin protein, but failed to reduce PC-3 growth (Miyake et al., 2000a). However, the combination of systemic clusterin ASO with paclitaxel enhanced apoptosis and reduced PC-3

(Miyake et al., 2000a; Miyake et al., 2003) and LNCaP (Miyake et al., 2000b) cell growth and tumor volume. Hence, our approach in this work was the targeting of clusterin ASO and paclitaxel or docetaxel directly into tumors by first incorporating the ASO and cytotoxic agents into an injectable paste. Following injection into tumors *in vivo* the pastes formed semi-solid implants in less than one hour. Intratumoral injection of clusterin ASO CC paste with paclitaxel or docetaxel into PC-3 tumors grown in mice showed a synergistic effect on tumor volume compared to paste with clusterin ASO, paclitaxel, or docetaxel alone. Similarly, intratumoral injection of clusterin ASO CC paste with paclitaxel into LNCaP tumors grown in mice resulted in a synergistic effect on tumor volume and serum PSA level compared to paste with clusterin ASO or paclitaxel alone.

In this work, efficacy was achieved for four weeks against PC-3 and LNCaP tumors grown in mice following a single intratumoral injection of biodegradable triblock polymeric paste loaded with clusterin ASO complexed with chitosan particles and combined with paclitaxel or docetaxel. Using 2 mg of clusterin ASO and 1 mg of paclitaxel or docetaxel, these formulations achieved efficacy against PC-3 and LNCaP tumors with no observed toxicity. Our research group observed similar efficacy following the single intratumoral injection of 10% w/w paclitaxel loaded polymeric paste (equivalent to 10 mg of paclitaxel per 25 g mouse) without clusterin ASO into PC-3 tumors. At this higher intratumoral dose of paclitaxel, areas of redness close to the injection site and evidence of inhibition of wound healing were observed (Jackson et al., 2000). Previous studies using systemically administered clusterin ASO and paclitaxel used a total of approximately 5 to 7 mg clusterin ASO (based on an average mouse weight of 25 mg and 10 to 12.5 mg clusterin/kg body

weight injected intraperitoneally daily for 15 to 18 days) and 2.5 or 5 mg paclitaxel (0.5 mg injected intravenously daily for 5 or 10 days) (Miyake et al, 2000a; Miyake et al., 2000b).

This study provides proof of principle data for an intratumorally administered sustained release formulation of clusterin ASO and paclitaxel or docetaxel as a treatment for solid prostate tumors.

4.6 CONCLUSIONS

1. Treatment of mice bearing PC-3 tumors with an intratumoral, controlled delivery system for clusterin ASO based on complexed clusterin ASO:chitosan dispersed in a biodegradable polymer paste with paclitaxel or docetaxel, reduced mean tumor volume by greater than 50% at four weeks.
2. Treatment of mice bearing LNCaP tumors with an intratumoral, controlled delivery system for clusterin ASO based on complexed clusterin ASO:chitosan dispersed in a biodegradable polymer paste with paclitaxel, reduced mean tumor volume and serum PSA level by more than 50% and 70%, respectively.

5. SUMMARIZING DISCUSSION, CONCLUSIONS AND FUTURE WORK

5.1 SUMMARIZING DISCUSSION

Paclitaxel and docetaxel have been shown to exert apoptotic effects by promoting the formation and inhibiting the depolymerization of microtubules, and by phosphorylating the oncogenic protein Bcl-2 (Berchem et al., 1999; Leung et al., 2000; Stein, 1999a). However, when administered intravenously in the clinic against prostate cancer, these agents have shown only modest responses (Sinibaldi et al., 2002; Kuruma et al., 2003). Pro-apoptotic stimulation of neoplastic prostate cells mediates a chemoresistant phenotype, in part, by the overexpression of clusterin protein, which inhibits apoptosis (July et al., 2002; Chi et al., 2005). Paclitaxel and clusterin ASO combination therapy, administered systemically in human prostate cancer PC-3 (Miyake et al., 2000a) and LNCaP (Miyake et al., 2000b) mice xenograft models, resulted in enhanced apoptosis, decreased cancer cell growth and reduced tumor volume. Intra-tumoral administration of paclitaxel formulated as controlled release biodegradable polymeric microspheres (Lapidus et al., 2004) or paste (Jackson et al., 2000) or docetaxel loaded into biodegradable microspheres (Farokhzad et al., 2006) have been investigated in terms of their ability to decrease systemic drug levels and corresponding systemic toxicities. These formulations have been shown to be efficacious against human prostate tumors in mice xenograft models.

The anatomical location of the prostate gland allows for brachytherapy for localized prostate tumors to be routinely carried out using transrectal ultrasound to guide the transperineal placement of the radioactive seed implants (Konstantinos, 2005). However, approximately half of these patients have post-radiation recurrences of prostate cancer and yet there is no effective treatment for these patients. It is therefore conceivable that prostate tumors in post-radiation

failure patients could be locally treated by direct injection of the prostate with an intratumoral drug delivery system (Jackson et al., 2000). Thus, we proposed that an intratumoral injection of a controlled release clusterin ASO and paclitaxel or docetaxel delivery system should maintain effective concentrations of the drugs in the tumor, resulting in regression of the tumor.

It was necessary to develop a formulation strategy to produce a controlled release of clusterin ASO from a polymer matrix which would also serve to protect the ASO from potential degradation by nucleases. We proposed that complexing polyanionic clusterin ASO with a polycationic polymer microparticle and incorporating this into a polymeric paste might help to control the release of the ASO from the paste. Microparticulate chitosan was chosen as a suitable polycationic polymeric biomaterial for this purpose. The amine group on the N-D-glucosamine residue of chitosan is capable of accepting a proton in acidic solutions. Unlike the colloidal or coacervate complexes formed from solutions of ASO mixed with chitosan in weak acid, we loaded clusterin ASO into chitosan microparticles by a solvent loading process to form clusterin ASO:chitosan microparticulate complexes (CC complexes).

The goals of this work were to develop and characterize controlled release polymeric paste formulations of clusterin ASO and paclitaxel or docetaxel and to investigate the *in vivo* efficacy of the formulations following intratumoral injection in human prostate cancer murine xenograft models. We proposed the following ideal properties of the polymeric paste formulation for this purpose: the formulation should be composed of biocompatible and biodegradable polymeric materials; the formulation should be readily sterilized, easily injected into tissue and form a depot following injection; and the formulation should maintain the stability of the drugs within the matrix while releasing the drugs in a controlled manner at the tumor site for one month or greater.

For the formulation characterization work, the development of suitable assays for the quantification of clusterin ASO were required and these were described in Chapter 2. Anion exchange HPLC and CGE assays were developed and qualified for the analysis of clusterin ASO over the range of 1 to 50 and 0.13 to 6.3 $\mu g \cdot mL^{-1}$, respectively. Anion exchange HPLC was used as the routine method for analysis of clusterin ASO when little or no degradation of the ASO was anticipated. CGE was selected as the method for analysis of the full length 21-mer clusterin ASO and its 20-, 19- and 18-mer degradation product oligonucleotides in human plasma since this method was able to separate and quantitate oligonucleotides differing in length by only 1 mer. An extraction and desalting method was developed to prepare plasma samples for CGE analysis, to overcome salt or buffer interfering with the electrokinetic injection and detection of oligonucleotide samples.

In Chapter 3 the characterization studies of clusterin ASO:chitosan microparticulate complexes (CC complexes) were reported. The insoluble chitosan microparticles swelled about 600% in aqueous media. This enabled us to readily load clusterin ASO into the chitosan by a process of soaking the chitosan microparticles in the clusterin ASO aqueous solution where the negatively charged ASO complexed with the positively charged amine groups on the chitosan polymer chains of the swollen chitosan hydrogel matrix. Zeta potential and binding studies demonstrated that the complexation of clusterin ASO to chitosan was dependent on the ASO:chitosan ratio and the pH.

CC complexes were difficult to inject through syringe/needle assemblies due to both aggregation and sedimentation. Issues of aggregation and sedimentation were overcome by incorporating the CC complexes into a polymeric paste consisting of the triblock copolymer PLC-block-PEG-block-PLC blended with MePEG in a 40/60 w/w ratio (CC pastes) and the

formulation was readily injected through a 22 gauge needle at ambient temperature. Addition of PBS release media at 37°C to the CC paste formulations would result in solidification of the paste. From previous work (Jackson et al., 2000; Jackson et al., 2004) we established that the hydrophilic MePEG rapidly partitioned and diffused out from the paste into the surrounding aqueous media. The remaining hydrophobic triblock copolymer-rich phase with dispersed CC complexes, with or without paclitaxel or docetaxel, would then solidify due to an increased melting temperature of the triblock copolymer and precipitation of the hydrophobic paclitaxel or docetaxel (Jackson et al., 2000; Jackson et al., 2004). The drug release profile of paclitaxel loaded CC pastes demonstrated a very slow, controlled release of paclitaxel over several weeks, primarily via a diffusion mechanism. The drug release profile of docetaxel showed a rapid burst phase followed by a slow controlled release phase over several weeks. Docetaxel released more rapidly from the paste probably because it is not as hydrophobic as paclitaxel and it is well established in the literature that hydrophilic drugs are released more rapidly from polyesters (Grassi and Grassi, 2005).

Release studies of clusterin ASO investigated the influence of ASO:chitosan ratios, pH, phosphate ion concentration and the presence or absence of the polymer paste matrix. The data demonstrated that complexing of polyanionic clusterin ASO to the cationic amine groups within the swollen chitosan hydrogel microparticles strongly influenced release profiles. Increasing either the amount of chitosan in the complexes relative to clusterin ASO, or changing the pH from above the pKa of chitosan (observed to be between 6.2 to 6.7) to close to or below the pKa, resulted in slower overall ASO release rates from the complexes. This was clearly a result of the increased number of positively charged sites within in the chitosan causing more extensive binding or complexation of clusterin ASO and therefore slower release of ASO from

these sites and into the release medium. The effect of increasing the phosphate ion concentration in the release medium, that is, increasing the ionic strength, resulted in more rapid release of clusterin ASO from CC complexes due to a shielding or competition of phosphate ions with clusterin ASO for the positively charged chitosan binding sites.

Previous work by others showed the sustained release of ASOs *in vitro* from PLGA microspheres, however, loading efficiencies were very low with only approximately 3 to 300 μg ASO loaded into 100 mg of PLGA microspheres (Hussain et al, 2002; Lewis et al., 1998; De Rosa et al., 2003). The low loadings of ASO into the microspheres, even using a water-in-oil-in-water double emulsion microsphere preparation method, were likely due to the hydrophilic nature of the ASO and the hydrophobicity of PLGA and its oil-phase solvent. We chose a dose of 2 mg of clusterin ASO for evaluation in the animal models in chapter 4 and suggest that lower ASO loadings would provide lower or no efficacy than we observed with 2 mg. However, to our knowledge, ASO loaded PLGA microspheres have not been investigated in *in vivo* efficacy models. We found that 2 mg or greater amounts of clusterin ASO could be loaded into 100 mg of polymeric triblock/MePEG paste by physical blending, with or without first complexing the ASO to chitosan microparticles. De Rosa (2003) improved the loading efficiency of ASOs in PLGA microspheres by first complexing the ASO with PEI. However; less than 10% of the ASO was released from the microspheres as the ASO/PEI complex over 45 days or "...the percentage of released complex even decreased with time." (De Rosa, 2003). Our data show that by varying the ratio of clusterin ASO:chitosan and by incorporating the ASO or CC complexes into biodegradable paste that the cumulative release of clusterin ASO over 4 weeks could be varied from approximately 10 to 100% of the loaded ASO.

Clusterin ASO released more slowly and to a lesser extent from CC paste containing paclitaxel (Figure 3.9) than from CC paste without paclitaxel (Figure 3.5). Previous work by Jackson et al. (2004) demonstrated that triblock/MePEG polymeric pastes containing paclitaxel or other hydrophobic drugs set to a semi-solid depot with greater structural integrity and remained as an intact pellet for a longer period of time in aqueous media under stirring than triblock/MePEG polymeric pastes containing hydrophilic drugs or no drug. The increased structural integrity of the paste with paclitaxel in aqueous media may have been due to the hydrophobic drug precipitating out as the MePEG diffused away from the paste, leaving solid paclitaxel dispersed throughout the semi-solid, waxy triblock copolymer-rich phase of the remaining formulation (Jackson, 2004). The CC paste with paclitaxel likely also had greater structural integrity and increased hydrophobicity than CC paste without paclitaxel, resulting in fewer aqueous pores and channels forming in the remaining triblock-rich waxy paste and a corresponding reduction in both the rate of swelling of the CC complexes in the paste and diffusion of the hydrophilic clusterin ASO through and out of the paste.

Release and degradation studies were carried out in human plasma *in vitro* to determine the ability of the CC complex and CC paste formulations to protect ASO from degradation by nucleases. The data showed that degradation of clusterin ASO occurred in the presence of plasma and suggested that while chitosan (CC complexes) did not protect the ASO from degradation, the presence of the polymer paste matrix surrounding the microparticulate CC complexes inhibited the degradation of clusterin ASO.

Studies were conducted to establish that clusterin ASO released from CC paste formulations could be taken up into cells in a bioactive form and inhibit the expression of clusterin protein. Western blots of PC-3 cells treated *in vitro* with clusterin ASO released from

polymeric paste, CC complexes and CC pastes *in vitro* demonstrated that clusterin ASO was released from the various formulations in a bioactive form.

We believe that, given the negligible water solubility of chitosan at a pH of 7.4 (Henriksen et al., 1997; Richardson et al., 1999) there is very little likelihood that there are dissolved chitosan species complexing with clusterin ASO. Thus, we suggest that ASO released from CC complexes and the CC pastes is primarily in the free form and not complexed with chitosan. A schematic of a proposed mechanism of release of clusterin ASO from CC paste *in vitro* is shown in Figure 5.1. Initial incubation of the CC paste in an aqueous media results in water diffusing into the paste (see pathway 1). The water soluble MePEG diffuses rapidly out of the paste, leaving interconnected aqueous pores and channels in the remaining semi-solid/waxy triblock copolymer (see pathway 2). This allows water to contact and swell the chitosan microparticles (see pathway 3). As clusterin ASO is released from the CC complexes, free clusterin ASO diffuses through the aqueous pores and channels in the triblock copolymer and is released into the media (see pathway 4). After approximately one week, most of the clusterin ASO remaining in the chitosan particles is strongly bound to the chitosan through electrostatic complexes and is not released or only very slowly released from CC complexes *in vitro* over the next 3 weeks.

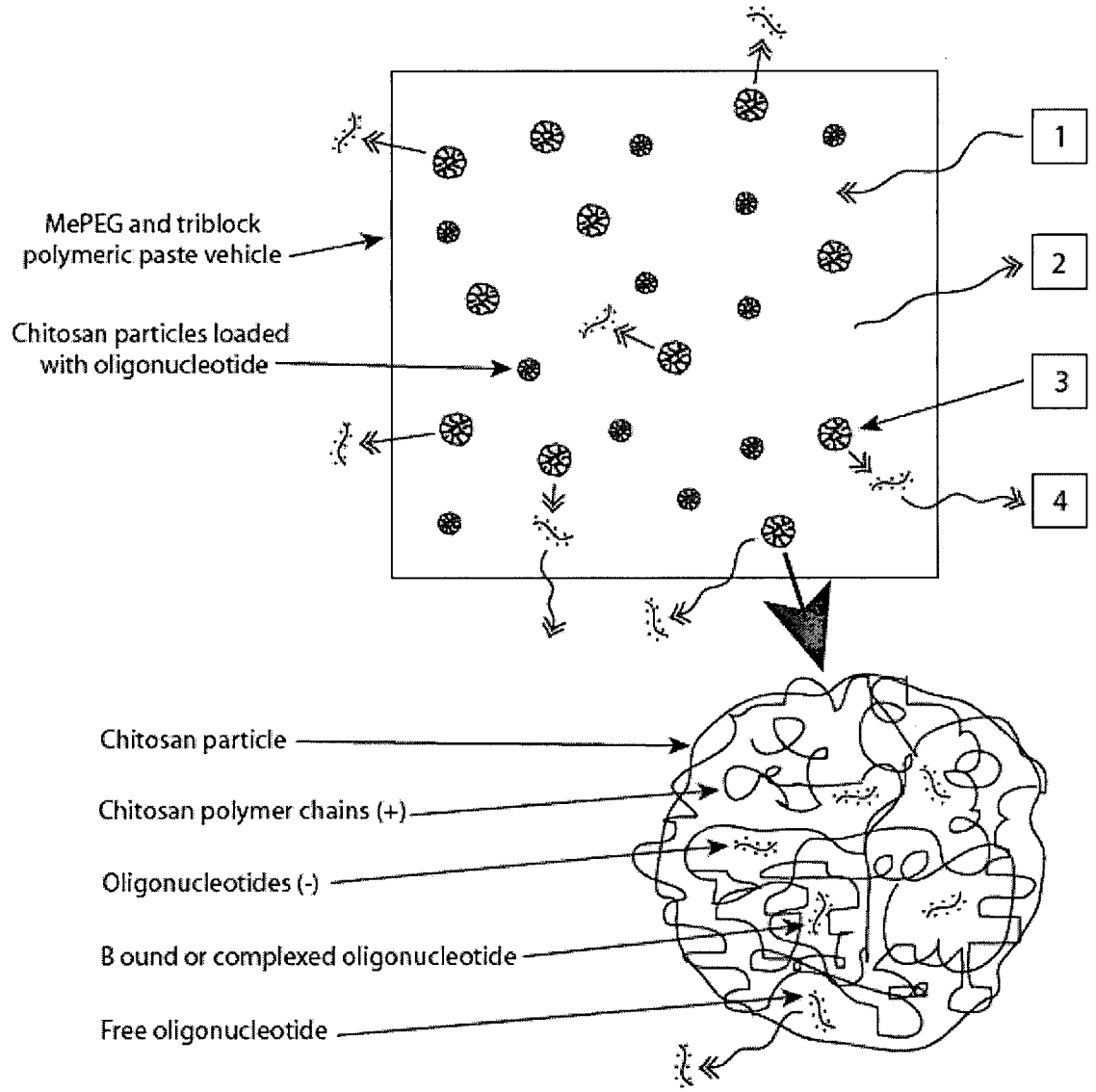

Figure 5.1 Schematic illustrating the proposed mechanism of ASO release from CC paste. ASO release occurs as follows:

1. Water diffuses into the MePEG and triblock polymeric paste vehicle.
2. Water-soluble MePEG diffuses out of the polymeric paste, resulting in the formation of pores and channels in the remaining triblock paste.
3. Water swells chitosan particles.
4. "Free" oligonucleotide diffuses through pores and channels out of the polymeric paste.

Prior to conducting most of the extensive characterization studies described in Chapter 3, we chose to conduct the proof of principle animal efficacy studies. We selected a clusterin ASO:chitosan ratio of 1:2 and these CC complexes were dispersed in polymeric paste together with paclitaxel or docetaxel. The use of the 1:2 ASO:chitosan ratio in the CC pastes was based on continuous release of clusterin ASO *in vitro* over 4 weeks and ease of injection. The *in vivo* efficacy studies of intratumoral clusterin ASO and paclitaxel or docetaxel loaded CC paste were conducted using human prostate PC-3 or LNCaP tumors in mice and are discussed in Chapter 4. The tumor volumes of PC-3 and LNCaP tumors were evaluated and the serum PSA levels of LNCaP tumor bearing mice were determined for 4 weeks, following a single intratumoral injection. Treatment of mice bearing PC-3 tumors with 2 mg clusterin ASO and 1 mg paclitaxel or docetaxel loaded CC paste resulted in reduced mean tumor volume by greater than 50% at 4 weeks. Treatment of mice bearing LNCaP tumors with 2 mg clusterin ASO and 1 mg paclitaxel loaded CC paste resulted in decreased mean tumor volume and serum PSA level by more than 50 and 70%, respectively. Previous studies in PC-3 tumor-bearing mice showed approximately 50% reduction in tumor volume at 4 weeks following the administration of 10 $mg \cdot kg^{-1}$ clusterin ASO in solution via intraperitoneal injection daily for 28 d (estimated total cumulative dose of 7 mg clusterin ASO for a 25 g mouse) combined with 0.5 mg paclitaxel in a micellar formulation administered via intravenous injection daily on days 10 to 14 and 24 to 28 (total cumulative dose of 5 mg paclitaxel) (Miyake et al., 2000a). Previous investigations in Shionogi tumor-bearing mice demonstrated approximately 35% reduction in tumor volume at 4 weeks following the administration of 12.5 $mg \cdot kg^{-1}$ clusterin ASO in solution via intraperitoneal injection daily for 15 days (estimated total cumulative dose of approximately 4.7 mg clusterin ASO for a 25 g mouse) combined with 0.5 mg paclitaxel in a micellar formulation administered

via intravenous injection daily on days 10 to 14 (total cumulative dose of 2.5 mg paclitaxel) (Miyake et al., 2000b). The data presented, suggest that for human prostate tumors in mice, that a single intratumoral administration of 2 mg clusterin ASO and 1 mg paclitaxel or docetaxel loaded CC paste had equal or greater efficacy than repeated systemic injections of a cumulative total of approximately 5 to 7 mg clusterin ASO with a total of 2.5 to 5 mg paclitaxel. Furthermore, the data suggest that clusterin ASO was being released in a sustained manner from CC paste *in vivo* for at least approximately 4 weeks. We speculate that *in vivo* the presence of salt ions and the likely enzymatic degradation of chitosan assist in the release of clusterin ASO from the CC complexes and CC paste. We believe that our approach of using site directed, controlled release delivery of clusterin ASO plus taxane should have the potential to make a significant impact on improving the delivery of these agents to prostate cancer patients.

Complexing polycationic polysaccharides to ASOs prior to incorporating the ASOs into biodegradable polymeric matrices has not, to our knowledge, been evaluated (Springate et al., 2005). Elucidation of this new knowledge is fundamental to understanding the processes of, and the development of new formulation strategies for, decreasing *in vivo* degradation of ASOs and controlling ASO release from biodegradable polymeric matrices. These studies are fundamental to future work and our long-term goal, in which delivery systems for intratumoral administration may be developed for rapidly degraded and eliminated drugs such as clusterin ASO. Although these studies are focused on prostate cancer, the research findings may also be applied to future chemotherapeutic treatment modalities for other localized tumors.

It will be important to understand the role of CC paste in future preclinical studies. Future studies should evaluate controlled release compared to current treatment regimens of continuous injections of high levels of clusterin ASO and taxane. The CC paste loaded with

clusterin ASO plus taxane should be administered via a single intratumoral injection in a human prostate tumor mouse xenograft model and compared to both the systemic and the intratumoral administrations of clusterin ASO solution plus commercial preparation of taxane. Acute and longer term toxicity of the CC paste formulation should be evaluated by administering intraperitoneal or subcutaneous injections in mice with alternating increasing doses of clusterin ASO and paclitaxel or docetaxel and evaluating the mice at 1, 3, 15 and 30 days. It is necessary to understand the plasma and tissue uptake, distribution and excretion of the drugs and polymers of the CC paste. As tumor tissue is different from normal tissue, these parameters should be characterized by administering intratumoral injections of the CC pastes in a human prostate tumor murine xenograft model. Based on the characterization, drug release and efficacy data, we anticipate that this formulation could be extended to evaluate the delivery of other polyanionic therapeutic oligonucleotides and other tumor models.

5.2 CONCLUSIONS

1. An HPLC method was developed to quantify docetaxel. The existing paclitaxel and new docetaxel HPLC methods were acceptable with linear ranges of 1 to 50 and 1 to 100 $\mu g \cdot mL^{-1}$, respectively.

2. An anion exchange HPLC method was developed and qualified for the analysis of clusterin ASO in the range of 1 to 50 $\mu g \cdot mL^{-1}$. A CGE method was developed and qualified for the analysis of 21-mer clusterin ASO and its 20-, 19- and 18-mer oligonucleotide degradation products in plasma in the range of 0.13 to 6.3 $\mu g \cdot mL^{-1}$.

3. Clusterin ASO:chitosan ratio and pH both influenced the electrostatic interaction and binding of clusterin ASO with chitosan in CC complexes.

4. The rate and extent of clusterin ASO release was influenced by clusterin ASO:chitosan ratio, pH and phosphate concentration. The release profiles were also related to whether the clusterin ASO was incorporated into polymeric paste.

5. Our data suggest that CC paste may have protected clusterin ASO from nuclease degradation *in vitro* in human plasma.

6. Clusterin ASO released from the various formulations suppressed the expression of clusterin protein in PC-3 cells *in vitro*.

7. Paclitaxel, docetaxel and clusterin ASO were released *in vitro* in a controlled manner from CC paste formulations used for *in vivo* evaluation.

8. Treatment of mice bearing PC-3 tumors with an intratumoral, controlled delivery system for clusterin ASO based on complexed clusterin ASO:chitosan microparticles dispersed in a biodegradable polymer paste with paclitaxel or docetaxel, reduced mean tumor volume by greater than 50% at four weeks.

9. Treatment of mice bearing LNCaP tumors with an intratumoral, controlled delivery system for clusterin ASO based on complexed clusterin ASO:chitosan microparticles dispersed in a biodegradable polymer paste with paclitaxel, reduced mean tumor volume and serum PSA level by more than 50% and 70%, respectively.

6. REFERENCES

Agalliu, I, D W Lin, C A Salinas, Z Feng, J L Stanford. Polymorphisms in the glutathione S-transferase M1, T1, and P1 genes and prostate cancer prognosis. *The Prostate* (2006) 66:1535-1541.

Agrawal, S, J Y Tang, D M Brown. Analytical study of phosphorothioate analogues of oligodeoxynucleotides using high-performance liquid chromatography. *Journal of Chromatography* (1990) 509:396-399.

Agrawal, S, J Temsemani, J Y Tang. Pharmacokinetics, biodistribution, and stability of oligodeoxynucleotide phosphorothioates in mice. *Proceedings of the National Academy of Sciences of the United States of America* (1991) 88:7595-7599.

Akhtar, S, M D Hughes, A Khan, M Bibby, M Hussain, Q Nawaz, J Double, P Sayyed. The delivery of antisense therapeutics. *Advanced Drug Delivery Reviews* (2000) 44:3-21.

Al Malyan, M, C Becchi, L Nikkola, P Viitanen, S Boncinelli, F Chiellini, N Ashammakhi. Polymer-based biodegradable drug delivery systems in pain management. *Journal of Craniofacial Surgery* (2006) 17:302-313.

Albrecht, T, R Schwab, C Peschel, H J Engels, T Fischer, C Huber, W E Aulitzky. Cationic lipid mediated transfer of c-abl and bcr antisense oligonucleotides to immature normal myeloid cells: uptake, biological effects and modulation of gene expression. *Annals of Hematology* (1996) 72:73-79.

Allerson, C R, N Sioufi, R Jarres, T P Prakash, N Naik, A Berdeja, L Wanders, R H Griffey, E E Swayze, B Bhat. Fully 2'-modified oligonucleotide duplexes with improved in vitro potency and stability compared to unmodified small interfering RNA. *Journal of Medicinal Chemistry* (2005) 48:901-904.

Amantana, A, C A London, P L Iversen, G R Devi. X-linked inhibitor of apoptosis protein inhibition induces apoptosis and enhances chemotherapy sensitivity in human prostate cancer cells. *Molecular Cancer Therapeutics* (2004) 3:699-707.

Anthonsen, M W, K M Vårum, O Smidsrod. Solution properties of chitosans: conformation and chain stiffness of chitosan with different degrees of *N*-acetylation. *Carbohydrate Polymers* (1993) 22:193-201.

Aynie, I, C Vauthier, M Foulquier, C Malvy, E Fattal, P Couvreur. Development of a quantitative polyacrylamide gel electrophoresis analysis using a multichannel radioactivity counter for the evaluation of oligonucleotide-bound drug carrier. *Analytical Biochemistry.240(2):202-9,* (1996).

Baker, R W. *Controlled Release of Biologically Active Agent*, New York, John Wiley & Sons (1987).

Baker, S D, A Sparreboom, J Verweij. Clinical pharmacokinetics of docetaxel: recent developments. *Clinical Pharmacokinetics* (2006) 45:235-252.

Baloglu, E, M L Miller, E E Roller, E E Cavanagh, B A Leece, V S Goldmacher, R V Chari. Synthesis and biological evaluation of novel taxoids designed for targeted delivery to tumors. *Bioorganic & Medicinal Chemistry Letters* (2004) 14:5885-5888.

Behrens, R J, J L Gulley, W L Dahut. Pulmonary toxicity during prostate cancer treatment with docetaxel and thalidomide. *American Journal of Therapeutics* (2003) 10:228-232.

Belenky, A, D L Smisek, A S Cohen. Sequencing of antisense DNA analogues by capillary gel electrophoresis with laser-induced fluorescence detection. *Journal of Chromatography A* (1995) 700:137-149.

Benesova-Minarikova, L, L Fantova, M Minarik. Multicapillary electrophoresis of unlabeled DNA fragments with high-sensitive laser-induced fluorescence detection by counter-current migration of intercalation dye. *Electrophoresis* (2005) 26:4064-9.

Berchem, G J, M Bosseler, N Mine, B Avalosse. Nanomolar range docetaxel treatment sensitizes MCF-7 cells to chemotherapy induced apoptosis, induces G2M arrest and phosphorylates bcl-2. *Anticancer Research* (1999) 19:535-540.

Bergan, R, Y Connell, B Fahmy, E Kyle, L Neckers. Aptameric inhibition of $p210^{bcr\text{-}abl}$ tyrosine kinase autophosphorylation by oligodeoxynucleotides of defined sequence and backbone structure. *Nucleic Acids Research* (1994) 22:2150-2154.

Berton, M, E Allémann, C A Stein, R Gurny. Highly loaded nanoparticulate carrier using an hydrophobic antisense oligonucleotide complex. *European Journal of Pharmaceutical Sciences* (1999) 9:163-170.

Bhujwalla, Z M, D Artemov, E Aboagye, E Ackerstaff, R J Gillies, K Natarajan, M Solaiyappan. The physiological environment in cancer vascularization, invasion and metastasis. *Novartis Foundation Symposium* (2001) 240:23-38.

Billmeyer, F W. *Textbook of polymer science*, New York, Wiley (1984).

BioMed Central website at *www.biomedcentral.com.*

Biroccio, A, C D'Angelo, B Jansen, M E Gleave, G Zupi. Antisense clusterin oligodeoxynucleotides increase the response of HER-2 gene amplified breast cancer cells to Trastuzumab. *Journal of Cellular Physiology* (2005) 204:463-469.

Blackadder, D A. *Some Aspects of Basic Polymer Science*, London, London Chemical Society (1975).

Bochot, A, E Fattal, A Gulik, G Couarraze, P Couvreur. Liposomes dispersed within a thermosensitive gel: a new dosage form for ocular delivery of oligonucleotides. *Pharmaceutical Research* (1998) 15:1364-1369.

Bock, L C, L C Griffin, J A Latham, E H Vermaas, J J Toole. Selection of single-stranded DNA molecules that bind and inhibit human thrombin. *Nature* (1992) 355:564-566.

Bono, A V. The global state of prostate cancer: epidemiology and screening in the second millennium. *BJU International* (2004) 94 Suppl 3:1-2.

Brannon-Peppas, L, J O Blanchette. Nanoparticle and targeted systems for cancer therapy. *Advanced Drug Delivery Reviews* (2004) 56:1649-1659.

Brem, H, P Gabikian. Biodegradable polymer implants to treat brain tumors. *Journal of Controlled Release* (2001) 74:63-67.

Brignole, C, G Pagnan, D Marimpietri, E Cosimo, T M Allen, M Ponzoni, F Pastorino. Targeted delivery system for antisense oligonucleotides: a novel experimental strategy for neuroblastoma treatment. *Cancer Letters* (2003) 197:231-235.

Brown, M D, A G Schatzlein, I F Uchegbu. Gene delivery with synthetic (non viral) carriers. *International Journal of Pharmaceutics* (2001) 229:1-21.

Bruno, R, N Vivier, C Veyrat-Follet, G Montay, G R Rhodes. Population pharmacokinetics and pharmacokinetic-pharmacodynamic relationships for docetaxel. *Investigational New Drugs.* (2001)163-169.

Bubendorf, L, M Kolmer, J Kononen, P Koivisto, M Spyro, Y Chen, E Mahlamäki, P Schraml, H Moch, N Willi, A G Elkahloun, T G Pretlow, T C Gasser, M J Mihatsch, G Sauter, O-P Kallioniemi. Hormone therapy failure in human prostate cancer: analysis by complementary DNA and tissue microarrays. *Journal of the National Cancer Institute* (1999) 91:1758-1764.

Burt, H M, J K Jackson, S K Bains, R T Liggins, A M Oktaba, A L Arsenault, W L Hunter. Controlled delivery of taxol from microspheres composed of a blend of ethylene-vinyl acetate copolymer and poly (d,l-lactic acid). *Cancer Letters* (1995) 88:73-79.

Caccamo, A E, S Desenzani, L Belloni, A F Borghetti, S Bettuzzi. Nuclear clusterin accumulation during heat shock response: implications for cell survival and thermo-tolerance induction in immortalized and prostate cancer cells. *Journal of Cellular Physiology.* (2006) 207:208-219.

Cao, C, E T Shinohara, H Li, K J Niermann, K W Kim, K R Sekhar, M Gleave, M Freeman, B Lu. Clusterin as a therapeutic target for radiation sensitization in a lung cancer model. *International Journal of Radiation Oncology, Biology, Physics* (2005) 63:1228-1236.

Capaccioli, S, G Di Pasquale, E Mini, T Mazzei, A Quattrone. Cationic lipids improve antisense oligonucleotide uptake and prevent degradation in cultured cells and in human serum. *Biochemical & Biophysical Research Communications.* (1993) 818-825.

Caplen, N J, S Mousses. Short interfering RNA (siRNA)-mediated RNA interference (RNAi) in human cells. *Annals of the New York Academy of Sciences* (2003) 1002:56-62.

Carreño-Gómez, B, R Duncan. Evaluation of the biological properties of soluble chitosan and chitosan microspheres. *International Journal of Pharmaceutics* (1997) 148:231-240.

Carson, C C, III. Carcinoma of the prostate: overview of the most common malignancy in men. *North Carolina Medical Journal* (2006) 67:122-127.

Chang, B L, S L Zheng, G A Hawkins, S D Isaacs, K E Wiley, A Turner, J D Carpten, E R Bleecker, P C Walsh, J M Trent, D A Meyers, W B Isaacs, J Xu. Joint effect of HSD3B1 and HSD3B2 genes is associated with hereditary and sporadic prostate cancer susceptibility. *Cancer Research* (2002) 62:1784-1789.

Chavany, C, T Le Doan, P Couvreur, F Puisieux, C Helénè. Polyalkylcyanoacrylate nanoparticles as polymeric carriers for antisense oligonucleotides. *Pharmaceutical Research* (1992) 9:441-449.

Chen, S-H, M Qian, J M Brennan, J M Gallo. Determination of antisense phosphorothioate oligonucleotides and catabolites in biological fluids and tissue extracts using anion-exchange high-performance liquid chromatography and capillary gel electrophoresis. *Journal of Chromatography B* (1997) 692:43-51.

Chen, J, W-L Yang, J Qian, J-L Xue, S-K Fu, D-R Lu. Transfection of mEpo gene to intestinal epithelium *in vivo* mediated by oral delivery of chitosan-DNA nanoparticles. *World Journal of Gastroenterology* (2003) 20:112-116.

Chenite, A, C Chaput, D Wang, C Combes, M D Buschmann, C D Hoemann, J C Leroux, B L Atkinson, F Binette, A Selmani. Novel injectable neutral solutions of chitosan form biodegradable gels in situ. *Biomaterials* (2000) 21:2155-2161.

Chi, K N, E Eisenhauer, L Fazli, E C Jones, S L Goldenberg, J Powers, D Tu, M E Gleave. A phase I pharmacokinetic and pharmacodynamic study of OGX-011, a 2'-methoxyethyl antisense oligonucleotide to clusterin, in patients with localized prostate cancer. *Journal of the National Cancer Institute* (2005) 97:1287-1296.

Chien, Y. *Novel Drug Delivery Systems*, London, Informa Healthcare (1991).

Chmurny, G N, B D Hilton, S Brobst, S A Look, K M Witherup, J A Beutler. 1H- and 13C-nmr assignments for taxol, 7-epi-taxol, and cephalomannine. *Journal of Natural Products* (1992) 55:414-423.

Cho-Chung, Y S, A M Gewirtz, C A Stein. Introduction. *Annals of the New York Academy of Sciences* (2003) 1002:xi-xii.

Chung, L W, A Baseman, V Assikis, H E Zhau. Molecular insights into prostate cancer progression: the missing link of tumor microenvironment. *Journal of Urology* (2005) 173:10-20.

Clarke, S J, L P Rivory. Clinical pharmacokinetics of docetaxel. *Clinical Pharmacokinetics* (1999) 36:99-114.

Cleek, R L, A A Rege, L A Denner, S G Eskin, A G Mikos. Inhibition of smooth muscle cell growth *in vitro* by an antisense oligodeoxynucleotide released from poly(DL-lactic-co-glycolic acid) microspheres. *Journal of Biomedical Materials Research* (1997) 35:525-530.

Collins, E A, J Bares, J F Billmeyer. *Experiments in Polymer Science*, New York, John Wiley & Sons (1973).

Cowie, J M G. *Polymers: chemistry and physics of modern materials*, Aylesbury, Bucks, International Textbook Company Limited (1973) 6-9.

Cowman, M K, S Matsuoka. Experimental approaches to hyaluronan structure. *Carbohydrate Research* (2005) 340:791-809.

Cox, M C, C D Scripture, W D Figg. Leuprolide acetate given by a subcutaneous extended-release injection: less of a pain? *Expert Review of Anticancer Therapy* (2005) 5:605-611.

Craft, N, Y Shostak, M Carey, C L Sawyers. A mechanism for hormone-independent prostate cancer through modulation of androgen receptor signaling by the HER-2/neu tyrosine kinase. *Nature Medicine* (1999) 5:280-285.

Cresteil, T, B Monsarrat, P Alvinerie, J M Treluyer, I Vieira, M Wright. Taxol metabolism by human liver microsomes: identification of cytochrome P450 isozymes involved in its biotransformation. *Cancer Research* (1994) 54:386-392.

Crook, J, H Lukka, L Klotz, N Bestic, M Johnston, Genitourinary Cancer Disease Stie Group of the Cancer Care Ontario Practice Guidelines Initiative. Systematic overview of the evidence for brachytherapy in clinically localized prostate cancer. *Canadian Medical Association Journal* (2001) 164:975-981.

Crooke, S T. Advances in understanding the pharmacological properties of antisense oligonucleotides. *Advances in Pharmacology* (1997) 40:1-49.

Crooke, S T. Molecular mechanisms of action of antisense drugs. *Biochimica et Biophysica Acta* (1999) 1489:31-44.

Crooke, S T. Evaluating the mechanism of action of antiproliferative antisense drugs. *Antisense & Nucleic Acid Drug Development* (2000) 10:123-126.

Cui, J Q, Y F Shi, H J Zhou. Effect of antisense oligodeoxynucleotide of small subunit component of human ribonucleotide reductase on human choriocarcinoma cell line in vitro. *Chinese Journal of Obstetrics & Gynecology* (2004) 39:465-468.

De Rosa, G, F Quaglia, M I La Rotonda, M Appel, H Alphandary, E Fattal. Poly(lactide-*co*-glycolide) microspheres for the controlled release of oligonucleotide/polyethylenimine complexes. *Journal of Pharmaceutical Sciences* (2002) 91:790-799.

de Semir, D, A Avinyó, S Larriba, V Nunes, T Casals, X Estivill, J M Aran. Quantitative Assessment of Chimeraplast Stability in Biological Fluids by Polyacrylamide Gel Electrophoresis and Laser-Assisted Fluorescence Analysis. *Pharmaceutical Research* (2002) 19:914-918.

De Smedt, S C, J Demeester, W E Hennink. Cationic polymer based gene delivery systems. *Pharmaceutical Research* (2000) 17:113-126.

DeDionisio, L. Capillary gel electrophoresis and the analysis of DNA phosphorothioates. *Journal of Chromatography A* (1993) 652:101-108.

DeDionisio, L, D H Lloyd. Capillary gel electrophoresis and antisense therapeutics. Analysis of DNA analogues. *Journal of Chromatography A* (1996) 735:191-208.

DeDionisio, L A, A M Raible, J S Nelson. Analysis of an oligonucleotide N3'-->P5' phosphoramidate/phosphorothioate chimera with capillary gel electrophoresis. *Electrophoresis* (1998) 19:2935-2938.

Dhanikula, A B, D R Singh, R Panchagnula. In vivo pharmacokinetic and tissue distribution studies in mice of alternative formulations for local and systemic delivery of Paclitaxel: gel, film, prodrug, liposomes and micelles. *Current Drug Delivery* (2005) 2:35-44.

Di Martino, A, M Sittinger, M V Risbud. Chitosan: a versatile biopolymer for orthopaedic tissue-engineering. *Biomaterials* (2005) 26:5983-5990.

Duggan, B J, S Gray, S R Johnston, K Williamson, H Miyake, M Gleave. The role of antisense oligonucleotide in the treatment of bladder cancer. *Urological Research* (2002) 30:137-147.

Edelman, E R, M Simons, M G Sirois, R D Rosenberg. c-myc in vasculoproliferative disease. *Circulation research* (1995) 76:176-182.

Eder, I E, J Hoffmann, H Rogatsch, G Sch+ñfer, D Zopf, G Bartsch, H Klocker. Inhibition of LNCaP prostate tumor growth in vivo by an antisense oligonucleotide directed against the human androgen receptor. *Cancer Gene Therapy* (2002) 9:117.

Eliaz, R E, F C Szoka, Jr. Robust and prolonged gene expression from injectable polymeric implants. *Gene Therapy* (2002) 9:1230-1237.

Epa, W R, U Greferath, A Shafton, P Rong, L M Delbridge, A Bennie, G L Barrett. Downregulation of the p75 neurotrophin receptor in tissue culture and in vivo, using beta-cyclodextrin-adamantane-oligonucleotide conjugates. *Antisense & Nucleic Acid Drug Development* (2000) 10:469-478.

Erbacher, P, S Zou, T Bettinger, A-M Steffan, J-S Remy. Chitosan-based vector/DNA complexes for gene delivery: biophysical characteristics and transfection ability. *Pharmaceutical Research* (1998) 15:1332-1339.

Eremeeva, T. Size-exclusion chromatography of enzymatically treated cellulose and related polysaccharides: a review. *Journal of Biochemical & Biophysical Methods* (2003) 56:253-264.

Evans, E E, S P Kent. The us of basic polysaccharides in histochemistry and cytochemistry: IV. Precipitation and agglutination of biological materials by *Aspergillus* polysaccharide and deacetylated chitin. *The journal of histochemistry and cytochemistry* (1962) 10:24-28.

Evelhoch, J L. pH and therapy of human cancers. *Novartis Foundation Symposium* (2001) 240:68-84.

Farokhzad, O C, J Cheng, B A Teply, I Sherifi, S Jon, P W Kantoff, J P Richie, R Langer. Targeted nanoparticle-aptamer bioconjugates for cancer chemotherapy in vivo. *Proceedings of the National Academy of Sciences of the United States of America* (2006) 103:6315-6320.

Felgner, P L, Y Barenholz, J P Behr, S H Cheng, P Cullis, L Huang, J A Jessee, L Seymour, F Szoka, A R Thierry, E Wagner, G Wu. Nomenclature for synthetic gene delivery systems. *Human Gene Therapy* (1997) 8:511-512.

Ferreiro, M G, L Tillman, G Hardee, R Bodmeier. Characterization of complexes of an antisense oligonucleotide with protamine and poly-L-lysine salts. *Journal of Controlled Release* (2001) 73:381-390.

Ferreiro, M G, L G Tillman, G Hardee, R Bodmeier. Alginate/poly-L-lysine microparticles for the intestinal delivery of antisense oligonucleotides. *Pharmaceutical Research* (2002) 19:755-764.

Fornaro, M, J Plescia, S Chheang, G Tallini, Y-M Zhu, M King, D C Altieri, L R Languino. Fibronectin protects prostate cancer cells from tumor necrosis factor-a-induced apoptosis via the AKT/survivin pathway. *The Journal of Biological Chemistry* (2003) 278:50402-50411.

Frasoldati, A, M Zoli, F F Rommerts, G Biagini, F M Faustini, C Carani, L F Agnati, P Marrama. Temporal changes in sulphated glycoprotein-2 (clusterin) and ornithine decarboxylase mRNA levels in the rat testis after ethane-dimethane sulphonate-induced degeneration of Leydig cells. *International Journal of Andrology.18(1):46-54,* (1995).

Freiberg, S, X X Zhu. Polymer microspheres for controlled drug release. *International Journal of Pharmaceutics* (2004) 282:1-18.

Freier, T, H S Koh, K Kazazian, M S Shoichet. Controlling cell adhesion and degradation of chitosan films by *N*-acetylation. *Biomaterials* (2005) 26:5872-5878.

Froim, D, C E Hopkins, A Belenky, A S Cohen. Method for phosphorothioate antisense DNA sequencing by capillary electrophoresis with UV detection. *Nucleic Acids Research* (1997) 24:4219-4223.

Fung, L K, W M Saltzman. Polymeric implants for cancer chemotherapy. *Advanced Drug Delivery Reviews* (1997) 26:209-230.

Gait, M J. Peptide-mediated cellular delivery of antisense oligonucleotides and their analogues. *Cellular and Molecular Life Sciences* (2003) 60:844-853.

Gao, S, J Chen, L Dong, Z Ding, Y-H Yang, J Zhang. Targeting delivery of oligonucleotide and plasmid DNA to hepatocyte via galactosylated chitosan vector. *European Journal of Pharmaceutics and Biopharmaceutics* (2005) 60:327-334.

Geary, R S, T A Watanabe, L Truong, S Freier, E A Lesnik, N B Sioufi, H Sasmor, M Manoharan, A A Levin. Pharmacokinetic properties of 2'-O-(2-methoxyethyl)-modified oligonucleotide analog in rats. *The Journal of Pharmacology and Experimental Therapeutics* (2001) 296:890-897.

Gibbons, N B, R W Watson, R N Coffey, H P Brady, J M Fitzpatrick. Heat-shock proteins inhibit induction of prostate cancer cell apoptosis. *The Prostate* (2000) 45:58-65.

Gibson, I. Antisense approaches to the gene therapy of cancer - 'Recnac'. *Cancer and Metastasis Reviews* (1996) 15:287-299.

Gilar, M, A Belenky, D L Smisek, A Bourque, A S Cohen. Kinetics of phosphorothioate oligonucleotide metabolism in biological fluids. *Nucleic Acids Research* (1997) 25:3615-3620.

Gleave, M E, N Bruchovsky, M J Moore, P Venner. Prostate cancer: 9. Treatment of advanced disease. *Canadian Medical Association Journal* (1999) 160:225-232.

Gleave, M, H Miyake, K Chi. Beyond simple castration: targeting the molecular basis of treatment resistance in advanced prostate cancer. *Cancer Chemotherapy and Pharmacology* (2005) 56 (Suppl 1):s47-s57.

Gleave, M, K N Chi. Knock-down of the cytoprotective gene, clusterin, to enhance hormone and chemosensitivity in prostate and other cancers. *Annals of the New York Academy of Sciences* (2005) 1058:1-15.

Gleave, M, W K Kelly. High-risk localized prostate cancer: a case for early chemotherapy. *Journal of Clinical Oncology* (2005) 23:8186-8191.

Gleave, M, H Miyake. Use of antisense oligonucleotides targeting the cytoprotective gene, clusterin, to enhance androgen- and chemo-sensitivity in prostate cancer. *World Journal of Urology* (2005) 23:38-46.

Gleave, M E, B P Monia. Antisense therapy for cancer. *Nature Reviews.Cancer* (2005) 5:468-479.

Godbey, W T, K K Wu, A G Mikos. Tracking the intracellular path of poly(ethylenimine)/DNA complexes for gene delivery. *Proceedings of the National Academy of Sciences of the United States of America* (1999) 96:5177-5188.

Goldenberg, S L, E W Ramsey, M A S Jewett. Prostate cancer: 6. Surgical treatment of localized disease. *Canadian Medical Association Journal* (1998) 159:1265-1271.

Grassi, M, G Grassi. Mathematical modelling and controlled drug delivery: matrix systems. *Current Drug Delivery* (2005) 2:97-116.

Grate, D, C Wilson. Inducible regulation of the *S. cerevisiae* cell cycle mediated by an RNA aptamer-ligand complex. *Bioorganic & Medicinal Chemistry* (2001) 9:2565-2570.

Gray, D M, S H Hung, K H Johnson. Absorption and circular dichroism spectroscopy of nucleic acid duplexes and triplexes. *Methods in Enzymology* (1995) 246:19-34.

Gronberg, H. Prostate cancer epidemiology. *Lancet* (2003) 361:859-864.

Grulke, E A. Polymer process engineering, Englewood Cliffs, Prentice-Hall (1994).

Guerin, C, A Olivi, J D Weingart, H C Lawson, H Brem. Recent advances in brain tumor therapy: local intracerebral drug delivery by polymers. *Investigational New Drugs* (2004) 22:27-37.

Hail, M E, B Elliott, K Anderson. High-throughput analysis of oligonucleotides using automated electrospray ionization mass spectrometry. *American Biotechnology Laboratory* (2004) 12-14.

Hall, C. Polymer Materials: An Introduction for Technologists and Scientists, New York, John Wiley & Sons (1988).

Hardardottir, I, S T Kunitake, A H Moser, W T Doerrler, J H Rapp, C Grunfeld, K R Feingold. Endotoxin and cytokines increase hepatic messenger RNA levels and serum concentrations of apolipoprotein J (clusterin) in Syrian hamsters. *Journal of Clinical Investigation* (1994) 94:1304-1209.

Harding, S E. The intrinsic viscosity of biological macromolecules. Progress in measurement, interpretation and application to structure in dilute solution. *Progress in Biophysics and Molecular Biology* (1997) 68:207-262.

Hasirci, V, K Lewandrowski, J D Gresser, D L Wise, D J Trantolo. Versatility of biodegradable biopolymers: degradability and an in vivo application. *Journal of Biotechnology* (2001) 86:135-150.

Hayatsu, H, T Kubo, Y Tanaka, K Negishi. Polynucleotide-chitosan complex, an insoluble but reactive form of polynucleotide. *Chemical & Pharmaceutical Bulletin* (1997) 45:1363-1368.

Heirwegh, K P, J A Meuwissen, R Lontie. Selective absorption and scattering of light by solutions of macromolecules and by particulate suspensions. *Journal of Biochemical & Biophysical Methods* (1987) 14:303-322.

Henriksen, I, S R Vågen, S A Sande, G Smistad, J Karlsen. Interactions between liposomes and chitosan II: effect of selected parameters on aggregation and leakage. *International Journal of Pharmaceutics* (1997) 146:193-204.

Henry, S P, R S Geary, R Yu, A A Levin. Drug properties of second-generation antisense oligonucleotides: how do they measure up to their predecessors? *Current Opinion in Investigational Drugs* (2001) 2:1444-1449.

Higuchi, T. Rate of release of medicaments from ointment bases containing drugs in suspension. *Journal of Pharmaceutical Sciences* (1961) 50:875.

Ho, H-A, M Boissinot, M G Bergeron, G Corbeil, K Doré, D Boudreau, M Leclerc. Colorimetric and fluorometric detection of nucleic acids using cationic polythiophene derivatives. *Angewandte Chemie International Edition* (2002) 41:1548-1551.

Hon, D N S. Chitin and chitosan: medical applications, in S Dumitriu (ed), *Polysaccharides in Medicinal Applications*, New York, Marcel Dekker, Inc. (1996) 631-649.

Horvath, A, J Aradi. Advantages of sodium perchlorate solution as mobile phase for purification of synthetic oligonucleotides by anion exchange chromatography. *Analytical Biochemistry* (2005) 338:341-343.

Hu, Q, C R Shew, M B Bally, T L Madden. Programmable fusogenic vesicles for intracellular delivery of antisense oligodeoxynucleotides: enhanced cellular uptake and biological effects. *Biochimica et Biophysica Acta* (2001) 1514:1-13.

Huggins, M L. The viscosity of dilute solutions of long-chain molecules. IV. Dependence on concentration. *Journal of the American Chemical Society* (1942) 84:2716-2718.

Huizing, M T, A C Keung, H Rosing, d K van, V, W W Bokkel Huinink, I M Mandjes, A C Dubbelman, H M Pinedo, J H Beijnen. Pharmacokinetics of paclitaxel and metabolites in a randomized comparative study in platinum-pretreated ovarian cancer patients. *Journal of Clinical Oncology* (1993) 11:2127-2135.

Huizing, M T, J B Vermorken, H Rosing, W W Bokkel Huinink, I Mandjes, H M Pinedo, J H Beijnen. Pharmacokinetics of paclitaxel and three major metabolites in patients with advanced breast carcinoma refractory to anthracycline therapy treated with a 3-hour paclitaxel infusion: a European Cancer Centre (ECC) trial. *Annals of Oncology* (1995) 6:699-704.

Hussain, M, G Beale, M Hughes, S Akhtar. Co-delivery of an antisense oligonucleotide and 5-fluorouracil using sustained release poly(lactide-co-glycolide) microsphere formulations for potential combination therapy in cancer. *International Journal of Pharmaceutics* (2002) 234:129-138.

ICH (International Committee on Harmonization). *Guidance for Industry. Q2B Validation of Analytical Procedures: Methodology* (1996).

Illum, L, I Jabbal-Gill, M Hinchcliffe, A N Fisher, S S Davis. Chitosan as a novel nasal delivery system for vaccines. *Advanced Drug Delivery Reviews* (2001) 51:81-96.

Ishihara, M, K Obara, S Nakamura, M Fujita, K Masuoka, Y Kanatani, B Takase, H Hattori, Y Morimoto, M Ishihara, T Maehara, M Kikuchi. Chitosan hydrogel as a drug delivery carrier to control angiogenesis. *Journal of Artificial Organs* (2006) 9:8-16.

Ishii, T, Y Okahata, T Sato. Mechanism of cell transfection with plasmid/chitosan complexes. *Biochimica et Biophysica Acta* (2001) 1514:51-64.

Islam, A, S L Handley, K S Thompson, S Akhtar. Studies on uptake, sub-cellular trafficking and efflux of antisense oligodeoxynucleotides in glioma cells using self-assembling cationic lipoplexes as delivery systems. *Journal of Drug Targeting* (2000) 7:373-382.

Jaaskelainen, I, J Monkkonen, A Urtti. Oligonucleotide-cationic liposome interactions. A physicochemical study. *Biochimica et Biophysica Acta* (1994) 1195:115-123.

Jackson, J K, M E Gleave, V Yago, E Beraldi, W L Hunter, H M Burt. The suppression of human prostate tumor growth in mice by the intratumoral injection of a slow-release polymeric paste formulation of paclitaxel. *Cancer Research* (2000) 60:4146-4151.

Jackson, J K, L S Liang, W L Hunter, M Reynolds, J A Sandberg, C Springate, H M Burt. The encapsulation of ribozymes in biodegradable polymeric matrices. *International Journal of Pharmaceutics* (2002) 243:43-55.

Jackson, J K, X Zhang, S Llewellen, W L Hunter, H M Burt. The characterization of novel polymeric paste formulations for intratumoral delivery. *International Journal of Pharmaceutics* (2004) 270:185-198.

Jaganathan, K S, Y U B Rao, P Singh, D Prabakaran, S Gupta, A Jain, S P Vyas. Development of a single dose tetanus toxoid formulation based on polymeric microspheres: a comparative study of poly(D,L-lactic-co-glycolic acid) versus chitosan microspheres. *International Journal of Pharmaceutics* (2005) 294:23-32.

Jain, R K. Transport of molecules, particles, and cells in solid tumors. *Annual Review of Biomedical Engineering* (1999) 1:241-263.

Jameela, S R, A Jayakrishnan. Glutaraldehyde cross-linked chitosan microspheres as a long acting biodegradable drug delivery vehicle: studies on the *in vitro* release of mitoxantrone and *in vivo* degradation of microspheres in rat muscle. *Biomaterials* (1995) 16:769-775.

Juliano, R L. Peptide-oligonucleotide conjugates for the delivery of antisense and siRNA. *Current Opinion in Molecular Therapeutics* (2005) 7:132-136.

Jones, S E, C Jomary. Molecules in focus. Clusterin. *The International Journal of Biochemistry and Cell Biology* (2002) 34:427-431.

July, L V, M Akbari, T Zellweger, E C Jones, S L Goldenberg, M E Gleave. Clusterin expression is significantly enhanced in prostate cancer cells following androgen withdrawal therapy. *The Prostate* (2002) 50:179-188.

Kanjickal, D G, S T Lopina. Modeling of drug release from polymeric delivery systems--a review. *Critical Reviews in Therapeutic Drug Carrier Systems* (2004) 21:345-386.

Kasaai, M R, J Arul, G Charlet. Intrinsic viscosity-molecular weight relationship for chitosan. *Journal of Polymer Science Part B: Polymer Physics* (2000) 38:2591-2598.

Kelly, W K, A X Zhu, H Scher, T Curley, M Fallon, S Slovin, L Schwartz, S Larson, W Tong, B Hartley-Asp, C Pellizzoni, M Rocchetti. Dose escalation study of intravenous estramustine phosphate in combination with paclitaxel and carboplatin in patients with advanced prostate cancer. *Clinical Cancer Research* (2003) 9:2098-2107.

Kim, S Y, Y M Lee, D J Baik, J S Kang. Toxic characteristics of methoxy poly(ethylene glycol)/poly(epsilon-caprolactone) nanospheres; in vitro and in vivo studies in the normal mice. *Biomaterials* (2003) 24:55-63.

Kiyama, S, K Morrison, T Zellweger, M Akbari, M Cox, D Yu, H Miyake, M E Gleave. Castration-induced increases in insulin-like growth factor-binding protein 2 promotes proliferation of androgen-independent human prostate LNCaP tumors. *Cancer Research* (2003) 63:3575-3584.

Klinman, D M, R Zeuner, H Yamada, M Gursel, D Currie, I Gursel. Regulation of CpG-induced immune activation by suppressive oligodeoxynucleotides. *Annals of the New York Academy of Sciences* (2003) 1002:112-123.

Knaul, J Z, M R Kasaai, V T Bui, K A M Creber. Characterization of deacetylated chitosan and chitosan molecular weight review. *Canadian Journal of Chemistry* (1998) 76:1699-1706.

Kondo, Y, S Koga, T Komata, S Kondo. Treatment of prostate cancer *in vitro* and *in vivo* with 2-5A-anti-telomerase RNA component. *Oncogene* (2000) 19:2205-2211.

Konstantinos, H. Prostate cancer in the elderly. *International Urology & Nephrology* (2005) 37:797-806.

Köping-Höggård, M, I Tubulekas, H Guan, K Edwards, M Nilsson, K M Vårum, P Artursson. Chitosan as a nonviral gene delivery system. Structure-property relationships and characteristics compared with polyethyleneimine *in vitro* and after lung administration *in vivo*. *Gene Therapy* (2001) 8:1108-1121.

Köping-Höggård, M. Relationship between the physical shape and the efficiency of oligomeric chitosan as a gene delivery system *in vitro* and *in vivo*. *The Journal of Gene Medicine* (2003) 5:130-141.

Kraemer, E O. Molecular weights of celluloses and cellulose derivatives. *Industrial and Engineering Chemistry* (1938) 30:1200-1203.

Kraft, P, P Pharoah, S J Chanock, D Albanes, L N Kolonel, R B Hayes, D Altshuler, G Andriole, C Berg, H Boeing, N P Burtt, B Bueno-de-Mesquita, E E Calle, H Cann, F Canzian, Y C Chen, D E Crawford, A M Dunning, H S Feigelson, M L Freedman, J M Gaziano, E Giovannucci, C A Gonzalez, C A Haiman, G Hallmans, B E Henderson, J N Hirschhorn, D J Hunter, R Kaaks, T Key, L Le Marchand, J Ma, K Overvad, D Palli, M C Pike, E Riboli, C Rodriguez, W V Setiawan, M J Stampfer, D O Stram, G Thomas, M J Thun, R Travis, A Trichopoulou, J Virtamo, S Wacholder. Genetic variation in the HSD17B1 gene and risk of prostate cancer. *PLoS Genetics* (2005) 1:e68.

Krieg, A M, J Tonkinson, S Matson, Q Zhao, M Saxon, L M Zhang, U Bhanja, L Yakubov, C A Stein. Modification of antisense phosphodiester oligodeoxynucleotides by a 5' cholesteryl moiety increases cellular association and improves efficacy. *Proceedings of the National Academy of Sciences of the United States of America* (1993) 90:1048-1052.

Krieg, A M, A-K Yi, S Matson, T J Waldschmidt, G A Bishop, R Teasdale, G A Koretzky, D M Klinman. CpG motifs in bacterial DNA trigger direct B-cell activation. *Nature* (1995) 374:546-549.

Krieg, A M. Immune stimulation by oligonucleotides, in ST Crooke (ed), *Antisense drug technology. Principles, strategies, and applications*, New York, Marcel Dekker, Inc. (2001) 471-515.

Kuhn, J G. Pharmacology and pharmacokinetics of paclitaxel. *Annals of Pharmacotherapy* (1994) 28:S15-S17.

Kuruma, H, T Fujita, T Shitara, S Egawa, E Yokoyama, S Baba. Weekly paclitaxel plus estramustine combination therapy in hormone-refractory prostate cancer: A pilot study. *International Journal of Urology* (2003) 10:470-475.

Kyprianou, N, H F English, J T Isaacs. Programmed cell death during regression of PC-82 human prostate cancer following androgen ablation. *Cancer Research* (1990) 50:3748-3753.

Langer, R. New methods of drug delivery. *Science* (1990) 249:1527-1533.

Lapidus, R G, W Dang, D M Rosen, A M Gady, Y Zabelinka, R O'Meally, T L DeWeese, S R Denmeade. Anti-tumor effect of combination therapy with intratumoral controlled-release paclitaxel (Paclimer® microspheres) and radiation. *The Prostate* (2004) 58:291-298.

Lee, K Y, W S Ha, W H Park. Blood compatibility and biodegradability of partially N-acylated chitosan derivatives. *Biomaterials* (1995) 16:1211-1216.

Lee, M, J-W Nah, Y Kwon, J J Koh, K S Ko, S W Kim. Water-soluble and low molecular weight chitosan-based plasmid DNA delivery. *Pharmaceutical Research* (2001) 18:427-431.

Leeds, J M, M J Graham, L Truong, L L Cummins. Quantitation of phosphorothioate oligonucleotides in human plasma. *Analytical Biochemistry* (1996) 235:36-43.

Leeds, J M, L L Cummins. Analytical methods for antisense drugs, in ST Crooke (ed), *Antisense drug technology. Principles, strategies, and applications*, New York, Marcel Dekker, Inc. (2001) 57-82.

Legrier, M E, G de Pinieux, F Poirson-Bichat, F Apiou, A M Dutrillaux, K Boye, A Sihassen, R Lidereau, J Bara, F Arvelo, B Dutrillaux, M F Poupon. A new model of human prostate cancer, the PAC120 xenograft. *Pathologie Biologie* (2003) 51:1-4.

Leonetti, J P, N Mechti, G Degols, C Gagnor, B Lebleu. Intracellular distribution of microinjected antisense oligonucleotides. *Biochemistry* (1991) 88:2702-2706.

Leong, K W, H Q Mao, L Truong, K Roy, S M Walsh, J T August. DNA-polycation nanospheres as non-viral gene delivery vehicles. *Journal of Controlled Release* (1998) 53:183-193.

Leung, S Y, J Jackson, H Miyake, H Burt, M E Gleave. Polymeric micellar paclitaxel phosphorylates Bcl-2 and induces apoptotic regression of androgen-independent LNCaP prostate tumors. *The Prostate* (2000) 44:156-63.

Levy, I G, N A Iscoe, L H Klotz. Prostate cancer: 1. The descriptive epidemiology in Canada. *Canadian Medical Association Journal* (1998) 159:509-513.

Lewis, K J, W J Irwin, S Akhtar. Development of a sustained-release biodegradable polymer delivery system for site-specific delivery of oligonucleotides: characterization of P(LA-GA) copolymer microspheres *in vitro*. *Journal of Drug Targeting* (1998) 5:291-302.

Li, S, P Dobrzynski, J Kasperczyk, M Bero, C Braud, M Vert. Structure-property relationships of copolymers obtained by ring-opening polymerization of glycolide and epsilon-caprolactone. Part 2. Influence of composition and chain microstructure on the hydrolytic degradation. *Biomacromolecules* (2005) 6:489-497.

Liggins, R T, W L Hunter, H M Burt. Solid-state characterization of paclitaxel. *Journal of pharmaceutical sciences* (1997) 86:1458-1463.

Liggins, R T, S D'Amours, J S Demetrick, L S Machan, H M Burt. Paclitaxel loaded poly(L-lactic acid) microspheres for the prevention of intraperitoneal carcinomatosis after a surgical repair and tumor cell spill. *Biomaterials* (2000) 21:1959-1969.

Liggins, R T, H M Burt. Polyether-polyester diblock copolymers for the preparation of paclitaxel loaded polymeric micelle formulations. *Advanced Drug Delivery Reviews* (2002) 54:191-202.

Lim, L Y, E Khor, O Koo. Gamma irradiation of chitosan. *Journal of Biomedical Materials Research* (1998) 43:282-290.

Lim, L Y, E Khor, C E Ling. Effects of dry heat and saturated steam on the physical properties of chitosan. *Journal of Biomedical Materials Research* (1999) 48:111-116.

Lindstrom, S, F Wiklund, H O Adami, K A Balter, J Adolfsson, H Gronberg. Germ-line genetic variation in the key androgen-regulating genes androgen receptor, cytochrome P450, and steroid-5-alpha-reductase type 2 is important for prostate cancer development. *Cancer Research* (2006) 66:11077-11083.

Logothetis, C J. Docetaxel in the integrated management of prostate cancer. Current applications and future promise. *Oncology* (2002) 16:63-72.

Loke, S L, C A Stein, X H Zhang, K Mori, M Nakanishi, C Subasinghe, J S Cohen, L M Neckers. Characterization of oligonucleotide transport into living cells. *Proceedings of the National Academy of Sciences of the United States of America* (1989) 86:3474-3478.

Lungwitz, U, M Breunig, T Blunk, A Gopferich. Polyethylenimine-based non-viral gene delivery systems. *European Journal of Pharmaceutics & Biopharmaceutics* (2005) 60:247-266.

Luo, Y, G D Prestwich. Cancer-targeted polymeric drugs. *Current Cancer Drug Targets* (2002) 2:209-226.

Lysik, M A, S Wu-Pong. Minireview. Innovations in oligonucleotide drug delivery. *Journal of Pharmaceutical Sciences* (2003) 92:1559-1573.

MacLaughlin, F C, R J Mumper, J Wang, J M Tagliaferri, I Gill, M Hinchcliffe, A P Rolland. Chitosan and depolymerized chitosan oligomers as condensing carriers for in vivo plasmid delivery. *Journal of Controlled Release* (1998) 56:259-272.

Managit, C, S Kawakami, F Yamashita, M Hashida. Effect of galactose density on asialoglycoprotein receptor-mediated uptake of galactosylated liposomes. *Journal of Pharmaceutical Sciences* (2005) 94:2266-2275.

Mao, H Q, K Roy, L Troung, K A Janes, K Y Lin, Y Wang, J T August, K W Leong. Chitosan-DNA nanoparticles as gene carriers: synthesis, characterization and transfection efficiency. *Journal of Controlled Release* (2001) 70:399-421.

Marchettini, P, O A Stuart, F Mohamed, D Yoo, P H Sugarbaker. Docetaxel: pharmacokinetics and tissue levels after intraperitoneal and intravenous administration in a rat model. *Cancer Chemotherapy & Pharmacology* (2002) 49:499-503.

Martin, A N, P Bustamante, A H C Chun, *Physical Pharmacy: Physical Chemical Principles in the Pharmaceutical Sciences*, Baltimore, Williams & Wilkins (1993) 562-563.

Materials Science and Engineering Laboratory NIST Center for Neutron Research website: *http://www.ncnr.nist.gov.*

Maurer, N, A Mori, L Palmer, M A Monck, K W C Mok, B Mui, Q F Akhong, P R Cullis. Lipid-based systems for the intracellular delivery of genetic drugs. *Molecular Membrane Biology* (1999) 16:129-140.

McKenzie, S, N Kyprianou. Apoptosis evasion: the role of survival pathways in prostate cancer progression and therapeutic resistance. *Journal of Cellular Biochemistry* (2006) 97:18-32.

McSheehy, P M J, H Troy, L R Kelland, I R Judson, M O Leach, J R Griffiths. Increased tumour extracellular pH induced by Bafilomycin A_1 inhibits tumour growth and mitosis in vivo and alters 5-fluorouracil pharmacokinetics. *European Journal of Pharmaceutical Sciences* (2003) 39:532-540.

Meidan, V M, J S Cohen, N Amariglio, D Hirsch-Lerner, Y Barenholz. Interaction of oligonucleotides with cationic lipids: the relationship between electrostatics, hydration and state of aggregation. *Biochimica et Biophysica Acta* (2000) 1464:251-261.

Meidan, V M, J Glezer, N Amariglio, J S Cohen, Y Barenholz. Oligonucleotide lipoplexes: the influence of oligonucleotide composition on complexation. *Biochimica et Biophysica Acta* (2001) 1568:177-182.

Mellman, I. Endocytosis and molecular sorting. *Annual Review of Cell & Developmental Biology* (1996) 12:575-625.

Meluch, A A, F A Greco, L H Morrissey, E L Raefsky, R G Steis, J A Butts, J D Hainsworth, Minnie Pearl Cancer Research Network. Weekly paclitaxel, estramustine phosphate, and oral etoposide in the treatment of hormone-refractory prostate carcinoma: results of a Minnie Pearl Cancer Research Network phase II trial. *Cancer* (2003) 98:2192-2198.

Metelev, V, S Agrawal. Ion-exchange high-performance liquid chromatography analysis of oligodeoxyribonucleotide phosphorothioates. *Analytical Biochemistry* (1992) 200:342-346.

Mi, F-L, Y-C Tan, H-F Liang, H-W Sung. In vivo biocompatibility and degradability of a novel injectable-chitosan-based implant. *Biomaterials* (2002) 23:181-191.

Miyake, H, A Tolcher, M E Gleave. Antisense Bcl-2 oligodeoxynucleotides inhibit progression to androgen- independence after castration in the Shionogi tumor model. *Cancer Research* (1999) 59:4030-4034.

Miyake, H, K N Chi, M E Gleave. Antisense TRPM-2 oligodeoxynucleotides chemosensitize human androgen- independent PC-3 prostate cancer cells both in vitro and in vivo. *Clinical Cancer Research* (2000a) 6:1655-1663.

Miyake, H, C Nelson, P S Rennie, M E Gleave. Acquisition of chemoresistant phenotype by overexpression of the antiapoptotic gene testosterone-repressed prostate message-2 in prostate cancer xenograft models. *Cancer Research* (2000b) 60:2547-2554.

Miyake, H, B P Monia, M E Gleave. Inhibition of progression to androgen-independence by combined adjuvant treatment with antisense Bcl-xL and antisense Bcl-2 oligonucleotides plus taxol after castration in the Shionogi tumor model. *International Journal of Cancer* (2000c) 86:855-862.

Miyake, H, C Nelson, P S Rennie, M E Gleave. Testosterone-repressed prostate message-2 is an antiapoptotic gene involved in progression to androgen independence in prostate cancer. *Cancer Research* (2000d) 60:170-176.

Miyake, H, M Pollak, M E Gleave. Castration-induced Up-Regulation of Insulin-like Growth Factor Binding Protein-5 Potentiates Insulin-like Growth Factor-I Activity and Accelerates Progression to Androgen Independence in Prostate Cancer Models. *Cancer Research* (2000e) 60:3058-3064.

Miyake, H, A Tolcher, M E Gleave. Chemosensitization and delayed androgen-independent recurrence of prostate cancer with the use of antisense bcl-2 oligodeoxynucleotides. *Journal of the National Cancer Institute* (2000f) 92:34-41.

Miyake, H, M E Gleave, S Arakawa, S Kamidono, I Hara. Introducing the clusterin gene into human renal cell carcinoma cells enhances their metastatic potential. *The Journal of Urology* (2002a) 167:2203-2208.

Miyake, H, M Gleave, S Kamidono, I Hara. Overexpression of clusterin in transitional cell carcinoma of the bladder is related to disease progression and recurrence. *Urology* (2002b) 59:150-154.

Miyake, H, I Hara, S Kamidono, M Gleave, H Eto. Resistance to cytotoxic chemotherapy-induced apoptosis in human prostate cancer cells is associated with intracellular clusterin expression. *Oncology Reports* (2003) 10:469-473.

Miyake, H, K Yamanaka, M Muramaki, T Kurahashi, M Gleave, I Hara. Enhanced expression of the secreted form of clusterin following neoadjuvant hormonal therapy as a prognostic predictor in patients undergoing radical prostatectomy for prostate cancer. *Oncology Reports* (2005) 14:1371-1375.

Mohr, D, M Wolff, T Kissel. Gamma irradiation for terminal sterilization of 17beta-estradiol loaded poly-(D,L-lactide-co-glycolide) microparticles. *Journal of Controlled Release* (1999) 61:203-217.

Monsarrat, B, E Mariel, S Cros, M Gares, D Guenard, F Gueritte-Voegelein, M Wright. Taxol metabolism. Isolation and identification of three major metabolites of taxol in rat bile. *Drug Metabolism & Disposition* (1990) 18:895-901.

Montanari, L, F Cilurzo, L Valvo, A Faucitano, A Buttafava, A Groppo, I Genta, B Conti. Gamma irradiation effects on stability of poly(lactide-co-glycolide) microspheres containing clonazepam. *Journal of Controlled Release* (2001) 75:317-330.

Moul, J W, K Civitelli. Managing advanced prostate cancer with Viadur (leuprolide acetate implant). *Urologic Nursing* (2001) 21:385-388.

Murthy, N, J Campbell, N Fausto, A S Hoffman, P S Stayton. Design and synthesis of pH-responsive polymeric carriers that target uptake and enhance the intracellular delivery of oligonucleotides. *Journal of Controlled Release* (2003) 89:365-374.

Nakajima, S, Y Koshino, T Nomura, F Yamashita, S Agrawal, Y Takakura, M Hashida. Intratumoral pharmacokinetics of oligonucleotides in a tissue-isolated tumor perfusion system. *Antisense & Nucleic Acid Drug Development* (2000) 10:105-110.

Napoli, S, U Negri, F Arcamone, M L Capobianco, G M Carbone, C V Catapano. Growth inhibition and apoptosis induced by daunomycin-conjugated triplex-forming oligonucleotides targeting the c-myc gene in prostate cancer cells. *Nucleic Acids Research* (2006) 34:734-744.

Narayanan, R. Harnessing the power of antisense technology for combination chemotherapy. *Journal of the National Cancer Institute* (1997) 89:107-108.

Nemunaitis, J, J T Holmlund, M Kraynak, D Richards, J Bruce, N Ognoskie, T J Kwoh, R Geary, A Dorr, D Von Hoff, S G Eckhardt. Phase I evaluation of ISIS 3521, an antisense oligodeoxynucleotide to protein kinase C-alpha, in patients with advanced cancer. *Journal of Clinical Oncology* (1999) 17:3586-2595.

Neri, B, G Cipriani, C Fulignati, M Turrini, R Ponchietti, R Bartoletti, M A Della, C Di, V, A Dominici, D Maleci, A Raugei, D Villari, G Nicita. Weekly paclitaxel and epirubicin in the treatment of symptomatic hormone-refractory advanced prostate carcinoma: report of a phase II trial. *Anti-Cancer Drugs* (2005) 16:63-66.

Noe, C R, L Kaufhold. Chemistry of Antisense Oligonucleotides, in F Gualtieri, R Mannhold, H Kubinyi, and H Timmerman (eds), *New Trends in Synthetic Medicinal Chemistry (Methods and Principles in Medicinal Chemistry)*, Weinheim, Wiley-VCH Verlag GmbH (2000) 261-334.

Nordtveit, R J, K M Vårum, O Smidsrod. Degradation of partially *N*-acetylated chitosans with hen egg white and human lysozyme. *Carbohydrate Polymers* (1996) 29:163-167.

O'Brien, S M, C C Cunningham, A K Golenkov, A G Turkina, S C Novick, K R Rai. Phase I to II multicenter study of oblimersen sodium, a Bcl-2 antisense oligonucleotide, in patients with advanced chronic lymphocytic leukemia. *Journal of Clinical Oncology* (2005) 23:7697-7702.

Ojugo, A S E, P M J McSheehy, D J O McIntyre, C McCoy, M Stubbs, M O Leach, I R Judson, J R Griffiths. Measurement of the extracellular pH of solid tumors in mice by magnetic resonance spectroscopy: a comparison of exogenous ^{19}F and ^{31}P probes. *NMR in Biomedicine* (1999) 12:495-504.

Oupický, D, C Konák, K Ulbrich, M A Wolfert, L W Seymour. DNA delivery systems based on complexes of DNA with synthetic polycations and their copolymers. *Journal of Controlled Release* (2000) 65:149-171.

Papisov, I M, A A Litmanovich. Molecular "recognition" in interpolymer interactions and matrix polymerization in *Conducting Polymers/Molecular Recognition* in series *Advances in Polymer Science* (1988) 90:139-179.

Park, K, W S W Shalaby, H Park. *Biodegradable Hydrogels for Drug Delivery*, Lancaster, Technomic Publishing Company, Inc. (1993).

Park, I K, T H Kim, S I Kim, Y H Park, W J Kim, T Akaike, C S Cho. Visualization of transfection of hepatocytes by galactosylated chitosan-graft-poly(ethylene glycol)/DNA complexes by confocal laser scanning microscopy. *International Journal of Pharmaceutics* (2003) 257:103-110.

Patel, V R, M M Amiji. Preparation and characterization of freeze-dried chitosan-poly(ethylene oxide) hydrogels for site-specific antibiotic delivery in the stomach. *Pharmaceutical Research* (1996) 13:588-592.

Peng, J, X Xing, K Wang, W Tan, X He, S Huang. Influence of anions on the formation and properties of chitosan-DNA nanoparticles. *Journal of Nanoscience and Nanotechnology* (2005) 5:713-717.

Pennati, M, M Binda, G Colella, M Zoppe, M Folini, S Vignati, A Valentini, L Citti, M De Cesare, G Pratesi, M Giacca, M G Daidone, N Zaffaroni. Ribozyme-mediated inhibition of survivin expression increases spontaneous and drug-induced apoptosis and decreases the tumorigenic potential of human prostate cancer cells. *Oncogene* (2004) 23:386-394.

Perez-Marrero, R, R C Tyler. A subcutaneous delivery system for the extended release of leuprolide acetate for the treatment of prostate cancer. *Expert Opinion on Pharmacotherapy* (2004) 5:447-457.

Perugini, P, I Genta, B Conti, T Modena, F Pavanetto. Periodontal delivery of ipriflavone: new chitosan/PLGA film delivery system for a lipophilic drug. *International Journal of Pharmaceutics* (2003) 252:1-9.

Petrylak, D P, C M Tangen, M H Hussain, P N Lara, Jr., J A Jones, M E Taplin, P A Burch, D Berry, C Moinpour, M Kohli, M C Benson, E J Small, D Raghavan, E D Crawford. Docetaxel and estramustine compared with mitoxantrone and prednisone for advanced refractory prostate cancer. *New England Journal of Medicine* (2004) 351:1513-1520.

Petrylak, D P. The current role of chemotherapy in metastatic hormone-refractory prostate cancer. *Urology* (2005) 65(5 Suppl):3-7.

Pettaway, C A, S Pathak, G Greene, E Ramirez, M R Wilson, J J Killion, I J Fidler. Selection of highly metastatic variants of different human prostatic carcinomas using orthotopic implantation in nude mice. *Clinical Cancer Research* (1996) 2:1627-1636.

Pienta, K J. Preclinical mechanisms of action of docetaxel and docetaxel combinations in prostate cancer. *Seminars in Oncology* (2001) 28:3-7.

Pitt, C G, A Schindler. The design of controlled drug delivery systems based on biodegradable polymers, in ES Hafez and WA van Os (eds) *Biodegradables and Delivery Systems for Contraception*, Lancaster, MTP Press Ltd. (1980) 17-45.

Qian, F, N Nasongkla, J Gao. Membrane-encased polymer millirods for sustained release of 5-fluorouracil. *Journal of Biomedical Materials Research* (2002) 61:203-11.

Quinn, M, P Babb. Patterns and trends in prostate cancer incidence, survival, prevalence and mortality. Part II: individual countries. *BJU International* (2002) 90:174-184.

Raghunand, N, M I Altbach, R van Sluis, B Baggett, C W Taylor, Z M Bhujwalla, R J Gillies. Plasmalemmal pH-gradients in drug-sensitive and drug-resistant MCF-7 human breast carcinoma xenografts measured by ^{31}P magnetic resonance spectroscopy. *Biochemical Pharmacology* (1999) 57:309-312.

Raghunand, N, R J Gillies. pH and chemotherapy. *Novartis Foundation Symposium* (2001) 240:199-211.

Ramos, E A, J L V Relucio, C A T Torres-Villanueva. Gene expression in Tilapia following oral delivery of chitosan-encapsulated plasmid DNA incorporated into fish feeds. *Marine Biotechnology* (2005) 7:89-94.

Ranade, V V. Drug delivery systems: 3B. Role of polymers in drug delivery. *Journal of Clinical Pharmacology* (1990) 30:107-120.

Rao, S B, C P Sharma. Use of chitosan as a biomaterial: studies on its safety and hemostatic potential. *Journal of biomedical materials research* (1997) 34:21-28.

Raynaud, F I, R M Orr, P M Goddard, H A Lacey, H Lancashire, I R Judson, T Beck, B Bryan, F E Cotter. Pharmacokinetics of G3139, a phosphorothioate oligodeoxynucleotide antisense to bcl-2, after intravenous administration or continuous subcutaneous infusion to mice. *Journal of Pharmacology & Experimental Therapeutics* (1997) 281:420-427.

Renbutsu, E, M Hirose, Y Omura, F Nakatsubo, Y Okamura, Y Okamoto, H Saimoto, Y Shigemasa, S Minami. Preparation and biocompatibility of novel UV-curable chitosan derivatives. *Biomacromolecules* (2005) 6:2385-2388.

Richardson, S C, H V Kolbe, R Duncan. Potential of low molecular mass chitosan as a DNA delivery system: biocompatibility, body distribution and ability to complex and protect DNA. *International Journal of Pharmaceutics* (1999) 178:231-243.

Ringel, I, S B Horwitz. Taxol is converted to 7-epitaxol, a biologically active isomer, in cell culture medium. *Journal of Pharmacology & Experimental Therapeutics* (1987) 22:692-698.

Robaczewska, M, S Guerret, J-S Remy, I Chemin, W-B Offensperger, M Chevallier, J-P Behr, A J Podhajska, H E Blum, C Trepo, L Cova. Inhibition of hepadnaviral replication by polyethylenimine-based intravenous delivery of antisense phosphodiester oligodeoxynucleotides to the liver. *Gene Therapy* (2001) 8:874-881.

Robinson, J. *Controlled drug delivery: past, present and future, in K Park (ed), Controlled drug delivery: challenges and strategies*, Washington, American Chemical Society (1997) 1-7.

Romoren, K, S Pedersen, G Smistad, Ø Evensen, B J Thu. The influence of formulation variables on in vitro transfection efficiency and physicochemical properties of chitosan-based polyplexes. *International Journal of Pharmaceutics* (2003) 261:115-127.

Rosen, S L. *Fundamental principles of polymeric materials*, New York, John Wiley & Sons (1993). 53-81.

Roth, C M, S Sundaram. Engineering synthetic vectors for improved DNA delivery: insights from intracellular pathways. *Annual Review of Biomedical Engineering* (2004) 6:397-426.

Rothenfusser, S, V Hornung, M Ayyoub, S Britsch, A Towarowski, A Krug, A Sarris, N Lubenow, D Speiser, S Endres, G Hartmann. CpG-A and CpG-B oligonucleotides differentially enhance human peptide-specific primary and memory $CD8^+$ T-cell responses in vitro. *Immunobiology* (2004) 103:2162-2169.

Routh, J C, B C Leibovich. Adenocarcinoma of the prostate: epidemiological trends, screening, diagnosis, and surgical management of localized disease. *Mayo Clinic Proceedings* (2005) 80:899-907.

Rowinsky, E K, R C Donehower. Paclitaxel (taxol). *New England Journal of Medicine* (1995) 332:1004-1014.

Sahoo, S K, W Ma, V Labhasetwar. Efficacy of transferrin-conjugated paclitaxel-loaded nanoparticles in a murine model of prostate cancer. *International Journal of Cancer* (2004) 112:335-340.

Sato, T, T Ishii, Y Okahata. In vitro gene delivery mediated by chitosan. effect of pH, serum, and molecular mass of chitosan on the transfection efficiency. *Biomaterials* (2001) 22:2075-2080.

Schwartz, G G. Vitamin D and the epidemiology of prostate cancer. *Seminars in Dialysis* (2005) 18:276-289.

Schweitzer, M, J W Engels. Analysis of Oligonucleotides, in R Schlingensiepen, W Brysch, and K-H Schlingensiepen (eds) *Antisense - From Technology to Therapy*, Berlin, Blackwell Wissenschaft (1997) 78-103.

Seidman, A D, D Hochhauser, M Gollub, B Edelman, T J Yao, C A Hudis, P Francis, D Fennelly, T A Gilewski, M E Moynahan, V Currie, J Baselga, W Tong, M O'Donaghue, R Salvaggio, L Auguste, D Spriggs, L Norton. Ninety-six-hour paclitaxel infusion after progression during short taxane exposure: a phase II pharmacokinetic and pharmacodynamic study in metastatic breast cancer. *Journal of Clinical Oncology* (1996) 14:1877-1884.

Semple, S C, S K Klimuk, T O Harasym, N Dos Santos, S M Ansell, K F Wong, N Maurer, H Stark, P R Cullis, M J Hope, P Scherrer. Efficient encapsulation of antisense oligonucleotides in lipid vesicles using ionizable aminolipids: formation of novel small multilamellar vesicle structures. *Biochimica et Biophysica Acta* (2001) 1510:152-166.

Sensibar, J A, M D Griswold, S R Sylvester, R Buttyan, C W Bardin, C Y Cheng, S Dudek, C Lee. Prostatic ductal system in rats: regional variation in localization of an androgen-repressed gene product, sulfated glycoprotein-2. *Endocrinology* (1991) 128:2091-2102.

Sensibar, J A, D M Sutkowski, A Raffo, R Buttyan, M D Griswold, S R Sylvester, ., J M Kozlowski, C Lee. Prevention of cell death induced by tumor necrosis factor in LNCaP cells by overexpression of sulfated glycoprotein-2 (clusterin). *Cancer Research* (1995) 55:2431-2437.

Shah, V P, K K Midha, S Dighe, I J McGilveray, J P Skelly, A Yacobi, T Layloff, C T Viswanathan, C E Cook, R D McDowall, K A Pittman, S Spector. Analytical methods validation: bioavailability, bioequivalence and pharmacokinetic studies. *Pharmaceutical Research* (1992) 9:588-592.

Shah, V. *Guidance for industry: Bioanalytical methods validation for human studies. Draft guidance.* U.S. Department of Health and Human Services - Food and Drug Administration - Center for Drug Evaluation and Research (CDER) (1998).

Shaw, D R, P K Rustagi, E R Kandimalla, A N Manning, Z Jiang, S Agrawal. Effects of synthetic oligonucleotides on human complement and coagulation. *Biochemical Pharmacology* (1997) 53:1123-1132.

Shearwin, K E, D J Winzor. Thermodynamic nonideality in macromolecular solutions. Evaluation of parameters for the prediction of covolume effects. *European Journal of Biochemistry.* (1990)523-529.

Sherbet, G V. Hormonal influences on cancer progression and prognosis. *Vitamins & Hormones* (2005) 71:147-200.

Shi, F, A Nomden, V Oberle, J B F N Engberts, D Hoekstra. Efficient cationic lipid-mediated delivery of antisense oligonucleotides into eukaryotic cells: down-regulation of the corticotropin-releasing factor receptor. *Nucleic Acids Research* (2001) 29:2079-2087.

Shi, R. *Dissertation: Development and characterization of paclitaxel loaded polymeric films based on polysaccharides-graft-poly(e-caprolactone) for the prevention of surgical adhesions*, Vancouver, The University of British Columbia (2003) 31.

Shou, M, M Martinet, K R Korzekwa, K W Krausz, F J Gonzalez, H V Gelboin. Role of human cytochrome P450 3A4 and 3A5 in the metabolism of taxotere and its derivatives: enzyme specificity, interindividual distribution and metabolic contribution in human liver. *Pharmacogenetics* (1998) 8:391-401.

Shuttleworth, J, G Matthews, L Dale, C Baker, A Colman. Antisense oligodeoxyribonucleotide-directed cleavage of maternal mRNA in *Xenopus* oocytes and embryos. *Gene* (1988) 72:267-275.

Siepmann, J, A Gopferich. Mathematical modeling of bioerodible, polymeric drug delivery systems. *Advanced Drug Delivery Reviews* (2001) 48:229-247.

Sinha, V R, A Trehan. Biodegradable microspheres for protein delivery. *Journal of Controlled Release* (2003) 90:261-280.

Sinibaldi, V J, M A Carducci, S Moore-Cooper, M Laufer, M Zahurak, M A Eisenberger. Phase II evaluation of docetaxel plus one-day oral estramustine phosphate in the treatment of patients with androgen independent prostate carcinoma. *Cancer* (2002) 94:1457-1465.

Smith, D C, C H Chay, R L Dunn, J Fardig, P Esper, K Olson, K J Pienta. Phase II trial of paclitaxel, estramustine, etoposide, and carboplatin in the treatment of patients with hormone-refractory prostate carcinoma. *Cancer* (2003) 98:269-276.

So, A, S L Goldenberg, M E Gleave. Prostate specific antigen: an updated review. *The Canadian Journal of Urology* (2003) 10:2040-2050.

So, A, P Rocchi, M Gleave. Antisense oligonucleotide therapy in the management of bladder cancer. *Current Opinion in Urology* (2005) 15:320-327.

Solomon, O F, I Z Ciuta. Determination de la viscosité intrinsèque de solutions de polymers par une simple determination de la viscosité. *Journal of Applied Polymer Science* (1962) VI-24:683-686.

Soukchareun, S, J Haralambidis, G Tregear. Use of Nalpha-Fmoc-cysteine(S-thiobutyl) derivatized oligodeoxynucleotides for the preparation of oligodeoxynucleotide-peptide hybrid molecules. *Bioconjugate Chemistry* (1998) 9:466-475.

Spencer, C M, D Faulds. Paclitaxel. A review of its pharmacodynamic and pharmacokinetic properties and therapeutic potential in the treatment of cancer. *Drugs* (1994) 48:794-847.

Springate, C M K, J K Jackson, M E Gleave, H M Burt. Efficacy of an intratumoral controlled release formulation of clusterin antisense oligonucleotide complexed with chitosan containing paclitaxel or docetaxel in prostate cancer xenograft models. *Cancer Chemotherapy and Pharmacology* (2005) 56:239-247.

Stahel, R A, U Zangemeister-Wittke. Antisense oligonucleotides for cancer therapy - an overview. *Lung Cancer* (2003) 41 Supplement:S81-S88.

Stein, C A, J L Tonkinson, L M Zhang, L Yakubov, J Gervasoni, R Taub, S A Rotenberg. Dynamics of the internalization of phosphodiester oligodeoxynucleotides in HL60 cells. *Biochemistry* (1993) 32:4855-4861.

Stein, C A, A M Krieg. Editorial: Problems in interpretation of data derived from *in vitro* and *in vivo* use of antisense oligodeoxynucleotides. *Antisense Research and Development* (1994) 4:67-69.

Stein, C A. How to design an antisense oligodeoxynucleotide experiment: a consensus approach. *Antisense & Nucleic Acid Drug Development* (1998) 8:129-132.

Stein, C A. Mechanisms of action of taxanes in prostate cancer. *Seminars in Oncology* (1999a) 26:3-17.

Stein, C A. Two problems in antisense biotechnology: in vitro delivery and the design of antisense experiments. *Biochimica et Biophysica Acta* (1999b) 1489:45-52.

Stein, C A. Evaluating the mechanism of action of antiproliferative antisense drugs: a convergence of views? *Antisense & Nucleic Acid Drug Development* (2000) 10:127-127.

Stephenson, R A, C P Dinney, K Gohji, N G Ordonez, J J Killion, I J Fidler. Metastatic model for human prostate cancer using orthotopic implantation in nude mice. *Journal of the National Cancer Institute* (1992) 84:951-957.

Straubinger, R M. Biopharmaceutics of paclitaxel (Taxol): formulation, activity, and pharmacokinetics, in M Suffness (ed) *Taxol® Science and Applications*, Boca Raton, CRC Press, Inc. (1996) 237-258.

Strlic, M, J Kolar. Size exclusion chromatography of cellulose in LiCl/N,N-dimethylacetamide. *Journal of Biochemical & Biophysical Methods* (2003) 56:265-279.

Stuart, D D, G Y Kao, T M Allen. A novel, long-circulating, and functional liposomal formulation of antisense oligodeoxynucleotides targeted against *MDR1*. *Cancer Gene Therapy* (2000) 7:466-475.

Stulik, K, V Pacakova, M Ticha. Some potentialities and drawbacks of contemporary size-exclusion chromatography. *Journal of Biochemical & Biophysical Methods* (2003) 56:1-13.

Tannock, I F, R de Wit, W R Berry, J Horti, A Pluzanska, K N Chi, S Oudard, C Theodore, N D James, I Turesson, M A Rosenthal, M A Eisenberger, TAX 327 Investigators. Docetaxel plus prednisone or mitoxantrone plus prednisone for advanced prostate cancer. *New England Journal of Medicine* (2004) 351:1502-1512.

ten Tije, A J, J Verweij, W J Loos, A Sparreboom. Pharmacological effects of formulation vehicles : implications for cancer chemotherapy. *Clinical Pharmacokinetics* (2003) 42:665-685.

Tereshko, V, S Portmann, E C Tay, P Martin, F Natt, K-H Altmann, M Egli. Correlating structure and stability of DNA duplexes with incorporated 2'-*O*-modified RNA analogues. *Biochemistry* (1998) 37:10626-10634.

Thalmann, G N, P E Anezinis, S M Chang, H E Zhau, E E Kim, V L Hopwood, S Pathak, A C von Eschenbach, L W Chung. Androgen-independent cancer progression and bone metastasis in the LNCaP model of human prostate cancer. *Cancer Research* (1994) 54:2577-2581.

Thalmann, G N, R A Sikes, T T Wu, A Degeorges, S M Chang, M Ozen, S Pathak, L W Chung. LNCaP progression model of human prostate cancer: androgen-independence and osseous metastasis. *The Prostate* (2000) 44:91-103.

Tolcher, A W, L Reyno, P M Venner, S D Ernst, M Moore, R S Geary, K Chi, S Hall, W Walsh, A Dorr, E Eisenhauer. A randomized phase II and pharmacokinetic study of the antisense oligonucleotides ISIS 3521 and ISIS 5132 in patients with hormone-refractory prostate cancer. *Clinical Cancer Research* (2002) 8:2530-2535.

Tolcher, A W, K Chi, J Kuhn, M Gleave, A Patnaik, C Takimoto, G Schwartz, I Thompson, K Berg, S D'Aloisio, N Murray, S R Frankel, E Izbicka, E Rowinsky. A phase II, pharmacokinetic, and biological correlative study of oblimersen sodium and docetaxel in patients with hormone-refractory prostate cancer. *Clinical Cancer Research* (2005) 11:3854-3861.

Tomari, Y, P D Zamore. Perspective: machines for RNAi. *Genes & Development* (2005) 19:517-529.

Tonkinson, J L, C A Stein. Patterns of intracellular compartmentalization, trafficking and acidification of 5'-fluorescein labeled phosphodiester and phosphorothioate oligodeoxynucleotides in HL60 cells. *Nucleic Acids Research* (1994) 22:4268-4275.

Trougakos, I P, A So, B Jansen, M E Gleave, E S Gonos. Silencing expression of the clusterin/apolipoprotein J gene in human cancer cells using small interfering RNA induces spontaneous apoptosis, reduced growth ability, and cell sensitization to genotoxic and oxidative stress. *Cancer Research* (2004) 64:1834-1842.

Trougakos, I P, E S Gonos. Regulation of clusterin/apolipoprotein J, a functional homologue to the small heat shock proteins, by oxidative stress in ageing and age-related diseases. *Free Radical Research* (2006) 40:1324-1334.

University of South Carolina Upstate Faculty website: *http://www.faculty.uscupstate.edu/.*

Urien, S, J Barre, C Morin, A Paccaly, G Montay, J P Tillement. Docetaxel serum protein binding with high affinity to alpha 1-acid glycoprotein. *Investigational New Drugs* (1996) 14:147-151.

U.S. National Institute's of Health, National Cancer Institute's web site: *http://www.cancer.gov.*

USFDA (United States Food and Drug Administration). *Guidance for Industry. Analytical Procedures and Methods Validation. Chemistry, Manufacturing and Controls Documentation* (2000).

Vasey, P A, G C Jayson, A Gordon, H Gabra, R Coleman, R Atkinson, D Parkin, J Paul, A Hay, S B Kaye, Scottish Gynaecological Cancer Trials Group. Phase III randomized trial of docetaxel-carboplatin versus paclitaxel-carboplatin as first-line chemotherapy for ovarian carcinoma. *Journal of the National Cancer Institute* (2004) 96:1682-1691.

Vaughn, D J, A W Brown, Jr., W G Harker, S Huh, L Miller, D Rinaldi, F Kabbinavar. Multicenter Phase II study of estramustine phosphate plus weekly paclitaxel in patients with androgen-independent prostate carcinoma. *Cancer* (2004) 100:746-750.

Veeramachaneni, N K, H Kubokura, L Lin, J A Pippin, G A Patterson, J A Drebin, R J Battafarano. Down-regulation of beta catenin inhibits the growth of esophageal carcinoma cells. *The Journal of Thoracic and Cardiovascular Surgery* (2004) 127:92-98.

Venkatesh, S, T J Smith. Chitosan-membrane interactions and their probable role in chitosan-mediated transfection. *Biotechnology and Applied Biochemistry* (1998) 27 Pt 3:265-267.

Vinogradov, S V, T K Bronich, A V Kabanov. Self-assembly of polyamine-poly(ethylene glycol) copolymers with phosphorothioate oligonucleotides. *Bioconjugate Chemistry* (1998) 9:805-812.

Vinogradov, S V, E V Batrakova, A V Kabanov. Nanogels for oligonucleotide delivery to the brain. *Bioconjugate Chemistry* (2004) 15:50-60.

von Brocke, A, T Freudemann, E Bayer. Performance of capillary gel electrophoretic analysis of oligonucleotides coupled on-line with electrospray mass spectrometry. *Journal of Chromatography A* (2003) 991:129-141.

Wagner, E. Strategies to improve DNA polyplexes for in vivo gene transfer: will "artificial viruses" be the answer? *Pharmaceutical Research* (2004) 21:8-14.

Walder, R Y, J A Walder. Role of RNase H in hybrid-arrested translation by antisense oligonucleotides. *Proceedings of the National Academy of Sciences of the United States of America* (1988) 85:5011-5015.

Walter, K A, M A Cahan, A Gur, B Tyler, J Hilton, O M Colvin, P C Burger, A Domb, H Brem. Interstitial taxol delivered from a biodegradable polymer implant against experimental malignant glioma. *Cancer Research* (1994) 54:2207-2212.

Wang, H, D Yu, S Agrawal, R Zhang. Experimental therapy of human prostate cancer by inhibiting MDM2 expression with novel mixed-backbone antisense oligonucleotides: in vitro and in vivo activities and mechanisms. *The Prostate* (2003a) 54:194-205.

Wang, L, R K Prakash, C A Stein, R K Koehn, D E Ruffner. Progress in the delivery of therapeutic oligonucleotides: organ/cellular distribution and targeted delivery of oligonucleotides in vivo. *Antisense & Nucleic Acid Drug Development* (2003b) 13:169-189.

Wang, L, S Venkatraman, L Kleiner. Drug release from injectable depots: two different in vitro mechanisms. *Journal of Controlled Release* (2004) 99:207-216.

Wang, F, E Blanco, H Ai, D A Boothman, J Gao. Modulating beta-lapachone release from polymer millirods through cyclodextrin complexation. *Journal of Pharmaceutical Sciences* (2006) 95:2309-2319.

Wani, M C, H L Taylor, M E Wall, P Coggon, A T McPhail. Plant antitumor agents. VI. The isolation and structure of taxol, a novel antileukemic and antitumor agent from *Taxus brevifolia*. *Journal of the American Chemical Society* (1971) 93:2325-2327.

Waters, J S, A Webb, D Cunningham, P A Clarke, F Raynaud, F di Stefano, F E Cotter. Phase I Clinical and Pharmacokinetic Study of Bcl-2 Antisense Oligonucleotide Therapy in Patients With Non-Hodgkin's Lymphoma. *Journal of Clinical Oncology* (2000) 18:1812-1823.

Wiernik, P H, E L Schwartz, A Einzig, J J Strauman, R B Lipton, J P Dutcher. Phase I trial of taxol given as a 24-hour infusion every 21 days: responses observed in metastatic melanoma. *Journal of Clinical Oncology* (1987a) 5:1232-1239.

Wiernik, P H, E L Schwartz, J J Strauman, J P Dutcher, R B Lipton, E Paietta. Phase I clinical and pharmacokinetic study of taxol. *Cancer Research* (1987b) 47:2486-2493.

Wilks, E.S.. Polymer nomenclature: the controversy between source-based and structure-based representations (a personal perspective). *Progress in Polymer Science* (2000) 25:9-100.

Willems, A V, D L Deforce, C H Van Peteghem, J F Van Bocxlaer. Development of a quality control method for the characterization of oligonucleotides by capillary zone electrophoresis-electrospray ionization-quadrupole time of flight-mass spectrometry. *Electrophoresis* (2005) 26:1412-1423.

Williams, W A, A Hendrickson, A F Gillaspy, D W Dyer, L A Lewis. Oligonucleotide analysis by sequential injection before analysis (SIBA) capillary electrophoresis. *Analytical Biochemistry* (2003) 313:183-185.

Winternitz, C I, J K Jackson, A M Oktaba, H M Burt. Development of a polymeric surgical paste formulation for taxol. *Pharmaceutical Research* (1996) 13:368-375.

Winzor, D J. Analytical exclusion chromatography. *Journal of Biochemical & Biophysical Methods* (2003) 56:15-52.

Wong, T W, L W Chan, S B Kho, P W S Heng. Design of controlled-release solid dosage forms of alginate and chitosan using microwave. *Journal of Controlled Release* (2002) 84:99-114.

Wu, X S. Synthesis, characterization, biodegradation, and drug delivery application of biodegradable lactic/glycolic acid polymers: Part III. Drug delivery application. *Artificial Cells, Blood Substitutes, & Immobilization Biotechnology* (2004) 32:575-591.

Yakubov, L A, E A Deeva, V F Zarytova, E M Ivanova, A S Ryte, L V Yurchenko, V V Vlassov. Mechanism of oligonucleotide uptake by cells: involvement of specific receptors? *Proceedings of the National Academy of Sciences of the United States of America* (1989) 86:6454-6458.

Yamamoto, S, T Yamamoto, T Kataoka, E Kuramoto, O Yano, T Tokunaga. Unique palindromic sequences in synthetic oligonucleotides are required to induce INF and augment INF-mediated natural killer activity. *The Journal of Immunology* (1992) 148:4072-4076.

Yokomizo, A, H Koga, N Kinukawa, T Tsukamoto, Y Hirao, H Akaza, M Mori, S Naito. HPC2/ELAC2 polymorphism associated with Japanese sporadic prostate cancer. *The Prostate* (2004) 61:248-252.

Yomota, C, T Miyazaki, S Okada. Determination of the viscometric constants for chitosan and the application of universal calibration procedure in its gel permeation chromatography. *Colloid & Polymer Science* (1993) 271:76-82.

Yoo, H, P Sazani, R L Juliano. PAMAM dendrimers as delivery agents for antisense oligonucleotides. *Pharmaceutical Research* (1999) 16:1799-1804.

Yu, R Z, R S Geary, J M Leeds, T Watanabe, M Moore, J Fitchett, J Matson, T Burckin, M V Templin, A A Levin. Comparison of pharmacokinetics and tissue disposition of an antisense phosphorothioate oligonucleotide targeting human Ha-ras mRNA in mouse and monkey. *Journal of Pharmaceutical Sciences* (2001) 90:182-193.

Yu, X, P Trang, S Shah, I Atanasov, Y-H Kim, Y Bai, H Zhou, F Liu. Dissecting human cytomegalovirus gene function and capsid maturation by ribozyme targeting and electron cryomicroscopy. *Proceedings of the National Academy of Sciences of the United States of America* (2005) 102:7103-7108.

Zamecnik, P, J Aghajanian, M Zamecnik, J Goodchild, G Witman. Electron micrographic studies of transport of oligodeoxynucleotides across eukaryotic cell membranes. *Proceedings of the National Academy of Sciences of the United States of America* (1994) 91:3156-3160.

Zellweger, T, H Miyake, S Cooper, K Chi, B S Conklin, B P Monia, M E Gleave. Antitumor activity of antisense clusterin oligonucleotides is improved in vitro and in vivo by incorporation of 2'-O-(2-methoxy)ethyl chemistry. *J.Pharmacol.Exp.Ther.* (2001) 298:934-940.

Zellweger, T, S Kiyama, K Chi, H Miyake, H Adomat, K Skov, M E Gleave. Overexpression of the cytoprotective protein clusterin decreases radiosensitivity in the human LNCaP prostate tumour model. *BJU International* (2003) 92:463-469.

Zelphati, O, F C Jr Szoka. Mechanism of oligonucleotide release from cationic liposomes. *Proceedings of the National Academy of Sciences of the United States of America* (1996) 93:11493-11498.

Zentner, G M, R Rathi, C Shih, J C McRea, M H Seo, H Oh, B G Rhee, J Mestecky, Z Moldoveanu, M Morgan, S Weitman. Biodegradable block copolymers for delivery of proteins and water- insoluble drugs. *Journal of Controlled Release* (2001) 72:203-215.

Zhang, X, H M Burt, G Mangold, D Dexter, D Von Hoff, L Mayer, W L Hunter. Anti-tumor efficacy and biodistribution of intravenous polymeric micellar paclitaxel. *Anti-Cancer Drugs* (1997a) 8:696-701.

Zhang, X, H M Burt, D Von Hoff, D Dexter, G Mangold, D Degen, A M Oktaba, W L Hunter. An investigation of the antitumour activity and biodistribution of polymeric micellar paclitaxel. *Cancer Chemotherapy and Pharmacology* (1997b) 40:81-86.

Zhang, W, N Leighl, D Zawisza, M J Moore, E X Chen. Determination of GTI-2040, a novel antisense oligonucleotide, in human plasma by using HPLC combined with solid phase and liquid–liquid extractions. *Journal of Chromatography B* (2005) 829:45-49.

APPENDIX 1 – QUALIFICATION OF CLUSTERIN ASO HPLC ASSAY

Table A1.1 Accuracy of clusterin ASO HPLC calibration curve for day one of four days. The equation for the calibration curve derived for day one is y = 11880x – 3135.

Clusterin ASO concentration ($\mu g \cdot mL^{-1}$)	Peak area[a]	Bias (%)[b]			Mean bias (%)
		First standard	Second standard	Third Standard	
0.5	2796	16.1	0.7	14.1	10.3
1	7334	11.9	5.6	11.5	9.7
2	18247	6.0	4.6	14.3	8.3
5	55325	8.9	13.5	3.1	8.5
10	115939	6.8	8.3	4.5	6.5
20	241821	3.5	7.3	2.2	4.3
50	588325	4.1	3.6	3.1	3.6

[a] Peak area is the peak area observed for the standard used to derive the calibration curve.
[b] Bias is the ratio of the absolute value of the deviation of predicted value from the actual concentration measured and is expressed as a percentage.

Table A1.2 Accuracy of clusterin ASO HPLC calibration curve for day two of four days. The equation for the calibration curve derived for day two is y = 11140x – 3687.

Clusterin ASO concentration ($\mu g \cdot mL^{-1}$)	Peak area[a]	Bias (%)[b]			Mean bias (%)
		First standard	Second standard	Third standard	
0.5	2119	6.8	5.7	13.4	8.6
1	6108	5.2	6.9	12.1	8.0
2	18827	9.2	17.2	7.9	11.4
5	50423	4.8	13.2	12.9	10.3
10	108303	7.0	15.7	14.5	12.4
20	222095	9.4	17.9	14.6	14.0
50	552108	7.0	14.7	12.8	11.5

[a] Peak area is the peak area observed for the standard used to derive the calibration curve.
[b] Bias is the ratio of the absolute value of the deviation of predicted value from the actual concentration measured and is expressed as a percentage.

Table A1.3 Accuracy of clusterin ASO HPLC calibration curve for day three of four days. The equation for the calibration curve derived for day three is y = 10880x – 2755.

Clusterin ASO concentration ($\mu g \cdot mL^{-1}$)	Peak area[a]	Bias (%)[b]			Mean bias (%)
		First standard	Second standard	Third standard	
0.5	4202	50.4	41.5	19.2	37.0
1	8704	24.6	0.9	9.8	11.8
2	19603	7.6	8.4	5.2	7.1
5	51183	3.7	3.7	4.0	3.8
10	103246	4.8	1.8	1.5	2.7
20	212548	5.0	4.4	1.1	3.5
50	539695	4.9	1.5	2.4	2.9

[a] Peak area is the peak area observed for the standard used to derive the calibration curve.
[b] Bias is the ratio of the absolute value of the deviation of predicted value from the actual concentration measured and is expressed as a percentage.

Table A1.4 Accuracy of clusterin ASO HPLC calibration curve for day four of four days. The equation for the calibration curve derived for day four is y = 10890x -3258.

Clusterin ASO concentration ($\mu g \cdot mL^{-1}$)	Peak area[a]	Bias (%)[b]			Mean bias (%)
		First standard	Second standard	Third standard	
0.5	4471	41.0	40.0	38.9	40.0
1	8477	25.0	9.4	26.5	20.3
2	20377	19.0	4.9	12.4	12.1
5	48394	13.7	2.3	7.5	7.8
10	102926	13.1	3.7	11.5	9.4
20	213569	14.2	5.2	11.2	10.2
50	541456	15.3	7.1	12.8	11.7

[a] Peak area is the peak area observed for the standard used to derive the calibration curve.
[b] Bias is the ratio of the absolute value of the deviation of predicted value from the actual concentration measured and is expressed as a percentage.

Table A1.5 Summary of intra-day precision of clusterin ASO HPLC calibration curves.

Clusterin ASO concentration ($\mu g \cdot mL^{-1}$)	Day one		Day two		Day three		Day four	
	Mean Peak area[a]	CV (%)[b]	Mean Peak area	CV (%)	Mean peak area	CV (%)	Mean Peak Area	CV (%)
0.5	2345	21.6	2303	9.8	4548	16.4	4382	1.7
1	7525	4.6	7498	16.4	9190	12.1	9491	11.4
2	19270	10.8	20560	7.2	20227	2.5	20934	6.2
5	58912	8.1	55917	7.6	52902	2.2	53625	8.0
10	118915	5.9	118194	6.7	106342	3.3	112548	7.0
20	241465	3.8	243191	6.6	218025	3.2	230715	6.1
50	597203	3.4	600990	6.2	544356	3.0	588622	6.2

[a] Mean peak area is the mean calculated from four standards at each concentration each day.
[b] CV (coefficient of variation) is the quotient of the standard deviation divided by the mean and is expressed as a percentage.

Table A1.6 Summary of inter-day precision of clusterin ASO HPLC calibration curves.

Clusterin ASO concentration ($\mu g \cdot mL^{-1}$)	Mean peak area[a]	CV (%)[b]
0.5	3395	34.9
1	8426	15.5
2	20247	7.17
5	55339	7.67
10	113999	7.03
20	233349	6.45
50	582793	6.02

[a] Mean peak area is the mean calculated from four standards a day for four days (16 standards).
[b] CV (coefficient of variation) is the quotient of the standard deviation divided by the mean and is expressed as a percentage.

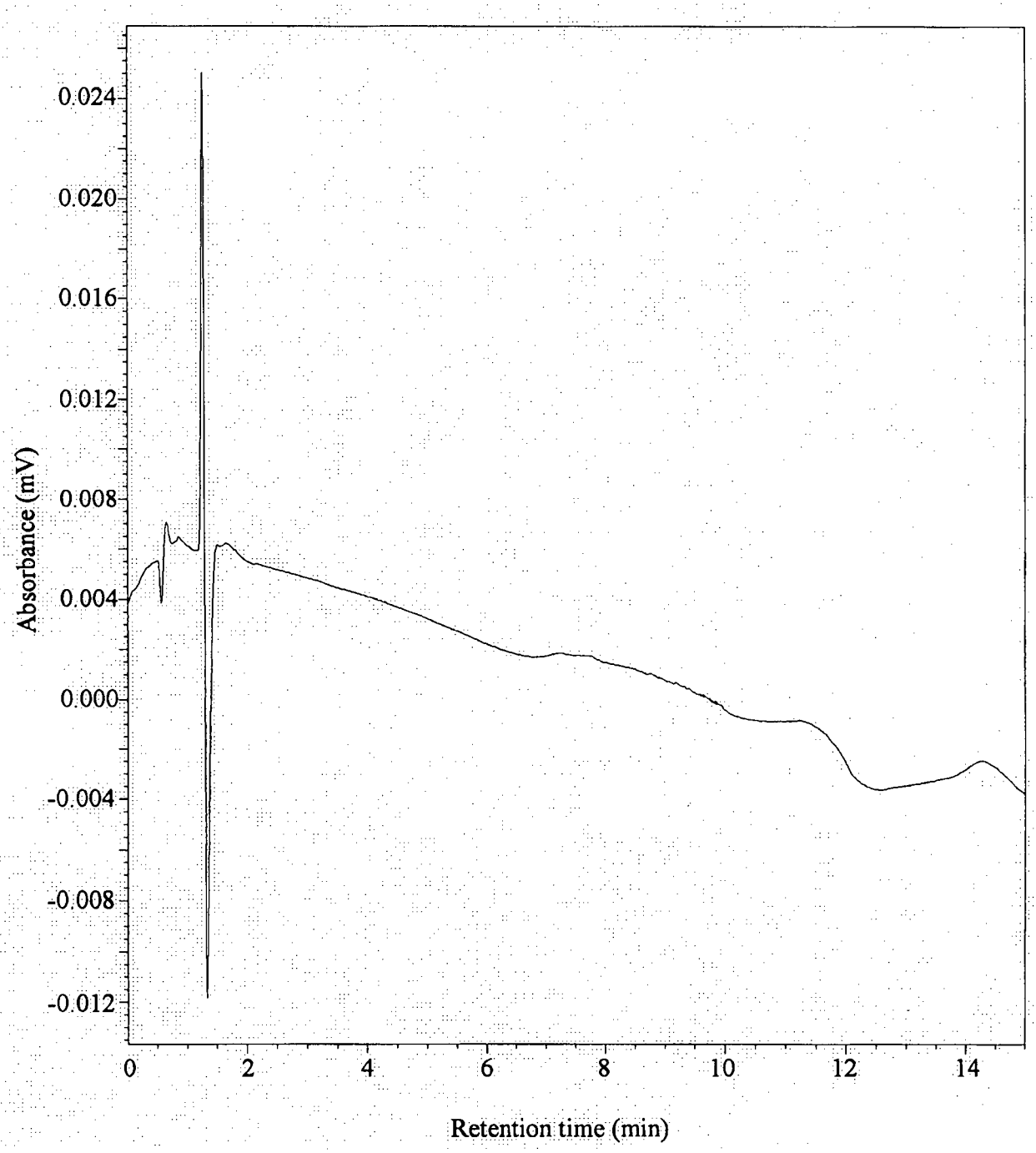

Figure A1.1 Representative blank sample HPLC chromatogram without baseline subtraction.

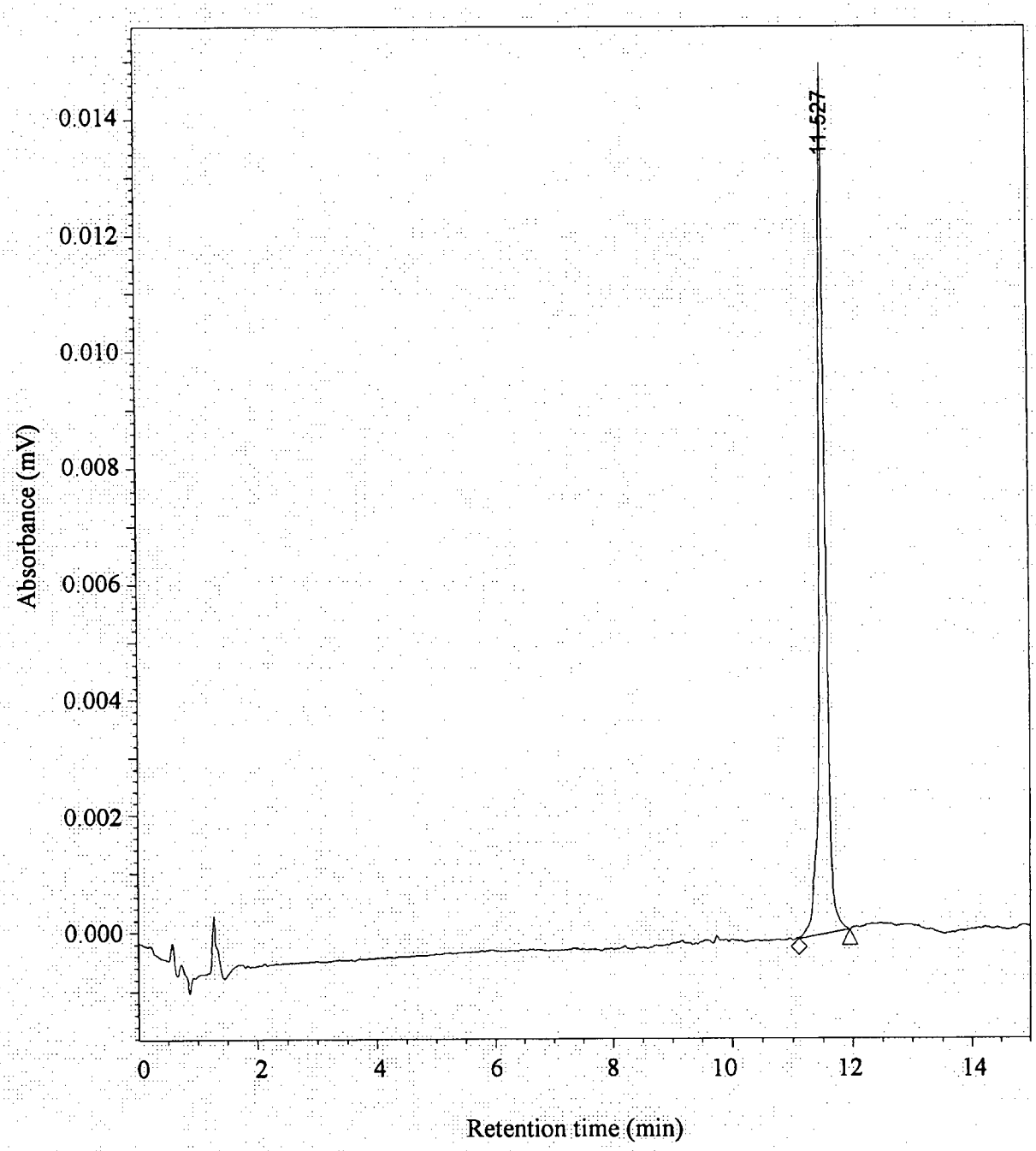

Figure A1.2 Representative clusterin ASO HPLC chromatogram. This chromatogram is from a 10 ug·mL^{-1} clusterin ASO standard and shows a retention time of 11.6 minutes.

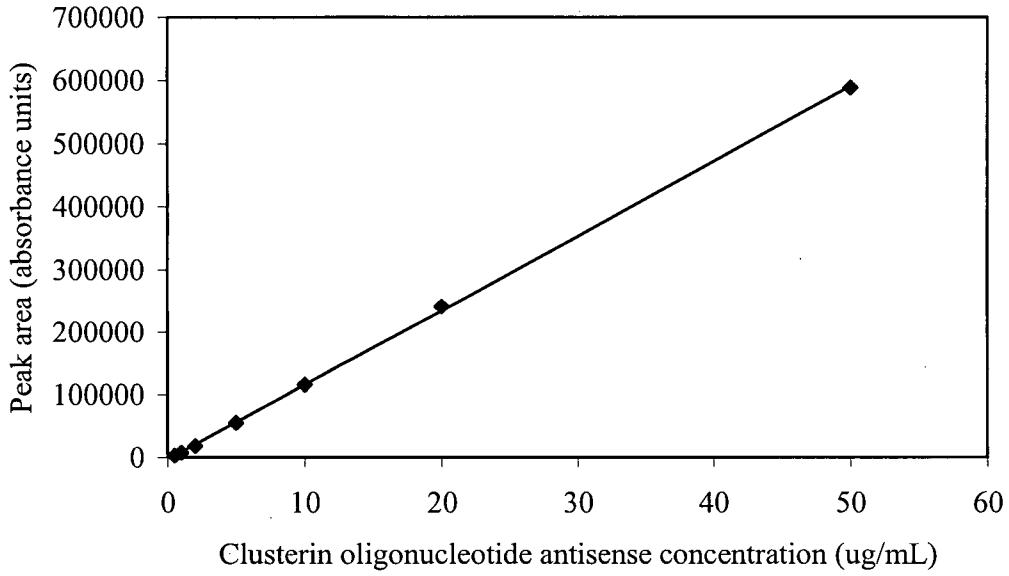

Figure A1.3 Representative clusterin ASO HPLC calibration curve. Sixteen different calibration curves were prepared (four a day for four days).

Regression analysis parameters ($y = mx + b$, R^2):
$m = 11{,}880$, $b = -3{,}135$, $R^2 = 1.000$

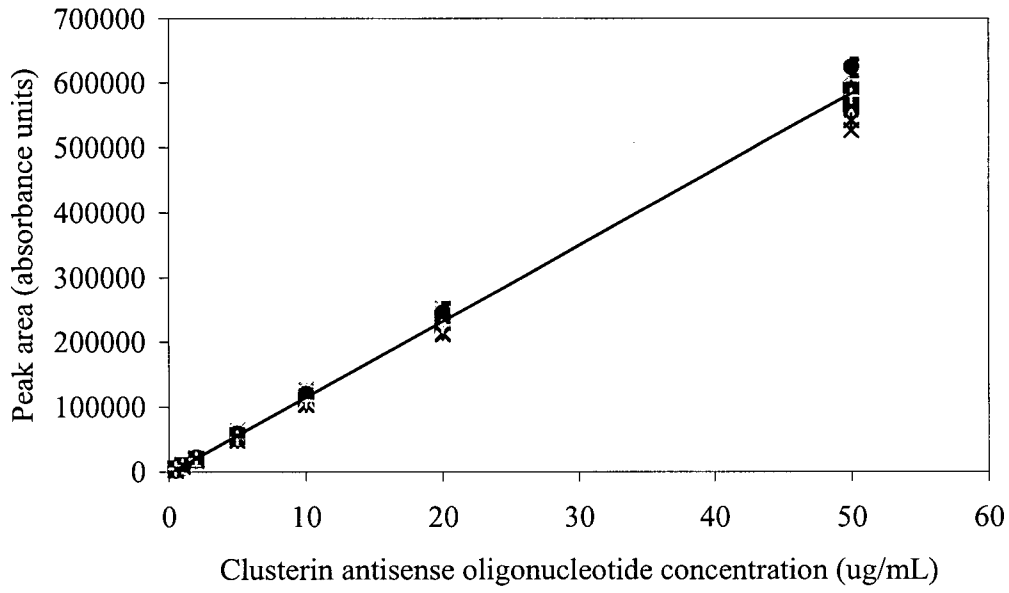

Figure A1.4 Clusterin ASO HPLC standard curve determined from sixteen calibration curves (four a day for four days).

Regression analysis parameters ($y = mx + b$, R^2):
$m = 11{,}720$, $b = -2{,}864$, $R^2 = 1.000$

APPENDIX 2 – QUALIFICATION OF CLUSTERIN ASO CAPILLARY GEL ELECTROPHORESIS ASSAY

Table A2.1 Summary of the characteristics of the capillary gel electrophoresis relative retention time of 21-mer clusterin ASO and its 20-, 19- and 18-mer degradation product standards (N, N-1, N-2 and N-3 oligonucleotides, respectively) to T_{25} internal standard.

Oligo[a]	N-3		N-2		N-1		N	
Oligo conc[b] ($\mu g \cdot mL^{-1}$)	Mean[c] relative R_t[d]	CV (%)	Mean relative R_t	CV (%)	Mean relative R_t	CV (%)	Mean relative R_t	CV (%)
0.065	0.884	1.0	0.895	0.3	0.910	0.1	0.928	0.1
0.20	0.881	0.7	0.893	0.1	0.909	0.2	0.926	0.0
0.59	0.879	0.4	0.891	0.2	0.907	0.1	0.925	0.0
1.8	0.876	0.1	0.880	2.1	0.906	0.0	0.923	0.1
5.3	0.876	0.2	0.891	0.1	0.907	0.1	0.923	0.1
All conc'ss	0.879	0.4	0.890	0.6	0.908	0.2	0.925	0.2

[a] Oligo = oligonucleotide.
[b] Conc = concentration. The concentration listed was the approximate concentration of the oligonucleotides (accurately measured).
[c] Mean is the mean of three standards on each of three separate days.
[d] R_t = retention time. Relative R_t is the quotient of the R_t of clusterin ASO divided by the R_t of T_{25} internal standard.

Table A2.2 Representative accuracy of clusterin ASO's 18-mer degradation product standard (N-3 oligonucleotide) capillary gel electrophoresis calibration curve for day one of two days. The equation for the calibration curve derived for day one is y = 0.958x – 0.253.

N-3 concentration ($\mu g \cdot mL^{-1}$)	Relative peak area[a]	Bias (%)[b]			Mean bias (%)
		First standard	Second standard	Third standard	
0.065	3.20	42.6	41.3	25.7	36.6
0.20	1.81	23.3	11.6	22.5	19.1
0.59	1.30	38.5	8.8	3.1	16.8
1.8	1.60	16.4	26.6	11.5	18.2
5.3	1.04	6.2	6.4	1.8	4.8

[a] Relative peak area is the ratio of the peak area of N-3 oligonucleotide and the peak area of the T_{25} internal standard, divided by the ratio of the concentration of N-3, N-2, N-1 or N oligonucleotide and the concentration of the T_{25} internal standard.
[b] Bias is the ratio of the deviation of predicted value from the actual measured value and is expressed as a percentage.

Table A2.3 Representative accuracy of clusterin ASO's 19-mer degradation product standard (N-2 oligonucleotide) capillary gel electrophoresis calibration curve for day one of two days. The equation for the calibration curve derived for day one is y = 0.750x – 0.289.

N-2 concentration ($\mu g \cdot mL^{-1}$)	Relative Peak area[a]	Bias (%)[b]			Mean bias (%)
		First standard	Second standard	Third standard	
0.065	5.53	46.8	51.0	44.9	47.6
0.20	2.50	34.1	16.9	0.5	17.1
0.59	2.43	8.4	23.4	0.6	10.8
1.8	2.12	21.8	25.2	16.3	21.1
5.3	1.34	7.2	5.4	2.2	4.9

[a] Relative peak area is the ratio of the peak area of N-2 oligonucleotide and the peak area of the T_{25} internal standard, divided by the ratio of the concentration of N-3, N-2, N-1 or N oligonucleotide and the concentration of the T_{25} internal standard.
[b] Bias is the ratio of the deviation of predicted value from the actual measured value and is expressed as a percentage.

Table A2.4 Representative accuracy of clusterin ASO's 20-mer degradation product standard (N-1 oligonucleotide) capillary gel electrophoresis calibration curve for day one of two days. The equation for the calibration curve derived for day one is $y = 0.671x - 0.127$.

N-1 concentration ($\mu g \cdot mL^{-1}$)	Relative Peak area[a]	Bias (%)[b]			Mean bias (%)
		First standard	Second standard	Third standard	
0.065	2.38	3.2	3.8	5.7	4.2
0.20	2.19	12.1	13.2	18.7	14.7
0.59	1.71	2.6	7.7	10.7	7.0
1.8	1.82	5.1	7.0	2.7	4.9
5.3	1.49	18.4	3.9	23.7	15.3

[a] Relative peak area is the ratio of the peak area of N-1 and the peak area of the T_{25} internal standard, divided by the ratio of the concentration of N-3, N-2, N-1 or N oligonucleotide and the concentration of the T_{25} internal standard.
[b] Bias is the ratio of the deviation of predicted value from the actual measured value and is expressed as a percentage.

Table A2.5 Representative accuracy of 21-mer clusterin ASO (N oligonucleotide) capillary gel electrophoresis calibration curve for day one of two days. The equation for the calibration curve derived for day one is $y = 0.725x$.

N concentration ($\mu g \cdot mL^{-1}$)	Relative peak area[a]	Bias (%)[b]			Mean bias (%)
		First standard	Second standard	Third standard	
0.065	2.92	35.2	48.2	50.1	44.5
0.20	2.09	20.4	1.1	40.6	20.7
0.59	1.55	0.4	29.2	14.0	14.6
1.8	2.01	21.3	18.2	12.2	17.2
5.3	1.40	17.3	5.6	4.9	9.3

[a] Relative peak area is the ratio of the peak area of N-3 oligonucleotide and the peak area of the T_{25} internal standard, divided by the ratio of the concentration of N-3, N-2, N-1 or N oligonucleotide and the concentration of the T_{25} internal standard.
[b] Bias is the ratio of the deviation of predicted value from the actual measured value and is expressed as a percentage.

Table A2.6 Summary of intra-day precision of 21-mer clusterin ASO and its 20-, 19- and 18-mer degradation product standards (N, N-1, N-2 and N-3 oligonucleotides, respectively) capillary gel electrophoresis calibration curves.

Oligo[a]	N-3		N-2		N-1		N	
Oligo conc[b] ($\mu g \cdot mL^{-1}$)	Mean[c] relative PA[d]	CV (%)[e]	Mean relative PA	CV (%)	Mean relative PA	CV (%)	Mean relative PA	CV (%)
0.065	2.32	27.3	3.06	6.5	2.35	6.0	2.75	62.2
0.20	1.66	18.8	2.48	8.3	1.90	4.4	2.23	23.7
0.59	1.47	15.7	2.49	11.6	1.81	5.6	1.52	19.6
1.8	1.38	12.8	1.72	3.6	1.77	4.4	1.24	6.9
5.3	1.05	5.2	1.38	6.5	1.64	12.4	1.38	10.9

[a] O ligo = oligonucleotide.
[b] Conc = concentration.
[c] Mean is the mean calculated from four standards on one day.
[d] PA = peak area. Relative peak area is the ratio of the peak area of N-3, N-2, N-1 or N oligonucleotide and the peak area of the T_{25} internal standard, divided by the ratio of the concentration of N-3, N-2, N-1 or N oligonucleotide and the concentration of the T_{25} internal standard.
[e] CV (coefficient of variation) is the quotient of the standard deviation divided by the mean and is expressed as a percentage.

Table A2.7 Summary of inter-day precision of of 21-mer clusterin ASO and its 20-, 19- and 18-mer degradation product standards (N, N-1, N-2 and N-3 oligonucleotides, respectively) capillary gel electrophoresis calibration curves.

Oligo[a]	N-3		N-2		N-1		N	
Oligo conc[b] ($\mu g \cdot mL^{-1}$)	Mean[c] relative PA[d]	CV (%)[e]	Mean relative PA	CV (%)	Mean relative PA	CV (%)	Mean relative PA	CV (%)
0.065	1.98	28.6	3.34	29.3	2.63	34.2	2.90	42.4
0.20	1.61	16.7	2.33	14.6	1.79	20.1	2.13	17.2
0.59	1.35	15.9	2.37	12.3	1.85	19.2	1.65	16.0
1.8	1.29	11.9	1.75	10.9	1.74	13.0	1.47	19.7
5.3	1.04	4.6	1.31	4.5	1.74	19.6	1.36	9.2

[a] Oligo = oligonucleotide.
[b] Conc = concentration. The concentration listed was the approximate concentration of the oligonucleotides (accurately measured).
[c] Mean is the mean calculated from eight standards (four standards a day for two days).
[d] PA = peak area. Relative peak area is the ratio of the peak area of N-3, N-2, N-1 or N oligonucleotide and the peak area of the T_{25} internal standard, divided by the ratio of the concentration of N-3, N-2, N-1 or N oligonucleotide and the concentration of the T_{25} internal standard.
[e] CV (coefficient of variation) is the quotient of the standard deviation divided by the mean and is expressed as a percentage

Table A2.8 Detection limit and quantitation limit as determined from Equation 10 and Equation 11, respectively, for the capillary gel electrophoresis assay of 21-mer clusterin ASO and its 20-, 19- and 18-mer degradation product standards (N, N-1, N-2 and N-3 oligonucleotides, respectively).

Oligonucleotide	Detection limit ($ng \cdot mL^{-1}$)	Quantitation limit ($ng \cdot mL^{-1}$)
N-3	40	121
N-2	36	110
N-1	44	133
N	35	107

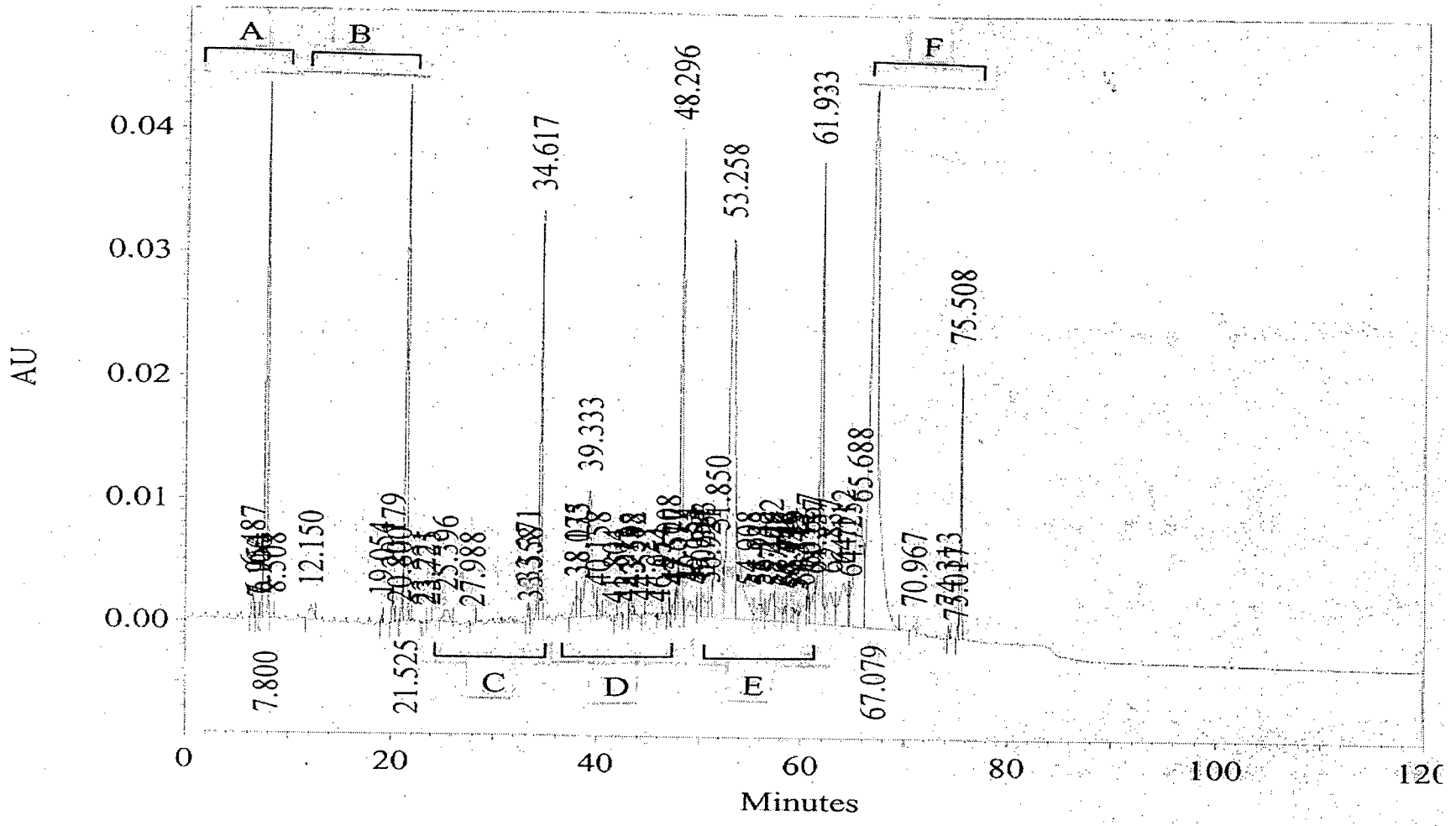

Figure A2.1 Representative CGE chromatogram of a blank and five different concentrations of clusterin ASO's 18-mer degradation product standard (N-3 oligonucleotide), each spiked with T_{25} internal standard and electrokinetically injected separately. **A)** Blank with T_{25} peak at 7.8 min. **B)** N-3 at 0.065 $\mu g \cdot mL^{-1}$ peak at 12.2 min with T_{25} peak at 21.5 min. **C)** N-3 at 0.19 $\mu g \cdot mL^{-1}$ peak at 25.4 min with T25 peak at 34.6 min. **D)** N-3 at 0.58 $\mu g \cdot mL^{-1}$ peak at 39.3 min with T_{25} peak at 48.3 min. **E)** N-3 at 1.7 $\mu g \cdot mL^{-1}$ peak at 53.3 min with T_{25} peak at 61.9 min. **F)** N-3 at 5.3 $\mu g \cdot mL^{-1}$ peak at 67.1 min with T_{25} peak at 75.5 min.

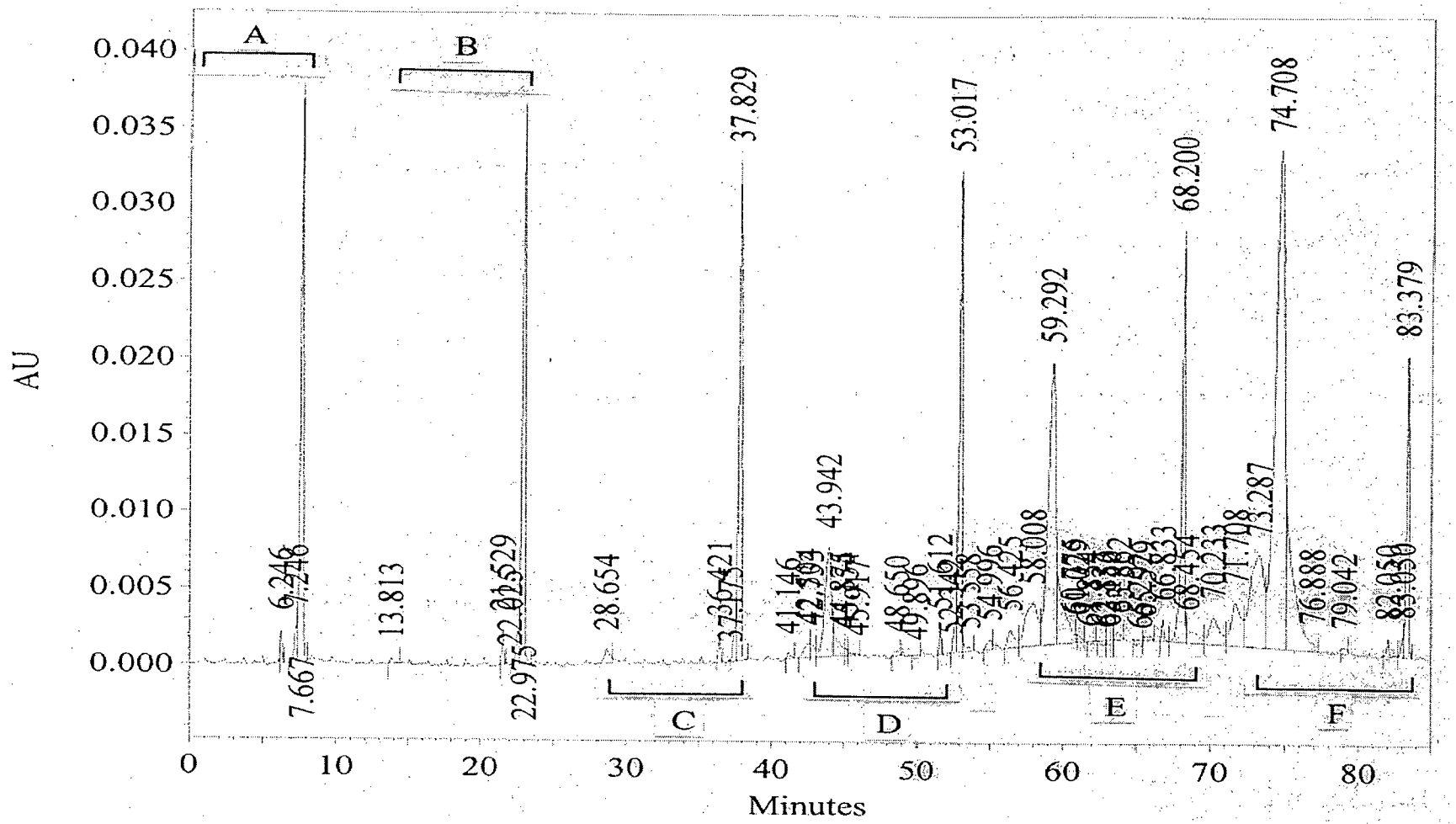

Figure A2.2 Representative CGE chromatogram of a blank and five different concentrations of clusterin ASO's 19-mer degradation product standard (N-2 oligonucleotide), each spiked with T_{25} internal standard and electrokinetically injected separately. **A)** Blank with T_{25} peak at 7.7 min. **B)** N-2 at 0.060 $\mu g \cdot mL^{-1}$ peak at 13.8 min with T_{25} peak at 23.0 min. **C)** N-2 at 0.18 $\mu g \cdot mL^{-1}$ peak at 28.7 min with T25 peak at 37.8 min. **D)** N-2 at 0.54 $\mu g \cdot mL^{-1}$ peak at 43.9 min with T_{25} peak at 53.0 min. **E)** N-2 at 1.6 $\mu g \cdot mL^{-1}$ peak at 59.3 min with T_{25} peak at 68.2 min. **F)** N-2 at 4.8 $\mu g \cdot mL^{-1}$ peak at 74.7 min with T_{25} peak at 83.4 min.

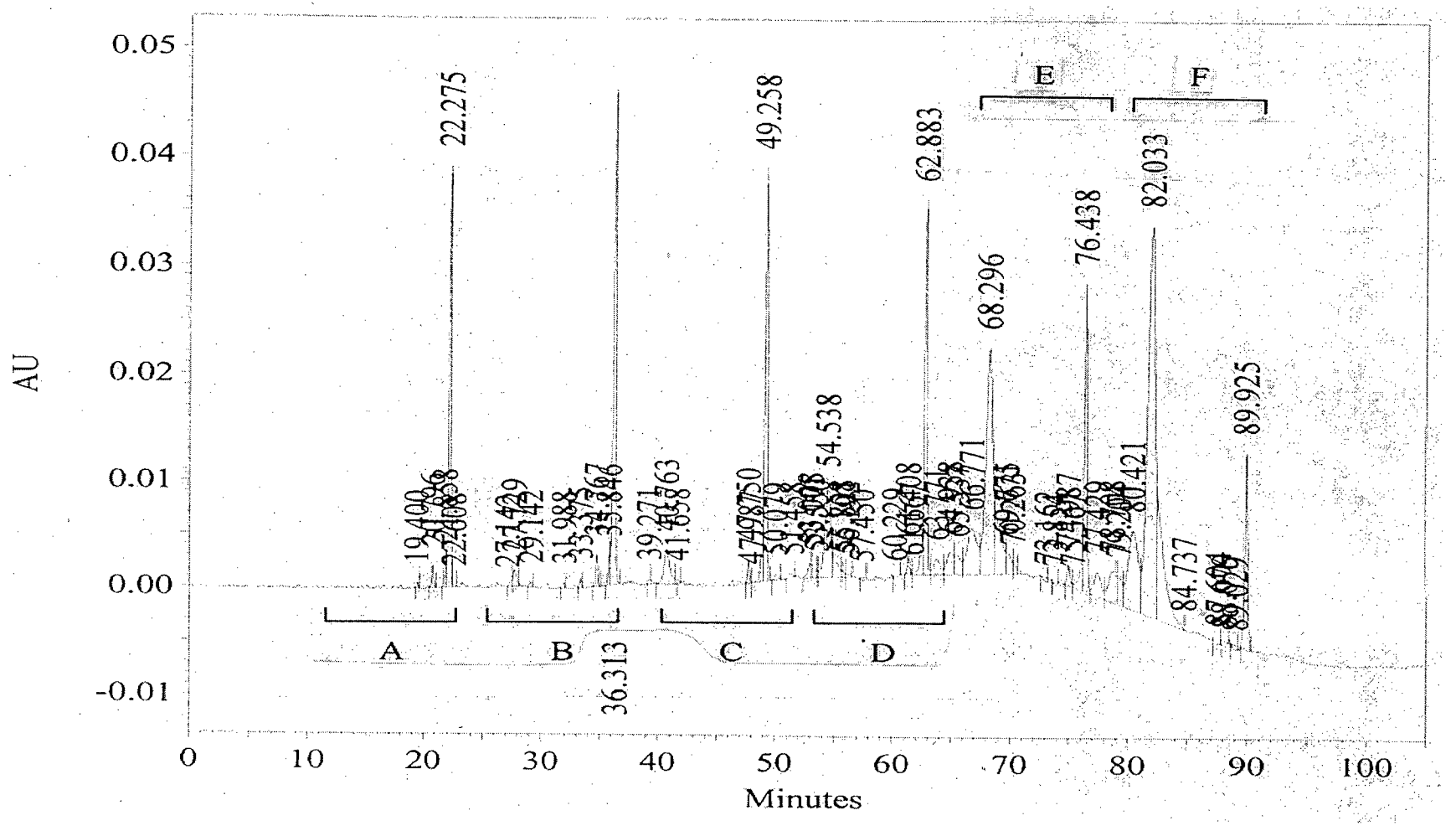

Figure A2.3 Representative CGE chromatogram of a blank and five different concentrations of clusterin ASO's 20-mer degradation product standard (N-1), each spiked with T_{25} internal standard and electrokinetically injected separately. **A)** Blank with T_{25} peak at 22.3 min. **B)** N-1 at 0.057 $\mu g \cdot mL^{-1}$ peak at 27.7 min with T_{25} peak at 36.3 min. **C)** N-1 at 0.17 $\mu g \cdot mL^{-1}$ peak at 40.8 min with T25 peak at 49.3 min. **D)** N-1 at 0.52 $\mu g \cdot mL^{-1}$ peak at 54.5 min with T_{25} peak at 62.9 min. **E)** N-1 at 1.5 $\mu g \cdot mL^{-1}$ peak at 68.3 min with T_{25} peak at 76.4 min. **F)** N-1 at 4.6 $\mu g \cdot mL^{-1}$ peak at 82.0 min with T_{25} peak at 89.9 min.

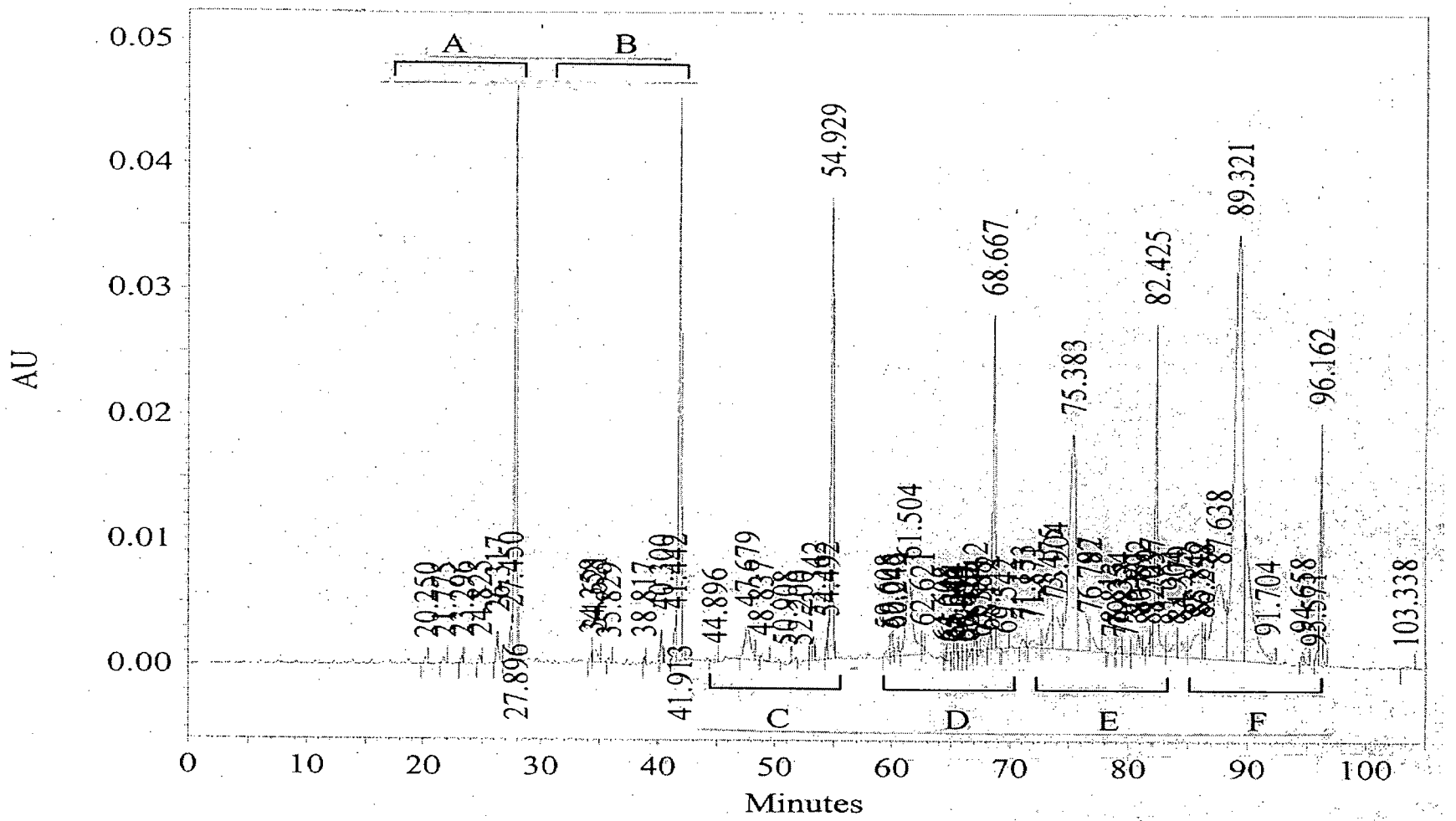

Figure A2.4 Representative CGE chromatogram of a blank and five 21-mer clusterin ASO standards (N oligonucleotide), each spiked with T_{25} internal standard and electrokinetically injected separately. **A)** Blank with T_{25} peak at 27.9 min. **B)** N at 0.051 $\mu g \cdot mL^{-1}$ peak at 34.6 min with T_{25} peak at 41.9 min. **C)** N at 0.15 $\mu g \cdot mL^{-1}$ peak at 47.7 min with T25 peak at 54.9 min. **D)** N at 0.46 $\mu g \cdot mL^{-1}$ peak at 61.5 min with T_{25} peak at 68.7 min. **E)** N at 1.4 $\mu g \cdot mL^{-1}$ peak at 75.4 min with T_{25} peak at 82.4 min. **F)** N at 4.2 $\mu g \cdot mL^{-1}$ peak at 89.3 min with T_{25} peak at 96.2 min.

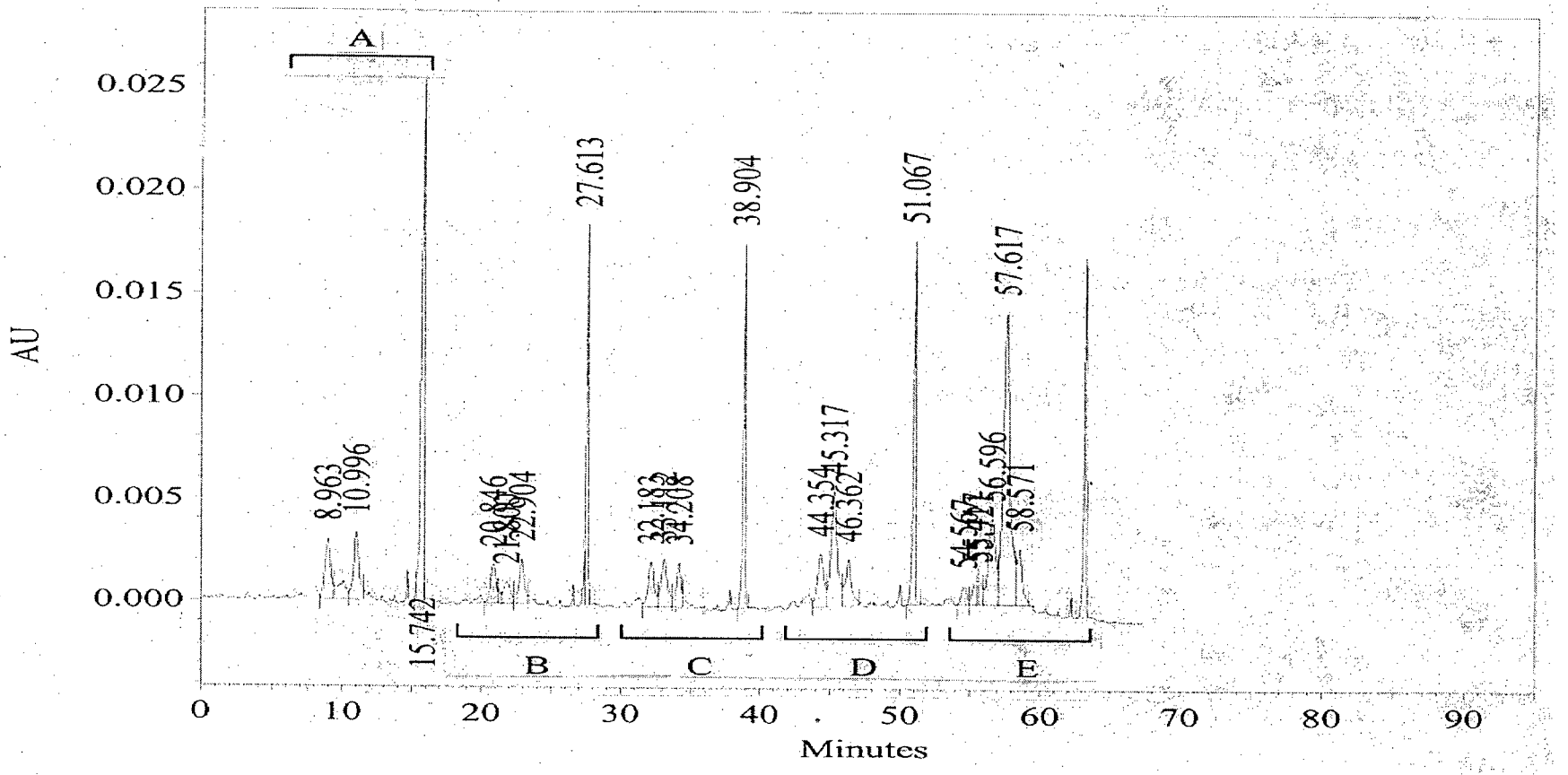

Figure A2.5. Representative CGE chromatogram of a blank and four different concentrations of clusterin ASO's 20-mer degradation product standard (N-1 oligonucleotide), each spiked with 0.23 $\mu g \cdot mL^{-1}$ each of 21-mer clusterin ASO (N oligonucleotide) and the 19-mer degradation product standard (N-2 oligonucleotide) and T_{25} internal standard and electrokinetically injected separately. **A)** Blank (no N-1) with N-2, N oligonucleotide and T_{25} peaks at 9.0, 11.0 and 15.7 min, respectively. **B)** N-1 at 0.082 $\mu g \cdot mL^{-1}$ peak at 21.8 min with N-2, N and T_{25} peaks at 20.8, 22.9 and 27.6 min, respectively. **C)** N-1 at 0.25 $\mu g \cdot mL^{-1}$ peak at 33.1 min with N-2, N and T25 peaks at 32.2, 34.2 and 38.9 min, respectively. **D)** N-1 at 0.74 $\mu g \cdot mL^{-1}$ peak at 45.3 min with N-2, N and T_{25} peaks at 44.4, 46.4 and 51.1 min, respectively. **E)** N-1 at 2.2 $\mu g \cdot mL^{-1}$ peak at 57.6 min with N-2, N and T_{25} peaks at 56.5, 58.6 and 63.4 min, respectively.

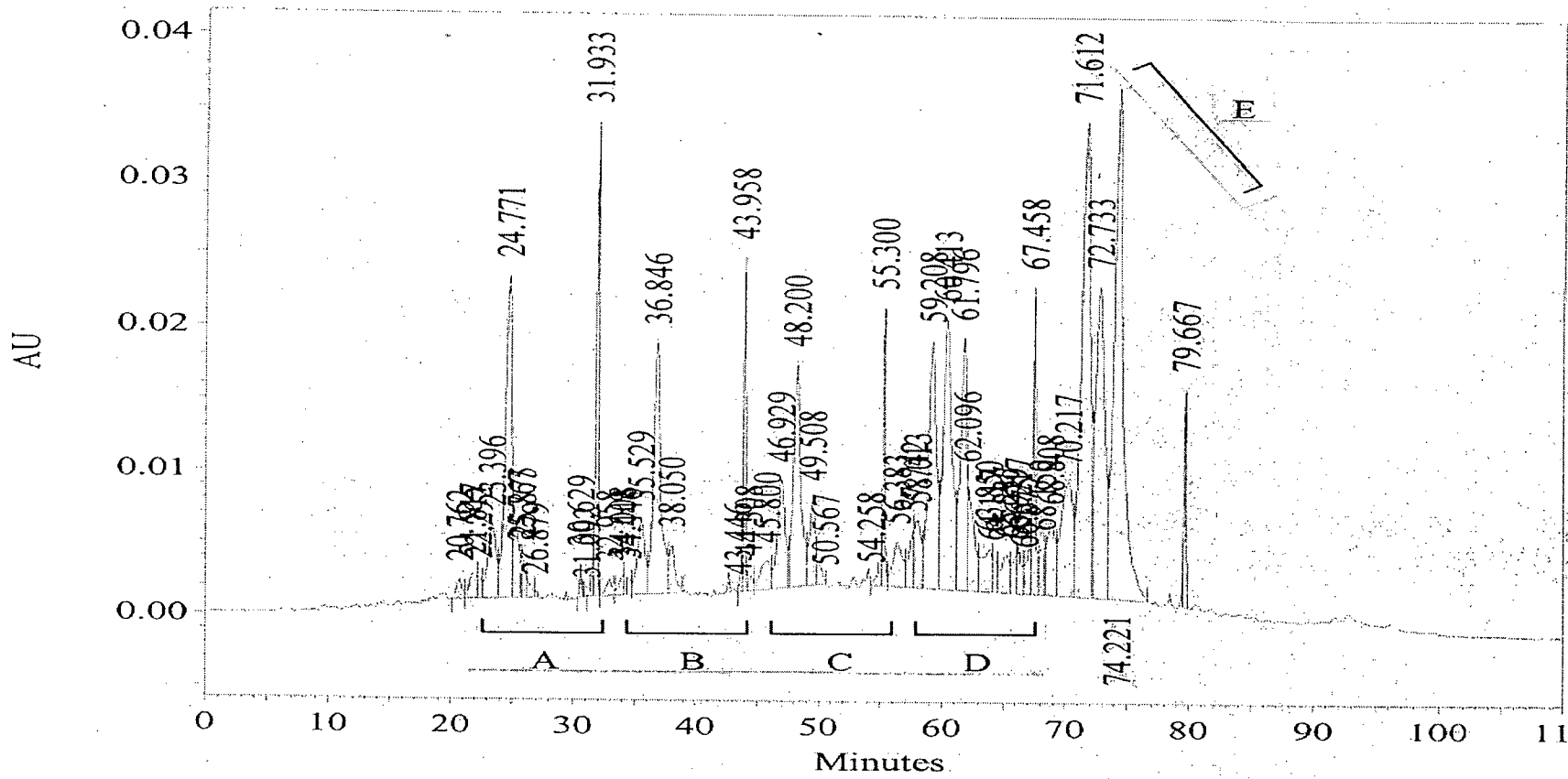

Figure A2.6. Representative CGE chromatogram of five clusterin ASO's 20-mer degradation product standard (N-1 oligonucleotide) at 2.2 $\mu g \cdot mL^{-1}$, each spiked with increasing amounts of 21-mer clusterin ASO(N oligonucleotide) and the 19-mer degradation product standard (N-2 oligonucleotide) and spiked with T_{25} internal standard and electrokinetically injected separately. **A)** N-1 peak at 24.8 min with N-2 at 0.076 $\mu g \cdot mL^{-1}$, N at 0.078 $\mu g \cdot mL^{-1}$ and T_{25} peaks at 23.4, 25.8 and 31.9 min, respectively. **B)** N-1 peak at 36.8 min with N-2 at 0.23 $\mu g \cdot mL^{-1}$, N at 0.23 $\mu g \cdot mL^{-1}$ and T_{25} peaks at 35.5, 38.1 and 44.0 min, respectively. **C)** N-1 peak at 48.2 min with N-2 at 0.68 $\mu g \cdot mL^{-1}$, N at 0.070 $\mu g \cdot mL^{-1}$ and T_{25} peaks at 46.9, 49.5 and 55.3 min, respectively. **D)** N-1 peak at 60.4 min with N-2 at 2.0 $\mu g \cdot mL^{-1}$, N at 2.1 $\mu g \cdot mL^{-1}$ and T_{25} peaks at 59.2, 61.8 and 67.5 min, respectively. **E)** N-1 peak at 72.7 min with N-2 at 6.1 $\mu g \cdot mL^{-1}$, N at 6.3 $\mu g \cdot mL^{-1}$ and T_{25} peaks at 71.6, 74.2 and 79.7 min, respectively.

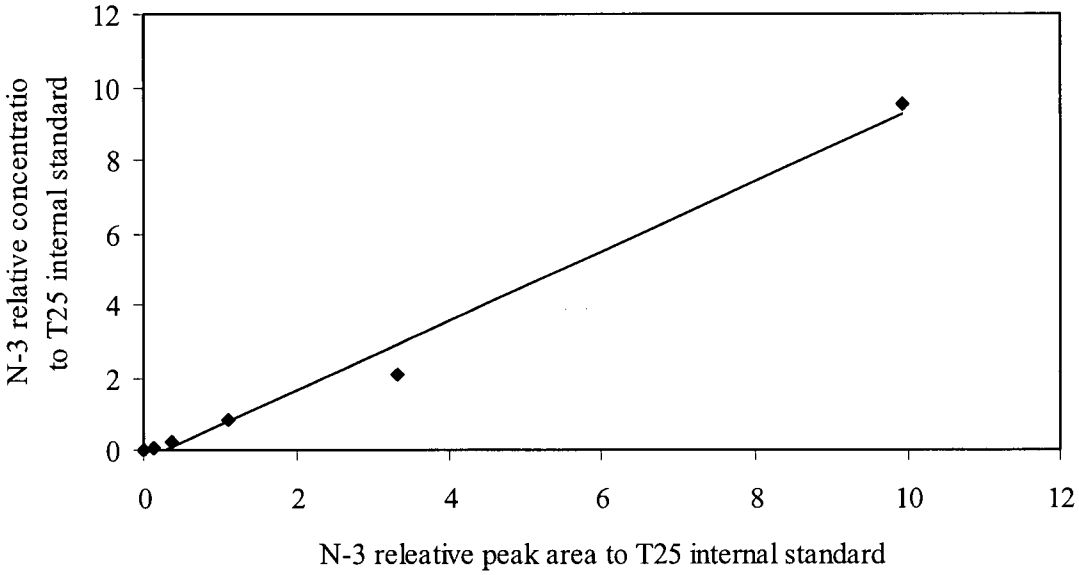

Figure A2.7 Representative clusterin ASO's 18-mer degradation product standard (N-3 oligonucleotide) capillary gel electrophoresis calibration curve.

Regression analysis parameters ($y = mx + b$, R^2):
$m = 0.9583$, $b = 0.2533$, $R^2 = 0.987$

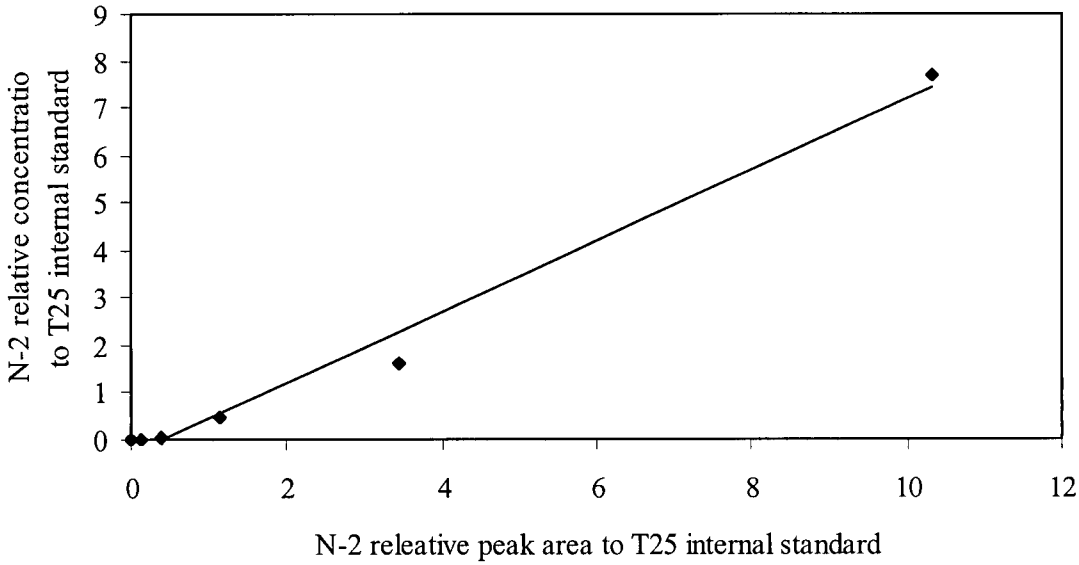

Figure A2.8 Representative clusterin ASO's 19-mer degradation product standard (N-2 oligonucleotide) capillary gel electrophoresis calibration curve.

Regression analysis parameters ($y = mx + b$, R^2):
$m = 0.7500$, $b = -0.2885$, $R^2 = 0.986$

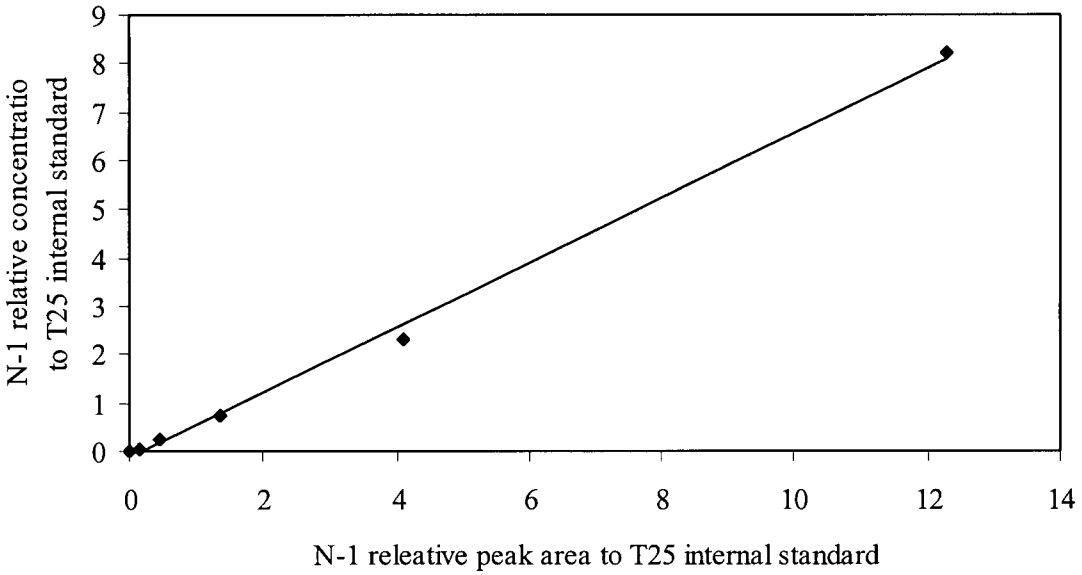

Figure A2.9 Representative clusterin ASO's 20-mer degradation product standard (N-1 oligonucleotide) capillary gel electrophoresis calibration curve.

Regression analysis parameters ($y = mx + b$, R^2):
$m = 0.6705$, $b = -0.127$, $R^2 = 0.997$

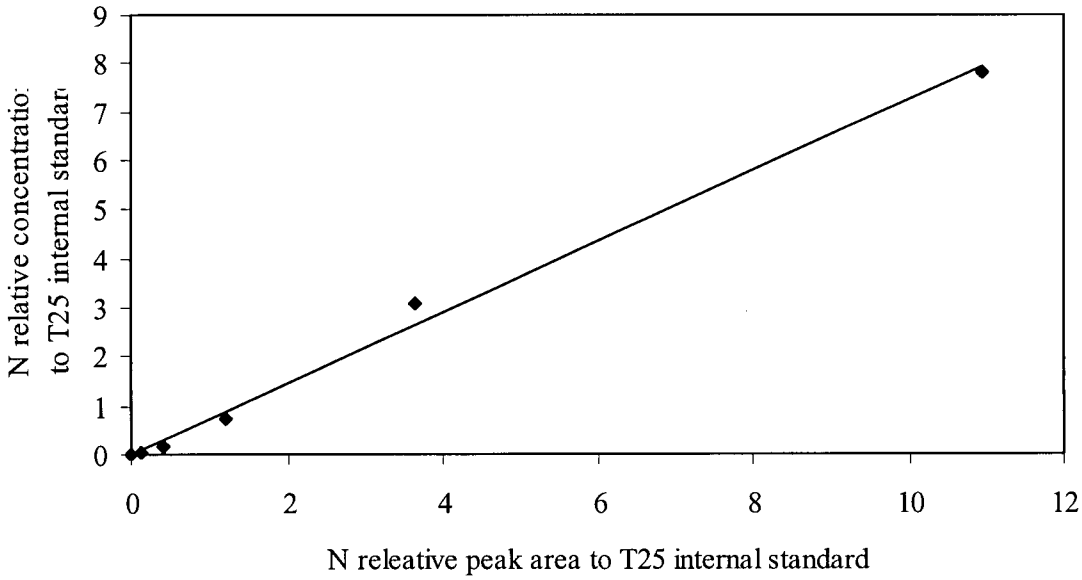

Figure A2.10 Representative 21-mer clusterin ASO (N oligonucleotide) capillary gel electrophoresis calibration curve.

Regression analysis parameters ($y = mx + b$, R^2):
$m = 0.7253$, $b = 0.0004$, $R^2 = 0.995$

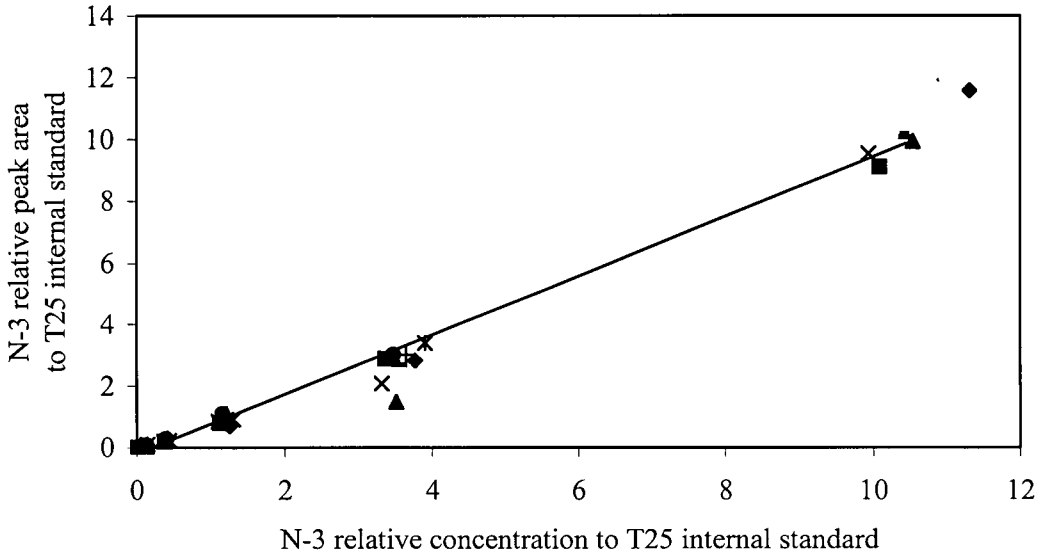

Figure A2.11 Clusterin ASO's 18-mer degradation product standard (N-3 oligonucleotide) capillary gel electrophoresis standard curve determined from eight standards for each concentration over two days.

Regression analysis parameters ($y = mx + b$, R^2):
$m = 0.9641$, $b = -0.2$, $R2 = 0.995$

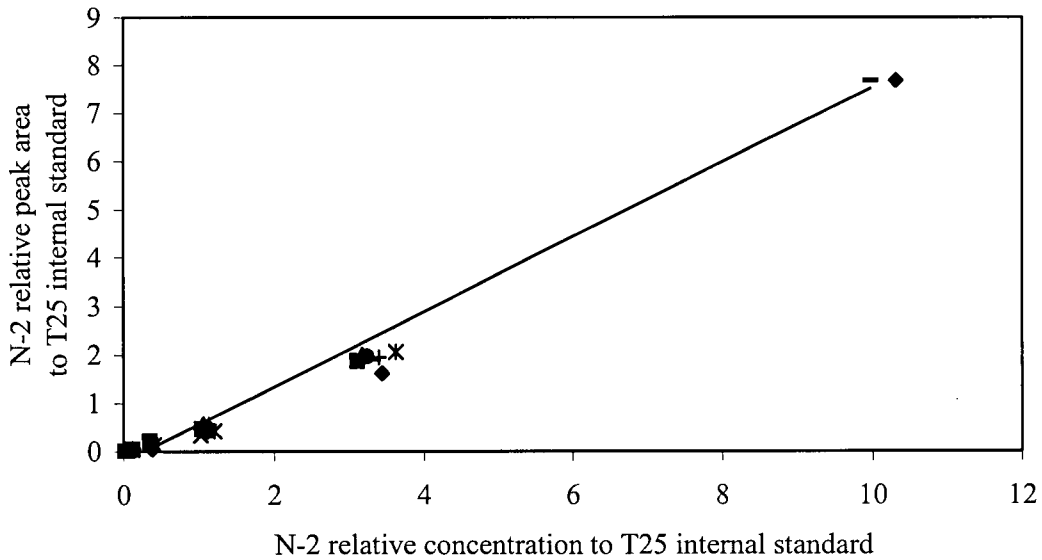

Figure A2.12 Clusterin ASO's 19-mer degradation product standard (N-2 oligonucleotide) capillary gel electrophoresis standard curve determined from eight standards for each concentration over two days.

Regression analysis parameters ($y = mx + b$, R^2):
$y = 0.7749$, $b = -0.2148$, $R^2 = 0.993$

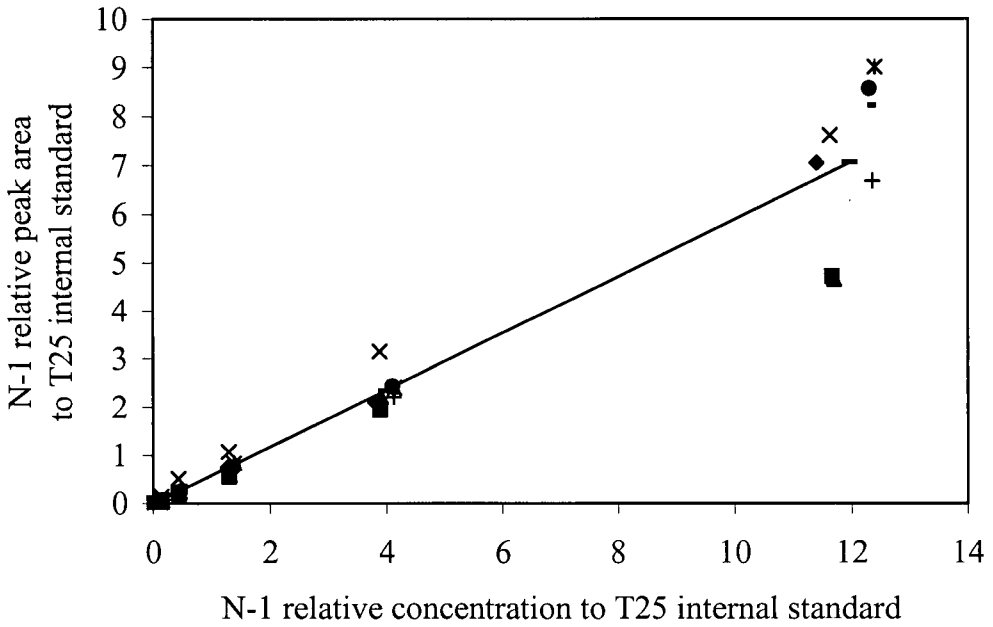

Figure A2.13 Clusterin ASO's 20-mer degradation product standard (N-1 oligonucleotide) capillary gel electrophoresis standard curve determined from eight standards for each concentration over two days.

Regression analysis parameters ($y = mx + b$, R^2):
$m = 0.5916$, $b = 0.018$, $R^2 = 1.000$

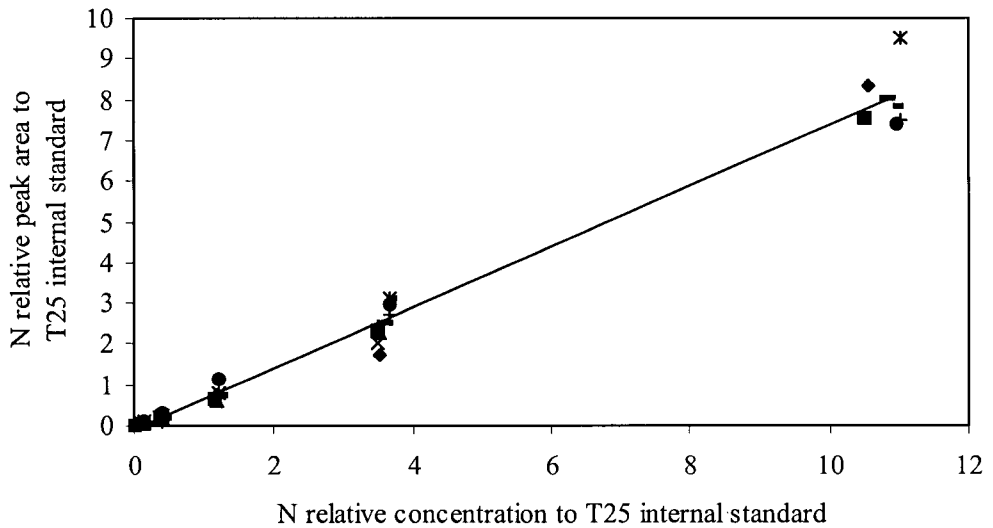

Figure A2.14 Clusterin ASO 21-mer (N oligonucleotide) capillary gel electrophoresis standard curve determined from eight standards for each concentration over two days.

Regression analysis parameters ($y = mx + b$, R^2):
$m = 0.7452$, $b = -0.083$, $R^2 = 1.000$

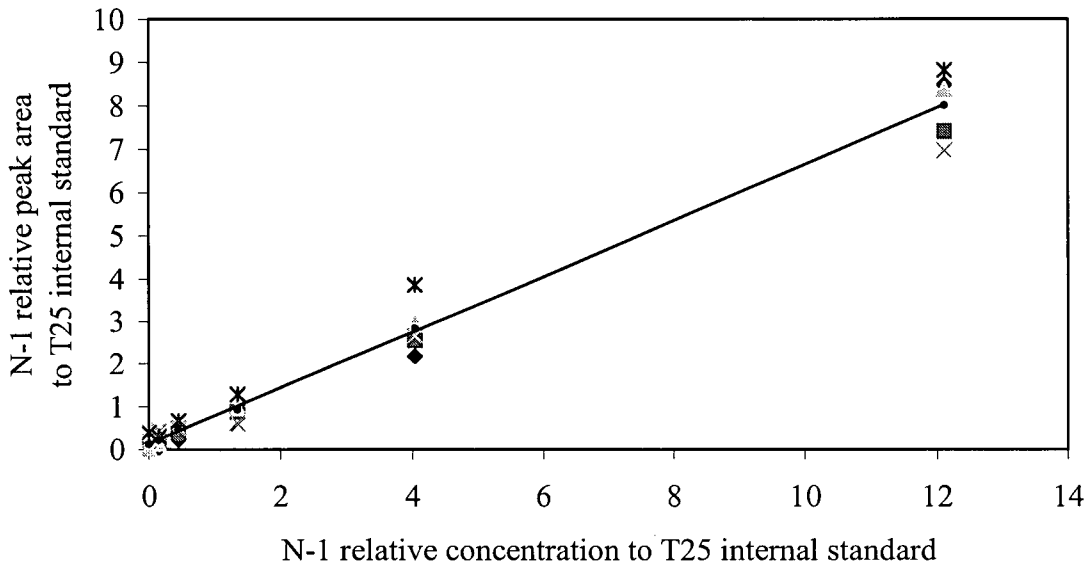

Figure A2.15 Representative clusterin ASO's 20-mer degradation product standard (N-1 oligonucleotide) capillary gel electrophoresis calibration curve determined from five standards for each concentration of N-1 over the concentration range of approximately 0.078 to 6.3 $\mu g \cdot mL^{-1}$. Clusterin ASO 21-mer (N oligonucleotide) and its 19-mer degradation product standard (N-2 oligonucleotide) were spiked in each sample to provide peaks that may potentially interfere with the N-1 peak.

Regression analysis parameters ($y = mx + b$, R^2):
$m = 0.6516$, $b = 0.1361$, $R^2 = 1.000$

APPENDIX 3 – MOLECULAR WEIGHT OF CHITOSAN

Introduction

Synthetic polymers generally consist of different numbers of polymer chains of different lengths or molecular weights. Thus, most polymers possess a distribution of molecular weights. The molecular weight may be represented by an average molecular weight or intrinsic viscosity ([η]) (Rosen, 1993). The molecular weight distribution may be expressed by two or more different types of average molecular weights or by its polydispersity index (PDI) (Cowie, 1973). The number average molecular weight (M_n) is given by

$$M_n = \frac{\sum n_i M_i}{\sum n_i}$$

Equation 1

where n_i is the number of molecules with the number of repeat units i and M_i is the molecular weight of the polymer chains with degree of polymerization i (Rosen, 1993). The weight average molecular weight (M_w) is given by

$$M_w = \frac{\sum w_i M_i}{\sum w_i}$$

Equation 2

where w_i is the weight fraction of the molecules with the number of repeat units i (Rosen, 1993). The PDI is given by (Cowie, 1973)

$$PDI = \frac{M_w}{M_n}$$

Equation 3

The [η] of a polymer in a defined solvent at a defined temperature, is dependent on its molecular weight. The viscosity of a polymer solution may be measured using a viscometer (Martin et al., 1993). If the viscosity of a number of different concentrations of polymer in dilute solution are measured, then Huggins plots may be constructed according to the following equation (Huggins, 1942)

$$\eta_{sp} / c = [\eta] + k_1[\eta]^2 c \qquad \textbf{Equation 4}$$

Kraemer plots may be constructed according to the following equation (Kraemer, 1938)

$$\ln(\eta_{rel} / c) = [\eta] + k_2[\eta]^2 c \qquad \textbf{Equation 5}$$

The Solomon-Ciuta equation may be used to calculate [η] with a single polymer concentration, without a plot (Solomon and Ciuta, 1962)

$$[\eta]_{SC} \simeq (2^{1/2} / c)\,((t_x / t_0) - 1 - (\ln(t_x / t_0))^{1/2} \qquad \textbf{Equation 6}$$

where $[\eta]$ is the intrinsic viscosity, η_{sp} is the specific viscosity, η_{rel} is the relative viscosity, c is the concentration of the polymer solution, k_1 and k_2 are constants, t_0 is the time for the solvent (no polymer) to flow through the viscometer and t_c is the time for the polymer solution at concentration c to flow through the viscometer. As the concentration of the polymer solution approaches zero, the values of η_{sp} / c and $\ln(\eta_{rel} / c)$ approach $[\eta]$. Thus the Huggins intrinsic viscosity ($[\eta]_H$) and Kraemer intrinsic viscosity ($[\eta]_K$) are then taken as the intercept value of the

linear regressions for each set of plots (that is, $c = 0$). In this work, the Solomon-Ciuta intrinsic viscosity ($[\eta]_{SC}$) was determined using different polymer concentrations and the intercept value of the linear regression averaged with the $[\eta]_H$ and $[\eta]_K$ to determine the $[\eta]$ value of chitosan.

A universal calibration curve may be constructed by plotting the log of the product of the molecular weight and $[\eta]$ of a set of polymer standards against their retention times (Collins et al., 1973). The M_{GPC} of a polymer sample may then be calculated from the universal calibration curve using the equation

$$M_{GPC} = 10^{(m \cdot Tr \cdot b)} / [\eta] \qquad \textbf{Equation 7}$$

where m is the slope and b is the intercept of the universal calibration curve and Tr is the retention time of the sample.

Materials, equipment and stock solutions

Chitosan, biomedical grade, lot 30310A, was obtained from Carbomer, Inc. (USA). Pullulan polysaccharide standards were obtained from Polymer Laboratories (USA) and included molecular weights of Mw 180 g·mol^{-1} (Mw/Mn 1.00), Mw 738 g·mol^{-1} (Mw/Mn 1.00), Mw 5.9k g·mol^{-1} (Mw/Mn 1.09), Mw 11.8k g·mol^{-1} (Mw/Mn 1.10), Mw 22.8k g·mol^{-1} (Mw/Mn 1.07), Mw 47.3k g·mol^{-1} (Mw/Mn 1.06), Mw 112k g·mol^{-1} (Mw/Mn 1.12), Mw 212k g·mol^{-1} (Mw/Mn 1.13), Mw 404k g·mol^{-1} (Mw/Mn 1.13) and Mw 788k g·mol^{-1} (Mw/Mn 1.23). ACS grade glacial acetic acid and ACS grade sodium acetate anhydrous were obtained from Fisher Scientific Company (USA).

Unless otherwise indicated, all GPC stock solutions and buffers were stirred or shaken until clear, filtered through a 0.45 μm filter, placed in glass bottles, capped and stored at

4°C until used. A stock solution of 0.5 $mol \cdot L^{-1}$ acetic acid was prepared by making 30.115 g glacial acetic acid up to 1 L with water. A stock solution of 0.5 $mol \cdot L^{-1}$ sodium acetate was prepared by making 41.304 g sodium acetate anhydrous up to 1 with water. A solution of 0.25 $mol \cdot L^{-1}$ acetic acid and 0.25 $mol \cdot L^{-1}$ sodium acetate was prepared by mixing 500 mL of 0.5 $mol \cdot L^{-1}$ acetic acid and 500 mL 0.5 $mol \cdot L^{-1}$ sodium acetate.

Ubbelohde viscometer was obtained from Cannon Instrument Company (USA). Ultrahydrogel 1000 and Ultrahydrogel 2000 columns both with 7.8 mm internal diameter x 30 cm length and 2410 refractive index detector were obtained from Waters (USA).

GPC used instrumentation consisting of 1 mL sample vials with lids, 600S controller, 600S, 717plus autosampler, 515 HPLC pump and Millenium^{32} Version 3.20 software and were obtained from Waters (USA).

Methods

The $[\eta]$ of chitosan was determined by constructing Huggins, Kraemer and Solomon-Ciuta plots. Four chitosan solutions in a range of concentrations from 0.2 to 0.8% w/v in a solution of 0.25 $mol \cdot L^{-1}$ acetic acid and 0.25 $mol \cdot L^{-1}$ sodium acetate were prepared. Plots were constructed by determining the viscosity of the chitosan solutions at 23 ± 1°C using an Ubbelohde viscometer. Each solution was measured three times and the mean value plotted. The $[\eta]$ of chitosan was taken as the mean of the intercept values of the three plots.

Pullulan standards were prepared as a 0.1% w/v solution and assayed by GPC at ambient temperature with an injection volume of 20 μL and a mobile phase of 0.25 $mol \cdot L^{-1}$

acetic acid and 0.25 mol·L^{-1} sodium acetate. The standards were eluted through Ultrahydrogel 2000 and Unltrahydrogel 1000 columns joined in series. A GPC universal calibration curve was constructed by plotting the log of the product of the MW and the [η] of the standards against the retention time of the peak of the standards. The MWs and the [η] reference values for the pullulan standards were obtained from the supplier and Yomota et al. (1993), respectively. Linearity of the GPC universal calibration curve was measured and expressed as R^2.

Results

The [η] value for chitosan was determined from Huggins, Kraemer and Solomon-Ciuta plots (shown in Figure A3.1) and found to be 4.5 ± 1.9 dL·g^{-1} in 0.25 mol·L^{-1} acetic acid and 0.25 mol·L^{-1} sodium acetate solution at 23 ± 1°C. The GPC universal calibration curve based on the plot of the product of the molecular weight and [η] against retention time of pullulan standards ranging in Mw 22.8k to 778k g·mol^{-1} is shown in Figure A3.2.

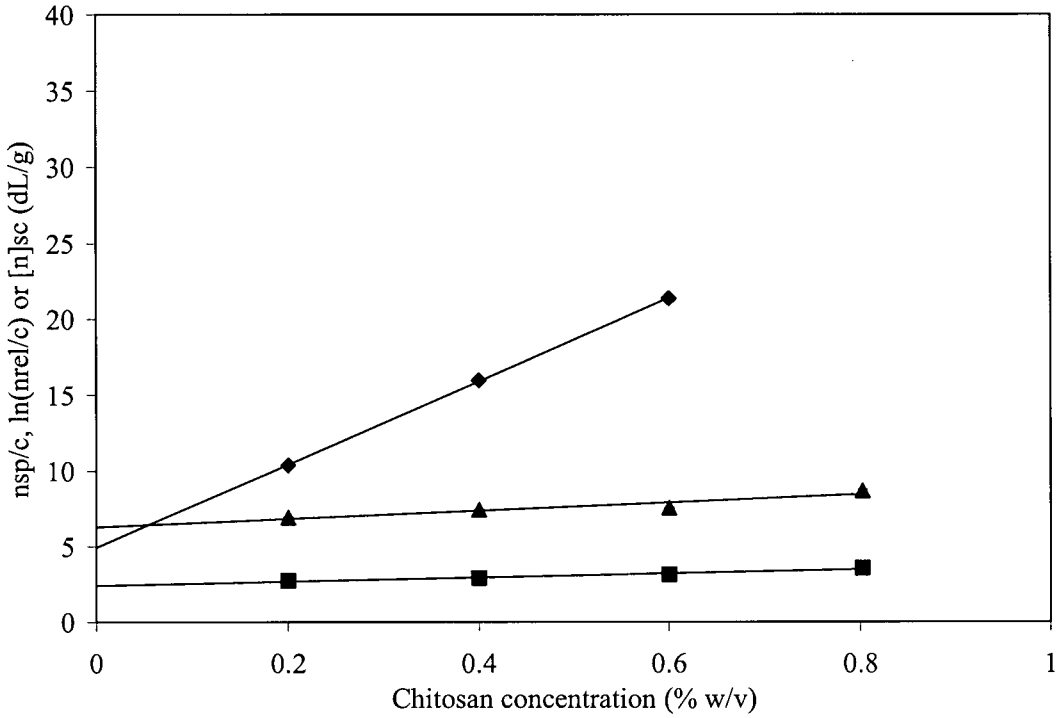

Figure A3.1 Huggins (♦; (η_{sp}/c)), Kraemer (■; ($\ln(\eta_{rel}/c)$) and Solomon-Ciuta (▲; ($[\eta]_{SC}$)) plots of viscosity data for chitosan in 0.25 mol·L^{-1} acetic acid and 0.25 mol·L^{-1} sodium acetate at 23 ± 1°C. η_{sp} is the specific viscosity, η_{rel} is the relative viscosity, c is the concentration of chitosan and ($[\eta]_{SC}$) is the Solomon-Ciuta intrinsic viscosity, for a specific concentration of chitosan. The Huggins, Kraemer and Solomon-Ciuta intrinsic viscosities are taken as the Y-intercept value of the linear regressions for each set of plots. Error bars were within the size of the data plots and therefore are not readily visualized on the figure.

Regression analysis parameters ($y = mx + b$, R^2) ± 95% confidence intervals:

Huggins plot:	$m = 27.4 \pm 2.4$, $b = 4.92 \pm 0.64$, $R^2 = 1.00$
Kraemer plot:	$m = 1.36 \pm 0.29$, $b = 2.41 \pm 0.10$, $R^2 = 0.957$
Solomon-Ciuta plot:	$m = 2.70 \pm 0.71$, $b = 6.27 \pm 0.26$, $R^2 = 0.881$

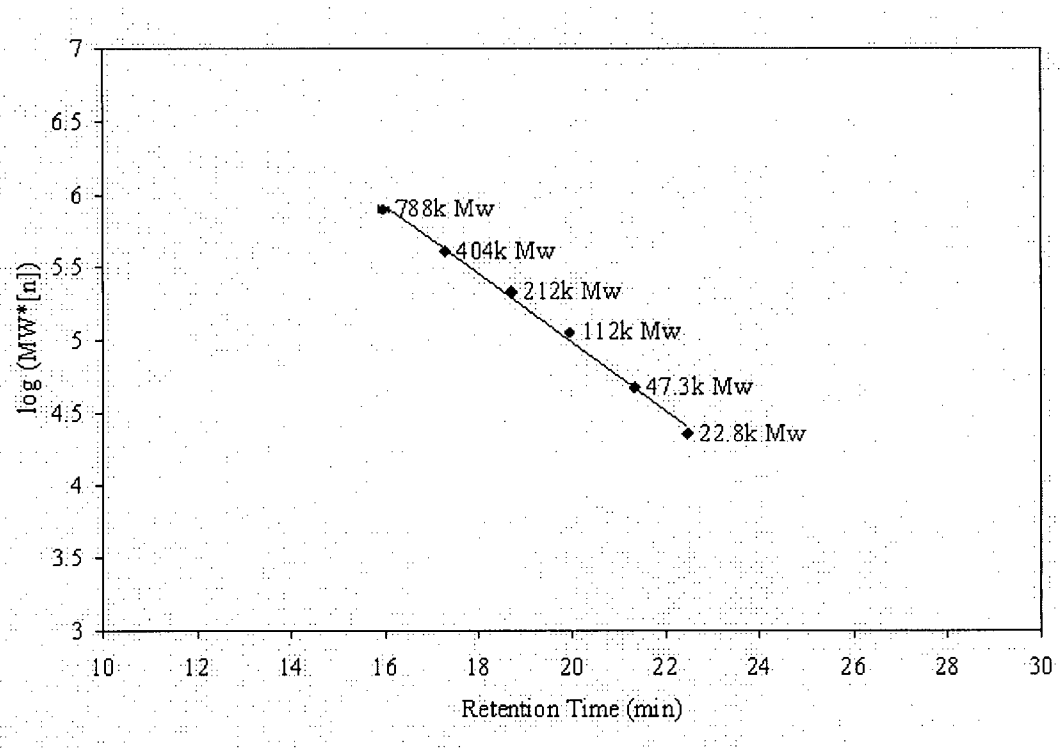

Figure A3.2 Representative gel permeation chromatography universal calibration curve of pullulan polysaccharide molecular weight standards. The Mw of each standard in $g \cdot mol^{-1}$ is listed beside its data point.

Regression analysis parameters ($y = mx + b$, R^2):

$m = -0.234$, $b = 9.66$, $R^2 = 0.995$

Discussion

The value of [η] of a polymer is dependent on molecular weight, the stiffness of the chains and the ionic strength of the media (Anthonsen et al., 1993). The [η] value of 4.5 $dL \cdot g^{-1}$ for the chitosan used in this work is within the range of [η] values of 2.9 to 9.8 $dl \cdot g^{-1}$ determined by Kasaai et al. (2000) under similar conditions using 75 to 80% deacetylated chitosan (compared to our 85% deacetylated chitosan) as the Mn was increased from 140k to 560k $g \cdot L^{-1}$. It is also similar to the range of [η] values of 1.85 to 7.80 $dl \cdot g^{-1}$ determined by Anthonsen et al. (1993) in 0.02 $mol \cdot L^{-1}$ acetic acid and sodium acetate with 0.1 $mol \cdot L^{-1}$ sodium chloride at pH 4.5 and 20°C, for a series of chitosans with Mn increasing from 35k to 245k $g \cdot mol^{-1}$. The large [η] standard deviation value of 1.9 $dL \cdot g^{-1}$ for the chitosan used in this project may be due to a number of errors as reviewed by Harding (1997), including curvature of the extrapolation curve and experimental errors such as the accuracy of the chitosan concentration, measurement of the chitosan solution flow time and the temperature of the water. The water bath used in this work was only capable of maintaining the temperature ± 1°C, while maintaining the temperature at ± 0.01°C is recommended (Harding, 1997). The R^2 value of 0.995 for the GPC universal calibration curve (Figure A3.2) showed the linearity of the method and demonstrated that the GPC method was appropriate for measurement of M_{GPC} in the range of 23k to 780k $g \cdot mol^{-1}$.